THE UNIVERSITY
of EDINBURGH

Role of the RING domain in MDM2-mediated ubiquitination of p53

Fiona Lickiss

Doctor of Philosophy

The University of Edinburgh

August 2014

Declaration

I hereby declare that I am the author of this thesis. The work herein is entirely my own unless otherwise clearly indicated and acknowledged. I can confirm that this thesis has been submitted for the degree of Doctor of Philosophy and no part of this work has been submitted for any other degree or professional qualification.

Fiona Lickiss

20th August 2014

Acknowledgements

Simply put, there are certain people without which the last four years would not have been possible. I'll begin in the lab…

Thank you Kathryn for your constant support and ideas, allowing me the opportunity to experience many new techniques, even braving ice storms along the way, and especially for guidance with and the reading of my thesis. Thank you Ted for your support and fresh ideas, especially regarding tricky cloning and peptide phage display. Thank you Malcolm for your support, advice and kind words regarding reports and presentations. Thank you Borick, Lenka, Petra and Martin for allowing me the opportunity to work in your lab, thank you for your expertise, patience and assistance. Thank you to everyone in the Ball and Hupp labs for answering my questions, checking my maths, opening bottles and being fantastic friends. Thanks for understanding and facilitating the fact that tea and cake fuel a scientist!

And outside the lab?

Thank you to all my friends, especially to everyone in 'Team Ming' for being the best friends a girl could wish for, thanks my lovelies for never talking about science and keeping me sane… refined drinks when this is over, yes? Thank you to everyone at over the wall, being part of the OTW family and entering the camp bubble cheers me up and puts absolutely everything back into perspective.

Thank you to my family, where would I be without you? Thanks Mum and Dad for your constant love and support, making sure I am well fed, providing me with my own personal taxi service and putting the world to rights in the Walnut Tree. Thank you Sarah for keeping me well dressed and being so thoughtful with messages and deliveries of hot chocolate! Thank you Auntie Annette and Uncle Paul for all the letters and emails, they always made my day. P.S. the hedgehogs are doing just fine… I love you all.

Thank you Mark for being the person who has to put up with 'science Fiona' the most. Thanks for being there through all the good and bad science days and for enduring your own personal science lessons that I am so convinced you find interesting. Thank you for the welcome distractions of recipe books and flowers and thank you for all the support whilst I have been writing, don't worry all the paper will be gone soon! I love you.

Abstract

The MDM2 protein regulates the tumour suppressor protein p53, acting as its chaperone, regulating its translation and targeting p53 for degradation by the 26s proteasome via its E3 ligase activity. The E3 ligase activity of MDM2 is dependent on its C-terminal RING domain. E3 ligases containing a RING domain are traditionally thought to catalyse the transfer of ubiquitin from their conjugating enzyme (E2) partner to the target protein, in the final step of the ubiquitination cascade. Various E2 enzymes have been shown to interact with their partner E3 ligases, yet evidence for the interaction between MDM2 and its partner E2, UbcH5α has not yet been shown. It has been reported that the reason for this lack of evidence is that the interaction between the two is highly unstable.

Here I show that MDM2 forms a stable isolatable interaction with UbcH5α, the C-terminal tail of MDM2 is not necessary for this interaction. Although RING E3 ligases were not previously thought to interact with ubiquitin, preliminary evidence is emerging that suggests that this interaction is possible indeed I show that MDM2 and ubiquitin form a stable complex. I demonstrate that UbcH5α and ubiquitin both interact with the RING of MDM2, specifically the 20 most C-terminal amino acids of MDM2. My results show that both these proteins can bind this region of the RING simultaneously. I also highlight specific residues including tyrosine 489 and arginine 479 important for UbcH5α and ubiquitin binding respectively and the negative affect that these mutations have on the E3 ligase activity of MDM2 towards p53. Furthermore I show by limited proteolysis and hydrogen deuterium exchange that UbcH5α can be allosterically activated by MDM2. A novel peptide phage display technique linked to next generation sequencing was developed to further confirm an allosteric change and demonstrates that UbcH5α has different binding specificity for peptides when in a free or ligand bound conformation.

MDM2 is a popular target for cancer therapeutics due to its dysregulation throughout many cancer types, including 30% of soft tissue sarcomas. Dissecting the mechanism of MDM2 function is an important step in identifying specific drugable interfaces on MDM2 and its interacting partners so that effective therapeutics can be designed.

ABBREVIATIONS

APS	Ammonium persulphate
ATP	Adenosine triphosphate
BLAST	Basic local alignment search tool
BME	β-mercaptoethanol
bp	Base pair
BSA	Bovine serum albumin
CDK	Cyclin dependant kinase
CHIP	C terminus HSC70 interacting protein
CK	Creatine phosphokinase
CP	Creatine phosphate
CPSA	Constant current chronopotentiometric stripping analysis
ΔT	Delta tail
DMSO	Dimethyl sulphoxide
DNA	Deoxyribonucleic acid
DTT	Dithiothreitol
DUB	Deubiquitinating enzyme
ECL	Enhanced chemiluminescence
E1	Ubiquitin activating enzyme
E2	Ubiquitin conjugating enzyme
EDTA	Ethylenediaminetetraacetic acid
ELISA	Enzyme linked immunosorbent assay
FL	Full length
GST	Glutathione S-transferase
HD	Hydrogen-deuterium
HDME	Hanging drop mercury electrode
HECT	Homologous to E6AP carboxyl terminus
HEPES	4-(2-hydroxyethyl)-1-piperazineethanesulfonic acid
His	Histidine
IPTG	Isopropyl β-D-1-thiogalactopyranoside
IMAC	Immobilised metal ion affinity chromatography
LB	Luria-Bertani

MAb	Monoclonal antibody
MDM2	Mouse double minute 2
MOPS	3-(N-morpholino)propanesulfonic acid
MS	Mass spectrometry
NGS	Next generation sequencing
NMR	Nuclear magnetic resonance
OD	Optical density
p53	Tumour suppressor protein 53
PAGE	Polyacrylamide gel electrophoresis
PBS	Phosphate buffered saline
PCNA	Proliferating cell nuclear antigen
PCR	Polymerase chain reaction
pRB	Retinoblastoma protein
RbR	Ring between ring
RECAMO	Regional centre for applied molecular oncology
RFU	Relative fluorescent units
RLU	Relative light units
RING	Really interesting new gene
RNA	Ribonucleic acid
RNF4	Ring finger protein 4
rpm	Revolutions per minute
SDS	Sodium dodecyl sulphate
SECMALS	Size exclusion chromatography linked to multi angle light scattering
SUMO	Small ubiquitin like molecule
TEMED	Tetramethylethylenediamine
TFA	Trifluoroacetic acid
TRIS	2-amino-2-hydroxymethyl-propane-1, 3 diol
UbcH5α	Ubiquitin conjugating enzyme human 5α
UBD	Ubiquitin binding domain
Ube1	Ubiquitin activating enzyme
UBL	Ubiquitin like
U-BOX	UFD2 homology
UPS	Ubiquitin proteasome system
UV	Ultraviolet

wt	Wild type

Table of Contents

Figures

Tables

Chapter 1: INTRODUCTION

1.1 Ubiquitination

1.1.1 Introduction

Ubiquitination is the ATP-dependant, covalent modification of a protein with ubiquitin. Ubiquitination is one of the most common post translational protein modifications but the nature of this modification is highly diverse.
Discovered in 1980[1] by virtue of the fact that proteins with polyubiquitin chains were observed that were subsequently targeted for degradation by the 26s proteasome[2]. Degradation of protein by the ubiquitin proteasome pathway (UPS) is the most prevalent method of protein degradation within the cell. Protein levels are dynamic and are kept stable by the strict relationship between protein synthesis and protein degradation, this tight level of control is critical for protein function and for rapid control during the response to cell stresses or environmental stimuli. In additional the UPS is important for the removal of misfolded and aggregated proteins from the cell[3]. Ubiquitination as a signal for protein degradation is the most well studied function of ubiquitin modification, there are however may other functions that ubiquitin can signal for, including many non-proteolytic outcomes such as sub-nuclear trafficking and localisation[4], DNA repair[5], protein function, activity of transcription factors and protein-protein interactions[6].

The ubiquitin signalling pathway is more diverse and complex than initial observations suggested. A chain of at least four ubiquitins (polyubiquitination) is required to signal for degradation, but chains of up to three ubiquitin molecules can exist and signal non-proteolytic events. Proteins can also be monoubiquitinated either at one site or multiple sites throughout the protein (multi-monoubiquitination) (**figure 1.1 i-iv**).

Ubiquitin is covalently linked to target proteins through its C-terminal glycine to a lysine residue on the substrate, though cases exist in which the N-terminal amino group of a protein is the point of ubiquitination instead of a lysine residue[7].

Ubiquitin itself contains 7 lysines that can be ubiquitinated in the formation of polyubiquitin chains. Chains can also form through the N-terminal methionine residue of ubiquitin, though this is less common. The first identified and best characterised of these polyubiquitin linkages are K48 linked chains. K63 linked chains are also well characterised but less is known about the nature of the other linkages (K6, K11, K27, K29 and K33), they are all abundant *in vivo* and they are all required for a fully functioning ubiquitin proteasome system[8]

Ubiquitin does not only form homogeneous chains i.e. chains in which ubiquitin molecules are linked via the same lysine, ubiquitin can also form heterogeneous chains. These heterogeneous chains can also form branched chains, in which two ubiquitin molecules are linked through adjacent lysines e.g. K6 and K11 on to the preceding ubiquitin molecule (**figure 1.1 vi-vii**). Branched chains do not associate with the proteasome, therefore do not appear to signal protein degradation[9].

Post-translational modification of substrates with smaller molecules is not restricted to ubiquitination, a number of ubiquitin-like proteins (UBLs) have been identified including small ubiquitin-like modifier (SUMO), neuronal-precursor-cell-expressed developmentally down regulated protein 8 (NEDD8) and human leukocyte antigen F-associated (FAT10). The UBLs all share a basic tertiary core structure and ubiquitin is able to form mixed chains with these UBLs[10] (**figure 1.1 viii**).
All these variable factors result in a large number of possible protein modifications by the UPS, and raises the question of how this complex system is controlled. Many advances in knowledge have been made yet still many methods of control remain a mystery.

Considering the diversity of ubiquitination and the role it plays in a broad range of cellular processes it is no surprise that dysregulation of the UPS has been implicated in a number of disease processes including Parkinson's disease and other neurodegenerative diseases[11], inflammatory diseases, such as asthma, muscle wasting diseases and cancer[12].

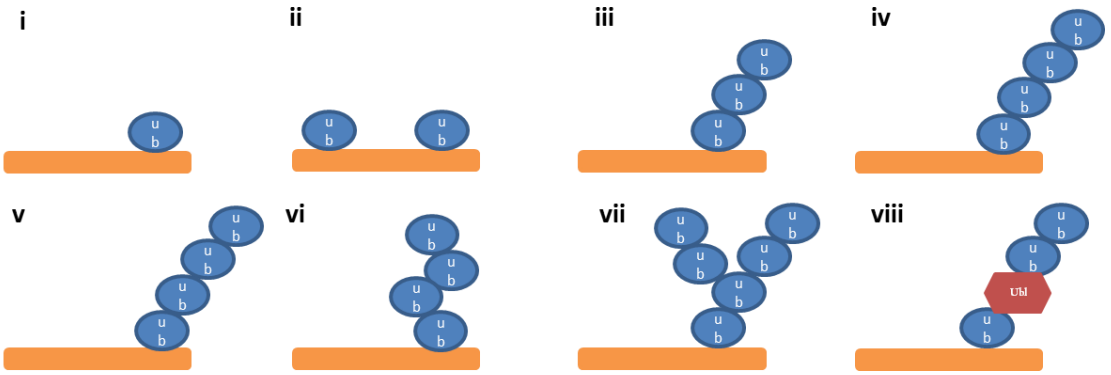

Figure 1.1: Diversity of ubiquitination. Ubiquitination is the addition of ubiquitin to a target protein, the nature of ubiquitination is diverse. Monoubiquitination is the addition of one ubiquitin molecule to a protein **(i)**. Monoubiquitination can happen at multiple different sites on a target protein resulting in multi-monoubiquitination **(ii)**. Chains of ubiquitin can be added to a target protein, these chains vary in length **(iii)**, a chain of at least four ubiquitin molecule signals for degradation by the 26s proteasome **(iv)**. Ubiquitin chains can be linked via the same lysine of ubiquitin **(v)** or linkage sites can be mixed throughout the chain **(vi)**, mixed linkages can result in branched ubiquitin chains **(vii)**. Ubiquitin can form mixed chains with other ubiquitin like proteins (UBLs) **(viii)**.

1.1.2 Ubiquitin

Ubiquitin is a small protein of 76 amino acids in length. It is highly conserved across eukaryotes, only 3 of the 76 amino acids differ between yeast and human versions, its ubiquitous presence inspired its name. UBLs are also present throughout eukaryotes, some such as SUMO and NEDD8 are present across the board whereas other such as FAT10 are present only in mammals[10].

The structure of ubiquitin includes an α helix and mixed 5 strand β sheet, there is a hydrophobic core between the β sheet and α helix, The overall structure of ubiquitin is extremely compact and tightly hydrogen bonded with only limited residues displaying any flexibility to allow for protein-protein interactions. The C-terminal tail is exposed to facilitate covalent linkage to target proteins (**figure 1.2**). The seven lysines involved in chain formation are all located on the surface of the protein[13].

Ubiquitin has three hydrophobic patches, each being responsible for interactions with its various binding partners and the proteasome. The hydrophobic patch of Ile44, Leu8, Val70 and His68 is involved in the majority of ubiquitin interactions, including most ubiquitin binding proteins and the proteasome[14,15]. The hydrophobic patch of IIle36, Leu71 and Leu73 is important for recognition by some HECT E3 ligases[16]. The final hydrophobic patch of Gln2, Phe4 and Thr14 is recognised by ubiquitin specific protease and some deubiquitinating enzymes (DUBs)[17].

1.1.3 Chain linkages

The 7 lysines of ubiquitin are integral to polyubiquitin chain formation; these chains also form a structure, and can be in a compact or open conformation. K6, K11 and K48 linked polyubiquitin chains tend to be compact with the distal and proximal ubiquitin moieties forming an intramolecular interface, on the other hand K63 linked polyubiquitin chains tend to be in an open conformation and the only point of contact is the linkage point[18].

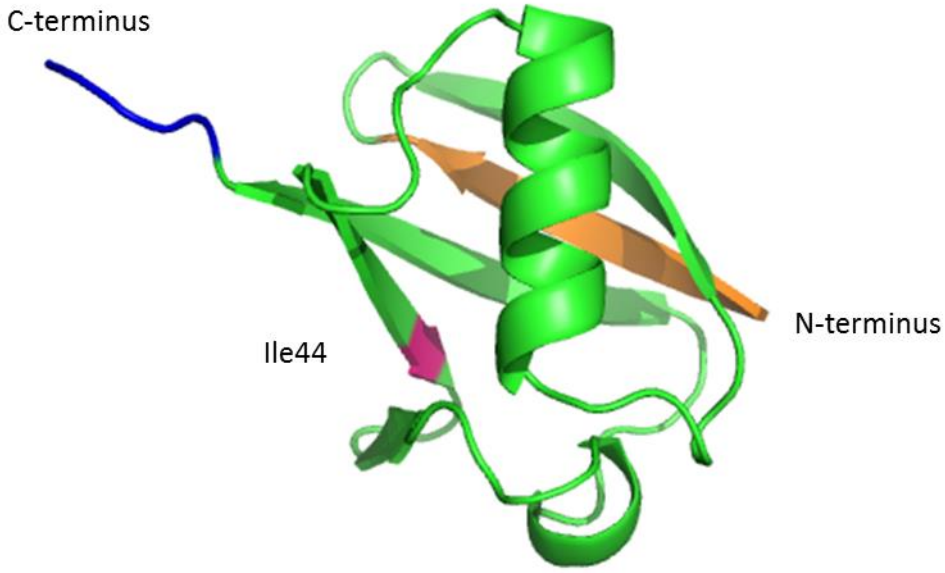

Figure 1.2: Structure of ubiquitin. This model was made in PYMOL and is based on the published crystal structure of ubiquitin[13]. The blue residues indicate the exposed C-terminus, the residues coloured orange show the N-terminus, and the residue coloured pink is Ile 44, a residue important for many of ubiquitins interactions with binding partners.

The open conformation of K63 linkages gives these ubiquitin chains more flexibility and allows them to adjust their conformation despite the rigidity of ubiquitin. Polyubiquitin chains are highly dynamic and the opposite of the usual conformation state can also be seen.

The cellular response to ubiquitination will vary depending on the lysine linkage point; it is becoming clearer that specific linkages signal for specific events. K48 linked polyubiquitin chains are the best characterised of all the lysine link points and are believe to be the principle signal for targeting substrates for proteasomal degradation. K48 is the most abundant linkage in resting cells, the ratio of chain linkages however may change under stress conditions or during disease. Monoubiquitination is known to signal non-proteolytic events, K63 linked polyubiquitin chains also signal non-proteolytic events, these chains mark proteins that contribute to DNA repair in response to stress[8] and are an important component of signalling cascades in the immune response. For example activation of the NF-κβ family of transcription factors occurs in response to numerous stimuli and is essential for cell transformation. In unstimulated cells NF-κβ is sequestered in the cytoplasm by its inhibitor Iκβ. Activation of NF-κβ is initiated by degradation of Iκβ which occurs primarily by the activation of the Iκβ kinase (IKK). NF-κβ is then free to enter the nucleus where it can act of a family of transcription factors. IKK phosphorylates Iκβ and this targets it for K48 linked polyubiquitination and its subsequent degradation by the 26S proteasome. In addition K63 linked polyubiquitination plays an important role in activating IKK. TRAF6 is an E3 ligase that facilitates the synthesis of K63 linked polyubiquitin chains and is an essential signalling protein in the immune and inflammatory pathways. TRAF6 mediates activation of the TAK1 kinase complex via K63 linked polyubiquitination, this subsequently activates IKK by phosphorylating Iκβ, therefore facilitating the release of NFκβ to act on its nuclear transcription factors[19].

Little is known about the other linkages. K6 linked polyubiquitin chains have been associated with proteins involved in DNA repair[20] whilst K27, K29 and K33 are the hardest to study as they are the least abundant linkages seen in resting cells[18]. K27 has been implicated in targeting proteins involved in mitochondrial biology[21]. Interestingly K11 linked polyubiquitin chains, like K48, may have a role in signalling

protein degradation[22]. Specifically K11 linkages are found in a subset of proteins that are part of the endoplasmic reticulum associated degradation pathway[8].

With the exception of K63 linked chains, it is likely that each different linkage signals proteasomal degradation of its substrate, yet the different linkages are formed in response to different stresses and signals within the cell and a lack of high affinity specific reagents makes it difficult to study the more minor forms of ubiquitin linkage. Ubiquitin chain linkages are generated for a specific purpose and target proteins are ubiquitinated on a certain residue, this shows that the system needs to be controlled at multiple levels to ensure the correct modification with the correct length and linkage of chain, if just one area of control is deregulated then there is the potential for disease to develop.

1.1.4 Ubiquitination cascade

The post translational modification of a protein with ubiquitin is an ATP dependant reaction that requires not only ATP but a group of enzymes. The core ubiquitin pathway components comprise of an activating enzyme (E1), a conjugating enzyme (E2) and a ligase (E3).

The first step in ubiquitin conjugation is to activate the C-terminus of ubiquitin, in eukaryotes this is a two-step reaction. The E1 has little affinity for ubiquitin by itself; MgATP binds to E1 before the two step reaction occurs in order to increase the affinity of E1 for ubiquitin. In the first step a ubiquitin-adenylate intermediate is formed, in the second step this intermediate reacts with the active cysteine on E1 to form a E1-ubiquitin thiol ester[23].This first, two-step reaction, is the same for all UBL proteins, each UBL has its own dedicated E1, except in the case of Atg8 and Atg12 which share a common E1[24]. The mechanism concerning the first part of this two-step reaction is highly conserved from *E.coli* to humans[10,25].

The next step in the conjugation cascade is the transfer of ubiquitin from the E1 cysteine to an E2 cysteine. The enzymes involved in the ubiquitination cascade are hierarchical in organisation; there is one E1, significantly more E2s, most likely because of the many downstream targets and a large number of E3s. This is slightly different for SUMO and NEDD8 they have one E1 and a few E3s but only one E2

each, Ubc12 for NEDD8 and Ubc9 for SUMO[10]. All E2 enzymes share a conserved globular domain of ~150 amino acids. The core domain consists of 4 standard α helices, a shortened α helix and a four stranded anti-parallel β sheet. The active site cysteine resides in a shallow cleft on the surface of the protein, residues surrounding this cysteine are highly conserved throughout the E2 family[26]. Free E2s bind very tightly to loaded E1s, the K_D is subnanomolar[27] but non covalent E2-ubiquitin binding affinities are very low[26], this highlights the importance of E1 in this cascade.

The final step in the conjugation cascade is the transfer of ubiquitin to the target substrate, this requires an E3 ligase. Each E3 interacts with one, or possibly a few, E2s, E2s will interact with many E3s. Each E3 recognises a specific substrate or set of substrates and substrate modification by ubiquitin is E3 dependant[28]. One of two events can happen in this final step. Either the E3 activates the E2 and ubiquitin is transferred directly to the target substrate from the E2 or the ubiquitin is transferred from the E2 to an active site cysteine on the E3 and then ubiquitin is transferred from the E3 to the target (**figure 1.3**). The ubiquitination conjugation pathway is extraordinary in its diversity of substrates, this diversity explains the large number of E3 ligase enzymes[29].

The many E2 and E3 enzyme pairings along with the diverse nature of ubiquitin modification illustrate what a complex system the ubiquitination pathway is. The exact nature of regulation of all the components and how specificity is controlled is still elusive in parts. It would appear that the E3 is responsible for substrate recognition, and it is the pairing of the E3 with a certain E2 that specifies the length and linkage of the ubiquitin chain[30]. Some E3s can interact with multiple E2s, such as BRCA1/BARD1[31]. Some of these pairings result in monoubiquitination of a substrate, other pairing result in the formation of polyubiquitin chains.

Substrate specific E3s may not apply to all UBLs; it may not be that all UBLs are conjugated to multiple downstream targets. SUMO however is conjugated to multiple downstream targets, like ubiquitin, and E3s dedicated to SUMO conjugation have been identified[32].

E2s were originally proposed to bring E3 and substrate together[33]. In principle this is remains true, three groups of E3 ligases have been subsequently identified and whilst they all catalyse the transfer of ubiquitin to their target the mechanisms of catalysis differ. E3 ligases belong to either the Homologous to E6AP Carboxyl Terminus (HECT), Really Interesting New Gene (RING) or UFD2 homology (U-box) family of proteins.

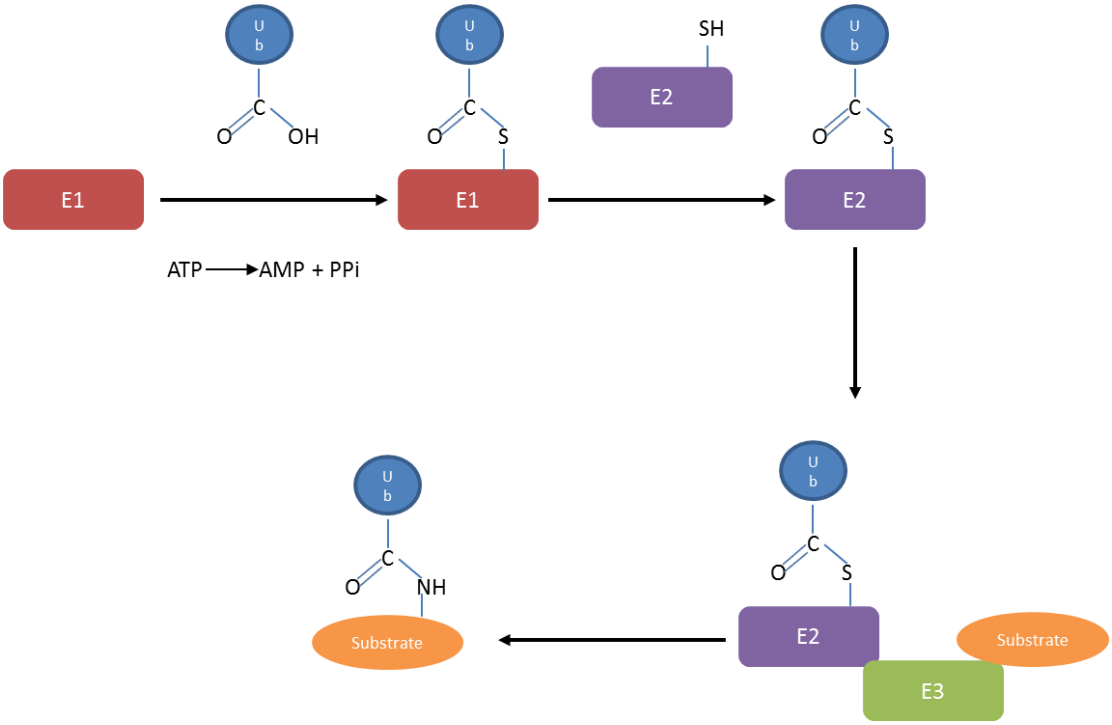

Figure 1.3: Ubiquitination cascade. An overview of the ubiquitination cascade showing ubiquitin transfer from ubiquitin activating enzyme (E1) to ubiquitin conjugating enzyme (E2) to substrate, via ligase enzyme (E3).

1.2 E3 ligases

1.2.1 RING E3 ligases

RING E3 ligases best fit the original proposed model of ubiquitin transfer. Originally RING E3 ligases were thought to act as a scaffold protein, binding their E2 and target substrate and catalysing the transfer of ubiquitin between the two[34,35]. To support this there are many examples of RING E3s binding to E2s, including BRCA1/BARD[36], RNF4[37] and CHIP[38]. Structures of E3s and E2s in complex show the E3 binding site is ~ 15Å away from the active site cysteine of the E2[39], this makes the proximity catalysis mechanism unlikely. Currently the mechanisms of how RING E3s catalyse the transfer of ubiquitin to the target is unclear, ideas regarding the allosteric activation of E2 have been proposed but not confirmed[35]. As to whether there is a universal mechanism of ubiquitin transfer for all RING E3s or mechanisms that are E3 and/or E2 specific remain to be seen.

The first RING described contained the zinc coordination sequence: Cys-X_2-Cys-X_{9-36}-Cys-X_{1-3}-His-X_{2-3}-Cys-X_2-Cys-X_{4-40}-Cys-X_2-Cys (x is any amino acid)[40]. As other RING containing proteins have been identified there have been some variations on the sequence above with regards to cysteines and histidines, though all RING domains still coordinate two zinc ions.

Two groups of RING E3s exist, those that act alone, such as MDM2 and c-Cbl and those that act as a component of a large multi protein complex, such as Rbx1/Roc1. There are further subgroups of multi protein complexes, the Skp1/Cullin/Fbox (SCF) group and the Anaphase Promoting Complex/Cyclosome (APC/C) group[41]. In these multi protein complexes the RING E3 subunit does not recognise the substrate; this is mediated by another subunit within the complex. Rbx1/Roc1 is an example of a RING E3 that can form an SCF, and other cullin RING ubiquitin ligase complexes with many alternative substrate recognition subunits, this adds to E3 diversity[42,43].

1.2.2 U-box E3 ligases

A relatively small number of E3 ligases contain the U-box E2 binding domain. It was originally proposed that the U-box would adopt a RING domain like conformation. Instead of zinc coordination, electrostatic interactions were proposed as the method of structural organisation[44]. The actual structure displays a hydrophobic core with two internal interaction centres comprising of hydrogen bonds and salt bridges. The spacing of the residues involved in these interactions are remarkably similar to the spacing of zinc coordinating residues in the RING domain[45]. This structure implied that U-box domains could bind E2s and facilitate ubiquitin conjugation. A number of binding studies confirmed this to be the case[46,47].

Relatively little is known about U-box E3s compared to RING E3s. The most well characterised U-box domain containing protein is Carboxyl-terminus of Hsc70 Interacting Protein (CHIP), the recognition of CHIPs target substrates, generally unfolded protein, is dependent on the association of CHIP with Hsp70 or Hsp90[48]. More recently however CHIP has been shown to ubiquitinate native proteins, such as IRF1, in an Hsp70- independent manner[49]. As with RING E3s the mechanism of ubiquitin transfer by U-box E3 ligases remains unclear.

1.2.3 HECT E3 ligases

The HECT E3s operate a different mechanism than RING and U-box E3s. They contain a conserved cysteine and this accepts ubiquitin from the E2 forming a thiol ester intermediate before transferring ubiquitin to the target[50](**figure 1.4**).

The first identified member of the HECT domain family of ligases was E6 Associated Protein (E6AP). When E6AP is bound to the E6 protein on an oncogenic human papillomavirus it can bind to and ubiquitinate the host p53, resulting in p53 degredation[51].

The HECT domain is 350 amino acids in length and all HECT domains exhibit similarity to that of E6AP. The HECT domain always resides at the C-terminus of a

protein; this is in contrast to RING domains which are found at differing points in proteins. Substrate specificity tends to be dictated by the N-terminus of the HECT domain containing proteins[52]. Modelling indicates that HECT domains have great flexibility and this this flexibility is important for their E3 activity[53].

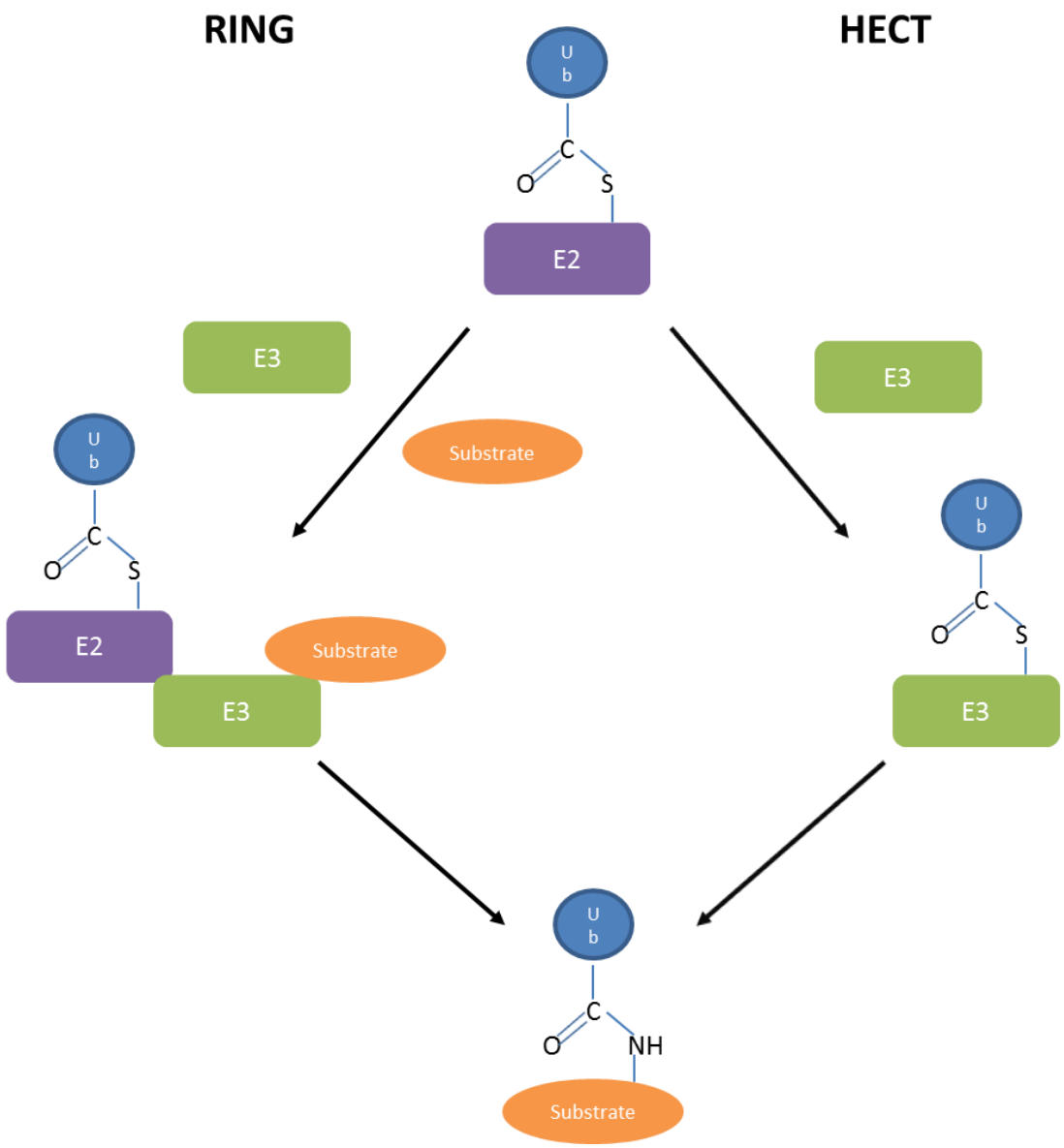

Figure 1.4: Mechanism of E3 ligase activity. Overview of the different mechanisms of activity that E3 ligases employ. RING E3 ligases catalyse the transfer of ubiquitin from the E3 to the substrate, the mechanism for this remains unknown. HECT E3 ligases accept ubiquitin from the E2, on to their active site cysteine, before transferring ubiquitin to the substrate.

1.2.4 Ring between ring E3 ligases

Ring Between Ring (RBR) E3s are a small sub class of RING E3 ligases, there are only thirteen in the human genome, they are few but are conserved across eukaryotes. This sub group of RING E3 blurs the boundaries between RING and HECT E3 mechanisms of action.

They were originally identified because they contain a standard RING domain but they also contain two additional domains. The RBRs contain a trio of closely spaced domains, a standard amino-terminal RING domain ($RING_1$), an InBetween Ring domain (IBR) and a second RING domain ($RING_2$). $RING_1$ is comparable to other RING E3s; the zinc coordination site follows the same conserved sequence of cysteine and histidine residues. $RING_2$ does not share this similarity; this domain is unique to RBRs[54,55].

The majority of RBRs are not yet well understood, their substrates and E2s are poorly defined. They have been implicated in regulation of translation[56] and NF-κβ signalling[57]. The most well characterised RBR is parkin, because of its association with Parkinson's disease[58], its list of substrates continues to grow[59] and the nature of the substrates suggest that parkin has a role in the degradation of misfolded or aggregated proteins.

A cysteine in the $RING_2$ domain, highly conserved throughout RBRs, functions like a HECT domain active site cysteine, it forms a thioester bond with ubiquitin before transferring it to the substrate. $RING_1$ can bind E2s and the E2 binding site is very similar to that identified in other RING E3 domains such as BRCA1. As RBRs contain a RING E3 domain that binds to E2s and an active site cysteine with activity comparable to HECT E3s they are thought of as RING/HECT hybrids[55].

1.2.5 E4s

As discussed a polyubiquitin chain consisting of at least four ubiquitin molecules can target a protein for degradation by the 26s proteasome system. It has been suggested

that ubiquitin chains are formed before addition to the substrate, this theory is supported by the presence of free, unanchored chains in the cell[60]. Conversely, *in vitro* experiments suggest that each ubiquitin is added sequentially to form polyubiquitin chains. Multiple rounds of the ubiquitination cascade described above seems the most likely mechanism for ubiquitin chain formation. Major conformational changes in the enzyme complex would be required to move along the ubiquitin chain. The three enzymes described above are not always sufficient for the formation of a polyubiquitin chain. For some E3 ligases an additional conjugation factor may be required, these extra factors are known as E4s.

UFD2, a protein found in yeast, was first identified as an E4[61]. Yeast UFD2 is implicated in cell survival under stress conditions and is essential for homoeostasis of unsaturated fatty acids. A mammalian E4 homologous to yeast UFD2 is required for the polyubiquitination of mammalian ataxin-3, ataxin-3 is responsible for spinocerebellar ataxia type 3, a neurodegenerative disorder[62], this highlights the importance of E4s, polyubiquitination and subsequent degradation of proteins. The yeast and human homologous E4s shared a U-box domain and it was initially considered that the U-box facilitated an interaction with the ubiquitin conjugated targets and that the U-box was essential for E4 activity.

E4s have since been identified that are not homologous to UFD2; CHIP is one such example, though it does still contain a U-box. CHIP is an E4 for parkin[63], interestingly CHIP has its own intrinsic E3 activity. Further E4s have been identified that are not homologous to UBD2 nor do they contain a U-box domain, one such example is p300, an E4 for MDM2. Unlike CHIP p300 does not have intrinsic E3 ligase activity but it is still able to target p53, monoubiquitinated by MDM2, for polyubiquitination[64].

The term E4 encompasses a wide range of enzymes, as of yet they do not appear to share a common feature, they do not share a common U-box domain, nor do they need to have their own E3 ligase activity. The mechanism of how they work alongside with their E3 to target proteins for polyubiquitination remains a mystery.

1.3 Ubiquitin binding proteins

Interaction of ubiquitin with the 26s proteasome is its most widely studied interaction, though this is only one of the many interacting partners of ubiquitin. Ubiquitin and ubiquitin chains can interact with a wide variety of proteins containing a ubiquitin binding domain (UBD). UBD is a general term for at least 16 very different domains that can interact with ubiquitin including Ubiquitin Interacting Motif (UIM), Ubiquitin Associated (UBA), and Zinc Finger Ubiquitin Binding domain (ZnF UBP). Different UBDs and/or different proteins containing UBDs can mediate distinct downstream cellular processes such as regulating the stability, function and localisation of the ubiquitin tagged proteins.

UBDs differ greatly in size, between 30-150 residues, but the majority of UBDs are α helical[65] and interact non covalently with one of two hydrophobic regions on the surface of ubiquitin[15]. Interaction with the hydrophobic patch including residues Leu 8, Ile 44 and Val 70 is linked to signalling for degradation. Interaction with the hydrophobic patch that includes Phe 4 and Ile44 is linked to non-proteolytic signalling[14]. UBDs do exist that do not centre on Ile 44 and the hydrophobic regions on the surface of ubiquitin[66] there is one such example in which the C-terminal di-glycine motif of ubiquitin is inserted into a deep binding pocket of ZnF UBP[67].

The majority of information for how each UBD distinguishes between different ubiquitin chain linkages is still unknown. Proteins containing repeats of the UIM can offer some insight. Two UIM motifs separated by different length spacers can recognise differently linked ubiquitin chains. For example, Rap80 contains two UIM's separated by a long spacer, these domain recognise ubiquitin molecules in an extended conformation, as often seen in K63 linked chains. Conversely ataxin-3 has repeats of UIM separated by a much shorter spacer, these recognise ubiquitin molecules in a more compact conformation, as often seen in K48 linked chains[68].

1.4 Deubiquitination enzymes

Ubiquitination of proteins is a reversible process; the removal of ubiquitin from a substrate is carried out by a group of enzymes known as deubiquitinating enzymes (DUBs). There are approximately 100 DUBs and these fall into 5 families based on their catalytic domain, there are four cys protease families and one metalloprotease family[69]. Some DUBs recognise specific chain linkages, others are non-specific and are able to recognise and cleave multiple chain linkages as well as mixed ubiquitin and UBL chains[70].

The removal of ubiquitin is very important for the regulation and function of a number of cellular processes. An important function of DUBs is to recycle ubiquitin. They associate with the 26s proteasome and remove ubiquitin from its substrate before it itself is unfolded and degraded[71]. Keeping levels of ubiquitin high is important for a rapid response to cell stresses and stimuli. DUBs are quite often seen in complex with E3s and they can affect the rate of ubiquitination of a substrate. E3s are prone to autoubiquitination in the absence of their target substrate; DUBs remove the ubiquitin saving the E3 from degradation so that they are able to respond to substrate increases. DUBs are also important for the intracellular localisation of proteins. The endocytic pathway depends on the tight regulation of ubiquitination and deubiquitination in order for vesicles to reach their target destination[72].

DUBs are also involved in cell death. Apoptotic cell death is mediated by intrinsic and external pathways that result in the activation of Cys-dependant Aspartyl-Specific Proteases (caspases), the main regulators of cell death. Several E3 ligases are known to have an important role in signalling for this apoptotic response. The interplay between ubiquitination and deubiquitination sets the threshold for apoptotic signalling. Deregulation of DUBs can disrupt apoptotic signalling resulting in diseases such as cancer and inflammatory disorders[69].

A20 is an example of a protein that has dual function as an E3 ligase and DUB. Its N-terminal domain is a DUB for K63 linked polyubiquitin mediators of the NF-κβ signalling pathway, such as TRAF6. Its C-terminal domain is a ubiquitin ligase for

K48 linked degradation of the same substrates. Interestingly A20 is not a general DUB, it does not recognise specific chains, e.g. K63 linked polyubiquitin chains, it instead has specificity for particular polyubiquitinated substrates, e.g. TRAF6 and removes the polyubiquitin chain without disassembling it. This limited DUB activity ensures the fidelity of A20 in regulating NF-κβ activation[73].

1.5 Functions of ubiquitination

1.5.1 Degradation

As previously described, chains of at least four ubiquitin molecules can target a protein for degradation by the 26s proteasome. Longer chains can increase the affinity of the protein for the proteasome, increasing the likelihood of successful degradation. In the majority of cases ubiquitin chains are linked by K48 or K11, though less abundant linkages K6, K27, K29 and K33 can also target proteins for degradation by the 26s proteasome.

Ubiquitin chains linked via K63 are regarded to signal for non-proteolytic events. Interestingly K63 and K48 linked chains bind to the 26s proteasome with similar affinity. Their structural differences account for how one linkage results in substrate degradation and the other does not. As outlined above K63 linked chains are in an open conformation, this open conformation increases the chains affinity for DUBs associated with the proteasome, and K63 linked chains are therefore disassembled quickly releasing the substrate before it reaches the proteasome. The decreased affinity that K48 has for the proteasome associated DUBs results in much slower chain disassembly increasing the likelihood of substrate unfolding[74].

There is the possibility that polyubiquitin chains may not always be sufficient for targeting the substrate to the proteasome. Some E3s can interact with the proteasome suggesting that they direct the substrate to the proteasome for efficient degradation[75]. While it is clear that some E3s can associate with the proteasome it is not clear whether association is necessary for substrate degradation. Studies in yeast have highlighted a role for polyubiquitin receptor proteins in the transport of

polyubiquitinated substrates to the proteasome[76]. The activity of these proteins associated with ubiquitin binding was facilitated by a variety of ubiquitin binding domains. For example UBA and UBL containing proteins RAD23 and Dsk1 respectively have been implicated as potential binding factors that can bind polyubiquitin chains and the proteasome[77,78]. A study has suggested that pathways operating downstream of polyubiquitination to target proteins to the proteasome exhibits substrate specificity and selection[78,79].

In addition to the well-studied role of ubiquitin in proteasomal degradation of proteins, ubiquitin has also been shown to be involved in lysozyme degradation and autophagy. K63 chains were thought to not signal for proteolytic events as proteins tagged with K63 linked chains were not targeted for degradation by the 26 proteasome. While they target proteins involved in the stress response, they may also signal for protein degradation, just not via the proteasome, K63 linked chains may play a role in targeting membrane proteins for degradation by the lysosome[80].

Aggregated proteins are harmful to the cell but are often too large to be removed by the proteasome, the process of autophagy is important for the removal of these aggregates. Autophagy receptors have been identified that can bind to ubiquitin, suggesting a role for the ubiquitination pathway in autophagy[81].

1.5.2 Signalling for degradation by ubiquitin

As described in detail above polyubiquitination is the main mechanism for protein degradation but what of the event prior to this, the event that signals for a protein to be degraded by the ubiquitination pathway. The ubiquitin proteasome system degrades a wide variety of proteins that contain specific degradation signals or degrons. Many types of degron signals exist, some better characterised then others, and some examples are outlined below.

The N-end rule pathway polyubiquitinates proteins that contain specific degrons called N-degrons. The main determent of an N-degron is a destabilising N-terminal residue of a substrate protein. The N-end rule states that the N-terminal amino acid of a protein determines its half life[82]. Recognition components of the N-end rule

pathway, called N-recognins, are specific E3 ligases that can target N-degrons[83]. Regulated degradation of specific proteins by the N-end rule pathway mediates a number of functions including sensing of oxygen, elimination of misfolded proteins, signalling by G proteins and regulation of DNA repair, neurogenesis and fat metabolism, to name a few.

The SFC family of E3 ligase contain an F-box domain. Degradation of most SFC substrates requires phosphorylation of specific Ser/Thr residues on the substrate, these short phosphorylated peptide motifs can bind to the F box, following binding to the F-box subsequent ubiquitination of the substrate can take place. The best characterised phosphodegrons are those involved in the elimination of cyclins and cyclin dependent kinase (CDK) inhibitors by the ubiquitin system. In the mammalian cell SCF complexes target phosphorylated forms of cyclin E and CDK inhibitor $p27^{KIP1}$[84,85]. The mechanisms by which phosphorylation drives substrate binding to SCF and subsequent ubiquitin conjugation are not fully understood.

Chaperone proteins have roles in the pathway of substrate recognition, ubiquitination and degradation. In many cases the exact roles of the chaperones are not defined. In the case of the E3 ligase CHIP it uses Hsp70 or Hsp90 as substrate recognition subunits, that bind to unstructured regions of aberrant proteins and position them for CHIP mediated ubiquitination[85]

The PEST sequence was identified in 1986 and is a peptide sequence rich in proline (P), glutamic acid (E), serine (S) and threonine (T). It is associated with proteins that have a short, less than 2 hours, half life[86]. Some PEST sequences appear to be constitutive proteolytic signals, others appear to be conditional signals and their mechanism of action varies[87].

1.5.3 Protein-protein interactions

When ubiquitin is bound to a protein it can affect that proteins interaction with its binding partners, it can facilitate protein: protein interactions a number of ways. Ubiquitin can induce a conformation change in the protein that it is bound to; this structural change can alter the interaction of binding partners. Ubiquitin is able to

provide, or extend, the interface between two binding partners; free ubiquitin chains can also provide an interface for two interacting proteins[88] (**figure 1.5**).

1.5.6 Cellular localisation

As discussed above ubiquitination of a substrate can affect the substrates interaction with its binding partners, a change in binding activity, either activating or inhibitory, can result in a change of localisation for the substrate. Ubiquitination can also affect localisation of a substrate by binding to and masking a signal important for localisation or, upon binding, mediate a conformation change resulting in the masking or unmasking of a localisation signal, e.g. nuclear export signal, or nucleolar localisation signal[89].

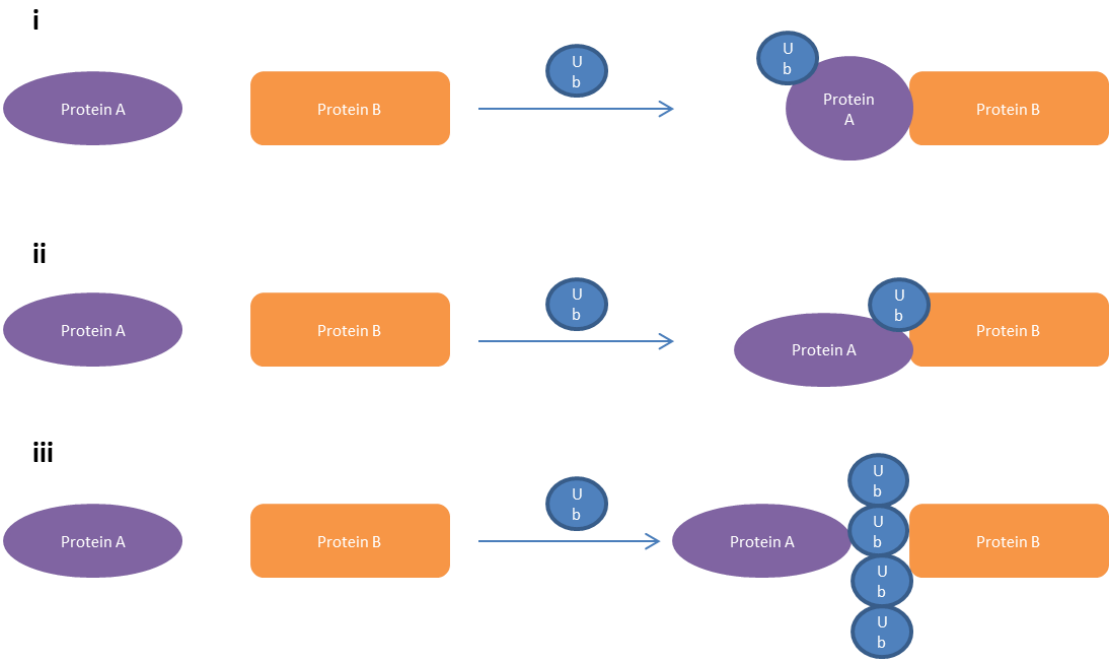

Figure 1.5: The role of ubiquitin on protein-protein interactions. Ubiquitination can result in the allosteric activation of the substrate, altering its binding to other proteins **(i)**. Ubiquitin can provide or extend a binding interface between two binding partners **(ii)**. Chains of ubiquitin can provide a binding interface between two proteins **(iii)**.

1.6 MDM2

1.6.1 Introduction

The Murine Double Minute 2 (*MDM2*) gene was first cloned as a gene amplified on double minute particles in a transformed murine cell line, hence its name[90]. At a similar time a protein identified as p90 co-purified with the tumour suppressor protein p53 in immunoprecipitation studies using cell extracts[91,92]. p90 was later identified as the *MDM2* gene product. Following this *MDM2* was studied as a gene amplified in many sarcomas[93]. MDM2 can act as a critical negative regulator of p53[94], at least in early development, as *MDM2* null mice were embryonic lethal but this could be rescued in mice that also had a p53 null background[95,96].

MDM2 is 491 amino acids in length and contains an N-terminal p53 binding domain, an acidic domain, a zinc finger and a C-terminal RING domain (**figure 1.6**). The RING domain of MDM2 has features that set it apart from other RING domains but its presence confirmed that MDM2 was an E3 ligase, in fact the RING of MDM2 is critical for its activity as an E3 ligase, and it specifically targets p53, among others, for degradation[97]. Not only does MDM2 target p53 for degradation by the 26S proteasome via its E3 ligase activity, it has also been shown to act on the translation of p53[98] and can chaperone p53[99].

A homologue of MDM2, known as MDM4 or MDMX, was identified more recently. Although the domains of MDM4 are homologous to those of MDM2, MDM4 is not able to substitute for MDM2 in early development and interestingly MDM4 does not display intrinsic E3 ligase activity towards p53[100,101]. MDM2 can associate with MDM4 to form a heterodimer, indeed it has been suggested that dimerisation of MDM2, as either a homodimer or as a heterodimer with MDM4, may be essential for the E3 ligase activity of MDM2[102].

Amplification of *MDM2* has been implicated in a wide variety of cancers, including 30 % of soft tissue sarcomas and 7 % of all solid tumours[103]. In addition to *MDM2* gene amplification, recent years have seen the identification of alternative and

aberrantly spliced forms of *MDM2* mRNA expressed in many tumour types, their expression is often associated with advanced levels of disease[104]. While it is true that gene amplification does lead to increased MDM2 protein levels and this is seen in various cancer, some tumours have been identified that contain elevated MDM2 protein without an increase in copy number. This implies that just looking at gene amplification will underestimate the number of tumours in which overexpression of the MDM2 protein contributes to cancer[105]. MDM2 is involved in a wide network of signalling pathways that rely on tight regulation for the normal function of the cell, overexpression of MDM2 protein could completely deregulate the normal signalling of these pathways. This will be discussed I further detail in following sections.

Despite being a popular research target, due to its dysregulation throughout many cancer types, there is still much that is not understood about the roles of MDM2 and also its mechanism of action in currently identified roles. Realistically our knowledge needs to improve to design effective therapeutics aimed at MDM2.

1.6.2 Structure

MDM2 is 491 amino acids in length. It contains an N-terminal p53 binding domain (aa 29-108), central acidic domain (aa 223-288), zinc finger (aa 289-331) and a C-terminal RING domain (aa 438-491). It also contains several localisation motifs, a nuclear localisation signal (starting at aa 178), nuclear exclusion signal (starting at aa 192) and a nucleolar localisation signal (aa 466, 478) (**figure 1.6)**. The sequence of MDM2 is conserved throughout eukaryotes; the three major domains of MDM2 are conserved in the most primitive of eukaryotes, the *Trichoplax adhaerans*[106].

Currently there is structural knowledge for only approximately 30 % of the MDM2 protein. Compared to the structural knowledge we have on other RING E3 ligases this is surprising, a possible reason for this lack of information could be that MDM2 contains large regions of intrinsic peptide disorder[107]. While there is no crystal structure for MDM2 in its entirety, there are crystal structures for the hydrophobic N-terminal p53 binding domain and the C-terminal zinc finger and RING domain. The structure and roles of the domains are discussed in further sections.

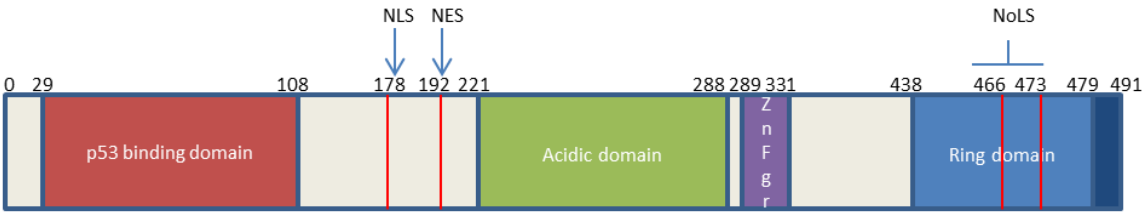

Figure 1.6: Schematic diagram of MDM2. This schematic shows the location of the domains and localisation sites within MDM2.

1.6.3 N-terminal domain

The N-terminal domain of MDM2 is 93 amino acids in length (residues 16-109) and was the first domain of MDM2 identified to bind to the tumour suppressor protein p53[108]. The N-terminal domain of MDM2 interacts with the activation domain (Box-1) in the N-terminal domain of p53[109] and hydrophobic residues of p53 are important for this interaction[110].

The N-terminal domain of p53 contains the Box-I motif, a domain defined using crystallographic studies. These crystal studies showed that the N-terminal domain of MDM2 contained a deep hydrophobic cleft in which the p53 Box-I peptide bound, in particular a triad of hydrophobic amino acids, Phe19, Trp23 and Leu26 insert deeply into this binding pocket. These amino acids are involved in the transactivation of p53[111], MDM2 binding to the N-terminal transactivation domain of p53 can therefore block p53-dependent transcription through steric mechanisms[112,113]. MDM2 competes with p300, a co-activating protein that binds to p53 for binding to the transactivating domain of p53[114]. Small molecules such as Nutlin compete with p53 for the hydrophobic binding pocket of MDM2 and release p53 from MDM2 mediated transrepression. Although Nutlin disrupts the high affinity interaction between the hydrophobic pocket and Box-I domain it is not an E3 ligase inhibitor, in fact an increase in p53 ubiquitination is seen when nutlin is added to cells. The E3 activity of MDM2 is enhanced because nutlin binding to the hydrophobic pocket increases the stability of a low affinity complex between of the acidic domain of MDM2 and the ubiquitination signal within p53[115,116], leading to ubiquitination. This allostery between domains will be discussed in further detail in following sections.

The N-terminal domain of MDM2 is flexible and can adopt different conformations depending on the length of the peptide bound to the hydrophobic pocket[117]. The differing conformations of MDM2 could be important for its diverse functions and should be an important consideration for the designing of anticancer drugs targeting the MDM2 protein.

In addition to residues 25-109 that form the p53 binding domain, the adjacent residues 12-24 form a pseudo substrate motif or ‘lid’ that can regulate the conformation of the

hydrophobic pocket. This 'lid' is strictly conserved across mammals[118]. The identification of the lid is not the first instance in which a lid or flap adjacent to an active site has been discovered[119]. The phosphorylation state of a serine at position 17 of the lid could be important for the interaction of MDM2 with different ligands. A phosphomimetic mutation, S17D, in the pseudo substrate motif directly affects the N-terminal MDM2 domain conformation, it opens the hydrophobic pocket and stabilises the full length MDM2-p53 complex[120]. The phosphorylation state of the lid and nature of the ligand bound are clearly important for the conformation of the N-terminal domain of MDM2, conformation could greatly increase downstream functions, and this is a very important point to consider when designing therapeutics targeted at MDM2.

1.6.4 Acidic domain

Adjacent to the N-terminal domain of MDM2 is a central domain rich in acidic amino acids and therefore known as the acidic domain (residues 221-228); the acidic domain is intrinsically disordered with no known structure.

The acidic domain of MDM2 binds to p14/19ARF. ARF is activated by inappropriate proliferative signals induced by oncoproteins such as Ras[121] and Myc[122]. ARF protein is nucleolar and by binding to MDM2 sequesters it in the nucleoli, inhibiting MDM2 nuclear export. p53 levels are therefore stabilised in the nucleoplasm where it can activate a p53-dependent stress response. Loss of ARF results in a predisposition to tumours in mice and an activation of ARF is commonly seen in tumour cell lines that retain wt p53[123].

MDM2 mutants in which the N-terminal domain was truncated still had E3 ligase activity towards p53; this suggested a secondary binding site between MDM2 and p53. Deletion of the acidic domain of MDM2 significantly reduced E3 activity suggesting that the secondary binding site lay within the acidic domain. Binding assays confirmed that the acidic domain of MDM2 could bind to p53[124]. NMR spectroscopy showed shifts within the Box-V domain of p53 upon MDM2 binding[116] and the acidic domain was subsequently shown to bind to the consensus sequence SxxLxGxxxF within the Box-V domain of p53[109].

As previously mentioned ligand binding to the hydrophobic pocket of MDM2 increased the stability of binding between the acidic domain of MDM2 and the Box-V domain of p53. The domains of MDM2 do not act independently of one another and the interaction between the hydrophobic pocket and acidic domain of MDM2, in the degradation of p53 is an excellent example of the allosteric control of MDM2 activity. There is an intrinsic conformational restraint to ubiquitination of the native p53 tetramer; this restraint is released when the binding of the N-terminal domain of MDM2 to the Box-1 domain of p53 alters the structure of the tetramer. This exposes the ubiquitination signal within p53, the Box-V domain, the acidic domain is then able to bind, in a stable manner, resulting in the ubiquitination and subsequent degradation of p53[116].

1.6.5 Zinc finger

The central region of MDM2 is very unstructured apart from the following motif: X_4-W-X-C-X_{2-4}-C-X_3-N-X_6-C-X_2-C-X_5 (where x is any amino acid). This matches the consensus sequence for RanBP2/NZF C_4 zinc fingers. C_4 zinc fingers are ubiquitous and multi-functional domains found in isolation or in tandem in a wide variety of proteins[125,126]. Little is known about the role(s) of the C_4 zinc finger of MDM2. The solution structure of the C_4 zinc finger of MDM2 identified a structure similar to that of the zinc ribbon structural motif. Zinc ribbon domains are found in proteins involved in transcription, translation, DNA replication and signal transduction where they mediate a variety of protein-protein, protein-DNA and protein-RNA interactions. The C_4 zinc finger of MDM2 shares sequence similarity with the zinc ribbon family including the highly conserved Trp and Asn residues[126].

Cancer types including follicular non-Hodgkin's lymphoma, leukaemia, hepatocellular carcinoma and osteosarcoma exhibited large quantities of MDM2 mRNA in the absence of MDM2 gene amplification. Instead they carried mis-sense, non-sense and frame shift mutations in the zinc finger of MDM2. The mis-sense mutations were found in tumour cells that contained a significant accumulation of MDM2 and a lack of nuclear p53[127]. Following nucleolar stress ribosomal proteins L5, L11 and L23 bind to MDM2 blocking MDM2-mediated p53 degradation. Mis-

sense mutations in the zinc finger domain disrupt the interaction of MDM2 with ribosomal proteins L5 and L11. Unlike wt MDM2 whose p53 suppressive activity can be inhibited by L11, the mis-sense mutants escape inhibition by L11, increasing MDM2 levels and decreasing levels of p53[128].

1.6.6 RING domain

MDM2 contains a C-terminal RING domain , a fact that took a while to confirm due to the unique nature of the MDM2 RING when compared to the RING domain of other E3 ligases. RING domains coordinate two metal ions and the coordination sites are either $Cys_3His_2Cys_3$, $Cys_3HisCys_4$ or Cys_4His_4, the spacing between the 4th and 5th coordination sites is also highly conserved. MDM2 can bind two zinc ions, but shares no direct sequence homology with other RINGS and the spacing between the 4th and 5th coordinating residue is not conserved. This led to the general consensus that MDM2 did contain a RING domain but there was some dispute over its zinc coordinating residues[129]. It was not until the solution structure of the MDM2 RING was solved that the true zinc coordinating residues were identified. MDM2 has a unique, among known RING domains, $Cys_2His_2Cys_4$ metal coordinating site in which two molecules of zinc are coordinated in a 'cross brace' configuration[130].

Before the identification of the RING domain MDM2 had been identified as an E3 ligase towards p53 and itself[131]. The C-terminal RING domain is essential for this activity[132], what is more the 12 amino acid 'tail' of MDM2 is required for E3 activity[133]. Mutating the zinc coordinating residues diminished E3 ligase activity of MDM2 suggesting that the tertiary structure of the RING is important for E3 function.

As well as the crucial role of the RING in the E3 ligase activity of MDM2, the RING has other functions. The RING binds to RNA[134], with residues 425-491 being both necessary and sufficient for binding RNA and binding is not zinc-dependant[129].
The RING domain contains a cryptic nucleolar localisation signal (aa 466-473), this sequence is exposed as a consequence of binding between MDM2 and p14/19ARF, which is essential for MDM2 nucleolar localisation[135]. The RING domain also contains a conserved Walker A or P loop motif, a motif that is a common feature of ATP/GTP binding proteins. The consensus sequence of the P loop is

GXXXXGK(T/S) (where X is any amino acid); in MDM2 the sequence is GCIVHGKT. This sequence is present in all MDM2 homologues including MDM4. In the MDM2 RING the motif resides between the 4th and 5th zinc coordinating residues. Among all known E3 ligases MDM2 is unique in possessing this motif. ATP binding is not required for E3 ligase activity. P loop mutants are impaired in p14^{ARF} independent nucleolar localisation, this is consistent with the fact that ATP bound MDM2 is preferentially localised to the nucleolus[136].

Although there is no structure of MDM2 in its entirety the solution structure for the RING of MDM2 has been solved. In this structure MDM2 is found in a homodimer, though it could also form a stable complex with MDM4. Each subunit of the homodimer folds into a compact globular domain with a short three stranded anti-parallel β sheet, a three turn α helix and several extended loops which are primarily involved in zinc coordination. The subunit structure is stabilised by the two zinc binding sites. Each subunit has a small hydrophobic core, the zinc binding sites are located at each end of this core, clamping the subunit together (**figure 1.7**)[130]. The solution structure showed that MDM2 could dimerise as either a homodimer or heterodimer, dimerisation of MDM2 will be discussed shortly but the RING domain of MDM2 is the region of MDM2 thought to be critical for this dimerisation. There also exists a crystal structure of the MDM2 RING[137] in a heterodimer with the MDM4 RING, as with the solution structure this crystal structure shows MDM2 in dimeric form.

As previously mentioned the domains of MDM2 do not function in isolation but are allosterically linked to one another. A gain in the ability of MDM2 to transrepress p53 dependant transcription was seen when zinc coordinating residues within the RING were mutated. This indicates that there is cross talk between the C-terminal RING and N-terminal p53 binding domains[138].

The N-terminal hydrophobic pocket is highly flexible and mutants in the RING allosterically modulated not only the affinity of the pocket but also its specificity. This suggests that binding of interacting proteins to the RING in cells is likely to act on MDM2 transrepression activity, and is worth considering when investigating the effacy of drugs that target their hydrophobic pocket in tumour cells[138].

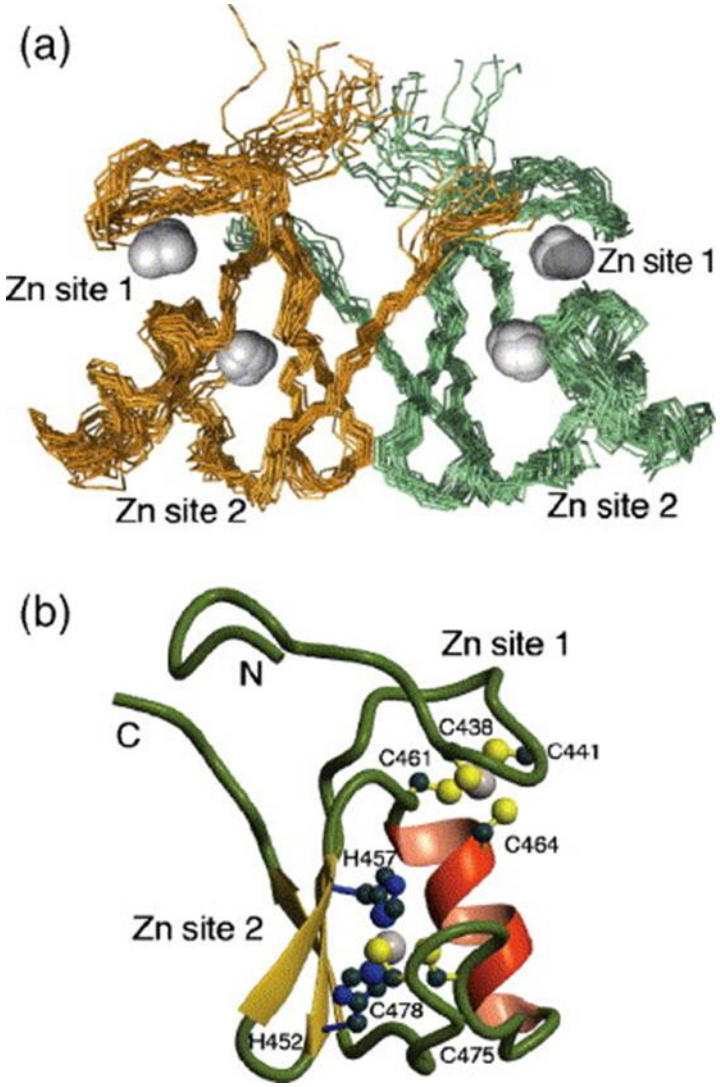

Figure 1.7: Solution structure of MDM2 RING (429-491) domain. a) Superposition of the 20 lowest energy structures of the MDM2 (429-491) homodimer, with the two subunits shown in yellow and green. Zinc ions are shown as grey spheres. **b)** Ribbon representation of the lowest energy structure of a single subunit of MDM2 (429-491) showing secondary structures and the localisation of two zinc binding sites. The side chains contacting the zinc ligand are shown as balls and coloured black (C), blue (N) and yellow (S)[130].

1.6.7 Dimerisation of MDM2

MDM2 can form homodimers[130,139] or heterodimers with its homologue MDM4[140], heterodimers appear to be preferential[139], forming a more stable complex[130].

The solution structure of the MDM2 RING homodimer shows that the residues involved in the interface primarily include Val451, Lys453, Thr455, Gly456, Leu458, Met459, Val486, Leu487, Thr488, Tyr489, Phe490, Pro491[130]. Six of these residues lie in the 12 amino acid tail of MDM2, the necessity of the tail in the dimerisation of MDM2 has been implicated[141].

Many RING/U box domains are found in a dimeric form, such as the heterodimer BRCA1/BARD[142], the homodimer CHIP[143] and the U box homodimer Prp19[144]. The formation of the dimer for these E3 ligases is important for their activity. The structures of these dimeric RING domains have been well characterised. When the homodimer of MDM2, from the solution structure, was compared with these characterised dimeric RING domains the relative positioning of the subunits was similar, however the two MDM2 subunits are at a different angle with respect to each other compared to the other structures, the other structures are symmetrical, this can be seen in **figure 1.8**[130].

For some other RING containing E3 ligases dimerisation is not required for their activity. Whether or not MDM2 is required to form a dimer for E3 ligase activity remains controversial. Some studies report that E3 ligase activity of MDM2 towards p53 is seen regardless of whether MDM2 is present as a monomer or dimer[141], others report that MDM2 must be a dimer to be active[102].

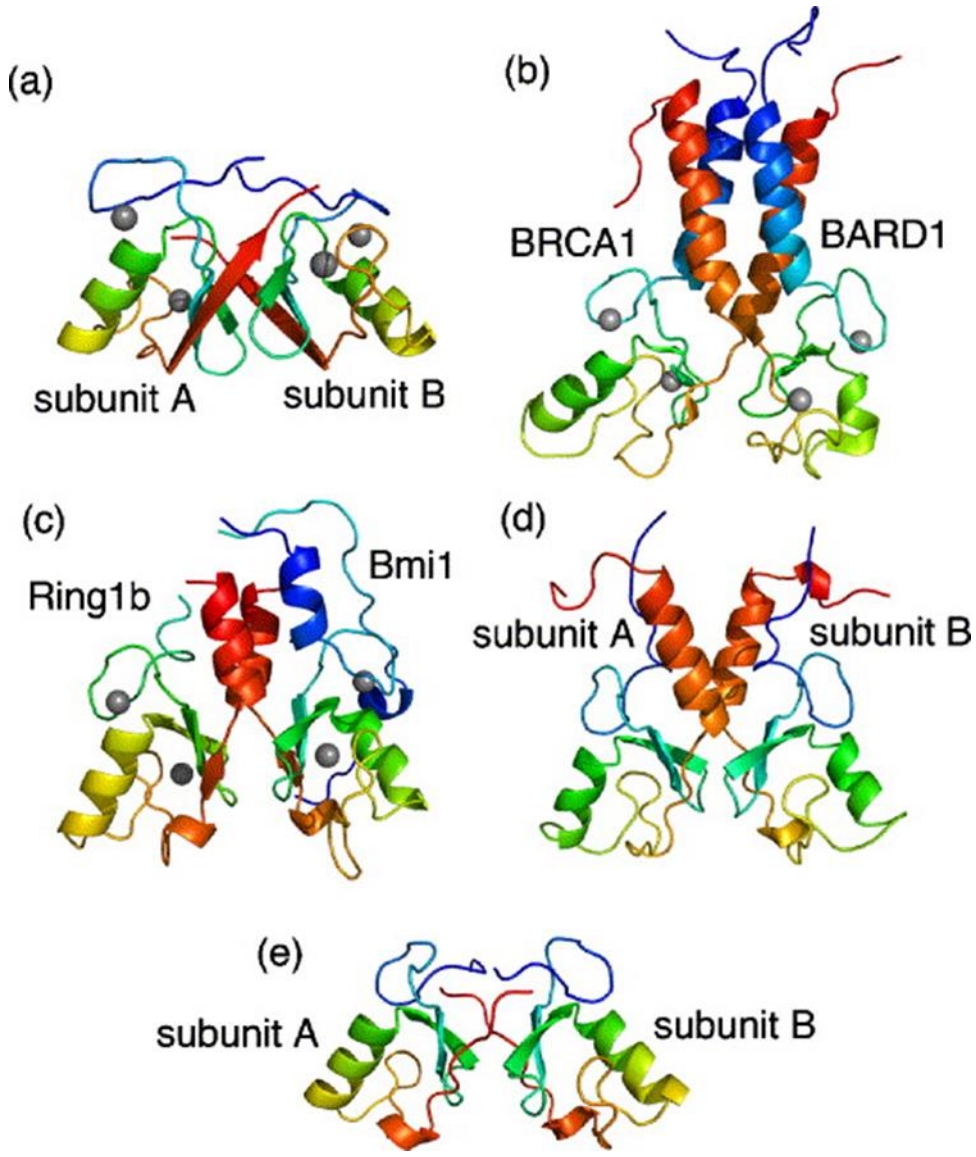

Figure 1.8: Comparison of MDM2 dimer organisation with other RING/U-box dimers. a) MDM2 (429-491) RING domain homodimer. **b)** BRCA1/BARD1 heterodimer. **c)** Ring1b/Bmi1 heterodimer. **d)** Zebra fish CHIP U-box homodimer. **e)** Prp19 U-box homodimer. Both subunit chains in all structures are coloured in a rainbow scheme, from blue at the N-terminus to red at the C-terminus[130].

If MDM2 was required to be a dimer for E3 activity it is unclear whether it would be as a homodimer, heterodimer or even both. BRCA1/BARD is an example of an E3 ligase that is active as a heterodimer. BARD does not have E3 ligase activity but stabilises and enhances the E3 activity of BRCA1[145]. It might be that MDM2 and MDM4 cooperate in a manner similar to this, or it might be that their dimerisation is related to other functions, such as each others cellular localisation or cellular levels, this will be covered in later sections.

1.7 Roles of MDM2, p53 dependant

1.7.1 p53

p53 was identified in 1979, it was initially thought to be oncogenic as it collaborated with the oncogene Ras, not unlike the previously identified oncogene myc[146]. These studies had been done using p53 synthesised from tumour samples. p53 subsequently cloned from the mRNA of normal cells supressed cell transformation indicating that p53 acts a tumour supressor[147].

Human p53 is a transcription factor comprised of four domains, an N-terminal transactivation domain, a central DNA binding domain, a tetramerisation domain and a C-terminal basic domain[148]. Tetramerisation is required for the tumour suppressor activity of p53[149] (**figure 1.9**) and mutations within the tetramerisation domain have been associated with cancer[150,151].

1.7.2 p53 pathway

The p53 pathway is composed of a network of genes and their products, that are targeted to respond to a number of stress signals, that impact upon mechanisms such as DNA replication , chromosome segregation and cell division[152]. Both intrinsic and external stresses on the cell can act upon the p53 pathway. Signals that activate p53 protein include damage to the integrity of the DNA template, irradiation of the cell, gamma or UV, alkylation of bases or reaction with oxidative free radicals. Different repair mechanisms are employed by the cell, depending on the type of damage[153].

Differing types of DNA damage activate different enzyme activities that modify p53 differently i.e. ubiquitination, phosphorylation, sumoylation, acetylation and methylation[154]. For example gamma radiation activates ATM kinase that can phosphorylate p53 and p53 is phosphorylated and acetylated in response to hypoxia, spindle poisons and inflammation of tissues[152].

Figure 1.9: Crystal structure of the p53 tetramerisation domain. The tetramerisation domain of p53 is revealed here by X-ray crystallography. The four helical domains of each subunit, each show in a different colour, are assembled into two pairs and the pairs assembled at right angles to one another[155].

The modifications of p53 alter its activity in two ways, firstly the half-life of the protein increases, resulting in an increased concentration of p53 in the cell. Secondly the ability of p53 to bind to specific DNA sequences, termed the p53 response element, and promote the transcription of genes regulated by these sequences is enhanced[156]. Once the p53 protein has been activated it initiates a transcriptional program that reflects the nature of the stress signal. The genes in this network initiate one of three responses, resulting in cell cycle arrest, cellular senescence or apoptosis.

An example of a p53 activated gene is p21, the p21 gene product plays a major role in cell cycle arrest, p21 inhibits cyclin E-cdk2. In the proliferating cell this cyclin dependant kinase acts upon Rb protein to depress E2F1 activity, this promotes the transcription of genes involved in preparing a cell to progress from the G to S phase of the cell cycle. Stress signals halt this proliferation pathway is a p53-dependant manner[156].

p53 dependant pathways leading to cellular senescence are less well characterised than pathways involved in cell cycle arrest and apoptosis. Introduction of the Ras oncogene into primary cell culture mediates a p53 dependent senescence. Activation of p53 by a number of oncogenes, including E2F1[157], myc[122] and Ras[121], is mediated in part by a positive feedback loop that results in transcription of $p14/19^{ARF}$. This in turn inhibits MDM2, resulting in increased p53 levels in the cell.

p53 dependant apoptosis is widely studied. Several p53 dependant genes (including bax and puma) enhance the secretion of cytochrome c into the cytoplasm from the mitochondria, this interacts with APAF-1 (another p53 regulated protein) initiating a protease cascade that leads to activation of caspases followed by apoptosis. This pathway is known as the intrinsic apoptotic pathway and is activated by a number of stress signals. p53 also regulates a series of genes that initiate the extrinsic apoptotic pathway e.g. fas ligand, resulting again in the activation of caspases and apoptosis[156].

In addition to activating genes involved in cell cycle arrest, cellular senescence or apoptosis p53 also regulates genes that produce secreted proteins such as maspin and thrombospondin. These secreted proteins are employed to communicate signals to surrounding cells, informing them of stress response[158].

p53 is a highly popular research target as it is the gene found to be most frequently mutated in human cancer cell genomes examined to date, being present in mutant forms in approximately 50 % of all human tumours. Point mutated alleles of p53, almost always leading to amino acid substitution, represent the greatest majority of mutant p53 alleles found in human tumours, the vast majority of p53 mutations affect the DNA binding domain of p53[159], supporting the concept that gene regulation is the most important function of p53.

p53 clearly activates and interacts with many genes and gene products involved in cell cycle regulation, outlined above is just a very small example. The regulation and control of p53 in proliferating cells and in response to stress must be tightly controlled or disease, such as cancer can develop. As a result it is not only p53 that is a popular research target, downstream targets of p53 and its regulators are also possible therapeutic targets. MDM2 is one of the p53 regulators that has received much attention as a therapeutic target.

1.7.3 Inhibition of p53 induced gene expression

MDM2 interacts with the activation domain of p53, the region of p53 that is important for p53 transcriptional activity[110]. p300 is a coactivating protein that binds to p53 enhancing the expression of its downstream target genes, MDM2 competes with p300 for the transactivation domain of p53[114]. As outlined previously the N -terminal hydrophobic domain of MDM2 binds to the N-terminal transactivation domain of p53 and blocks p53 dependant transcription, interestingly the MDM2 RING domain is completely dispensable for MDM2 to act as a direct transrepessor of p53[113].

It is possible that MDM2 inhibits p53 induced gene expression via a dual mechanism. It has been shown that the adenovirus E1B contains an inhibitory domain that is targeted to the p53 promoter by interacting with p53. Once at the promoter E1B inhibits expression of p53 induced genes, by inhibiting additional activators or repressing the activity of the basal transcriptional machinery[160]. MDM2 may directly block p53 dependant transcription and also inhibit the ability of general transcription factors to potentiate mRNA synthesis[112], as with E1B. To support a dual mechanism hypothesis a similar mechanism has been proposed, in which Rb protein inhibits E2F

dependant transcription by both masking the activator of E2F and inhibiting transcription machinery[161].

1.7.4 Translation of p53

A study showed that MDM2 could induce translation of p53 and that this translation induction required MDM2 to interact with the nascent polypeptide of p53[98]. This information combined alongside the fact that MDM2 interacts with L5/5S ribosomal complex[128] and RNA[134] produced a model in which MDM2 is recruited to active polyribosomes by nascent p53 N-termini, resulting in *cis* regulation of p53 mRNA translation[98]. MDM2 induces translation of the p53 mRNA from two alternative sites. This produces full length p53 and another protein with a relative molecular mass of 47kDa, this protein is known as p53/47. MDM2 effects translation of p53 and p53/47 by directly interacting with p53 protein. p53/47 lacks an N-terminal MDM2 binding domain and as such is not degraded by MDM2. It does however have a fully functional tetramerisation domain and can oligomerise with full length p53. MDM2 can change the ratio of p53 and p53/47 by inducing translation of both then preferentially targeting p53 for degradation[98].

The N-terminus of p53 has two independent transcription activation domains[162]. p53/47 lacks the first (TAI) but contains the second (TAII). The different activation domains induce the expression of different downstream targets. TAI transactivates $p21^{WAF1}$ and TAII transactivates MDM2, Bax and GADD45. A change in the ratio of p53/47 and p53 will alter the ratio of these downstream targets,

The proportion of p53/47 to p53 has implications for the cells biological response to p53 activation. In one mouse model overexpression of p53/47 leads to p53 dependant cellular senescence and premature aging[163]. This model indicates that p53/47 may be a factor in directing the p53 dependant cell stress response (repair, senescence or apoptosis) and the synthesis of p53 and p53.47 have been shown to be regulated through distinct stress induced pathways, which help orchestrate the cellular outcome in response to stress[164]. It should be noted that there are many more p53 isoforms, above is one example.

There is currently not a large amount of information on p53/47. Further study is needed to ascertain its role in p53 activation, degradation and the cell response to different stresses.

1.7.5 Chaperone for p53

Molecular chaperones are defined as a vast class of structurally unrelated proteins that assist in correct non-covalent assembly of other polypeptide containing structures. They are not components of the assembled structure when they perform their biological functions[99]. Several studies show that MDM2 possesses similar activities as described for molecular chaperones[165] including binding to a nascent polypeptide chain[98], modulation of transcription factors[166], protection and activation of DNA polymerases[167] and involvement in ribosome assembly[168].

Hsp90 is a molecular chaperone that in an ATP-dependant reaction folds p53. MDM2 can work synergistically with Hsp90 enhancing the binding of p53 to promoter derived sequences[99]. Interestingly MDM2 alone could substitute for Hsp90 and, in an ATP-dependant reaction, promote the binding of p53 to the p21 promoter sequence. MDM2 protein possesses a nucleotide binding motif, mediated by the consensus P Walker motif, within its RING domain, this ATP binding site is not required for E3 ligase activity[136]. This study provided the first direct role for the ATP binding domain of MDM2.

MDM2 localises with latent p53 on the chromatin near $p21^{WAF1}$ and MDM2 genes before but not after DNA damage[169]. This chaperone study suggests that the transient complex of p53 with chaperones such a MDM2 may be important for the decision of whether to activate or degrade p53 by employing a series of post translational modifications such as ubiquitination, sumoylation, acetylation, methylation etc.

1.7.6 E3 ligase activity

As previously discussed MDM2 is an E3 ligase for p53. There are many questions concerning the mechanism of the E3 ubiquitin ligase activity of MDM2. The general mechanism for how all RING domain containing proteins facilitate the transfer of

ubiquitin from their partner E3 to the target substrate remains unknown. There are more unknowns specifically related to MDM2, it is currently unclear whether MDM2 must dimerise to be active as an E3[102,141], furthermore if MDM2 is required to dimerise for E3 activity it remains unclear whether it would form homodimers[139] or heterodimers[140] with its homologue MDM4. The MDM2 RING possesses a 12 amino acid 'free' tail, unlike other RINGS, and this tail is essential for E3 ligase activity[133] yet the reason(s) why remains unknown, it has been implicated in dimer formation[141] or it may be involved in the allosteric activation of it E2[35]. There is also a question as to whether MDM2 would polyubiquitinate p53, it has been suggested that MDM2 works alongside an E4, in this case p300[64], in order to polyubiquitinate p53 and target it for degradation, as by itself it has been suggested that MDM2 is a monoubiquitin ligase[170].

MDM2 regulates the degradation of p53 in normal unperturbed cells, recognising p53 as a target that should be ubiquitinated shortly after synthesis and therefore targeted for degradation. In some circumstances, specifically when cells are suffering certain types of stress or damage, p53 must be protected from MDM2 facilitated degradation so that it can accumulate to functionally significant levels in the cell.

Levels of p53 are controlled by feedback loops. Ten feedback loops have been identified in the p53 pathway. Of these seven are negative feedback loops, these down regulate p53 activity, and three are positive feedback loops, these up regulate p53 activity. All of these loops are auto regulatory in that that they are either induced by p53 activity at the transcriptional level, transcriptionally repressed by p53 or are regulated by p53 induced proteins. Six of these feedback loops act through MDM2 to mediate p53 activity[156].

1.7.7 Positive feedback loops

In response to DNA damage kinases such as ATM, Chk1 and Chk2 phosphorylate the N-terminus of p53 which prevents its association with MDM2. At the same time ATM can phosphorylate MDM2 resulting in its functional inactivation, this allows p53 to accumulate and activate a series off downstream positive feedback loops.

1.7.7.1 PTEN pathway

The P13 kinase (P13K) phosphorylates phosphatidylinositol (4,5)-bisphosphate ($PIP_{2)}$, phosphatidylinositol (3,4,5)-triphosphate ($PIP_{3)}$ can then activate Akt/PKB kinase which phosphorylates MDM2, this results in the translocation of MDM2 from the cytoplasm to the nucleus where it is able to act on p53. p53 protein induces transcription of PTEN genes, the PTEN protein is a phosphatase that dephosphorylates PIP_3 to PIP_2, this results in the inactivation of the Akt/PKB pathway and the up regulation of p53[156] (**figure 1.10**).

1.7.7.2 Retinoblastoma pathway

Retinoblastoma (Rb) protein is multiply phosphorylated by the cyclin dependant kinase Cyclin E-cdk2, this hyperphosphorylation state releases a group of transcription factors known as E2Fs allowing them to stimulate transcription of target genes, the target genes of E2Fs are involved in cell cycle progression. When p53 is activated it stimulates the synthesis of the p21 protein, this inhibits Cyclin E-cdk2 activity, Rb is able to bind E2F preventing it from facilitating transcription of its target genes. Hypophosphorylated Rb also forms complexes with MDM2 and p53, the outcome of which is high p53 activity and enhanced apoptotic activity[161,171] (**figure 1.10**).

1.7.7.3 p14/19ARF pathway

The p14/19ARF protein binds to MDM2 localising is to the nucleolus where it is unable to act on p53[123]. The transcription of the p19/14 ARF gene is positively regulated by ESF1[172] and β-catenin[173], in addition levels are increased by Ras[121] and myc[122] signalling. Interestingly p14/19 ARF activity is negatively regulated by p53 itself[156] (**figure 1.10**).

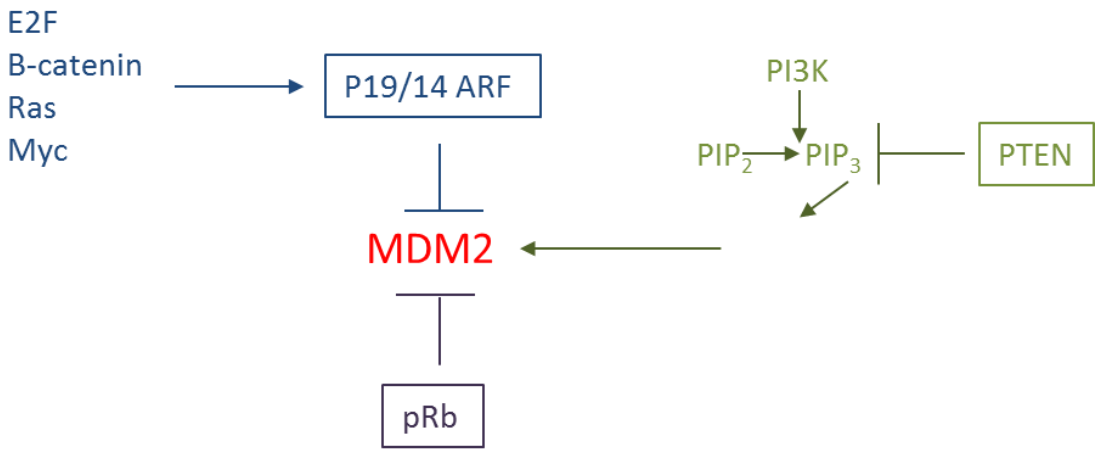

Figure 1.10: Diagram showing the involvement of MDM2 in the p53 positive feedback loops. MDM2 is inhibited by P19/14ARF. PTEN inhibits factors that activate MDM2. MDM2 is inhibited by pRb.

1.7.8 Negative feedback loops

1.7.8.1 Siah-1 pathway

The Siah-1 gene contains a p53 response element and p53 protein positively regulates the transcription of the RING domain containing ubiquitin ligase Siah-1[174]. Siah-1 interacts sequentially with siah interacting protein (SIP), Skp1 and EBI. EBI binds directly to β-catenin and initiates subsequent proteasome mediated degradation[175]. β-catenin levels regulate the p14/19 ARF gene[173], subsequently the protein sequesters MDM2 in the nucleolus allowing p53 levels to accumulate in the cell. Siah-1 down regulates this positive feedback loop, decreasing levels of p53 (**figure 1.11**).

1.7.8.2 Cyclin G pathway

Cyclin G is one of the most active of the p53 responsive genes; it is rapidly transcribed to high levels after p53 activation in a wide range of cell types[176-178]. Cyclin G protein forms a complex with PP2A phosphatase, this removes a phosphate residue from MDM2[179], this phosphate residue would have been previously added to MDM2 by Cyclin A-cdk2. Phosphorylation of MDM2 by Cyclin A-cdk2 inhibits its activity thus the Cyclin G PP2A phosphatase enhances MDM2 activity and inhibits p53[156]. Cyclin G null mouse fibroblasts have elevated p53 levels in an absence of stress[179], this indicates that this negative feedback loop acts upon basal levels of p53 in cells and not only on higher p53 levels induced after stress[156] (**figure 1.11**).

1.7.8.3 MDM2 feedback loop

MDM2 is a very important downstream target of p53; p53 induces the transcription of MDM2, an agent of its own destruction. This creates a negative feedback loop[156] that functions to ensure that p53 molecules are degraded soon after their synthesis, keeping very low steady state levels of p53 proteins in normal unperturbed cells. In human cancer cells that carry mutant p53 alleles the p53 protein is invariably present in high concentrations, in contrast to normal cells. This initially appears paradoxical since high levels of a tumour suppressor, such as p53, would seem incompatible with

malignant cell proliferation. This paradox is resolved by the fact that the great majority of mutations affecting the p53 gene cause the protein to lose its transcription activating activity. Consequently p53 is unable to induce MDM2 transcription and thus MDM2 synthesis. In the absence of MDM2 p53 escapes degradation and the result is an accumulation of high levels of inert p53[180] (**figure 1.11**).

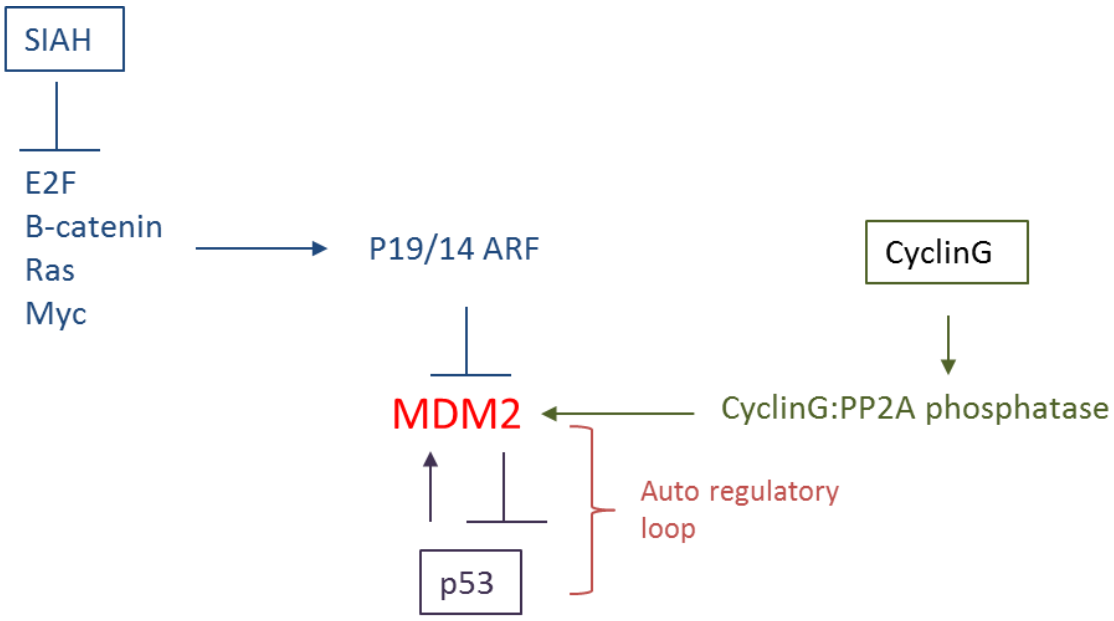

Figure 1.11: Diagram showing the involvement of MDM2 in the p53 negative feedback loops. SIAH inhibits factors that inhibit MDM2. Cyclin G activates MDM2. p53 activates MDM2.

1.8 Roles of MDM2, p53 independent

Although M2DM2 is an important regulator of p53 there is evidence that MDM2 has p53-independent functions, such as roles in DNA repair, transcription and ribosome biosynthesis. Evidence for p53 independent roles include the fact that MDM2 overexpression in tumours accompanied by mutant p53 or a lack of p53 is observed in a wide range of cancers and is associated with poor prognosis[181].

1.8.1 MDM4

MDM4, also known as MDMX, HDMX and HDM4, was identified in 1996. A protein 490 amino acids in length, it has high structural homology to MDM2. The highest level of sequence homology between the two proteins is in the N-terminal domain, in addition the zinc binding domain and C-terminal RING domain show high conservation too. Homology between the proteins is very low in the central acidic reigon[100,101].

Similarities between MDM2 and MDM4 include the ability of MDM4 to bind to p53 and block transactivation of a p53-responsive reporter genes[182]. In contrast MDM4 has no E3 ligase activity and cannot degrade p53, it is also unable to facilitate nuclear export. MDM4 is not induced in response to DNA damage and so, unlike MDM2, is unlikely to play a significant role in regulating p53 function in response to genotoxic stress[183].

When MDM2 knockout mice were created they were embryonic lethal[95], this indicates that MDM4 cannot compensate for MDM2 in early development. Interestingly the MDM4 knockout is also embryonic lethal thus neither homologue can compensate for each other, both MDM2 and MDM4 are essential regulators of p53 in early development[184].

Not long after the discovery of MDM4, MDM2 and MDM4 were found to form heterodimers, an interaction that is facilitated by their RING finger domains. Coexpression of MDM4 inhibited degradation of MDM2, suggesting a role for

MDM4 as a regulator of MDM2 levels[140]. This is true, they are actually dependant on each other for their function. When there is no MDM4 present in the cell, MDM2 is ineffective at down regulating p53 due to a very short half-life[184], association with MDM4 leads to an increase in steady state levels of MDM2[185]. MDM4 is cytoplasmic and requires MDM2 to locate to the nucleus where it can inactivate p53 by blocking its transactivation[184]. MDM4 is targeted for degradation by MDM2[186], DNA damage activates ATM which phosphorylates MDM4 at S403, this results in MDM2 targeting MDM4 for degradation, allowing a build-up of p53[145].

MDM4 has been shown to have a role in certain cancers; it has been described as an oncogene that becomes activated upon its overexpression. Screening showed that MDM4 was overexpressed in a wide variety of human tumours and amplified in 5 % of breast tumours screened, all which retained wt p53. In combination with oncogenic Ras, MDM4 overexpression contributes to cell immortalisation and neoplastic transformation[187]. As overexpression of MDM4 contributes to cancer it is a potential target for cancer therapy. Currently interest lies in developing small molecule inhibitors of the MDM4-p53 interaction[188].

1.8.2 DNA repair

Five primary human DNA repair pathways regulate the fidelity of duplex DNA and are able to counteract specific subsets of lesions that can potentially alter genomic integrity. An accumulation of DNA damage and/or the inability to repair damage directs human cells towards a tumorigenic phenotype[189]. The involvement of MDM2 in DNA repair is starting to be investigated.

Base exclusion repair (BER) attempts to fix single strand breaks, altered bases, and abasic sites[190]. Ape1 is a key enzyme in the BER pathway, its importance is demonstrated by embryonic lethality and apoptosis in cells lacking this enzyme[191-193]. Ape1 was found to be polyubiquitinated in the human cancer cell line HCT116, and MDM2 led to the ubiquitination of Ape1. Monoubiquitination of Ape1 appears to lead to its exclusion from the nucleus which may be a proapoptotic mechanism for interactions with Bcl2 in mitochondria versus DNA repair[194]. Considering that Ape1

has a critical role in the BER pathway. MDM2 may play a pivotal role in this DNA repair mechanism.

Homologous recombination (HR) repairs DNA double strand breaks. Nbs1 is a protein cofactor of the MRN complex that is involved in HR[189]. MDM2 interacts with Nbs1 and colocalises with Nbs1 at sites of double strand DNA damage[195] Overexpression of MDM2 leads to an inhibition of Nbs1 directed repair of double strand breaks[196], this information supports the role of MDM2 in oncogenesis.

DNA mismatch repair (MMR) facilitates the removal of incorrect nucleotides on the opposite DNA strand. Proliferating cell nuclear antigen (PCNA) is a protein involved in MMR. MDM2 is in part regulated by PCNA[189], yet it has not been investigated in context of the MMR pathway, MDM2 may have the potential to play a role in this pathway.

Nucleotide excision repair (NER) promotes the repair of bulky, helix distorting lesions. The general mechanism of NER involves scanning and detection of DNA lesions, formation of a denaturation bubble, damaged strand incision, removal of the lesion containing oligonucleotide, gap filling and DNA ligation[197]. Small DNA lesions are recognised by the XPC complex[198] and DDB is a protein that forms a complex with other protein components to form a ubiquitin ligase complex that regulates XPC through polyubiquitination[199] Preliminary studies suggest that MDM2 may interact with XPC[200-202] and/or DDB[203,204] and play a role in the NER pathway.

Non homologous end joining (NHEJ) repairs breaks induced by ionizing radiation, oxidative free radicals, inhibition of topoisomerases and other mechanical stresses[205]. Once DNA repair factors have executed their enzymatic function they are no longer needed around duplex DNA. MDM2 has been shown to interact with NHEJ proteins such as Ku70[206], interaction between MDM2 and NHEJ proteins represents a potential avenue for exiting repair factors from repaired DNA.

MDM2 interacts with DNA polymerase ε, as shown by a yeast two hybrid screen, *in vitro* binding assay and *in vivo* immunoprecipitation[208]. The C-terminal domain of DNA polymerase ε, to which MDM2 binds and the N-terminus of MDM2, to which DNA polymerase ε binds, are essential for the stimulation of DNA polymerase ε activity by MDM2. Proposed roles of DNA polymerase ε include DNA repair, recombination, damage sensing and chromatin remodelling[207].

1.8.3 Ribosomal proteins

MDM2 has a nuclear localisation signal (NLS) and resides in the nucleus; this is where ribosomes are biosynthesised and assembled. The interaction of MDM2 with ribosomal proteins L5, L11 and L23[209-211] suggests that MDM2 may play a role in ribosome assembly, transport or synthesis[212].

1.8.4 NF-κβ

MDM2 has been shown to induce the p65 subunit of NF-κβ through effects on the p65 promoter[213]. NF-κβ has various roles including inhibition of apoptosis in response to chemotherapy in certain cells. MM2 overexpression in leukaemia bone marrow cells has been associated with elevated expression of p65 and *in vitro* resistance to doxorubicin[214]. Further studies are required to establish whether the induction of p65 by MDM2 is an important p53-independnat role of MDM2 in tumorigenesis.

1.8.5 MDM2 binding protein

MDM2 binding protein (MTBP) has been identified as a protein that interacts with MDM2, a 380 amino acid region at the C-terminus of MTBP is sufficient for interaction with the acidic domain of MDM2[215]. Overexpression of MTBP inhibits proliferation and also metastasis of several human cancer cell lines, regardless of p53 status, suggesting that MTBP has a role in the suppression of tumorigeneis[216]. While overexpression of MDM2 can inhibit MTBP induced cell proliferation arrest it is currently unknown whether MDM2 can inhibit MTP mediated metastasis suppression.

1.9 Thesis objectives

The main objectives of this PhD were:

1. To investigate the mechanism of MDM2 E3 ligase activity
2. To investigate the oligomeric nature of MDM2
3. To investigate the role of the C-terminal tail of MDM2

This was done by employing a range of biochemical assays, including protein binding ELISAs, to investigate the binding of MDM2 to other ubiquitination cascade components (**Chapter 3**).

Biophysical assays, such as HD exchange, were utilised to further investigate the mechanism of MDM2 and the allosteric affect it has on UbcH5α (**Chapter 4**). Biophysical assays were also used to study the oligomeric nature of MDM2 (**Chapter 6**).

Peptide phage display was used in a novel way to confirm biochemical and biophysical data regarding the allosteric activation of UbcH5α as well as providing new information in regards to the binding partners of UbcH5α (**Chapter 5**).

In this thesis I outline how I have investigated the objectives and provide new evidence for the mechanistic action of MDM2.

Chapter 2: MATERIALS AND METHODS

2.1 Plasmids, chemicals and reagents

pGEx6-MDM2-WT and pET15b-mod-CHIP were a kind gift from Alicja Zylicz; pGex6-MDM2ΔT and pET14b-UbcH5α were from Susanna Pettersson; pT7-7Hup53 was from Ted Hupp.

The general chemicals and reagents used in this thesis were from Sigma or Merck-BDH, unless otherwise indicated.

Peptides were used for a number of biochemical and biophysical assays, the full sequence of the peptides, alongside their names, are detailed in **table 2** below.

Peptides were purchased from Chiron Mimotopes and were synthesised with an N-terminal biotin tag and Ser-Gly-Ser-Gly spacer.

Peptide name	**Protein peptide is derived from**	**Sequence**
Peptide 1	MDM2 RING	Biotin-SGSGCVICQGRPKNGCIVHGKTGH
Peptide 2	MDM2 RING	Biotin-SGSGGRPKNGCIVHGKTGHLMACF
Peptide 3	MDM2 RING	Biotin-SGSGGCIVHGKTGHLMACFTCAKK
Peptide 4	MDM2 RING	Biotin-SGSGGKTGHLMACFTCAKKLKKRN
Peptide 5	MDM2 RING	Biotin-SGSGLMACFTCAKKLKKRNKPCPV
Peptide 6	MDM2 RING	Biotin-SGSGTCAKKLKKRNKPCPVCRQPI
Peptide 7	MDM2 RING	Biotin-SGSGLKKRNKPCPVCRQPIQMIVL
Peptide 8	MDM2 RING	Biotin-SGSGNKPCPVCRQPIQMIVLTYFP
Peptide 9	MDM2 RING	Biotin-SGSGQPIQMIVLTYFP
N472A	MDM2 RING	Biotin-SGSGAKPCPVCRQPIQMIVLTYFP

K473A	MDM2 RING	Biotin-SGSGNAPCPVCRQPIQMIVLTYFP
P474A	MDM2 RING	Biotin-SGSGNKACPVCRQPIQMIVLTYFP
C475A	MDM2 RING	Biotin-SGSGNKPAPVCRQPIQMIVLTYFP
P476A	MDM2 RING	Biotin-SGSGNKPCAVCRQPIQMIVLTYFP
V477A	MDM2 RING	Biotin-SGSGNKPCPACRQPIQMIVLTYFP
C478A	MDM2 RING	Biotin-SGSGNKPCPVARQPIQMIVLTYFP
R479A	MDM2 RING	Biotin-SGSGNKPCPVCAQPIQMIVLTYFP
Q480A	MDM2 RING	Biotin-SGSGNKPCPVCRAPIQMIVLTYFP
P481A	MDM2 RING	Biotin-SGSGNKPCPVCRQAIQMIVLTYFP
I482A	MDM2 RING	Biotin-SGSGNKPCPVCRQPAQMIVLTYFP
Q483A	MDM2 RING	Biotin-SGSGNKPCPVCRQPIAMIVLTYFP
M484A	MDM2 RING	Biotin-SGSGNKPCPVCRQPIQAIVLTYFP
I485A	MDM2 RING	Biotin-SGSGNKPCPVCRQPIQMAVLTYFP
V486A	MDM2 RING	Biotin-SGSGNKPCPVCRQPIQMIALTYFP
L487A	MDM2 RING	Biotin-SGSGNKPCPVCRQPIQMIVATYFP
T488A	MDM2 RING	Biotin-SGSGNKPCPVCRQPIQMIVLAYFP
Y489A	MDM2 RING	Biotin-SGSGNKPCPVCRQPIQMIVLTAFP
F490A	MDM2 RING	Biotin-SGSGKPCPVCRQPIQMIVLTYAP
P491A	MDM2 RING	Biotin-SGSGNKPCPVCRQPIQMIVLTYFA
Box 1	p53	SGSGPPLSQETFSDLWKLLP
Peptide 12.1	p53	SGSGMPRFMDYWEGLN
Peptide 12.1$^{W\Delta A}$	p53	SGSGMPRFMDYAEGLN
Peptide 12	Aptamer screen	Biotin-SGSGAKFDMHIATRLS
Peptide 37	Aptamer screen	Biotin-SGSGFIPAQLHFHWRS
Peptide 58	Aptamer screen	FIPAQLQFHWRSGSG-Biotin
Peptide 68	Aptamer screen	KHSAFMWWTVKSGSG-Biotin

Table 2.1: Sequences of peptides used throughout PhD.

2.2 Microbiological Techniques

2.2.1 Bacterial cultures

Bacterial cultures were grown in Luria-Bertani (LB) broth in an incubator shaker at 37 ^{o}C, 220 rpm. Sterile vessels with 4x the capacity of the culture being grown were used for adequate aeration of the culture. Selective antibiotics were used at the following concentrations 100 µg/ml ampicillin and 25 µg/ml kanamycin.

LB plates were prepared by heating agar until liquid, cooling to 42 ^{o}C, adding selective antibiotic (at the concentrations above) and pouring into 90 mm petri dishes (Sterilin). The agar was further cooled until solid and the plates dried at 37 ^{o}C for 10 minutes-1 hour before use.

LB broth	LB agar
1 % (w/v) tryptone	1 % (w/v) tryptone
0.5 % (w/v) yeast extract	0.5 % (w/v) yeast extract
1 % (w/v) NaCl	1 % (w/v) NaCl
	1.5 % (w/v) agar
Autoclave, 121 ^{o}C, 20 minutes	Autoclave, 121 ^{o}C, 20 minutes

On occasion glucose was added to LB broth at a final concentration of 0.015 % (w/v).

During expression trials 2x TY media was used instead of LB broth, the protocol for bacterial growth is as described for LB broth.

2x TY media

1.6 % (w/v) tryptone
1 % (w/v) yeast extract
0.5 % (w/v) NaCl

2.2.2 Glycerol stocks

The preparation of glycerol stocks, for the long term storage of bacteria, was achieved by adding 800 µl of mid log phase bacterial culture ($OD_{600\ nm}$ ~ 0.6) to a cryotube (Nunc) along with 200 µl of sterile glycerol and mixing gently. The cells were rapidly frozen in liquid nitrogen and stored at -80 ^{o}C.

2.2.3 Preparation of competent cells, heat shock method

Bacterial cells from glycerol stocks were inoculated in 2 ml of LB broth, minus antibiotic, and incubated overnight at 37 ^{o}C and 220 rpm. 250 µl of the overnight culture was added to 50 ml fresh LB broth and incubated until the $OD_{600\ nm}$ was 0.4. The culture was centrifuged at 4000g for 15 minutes at 4 ^{o}C. The pellet was resuspended in 16 ml of ice cold buffer I, incubated on ice for 10 minutes and centrifuged as above. The pellet was gently resuspended in 2 ml of ice cold buffer II and incubated on ice for 10 minutes. Aliquots (30 µl) were prepared in pre-chilled sterile microcentrifuge tubes, rapidly frozen in liquid nitrogen and stored at -80 ^{o}C.

Buffer I	Buffer II
60 mM CH_3COOK	10 mM MOPS
10 mM RbCl	10 mM RbCl
10 mM $CaCl_2$	75 mM $CaCl_2$
40 mM MgCl	15 % (v/v) glycerol
15 % (v/v) glycerol	
pH 5.8 with CH_3COOH	pH 6.5 with NaOH
Sterilise by filtration	Sterilise by filtration

2.2.4 Transformation of bacteria, heat shock method

A thawed aliquot of competent bacterial cells (30 µl) was mixed with plasmid DNA (250 ng) and incubated on ice for 30 minutes. Cells were heat shocked at 42 ^{o}C in a water bath for 90 seconds and cooled on ice for a further two minutes. LB broth (1

ml), minus antibiotic, was added to the cells and they were incubated at 37 ^{o}C, 220 rpm for 60-90 minutes.
Aliquots (100 µl and 100 µl of a 1:10 dilution) were plated onto LB agar plates containing the appropriate selective antibiotic and incubated overnight at 37 ^{o}C.

2.3 Molecular biology methods

2.3.1 Plasmid DNA amplification

Plasmid DNA was amplified using either the Mini-prep or HiSpeed Maxi-prep kits from Qiagen, following the manufacturer's instructions. Plasmid DNA was eluted at room temperature in nuclease free water. Plasmid DNA was then quantified using a NanoDrop ND-1000 spectrophotometer, using nuclease free water as the blank before storing at -20 ^{o}C.

2.3.2 Agarose gel electrophoresis of DNA

Agarose gel electrophoresis was used to separate, identify and purify DNA fragments. Agarose gels (1 %) were prepared by dissolving agarose in 1xTAE. To detect the DNA either the fluorescent intercalating dye ethidium bromide (0.5 µg/ml) or SYBR®Safe (Invitrogen) were added to the gel prior to pouring the gel. The switch between ethidium bromide occurred as SYBR®Safe is now considered safer and less mutagenic then ethidium bromide. Loading dye (6x) was added to the DNA samples prior to loading onto the agarose gel; the gel was run in 1x TAE buffer at 100 V for ~1 hour.

1x TAE buffer	6x DNA loading dye
40 mM Tris	0.25 % (w/v) bromophenol blue
1 mM EDTA	0.25 % (w/v) xylene cyanol
pH 8	15 % (v/v) glycerol

2.3.3 DNA sequencing

Sequencing was carried out by Source Bioscience (LifeSciences). Plasmid DNA was obtained from clones by using the Qiagen Mini-prep kit, following manufacturer's instructions. Plasmids were sequenced using stock primers from source bioscience.

2.3.4 Cloning

2.3.4.1 Traditional cloning using restriction enzymes

Traditional cloning using restriction enzymes (RE) is done in three steps. 1) PCR amplification of the desired insert, including suitable restriction sites. 2) Restriction enzyme double digests of insert and vector. 3) Ligation of digested vector and insert.

2.3.4.2 PCR amplification

Suitable plasmid DNA for the insert was used as a template. Primers were designed that incorporated different RE sites into the 3' and 5' end. It is important to make sure that the inserted gene is in frame with any tags within the vector it is to be cloned. Nucleotide bases are added alongside the RE sites to allow for efficient binding. These nucleotides are random and are manipulated to get good G/C content and a suitable melting temperature.

Gene to be cloned	**Vector cloned into**	**Tag encoded by vector**	**Primers 5'-3'**	**Template**
MDM2 322-491	pET28b	N-terminal 6x His tag	Forward: GCTAAGTGGATCCA TGTTGGGCCCTTCGT GAG Reverse: GCACGTAGGTCGAA TTCACTAGGGGAAA TAAGTTAGC	pGEx6-MDM2-wt
MDM2 322-479	pET28b	N-terminal 6x His tag	Forward: As above Reverse: CGTAGGTCGAATTC ACTATCTACATACT GGGCAGGGC	pGEx6-MDM2-wt
MDM2 322-491	pET-15b	N-terminal 6x His tag	Forward: GCAGCTCATATGTG TTGGGCCCTTCG Reverse: GCATGGGATCCCTA GGGAAATAGG	pGEx6-MDM2-wt
MDM2 322-479	pET-15b	N-terminal 6x His tag	Forward: As above Reverse: CGTGGATCCCTATCT ACATACTGGGCAGG GC	pGEx6-MDM2-wt

Table 2.2: Primers used for traditional cloning

Key: Blue- Nucleotide bases added to allow for efficient RE binding

Red- RE recognition site

Green- Inserted base to make sure that my insert is in frame

Black- Desired gene

Black- Stop codon added in to truncate the gene

Restriction Enzyme	**Recognition sequence 5'-3'** **(/ indicates cut site)**
BamH1	G/GATCC
EcoRI	G/AATTC
NdeI	CA/TATG
Sa1I	G/TCGAC
ApaI	GGGCC/C
SfiI	GGCCNNNN/NGGCC

Table 2.3: Restriction enzymes used in traditional cloning

The PCR reaction was set up in nuclease free tubes using 2 x Pfu master mix (Rovalab) as follows:

- 25 µl 2x Pfu master mix[1]
- 5 µl Band doctor (Rovalab)
- 5 ng template DNA
- 1 µl forward primer (20 µM stock)
- 1 µl reverse primer (20 µM stock)
- Nuclease free water up to 50 µl

Thermal cycling conditions:

- Incubate at 95 ^{o}C for 2 minutes
- Incubate at 95 ^{o}C for 20 seconds
- Incubate at 68 ^{o}C for 40 seconds
- Incubate at 72 ^{o}C for 1 minute
- Cycle to step 2 for 30 cycles
- Incubate at 72 ^{o}C for 1 minute
- Hold at 4 ^{o}C forever

[1] pfu master mix contains pfu polymerase (isolated from *Polycoccus furiosus*) which, when compared to other polymerases such as Taq, has superior proofreading properties and higher thermostabilty. Its error rate is 1 in 1.3 million bases, but these higher proofreading capabilities results in slower DNA amplification (>10x slower than Taq).

Post PCR the amplified DNA was cleaned using the Qiagen PCR clean up kit and eluted in 50 µl of nuclease free water.

2.3.4.3 Restriction digests of vector and insert

Restriction digests were carried out using restriction enzymes (RE) and buffers from New England Biolabs and digest conditions recommended by the supplier.

Insert digest	Vector digest
40 µl PCR product	5 µg pet28b vector
5 µl EcoRI buffer	5 µl EcoRI buffer
0.5 µl BSA (10 mg/ml)	0.5 µl BSA (10 mg/ml)
1 µl BamH1	1 µl BamH1
1 µl EcoRI	1 µl EcoRI
Nuclease free water up to 50 µl	Nuclease free water up to 50 µl

It is important to add the RE last to each digest reaction.

Double digests were incubated at 37 ^{o}C for 90 minutes. Following the digest the RE were inactivated by incubating at 65 ^{o}C for 10 minutes.

Following the double digestion the digest mix was loaded onto a 1 % agarose gel. The gel was viewed under UV light and the bands corresponding to digested insert and vector cut out and purified using the Qiagen Gel extraction kit. Purified DNA was eluted in 50 µl nuclease free water.

2.3.4.4 Ligation of vector and insert

Ligation of vector and insert was carried out using T4 DNA ligase (Promega), following manufacturer's instructions.

A standard amount of vector (100 ng) was used and the amount of insert required was calculated using the following formula:

$$Insert_{ng} = \frac{Vector_{ng} \times Insert\ sixe_{kb}}{Vector\ size_{kb}} \times \text{Molar ratio of } \frac{insert}{vector}$$

A 1:1 and 3:1 molar ratio of insert to vector was always tested.

Ligation reactions were as follows:

- 1 µl ligase buffer (10x)
- 100 ng vector
- *X* ng insert
- 1 µl T4 DNA ligase
- Nuclease free water to 10 µl water

Occasionally if the vector was not particularly concentrated the reaction would have a total volume of 20 µl to compensate for the volume of vector used.

Ligation reactions were carried out at room temperature for 1 hour. Following which 2.5 µl of the mix was transformed into DH5α competent cells and plated onto ampicillin containing LB agar plates. Colonies were selected and plasmid DNA obtained using the Qiagen Mini-prep kit.

Site directed mutagenesis

Site directed mutagenesis was carried out using methods from Stratagene.

Mutation	**Vector backbone**	**Tag encoded by vector**	**Primer (mutated nucleotides in red)**	**Template**
MDM2ΔT	pGEx6	N terminal GST	Forward: CCCTGCCCAGTATGTAGACAATAGATTCAAATGATTGTGC Reverse: GCACAATCATTTGAATCTATTGTCTACATACTGGGCAGGG	pGEx6-FLMDM2
RING^{Y489A}	pET15b	N terminal 6x His	Forward: GATTGTGCTAACTGCTTTCCCCTAGG Reverse: CCTAGGGGAAAGCAGTTAGCACAATC	pET15b-RING^{491}
RING^{R479A}	pET15b	N terminal 6x His	Forward: CTGCCCAGTATGTGCTCAACCAATTCAAATGATTG Reverse: CAATCATTTGAATTGGTTGAGCACATACTGGGCAG	pET15b-RING^{491}

Table 2.4: Primers used in site directed mutagenesis

The PCR reaction was set up in nuclease free tubes using 2 x Pfu master mix (Rovalab) as follows:

- 25 µl 2x Pfu master mix
- 5 µl Band doctor (Rovalab)
- 20 ng template DNA
- 1 µl forward primer (20 µM stock)
- 1 µl reverse primer (20 µM stock)
- Nuclease free water up to 50 µl

Thermal cycling conditions:

- Incubate at 95 ^{o}C for 2 minutes
- Incubate at 95 ^{o}C for 1 minute
- Incubate at 60 ^{o}C for 1 minute
- Incubate at 72 ^{o}C for 5 minutes
- Cycle to step 2 for 16 cycles
- Incubate at 72 ^{o}C for 5 minutes
- Hold at 4 ^{o}C forever

Post PCR 1 µl DpnI (20000 U/ml, NEB) was added directly to each reaction tube and incubated at 37 ^{o}C for 1 hour. Dpn1 was inactivated after this time by incubating at 65 ^{o}C for 10 minutes.

PCR reactions (2.5 µl) were transformed into DH5α competent cells and plated onto ampicillin containing LB agar plates. Colonies were selected and plasmid DNA obtained using the Qiagen Mini-prep kit.

2.4 Biochemical techniques

2.4.1 Protein quantification

Protein concentration was estimated in a number of ways. 1) Using Bradford's reagent (Bio-Rad), following manufacturers instructions. Absorbance (595 nm) was measured using the victor 3 plate reader (Perkin Elmer). 2) Comparison against BSA concentration standards, run on a coomassie gel. 3) Quantification using a NanoDrop ND-1000 spectrophotometer, using the storage buffer of the protein to be quantified as the blank.

2.4.2 SDS-PAGE

Polyacrylamide gels were prepared as described by Laemmli, using the recipes listed below and the Biorad Mini-PROTEAN® 3 Cell.

The appropriate separating gel was cast and overlaid with isopropanol. The isopropanol acts in two ways, it levels out the top of the separating gel and prevents oxygen from reaching the gel, allowing the even polymerisation of the acrylamide. Once the separating gel had polymerised the isopropanol was removed and the stacking gel cast. Samples to be loaded were first mixed with sample buffer (2x) in a 1:1 ratio and heated for 3-5 minutes at 90 ^{o}C. Prestained protein markers (Fermentas) were loaded and used as size markers.

Gels were run at ~ 150 V for ~1 hour in running buffer (1x) and terminated once the dye front had reached the end of the gel.

<u>10 % separating gel</u>

30 % acrylamide mix	10 % (v/v)
1.5 M TRIS (pH 8.8)	0.39 M
10 % (w/v) SDS	0.1 % (v/v)
10 % (w/v) APS	0.1 % (v/v)
TEMED (v/v)	0.04 % (v/v)
H_2O to final volume	

<u>15 % separating gel</u>

30 % acrylamide mix	15% (v/v)
1.5 M TRIS (pH 8.8)	0.39 M
10 % (w/v) SDS	0.1 % (v/v)
10 % (w/v) APS	0.1 % (v/v)
TEMED (v/v)	0.04 % (v/v)
H_2O to final volume	

Stacking gel

30 % acrylamide mix	5 % (v/v)
1 M TRIS (pH 6.8)	0.13 M
10 % (w/v) SDS	0.1 % (v/v)
10 % (w/v) APS	0.1 % (v/v)
TEMED	0.1 % (v//v)
H_2O to final volume	

**Acrylamide mix (Protogel, National diagnostics) consists of 30 % acrylamide and 0.8 % (w/v) bis-acrylamide.*

2X Sample Buffer	Running Buffer
300 mM TRIS (pH 6.8)	192 mM glycine
5 % (w/v) SDS	25 mM TRIS
25 % (v/v) glycerol	0.1 % (w/v) SDS
400 mM DTT	
bromophenol blue to desired colour	

2.4.3 Precast gel protocol

All ubiquitination and discharge assay samples were run on precast gradient gels (4-12 % Bis-Tris Gels, Invitrogen) in MOPS buffer (1x) (Invitrogen) and run at 180 V for ~60 minutes.

2.4.4 Coomassie staining

To detect proteins, after SDS-PAGE, by coomassie staining, the gels were submerged in coomassie blue stain (20 ml) for 10-20 minutes. The stained gel was then destained for 10 minutes, the destain was then removed, fresh added and the gels left to destain for as long as desired (2 hours-overnight).

The destained the gels were rinsed in water and dried using a heated vacuum gel drier (Gel master model 1426, Welche Rietschle Thomas).

Stain	Destain
50 % (v/v) methanol	7.5 % (v/v) methanol
10 % (v/v) glacial acetic acid	10 % (v/v) glacial acetic acid
0.2 % (w/v) coomassie brilliant blue R-250	

2.4.5 Immuno blotting

Proteins separated using SDS-PAGE gels are transferred onto 0.2 µM nitrocellulose membrane (Protran, Schleicher and Schuell Biosciences). The transfer was carried out in tanks containing transfer buffer (1x) and an ice pack, to prevent overheating, at 100 V for 1 hour or 30 mV overnight. Transfer apparatus supplied by Biorad.

Following transfer the membrane was washed with Phosphate Buffered Saline (PBS) containing 0.1 % (v/v) TWEEN-20 (PBST), 3 washes at 5 minutes. The membrane was blocked with blocking buffer (3 % (w/v) (skimmed milk powder in PBST) for 30 minutes. The membrane was incubated with primary antibody (**table 6**) in blocking buffer for 1 hour at room temperature, alternatively overnight at 4 ^{o}C, and then washed with PBST, as above. The membrane was incubated with horseradish peroxidise conjugated secondary antibody (1:1000, Dako) in blocking buffer for 1 hour at room temperature, and again washed as above.

Antibody signal was detected using enhanced chemiluminescence (ECL). Blots were overlaid with a fresh mix of ECL I and ECL II (1:1) for 1 minute, blotted to dry and exposed to Hyperfilm ECL (Amersham) for the desired period of time. Film was developed using a Konica medical film processor (model SRX-101A).

1x Transfer Buffer
192 mM glycine
25 mM TRIS
20 % (v/v) methanol

ECL I	ECL II
100 mM TRIS (pH 8.5)	100 mM TRIS (pH 8.5)
2.5 mM luminol	0.02 % (v/v) H_2O_2
0.4 mM p-Coumaric acid	

2.4.6 Stripping nitrocellulose blots

Antibodies were stripped from membranes in order that the same blot could be probed with different antibodies. The membranes were incubated with stripping buffer for 30 minutes at room temperature with gentle agitation. Blots were thoroughly washed with PBST (3x 5 minutes), blocked with milk 3 % (w/v) /PBST, and then incubated with new antibodies as required.

Stripping buffer

62.5 mM TRIS (pH 6.8)
2 % (w/v) SDS
0.6 % (v/v) BME

The primary antibodies mentioned in this thesis, alongside their supplier and working dilution are listed in **Table 2.5**.

Antibody to	Type	Name	Supplier	Dilution
His tag	Mouse monoclonal	Anti-his	Novagen	1:1000
FL MDM2	Mouse monoclonal	3G5	Gift from B. Vojtesek	1:1000
FL MDM2	Mouse monoclonal	4B2	Gift from B. Vojtesek	1:1000
MDM2 RING	Mouse monoclonal	2A10	Gift from B. Vojtesek	1:1000
p53	Mouse monoclonal	DO-1	Gift from B. Vojtesek	1:2000
Ubiquitin	Mouse monoclonal	Anti-ub	Santa-cruz Biotechnology	1:1000

Table 2.5: Primary antibodies. Table showing all the primary antibodies, their source, and the dilution used at, throughout the course of my PhD.

2.5 Protein expression and purification

2.5.1 Purification of GST-tagged proteins

An overnight culture (10 ml) of BL21-DE3 competent cells containing pGEx6MDM2-wt or pcDNA-MDM2ΔT was added to LB broth (1 L) containing ampicillin (100 µg/ml). The cells were incubated at 37 ^{o}C (220 rpm) until the OD_{600} reached 0.4, protein expression was induced by the addition of IPTG (1 mM) and the culture incubated for a further 3 hours at 37 ^{o}C (220 rpm).

The culture was centrifuged at 6000g for 15 minutes at 4 ^{o}C and the supernatant discarded. The pellet was resuspended in lysis buffer (20 ml lysis buffer per 1 L pellet), rapidly frozen in liquid nitrogen and stored at -80 ^{o}C. When required the pellet was thawed in a water/ice bath. Sucrose (10 % w/v), lysozyme (5 mg), DTT (5 mM), Benzamadine (1 mM) and protease inhibitor (PI) mix (1 ml) were added and the resuspended pellet lysed on ice for 30-45 minutes. The cells were sonicated (Soniprep

150 sonicator), 3x 15 seconds (amplitude 10 microns) with 30 second intervals on ice. Sonicated samples were then centrifuged at 16000g for 30 minutes at 4 ^{o}C.

The supernatant was filtered (22 µM Millex® Syringe-driven filter unit, Millipore) and mixed with glutathione-sepharose 4B beads (1 ml, 50 % slurry) (Amersham GE), previously washed in sterile PBS (2x) and wash buffer (2x), and incubated for 1 hour at 4 ^{o}C on a rotating table.

The mix was transferred to a 5 ml disposable column (MoBiTec) and left to empty by gravity, following which the beads were washed with wash buffer (4x 5 ml). GST tagged proteins were eluted from the column using elution buffer (10x 0.5 ml), benzamadine (1 mM) and pefabloc (40 µg/ml) were added, and the eluted fractions aliquoted, rapidly frozen in liquid nitrogen and stored at -80 ^{o}C.

Lysis Buffer

50 mM TRIS pH8
150 mM NaCl
0.5 % (v/v) NP40

Wash Buffer

20 mM HEPES pH7.5
150 mM NaCl
1 mM DTT
0.1 % (V/V) NP40

Elution Buffer

25 mM HEPES pH 7.5
1 mM DTT
10 % (v/v) glycerol
150 mM NaCl
50 mM reduced glutathione pH 8

2.5.2 GST tag cleavage using PreScission Protease

Full length MDM2 was expressed with a GST tag. The linker region contained a site recognised by PreScission Protease (GE healthcare). In instances where untagged protein was required the following protocol was used.

GST tagged MDM2 was purified as described in 'Purification of GST tagged proteins' up to, and including, the wash step. The column was then washed with prescission buffer (0.5 ml) to equilibrate the beads. The column was capped and preScission buffer containing PreScission protease was added (40 µl in 0.5 ml). The column was left rotating at 4 ^{o}C overnight. The cleaved MDM2 was eluted by gravity, aliquoted, rapidly frozen in liquid nitrogen and stored at -80 ^{o}C.

PreScission Buffer

25 mM HEPES pH 7.5
1 mM DTT
10 % (v/v) glycerol
150 mM NaCl

2.5.3 Purification of his tagged proteins

An overnight culture (10 ml) of BL21-DE3 cells containing either pet15b-RING$^{322-479}$, pet15b-RING$^{322-491}$, pet15b-RING^{Y489A}, pet15b-RING^{R479A} or pet15b -UbcH5α was added to LB broth (1 L) containing ampicillin (100 µg/ml). In the case of UbcH5α glucose was added to the LB broth as described in 'Bacterial cultures'. The cells were incubated at 37 ^{o}C (220 rpm) until the OD_{600} reached 0.4, protein expression was induced by the addition of IPTG (1 mM) and the culture incubated for a further 3 hours at 37 ^{o}C.

The culture was centrifuged at 6000g for 15 minutes at 4 ^{o}C and the supernatant discarded. The pellet was resuspended in lysis buffer (20 ml lysis buffer per 1 L pellet), rapidly frozen in liquid nitrogen and stored at -80 ^{o}C.

When required the pellet was thawed in an ice/water bath. Imidazole (20 mM), lysozyme (100 µg/ml) and protease inhibitor (PI) mix (1 ml) were added and the

resuspended pellet lysed on ice for 35-45 minutes. The cells were then sonicated (Soniprep 150 sonicator), 3x 15 seconds (amplitude 100 microns) with 30 second intervals on ice. Sonicated samples were then centrifuged at 16000g for 30 minutes at 4 ^{o}C.

The centrifuged samples were filtered (22 µM Millex® Syringe drawn filter unit, Millipore) and mixed with Ni-NTA agarose beads (1 ml, 50 % slurry) (Qiagen), previously washed in sterile lysis buffer (2x) and wash buffer I (2x), and incubated for 1 hour at 4 ^{o}C on a rotating table.

The mix was transferred to a disposable column (5 ml, MoBiTec) and left to empty by gravity. The beads were washed with wash buffer I (2x 5 ml) followed by wash buffer II (3x 5 ml). His tagged proteins were eluted from the column using elution buffer (10x 0.5 ml).

In the case of UbcH5α the eluted fractions were aliquoted, rapidly frozen in liquid nitrogen and stored at -80 ^{o}C. In the case of all MDM2 RING proteins the eluted fractions were exchanged into a buffer compatible for their effective storage.

PI mix

469 nM leopeptin
1.5 nM aprotinin
28.7 nM pepstatin
5 nM soya bean trypsin inhibitor
10 mM benzamadine
20 mM pefabloc
10 mM EDTA

Lysis buffer

20 mM Tris (pH8)
150 mM NaCl
0.1 % v/v NP40
10 % v/v glycerol
10 mM $MgCl_2$

Wash buffer I

20 mM Tris (pH8)
150 mM NaCl
0.1 % v/v NP40
10 % v/v glycerol
10 mM $MgCl_2$
20 mM imidazole

Wash buffer

20 mM Tris (pH8)
150 mM NaCl
0.1 % v/v NP40
10 % v/v glycerol
10 mM $MgCl_2$
40 mM imidazole

Elution buffer

20 mM Tris (pH8)
150 mM NaCl
0.1 % v/vNP40
10 % v/v glycerol
10 mM $MgCl_2$
150 mM imidazole

2.5.4 Buffer exchange

MDM2 ring proteins had to be instantly buffer exchanged following protein purification to prevent their aggregation.

The eluate was collected and subsequently exchanged into MDM2 buffer, using Zeba Desalt Spin Columns (Pierce), according to the manufacturers instructions. Once exchanged BME (5 mM) was added to the eluate which was aliquoted and stored directly at -20 ^{o}C.

MDM2 buffer

50 mM tris, pH 7.5
150 mM NaCl
10 µM zinc

2.5.5 His-tag cleavage using free thrombin

For the removal of the his tag from UbcH5α, thrombin (GE healthcare) digestion was performed following elution from the nickel column.

The thrombin is supplied dry in 500U, this was dissolved in ice cold PBS (0.5 ml), aliquoted and stored at -20 ^{o}C. One unit theoretically cleaves 100 ng of protein in 16 hours at room temperature. Add 10 cleavage units (10 µl) per mg of protein mix gently and incubate for 16 hours at room temperature. Cleavage and the purity of the protein can be confirmed by coomassie staining.

2.5.6 UbcH5α purification in preparation for hydrogen-deuterium (HD) exchange

In the previously outlined his purification method NP-40 was used as the detergent. This interferes with the HD exchange apparatus; the following method purifies His-UbcH5α that is suitable for analysis by HD exchange.

An overnight culture (10 ml) of BL21-DE3 cells containing pet15b -UbcH5α was added to LB broth (1 L) containing ampicillin (100 µg/ml), glucose was added to the LB broth as described in 'Bacterial cultures'. The cells were incubated at 37 ^{o}C (220 rpm) until the OD_{600} reached 0.4, protein expression was induced by the addition of IPTG (1 mM) and the culture incubated for a further 3 hours at 37 ^{o}C.

The culture was centrifuged at 6000g for 15 minutes at 4 ^{o}C and the supernatant discarded. The pellet was resuspended in lysis buffer (20 ml lysis buffer per 1 L pellet), rapidly frozen in liquid nitrogen and stored at -80 ^{o}C.
When required the pellet was thawed in an ice/water bath. Imidazole (20 mM), lysozyme (100 µg/ml) and protease inhibitor (PI) mix (1 ml) were added and the resuspended pellet lysed on ice for 35-45 minutes. The cells were then sonicated (Soniprep 150 sonicator), 3x 15 seconds (amplitude 100 microns) with 30 second intervals on ice. Sonicated samples were then centrifuged at 16000g for 30 minutes at 4 ^{o}C.

The centrifuged samples were filtered (22 µM Millex® Syringe drawn filter unit, Millipore) and mixed with Ni-NTA agarose beads (1 ml, 50 % slurry) (Qiagen), previously washed in CV sterile lysis buffer (2x) and CV IMAC 5 (5x), and incubated for 1 hour at 4 ^{o}C on a rotating table.

The mix was transferred to a disposable column (5 ml MoBiTec) and left to empty by gravity. The beads were washed with IMAC 5 (5x CV) followed by IMAC 5 + detergent (25x CV) then washed with IMAC 25 (5x CV). His tagged UbcH5α was eluted from the column using IMAC 150 (10x 0.5ml). The eluted fractions were aliquoted, rapidly frozen in liquid nitrogen and stored at -80 ^{o}C.

Lysis Buffer

20 mM TRIS (pH8)
150 mM NaCl
0.1 % (w/v) n-Dodecyl-β-D-maltoside
10 % (v/v) glycerol
10 mM $MgCl_2$

IMAC 5

20 mM TRIS (pH8)
500 mM NaCl
5 mM imidazole

IMAC 25

20 mM TRIS (pH8)
500 mM NaCl
25 mM imidazole

IMAC 25 + detergent

20 mM TRIS (pH8)
500 mM NaCl
25 mM imidazole
0.5 % v/v Triton X-100
0.5 % v/v TWEEN 20

IMAC 150

20 mM TRIS (pH8)
500 mM NaCl
150 mM imidazole

2.6 Biochemical Assays

2.6.1 In vitro ubiquitination of p53

This activity assay measures the ability of a protein/peptide to ubiquitinate p53 *in vitro*.

Purified ubiquitin and Ubiquitin Activating Enzyme (UBE1) were from Boston Biochem, creatine phosphate (CP), creatine phosphokinase (CK) and ATP were from Sigma.
UbcH5α (E2) was purified as described in 'Purification of His tagged proteins'. p53 was purified from *E.coli* by Kathryn Ball and Ted Hupp.

Master mix (16 reactions)

The master mix and separate ubiquitination reaction tubes are all assembled on ice.

366 µl water
10 µl 1 M HEPES (pH 8)
2.4 µl 1 M $MgCl_2$
2 µl 10 % (v/v) Triton X-100
0.2 µl 1 M DTT
0.4 µl 1 M benzamadine
6 µl 0.2 M ATP
3.2 µl 10 mg/ml ubiquitin

At this point the tube was gently mixed by inversion, and briefly centrifuged to remove any solution detained in the lid.

12 µl 1 M CP
2 µl 10 mg/ml CK

Again the tube was gently mixed by inversion and briefly centrifuged.

0.7 µl 1 µg/µl UBE1
1µl 1 mg/ml E2
1µl 40 ng/µl p53[2]

The tube was gently mixed by inversion and briefly centrifuged.

The master mix was aliquoted into separate reactions (22 µl). There was always a control aliquot containing no E3 protein (or peptide). MDM2 proteins and/or peptides were titrated as desired. When peptides were used a DMSO only control was also present. The reactions were incubated in a waterbath at 30 ^{o}C for 15 minutes, on occasion the reaction was allowed to progress for 30 minutes.

The reaction was terminated by the addition of sample buffer (2x). Sample buffer was used at a 1:1 ratio with the total reaction volume i.e. master mix plus peptide, protein etc. Samples (16 µl) were loaded onto a 4-12 % gradient NuPAGE gel (Invitrogen) and run in MOPS buffer (1x) before analysis via immunoblotting.

2.6.2 In vitro discharge assay

This activity assay measures the ability of a protein/peptide to facilitate the discharge of ubiquitin from E2.

Purified components for this assay were either purchased or purified as described in the above method for ubiquitination of p53.

The master mix and separate discharge reaction tubes are all assembled on ice.

[2] The ratio of folded to unfolded p53 will vary with each batch purified. 40 ng/µl is total protein amount, both folded and unfolded. A titration of p53 established quantity of p53 required for this assay from this specific batch.

Master mix (16 reactions)

366 µl water
10 µl 1 M HEPES (pH 8)
2.4 µl 1 M $MgCl_2$
2 µl 10 % (v/v) Triton X-100
0.2 µl 1 M DTT
0.4 µl 1 M benzamadine
15 µl 20 µM ATP
3.2 µl 10 mg/ml ubiquitin

At this point the tube was gently mixed by inversion, and briefly centrifuged to remove any solution detained in the lid.

0.7 µl 1 µg/µl UBE1
1 µl 1 mg/ml E2

The tube was gently mixed by inversion and briefly centrifuged.

The master mix was aliquoted into separate reactions (22 µl). The reactions were incubated in a waterbath at 30 ^{o}C for 5 minutes, in order for the E2 to become charged with ubiquitin by the UBE1, and then placed back on ice.

Two controls exist for this assay; one contains no protein and/or peptide, to check for spontaneous discharge of ubiquitin from the E2. The second control has DTT added (1 µl, 1 M) to check for the presence of thioester and/or isopeptide bonds, thioester bonds are reversible by DTT. Protein and/or peptide was titrated into the remaining aliquots as desired. The reactions were incubated in a waterbath at 30 ^{o}C for 15 minutes.

The reaction was terminated by the addition of sample buffer (2x). Sample buffer was used at a 1:1 ratio with the total reaction volume i.e. master mix plus peptide, protein etc. Samples (16 µl) were loaded onto a 4-12 % gradient NuPAGE gel (Invitrogen) and run in MOPS buffer (1x) before analysis via immunoblotting.

2.6.3 Protein binding ELISA

The following proteins were used in protein binding ELISAS: FL-MDM2, ΔT-MDM2, $RING^{322-491}$, $RING^{322-479}$, $RING^{Y489A}$, $RING^{R479A}$ and His-UbcH5α purified using the protocol outlined previously. Additionally ubiquitin purchased from Boston Biochem was also used in these assays.

Purified protein (100 ng per well) was coated onto a Costar™ white 96 well plate (Fisher) in 0.1 M $NaHCO_3$ (50 µl) overnight at 4 ^oC. The following day wells were washed with PBST (5x 200 µl, 0.1 % (v/v) TWEEN-20) and blocked with PBS (200 µl) containing 3 % (w/v) BSA (PBS + BSA), for 1 hour at room temperature, with shaking. The wells were then washed with PBST as described above. A titration of protein 2 was added to wells (the wells preincubated with protein 1) in PBS + BSA (50 µl) and incubated for 1 hour at room temperature, with shaking. The wells were then washed as described above and incubated with primary antibody (to protein 2) diluted in PBS + BSA (50 µl) for 1 hour at room temperature, with shaking. The wells were washed as above then incubated with HRP-conjugated secondary antibody diluted in PBS + BSA (50 µl) for 1 hour at room temperature, with shaking. The wells were washed for a final time, as described above, and protein-protein binding was detected by electrochemical luminescence (50 µl ECL per well) and quantified using a luminometer (Labsystems Fluroscan Ascent FL).

2.6.4 Peptide binding ELISA

Streptavidin (1 µg per well) was coated onto a Costar™ white 96 well plate (Fisher) in water (50 µl) overnight at 37 ^oC. The following day wells were washed with PBST (5x 200 µl, 0.1 % (v/v) TWEEN-20) and then incubated with biotin tagged peptide, enough to saturate the streptavidin (500 ng per well), in water (50 µl). The wells were washed as above and blocked with Pierce Protein-Free Blocking Buffer (200 µl, Thermo Scientific), for 1 hour at room temperature, with shaking. The wells were then washed with PBST as described above. A titration of the protein of interest was added to wells (the wells preincubated with peptide) in Pierce Protein-Free Blocking Buffer (50 µl) and incubated for 1 hour at room temperature, with shaking. The wells were then washed as described above and incubated with primary antibody diluted in

Pierce Protein-Free Blocking Buffer (50 µl) for 1 hour at room temperature, with shaking. The wells were washed as above then incubated with HRP-conjugated secondary antibody diluted in Pierce Protein-Free Blocking Buffer (50 µl) for 1 hour at room temperature, with shaking. The wells were washed for a final time, as described above, and peptide-protein binding was detected by electrochemical luminescence (50 µl ECL per well) and quantified using a luminometer (Labsystems Fluroscan Ascent FL).

2.6.5 Competition ELISA

This ELISA was designed to investigate the inhibitory effect of certain peptides on protein-peptide binding.

The assay was carried out in a similar manner to the peptide binding ELISA detailed above, except that a fixed amount of protein was incubated with a titration of inhibitory peptide, in 0.1 M $NaHCO_3$ (50 µl) for 10 minutes at room temperature before titration onto the plate coated with a fixed amount of peptide 1.

2.6.6 Protein-peptide-protein ELISA

This ELISA was designed to investigate the interaction of two proteins with one peptide simultaneously.

Purified protein 1 (100 ng per well) was coated onto a Costar™ white 96 well plate (Fisher) in 0.1 M $NaHCO_3$ (50 µl) overnight at 4 ^{o}C. The following day wells were washed with PBST (5x 200 µl, 0.1 % (v/v) TWEEN-20) and blocked with Pierce Protein-Free Blocking Buffer (200 µl) for 1 hour at room temperature, with shaking. Peptide was added (500 ng per well) to the wells and incubated for 1 hour at room temperature, with shaking. The wells were then washed with PBST as described above. A titration of protein 2 was added to wells (the wells preincubated with protein 1 and peptide) in Pierce Protein-Free Blocking Buffer (50 µl) and incubated for 1 hour at room temperature, with shaking. The wells were then washed as described above and incubated with primary antibody (to protein 2) diluted in Pierce Protein-Free Blocking Buffer (50 µl) for 1 hour at room temperature, with shaking. The wells

were washed as above then incubated with HRP-conjugated secondary antibody diluted in Pierce Protein-Free Blocking Buffer (50 µl) for 1 hour at room temperature, with shaking. The wells were washed for a final time, as described above, and protein-peptide-protein binding was detected by electrochemical luminescence (50 µl ECL per well) and quantified using a luminometer (Labsystems Fluroscan Ascent FL).

2.6.7 AlphaScreen®

The AlphaScreen® is a sensitive bead-based proximity assay for the measurement of protein interactions. Low affinity interactions that can be difficult to measure using traditional binding assays can be assessed by AlphaScreen. There are a variety of beads to mix and match depending on the interaction to be studied. I used donor glutathione beads, as MDM2 had a GST tag, and Protein A beads preincubated with anti-his as UbcH5α had a His-tag.

The required area of a Costar™ white 96 well plate (Fisher) was blocked using dilution buffer (100 µl per well) for 1 hour at room temperature. The required amount of Donor beads (20 µl per well) were diluted 1:100 in dilution buffer, a titration of the first interacting protein was added to the diluted beads and incubated for 1 hour at room temperature in the dark. The amount of light the beads are exposed to should be kept to a minimum otherwise the final signal will be affected, pipette and incubate in the dark.

The required amount of Protein A beads (20 µl per well) were diluted 1:100 in dilution buffer, antibody specific for the second interacted protein was added and as before the mix incubated for 1 hour at room temperature in the dark. As a general rule an antibody used at 1:1000 in a protein binding ELISA works well at 0.05 µl per well in an AlphaScreen.

Following incubation Donor beads (20 µl); Protein A beads (20 µl) and second interacting protein (10 µl) were added to each well. The plate was wrapped in foil and incubated for 1 hour, with shaking.

Protein binding was detected by an Envision™ 2101 Multilabel Reader (Perkin Elmer). Fluorescence intensity was measured by using excitation wavelengths of 680 nm and emission wavelengths of 520-620 nm in Relative Fluorescent Units (RFU).

Dilution Buffer

50 mM Hepes pH 8
150 mM NaCl
0.5 % (w/v) BSA
0.05 % (v/v) TWEEN 20

2.6.8 Peptide phage display

Round 1

This experiment is set up in duplicate on two separate plates to analyse the data when comparing fast washes and slow washes. The first steps are simultaneous.

Purified protein (100 ng per well) was coated onto a Costar™ white 96 well plate (Fisher) in 0.1 M $NaHCO_3$ (50 µl) overnight at 4 ^{o}C. To analyse and compare page binding to protein peptide/ligand complexes the protein was pre incubated with peptide/ligand for 5 minutes at room temperature before adding 0.1 M $NaHCO_3$ (50 µl) and coating onto the plate.

The following day wells were washed with Tris buffered saline containing (3x, 0.1 % (v/v) TWEEN-20 (TBST) and then blocked with Tris buffered saline (TBS, 200 µl) containing 3 % (w/v) BSA. The phage (Ph.D™-12 phage display library, New England Biolabs) was added to wells (4 µl in 96 µl TBST), to those wells containing the protein peptide/ligand complex peptide/ligand was added at the same concentration that was used to coat the plate (4 µl phage library, x µl peptide/ligand, 100 µl-4 µl-x µl TBST). For the fast wash data the wells of one plate were washed with TBST (10x 200 µl). The phage was eluted with 0.2 M glycine-HCl pH2.2 (100 µl) containing BSA (1 mg/mg) for 15 minutes at room temperature with rocking. It is important that this step is not allowed to progress past 15 minutes. The eluted phage was transferred to a fresh eppendorf and 1M Tris-HCl (15 µl) was added to neutralise the phage solution. It is important that this neutralisation is carried out immediately. The eluted phage was then stored at 4 ^{o}C. For the slow data wells were washed with

TBST (6x 200 µl), 5 minutes per wash. In the wells that contained the protein peptide/ligand complex, peptide, at the same concentration used in the coating step, was added to the TBST wash. Following the washes the phage were eluted and neutralised as before. An overnight was set up with ER2738 cells (New England Biolabs) in LB (10 ml) containing tetracycline (1 µg/µl) at 37 ^{o}C, 220 rpm.

The overnight culture was diluted 1:200 in LB (20 ml) and grown for 1 hour at 37 ^{o}C, 220 rpm. It was then inoculated with the eluted phage (100 µl) and incubated for 4.5 hours at 37 ^{o}C, 220 rpm. The culture was centrifuged for 10 minutes, 12000g, 4 ^{o}C and the supernatant transferred to a fresh tube and centrifuged for 10 minutes, 12000g, 4 ^{o}C. The top 80 % of supernatant was transferred to a fresh tube and 20 % (w/v) PEG/2.5 M NaCl was added (1/6 of the supernatant volume) to precipitate the phage, the phage was precipitated overnight at 4 ^{o}C.In preparation of the second round the following day, purified protein (100 ng per well) was coated onto a Costar™ white 96 well plate (Fisher) in 0.1 M $NaHCO_3$ (50 µl) overnight at 4 ^{o}C. If protein peptide/ligand complexes were examined they too were coated onto plates as detailed above. As above the plates were set up in duplicate.

The following day the PEG solution was spun for 15 minutes, 12000g, 4 ^{o}C and the supernatant discarded, the tube was left upside down to drain for 10 minutes. The pellet was resuspended in TBS 200 µl, transferred to an eppendorf and centrifuged for 5 minutes, 13000 rpm, 4 ^{o}C. The supernatant was transferred to a new tube, and the amplified phage from round one was stored at 4 ^{o}C.

Round 2

Round 2 was carried out following the method for round one, except, instead of adding phage library to the wells, amplified phage (10 µl in 100 µl total volume in TBST or TBST+ peptide ligand) was added at this point in the method.

PCR

Both the eluted and amplified phage sequences from rounds 1 and 2 were amplified by PCR and sent for sequencing.

The PCR reaction was set up in nuclease free tubes as follows:

- 5 µl 5 M bertaine
- 10 µl 5x herculase II buffer
- 5 µl 132 mM trehalose
- 2.5 µl 10 mM dNTP
- 1 µl 100 mM reverse primer
- 1 µl herculase II enzyme
- 1 µl forward primer
- 10 µl phage
- Nuclease free water to 50 µl

Thermal cycling conditions were as follows:

- Incubate at 95 ^{o}C for 60 seconds
- Incubate at 95 ^{o}C for 15 seconds
- Incubate at 55 ^{o}C for 20 seconds
- Incubate at 70 ^{o}C for 60 seconds
- Cycle to step 2 for 30 cycles
- Incubate at 70 ^{o}C for 210 seconds
- Hold at 4 ^{o}C forever

2.6.9 Enzymatic protein digest

UbcH5α (12-20 µg), purified as described above, and peptide 8 (5 µg) were preincubated for 10 minutes at room temperature. Trypsin (0.5 mg/ml, Roche), glutamine-C (0.5 mg/ml, Roche) or arginine-A (0.5 mg/ml Roche) was added (1:50 (w/w) and the reaction mix incubated at 4 ^{o}C or 30 ^{o}C for 0-30 minutes. The reaction

was terminated at certain time points (0, 5, 10, 15 and 30 minutes) by the addition of SDS sample buffer (1x) containing DTT (1:4) and heating for 3 minutes at 80 ^{o}C. The samples (total reaction volume) were loaded onto an agarose gel (15 %) and digestion products were visualised by coomassie staining.

2.7 Biophysical assays

2.7.1 Gel filtration

Gel filtration was carried out using a Superdex 200 10/300 GL column (GE Healthcare Life Sciences). The column was equilibrated with MDM2 buffer and proteins were run through the column using this buffer, The manufacturers manual for the column was followed for standard column operating procedure and the RING proteins were run through the column at 0.5 ml/min.

MDM2 buffer

50 mM tris, pH 7.5
150 mM NaCl
10 µM zinc
5 mM BME

2.7.2 In gel enzymatic digestion of protein samples for mass spectrometry analysis

Coomassie stained protein bands were excised from the gel. Washed twice with deionised water and, if large, were cut into smaller pieces using a sterile pipette tip. Washing and hydration buffer (250 µl) was added and samples incubated at 30 ^{o}C for 20 minutes to destain. The supernatant was removed; equilibration and cleavage buffer (250 µl) was added to the samples and incubated at 30 ^{o}C for 30 minutes before the supernatant was removed. In the case of insufficient destaining the washing and equilibration steps were repeated.

The gel slices were dried by the addition of 100 % acetonitrile (100 µl), incubated at room temperature for 10 minutes, and then removed.

Trypsin (0.25 µl, 0.2 µg/µl, Roche) was mixed with equilibration and cleavage buffer (5 µl), added directly to each gel sample and cultivated at 4 ^{o}C for 20 minutes. Alternatively chymotrypsin (0.25 µl, 0.4 µg/µl, Roche) was mixed with 100 mM TRIS pH 8 (5 µl), added directly to each gel sample and cultivated at 4 ^{o}C for 20 minutes. From here on the method is identical regardless of which enzyme was used. Equilibration and cleavage buffer (40 µl) was added to completely submerge the gel piece and the samples incubated overnight at 37 ^{o}C. The digestion was terminated by the addition of 2 % (v/v) trifluoroacetic acid (TFA) (5 µl) in 98 % (v/v) acetonitrile to acidify the sample solution. The supernatant was transferred to a new eppendorf and the sample was dried using a speed vacuum. This could be stored at -20 ^{o}C before commencing the purification of the peptides for mass spec analysis.

Washing and rehydration buffer pH 7.8	Equilibration and cleavage buffer pH 7.8
200 mM ammonium bicarbonate	50 mM ammonium bicarbonate
40 % (v/v) acetonitrile	5 % (v/v) acetonitrile

2.7.3 Peptide purification for mass spectrometry

Peptides were purified using a C18 MicroTrap™ (MICHROM Bioresources, Inc.) column.

The dry peptides were dissolved in equilibration buffer (100 µl). The column was first washed with wash buffer (5x 25 µl) then equilibrated with equilibration buffer (5x 25 µl). The entire sample was loaded onto the column and any salts eluted with equilibration buffer (5x 25 µl). Peptides were eluted from the column using elution buffer (3x 25 µl), and the column washed with wash buffer (5x 25 µl). The peptide samples were dried using a speed vacuum and stored at -20 ^{o}C.

Wash Buffer

90 % (v/v) acetonitrile
0.4 % (v/v) TFA

Equilibration Buffer

0.4 % (v/v) TFA

Elution Buffer

50 % (v/v) acetonitrile
0.4 % (v/v) TFA

2.7.4 Hydrogen -deuterium exchange

UbcH5α (4 μM) was prepared in H_2O (control) and D_2O for set time intervals (1, 2, 5, 10, 30, 60 and 180 minutes) before the exchange was terminated by quenching with Trifluoroacetic acid.

UbcH5α and peptide 1 (control) or peptide 8 were incubated (molar ratios 1:1, 1:10 and 1:100, E2:peptide) at room temperature (30 minutes) to allow for complex formation. The samples were then prepared for exchange as for UbcH5α.

The samples were measured on the Orbitrap Elite mass spectrometer connected to HD robot and liquid chromatography. HD exchange analysis was done in MS mode in orbitrap analyser with 120 000 resolution. Two different fragmentation methods were applied, collision induced dissociation (CID) and higher-energy collisional dissociation (HCD) and peptide mapping was measured in MSMS mode with data dependant analysis (TOP3).

2.7.5 Thermal denaturation

Protein denaturation was measured by fluorescent SYPRO Orange Dye (Invitrogen). The stock (5000X) was diluted to a concentration of 50X, using buffer A and used at a final concentration of 5x in all denaturation experiments.

Ubiquitin (Bosten Biochem) was re-dissolved in sterile water (10 mg/ml) and diluted to concentrations between 2.5-10 µM with buffer A. If required, guanidine was added to the ubiquitin samples at concentrations between 0-4 M, with 0.5 M increments. Following the addition of SYPRO orange final sample volumes were made up to 50 µl with buffer A.

UbcH5α, purified as described in the methods above, was diluted to concentrations between 1.25-5 µM with buffer A. If required peptide 8 was added to UbcH5α (5 µM) samples at molar ratios of UbcH5α to peptide 8 between 1:1.25-1:10. DMSO was added to bring the final percentage of DMSO in the sample up to 2 %.
Following the addition of SYPRO orange final sample volumes were made up to 50 µl with buffer A.

Samples were aliquoted onto a 96 well PCR plate and sealed with optical quality sealing film (Bio-Rad). The plate was centrifuged at 100g for 2 minutes at 21^{o}C to ensure that no bubbles were present in the samples. Protein denaturation was measured using an iCycler iQ Real Time PCR system (Bio-Rad) by heating the samples from 20-90 ^{o}C at 1 ^{o}C increments, with 30 second incubations at each increment. Fluorescence intensity was measured using excitation wavelengths of 485 nm and emission wavelengths of 575 nm in RFU.

Buffer A pH 8

150 mM Hepes
20 mM Tris

Chapter 3: RESULTS

3.1 MDM2 binds to UbcH5α and ubiquitin

3.1.1 Introduction

As previously described MDM2 is a RING E3 ligase. At the start of my PhD a number of facts were known concerning the RING domain of MDM2. Firstly it has a 12 amino acid C-terminal tail; this free tail is not seen in all RING domains. The tail of MDM2 is critical for E3 ligase activity though it is not conclusively shown why. One suggestion for the role of the tail was it having a role in dimerisation, with a dimer being necessary for MDM2 E3 activity[141]. Secondly the MDM2 RING is the only RING protein to contain an ATP binding site within its RING domain[136]. The reason for this difference and the relevance to MDM2 activity it may have is unknown. Finally the RING contains a unique sequence for the coordination of two zinc ions[130]. It is possible that the novel coordination has more significance than is currently realised.

RING E3 ligases are widely thought to act as a scaffold, contacting their target substrate, and E2 charged with ubiquitin, before catalysing the transfer of ubiquitin from the E2 to the target. The mechanism of ubiquitin transfer is universally unclear across the range of E2:E3 binding partners.

In 1994 a novel human E2 was identified, it was highly similar to yeast UB4 and UB5, so was named UbcH5. As with all identified E2 proteins it contained a conserved active site cysteine[217].Discovery of two related human E2 proteins with 89 % similarity to UBCH5 resulted in it being subsequently named UbcH5α[218]. Interestingly this family of UbcH5 proteins were closely related to *Saccharomyces cerevisiae* UB4 and UB5, these yeast E2 proteins are involved in the stress response and target regulatory proteins for degradation[219]. One study identified that MDM2 was an E3 ligase for p53 and that the E2 protein required for successful ubiquitination of p53 by MDM2 was UbcH5α[131].

The binding of UbcH5α to a number of its E3 binding partners have been characterised including BRCA1/BARD1[36], RNF4[37], and CHIP[38]. A study into another binding partner of UbcH5α, u-Cbl, indicates a consensus E2:E3 contact surface, this predicted a contact area is ~15Å away from the active site cysteine of E2. This study claims that the interaction between UbcH5 and the RING domain is a low affinity interaction and therefore cannot be detected in pull down assays. They mutated hydrophobic residues within the RING that they concluded to be important based on the E2:E3 binding consensus sequence and they used changes in E3 activity as a test for E2 binding[34]. It has not been shown that UbcH5α can bind the RING in solution, so how is it possible to conclude that mutating certain residues results in a loss of E2 binding? Mutating certain residues certainly may affect E3 activity but this could be due to an affect other than E2 binding.

In the case of MDM2 understanding the mechanism of UbcH5α recruitment and binding is a particular problem, as the interaction is reported to be very unstable[220], this is similar to the low affinity for UbcH5α[137] displayed by u-Cbl.

Questions

1) Is MDM2 able to form a stable, isolatable complex with UbcH5α and if so which RING domain amino acids are required for UbCh5α binding?

2) Previous studies have suggested that MDM2 constructs in which the tail has been deleted are inactive as E3 ligases.

    a. How does the tail impact on RING activity?
    b. Is the tail required for UbcH5α binding?

3.1.2 Purification of recombinant MDM2

To study the interaction of MDM2 with ubiquitination pathway components I first cloned and purified various MDM2 proteins. The literature states that the RING is the domain responsible for E3 activity and that the 12 amino acid C-terminal tail is critical for this activity[133]. This led me to ask, what is the role of the tail in E3 activity? Does the loss of the tail result in loss of binding to certain ubiquitination components and does this result in a loss of activity? To investigate these questions I first wished to set up a number of *in vitro* assays that required purified MDM2. MDM2 was cloned and expressed in both a full length form and as an isolated RING; in both cases the constructs were made with and without the 12 amino acid tail **(figure 3.1)**.

Expression trials were carried out in order to determine the bacterial growth conditions for optimum expression of soluble MDM2 protein. As well as the commonly used LB broth 2x TY media and autoinduction media were trialled. The 2x TY media is simply a variation of LB broth. Autoinduction media is formulated to grow IPTG inducible strains of *E.coli.*, initially without induction, and then induce production of the target protein automatically, usually when cell density is high. Trace elements are also added to autoinduction media, the trace metals can potentially increase the yield of protein and/or correctly folded protein.

Three *E.coli* cell lines were tested in the trials. BL21 (DE3) is a common strain used for the expression of recombinant proteins within a T7 promoter based plasmid, when the proteins expressed are non-toxic to the bacteria. The BLD1 (DE3) STAR cells have the same properties as the BL21 (DE3) strain but also contain a genotype that promotes high mRNA stability and protein yield. The final strain tested was C41 (DE3); this strain is derived from BL21 (DE3) but contains a mutation which prevents cell death associated with toxic recombinant proteins.

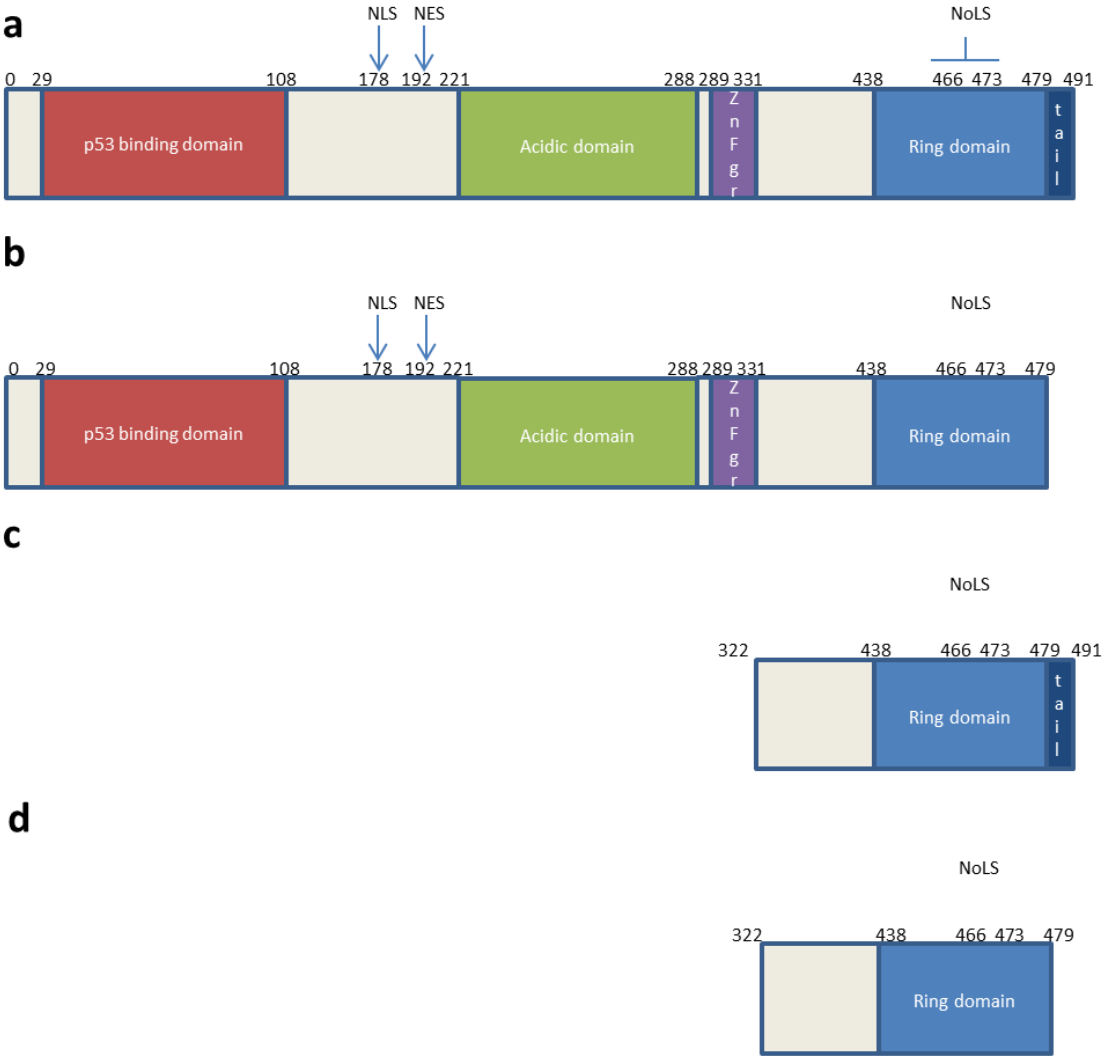

Figure 3.1: Schematic diagram showing the features of the four original MDM2 constructs. a) Full length MDM2 (FL MDM2) **b)** Full length MDM2 delta tail (MDM2ΔT) **c)** Extended RING domain of MDM2 (FL RING) **d)** Extended RING domain of MDM2 delta tail (RING ΔT). NLS- Nuclear localisation signal, NES- Nuclear exclusion signal, NoLS- Nucleolar localisation signal.

The optimum temperature for *E.coli* growth is 37 ^{o}C, they can tolerate lower temperatures though rate of growth will be slower. Growing *E.coli* at lower temperatures however can produce more soluble folded proteins; cells were therefore grown and induced at a range of temperatures (20, 30 and 37 ^{o}C).

Each *E.coli* strain was grown in each media at each temperature (data not shown). Although a high yield of protein is desirable should it be too high it can accumulate in insoluble inclusion bodies within the *E.coli*.
BL21-DE3 cells showed the best results, they produced much more soluble MDM2 protein when compared to the other strains. The main considerations were which media and temperature to use **(figure 3.2)**. When grown in LB media the BL21-DE3 cells look to promote less degradation of MDM2, within the soluble fraction, than when grown in autoinduction media **(figure 3.2a, lane 4 and figure 3.2b, lane 5)**. There appears to be less degradation of MDM2 protein, within the soluble fraction, when grown and induced at 20 ^{o}C compared to 37 ^{o}C **(figure 3.2b lanes 1 +5)** however there was a greater ratio of soluble protein at 37 ^{o}C when compared to 20 ^{o}C **(figure 3.2b lanes 1 +5)**. The levels of degradation of MDM2 are not greatly reduced when grown at 20 ^{o}C, not enough to make a significant difference, especially when compared to the actual soluble protein levels when grown at 37 ^{o}C. All this taken into account, MDM2 was from this point on grown in BL21-DE3 cells in LB media at 37 ^{o}C.

Optimum induction time, following addition of IPTG, varies from protein to protein. A couple of hours can be enough for proteins that are highly expressed, for proteins with lower expression levels induction may need to proceed for much longer. Interestingly, Interferon regulatory factor 1 (IRF1) a transcriptional activator or repressor of a wide variety of target genes, degrades very rapidly if left to induce for even a short period of time. Induction carried out for 30 minutes is the best compromise, enough useable protein has been produced and not so much had been degraded.

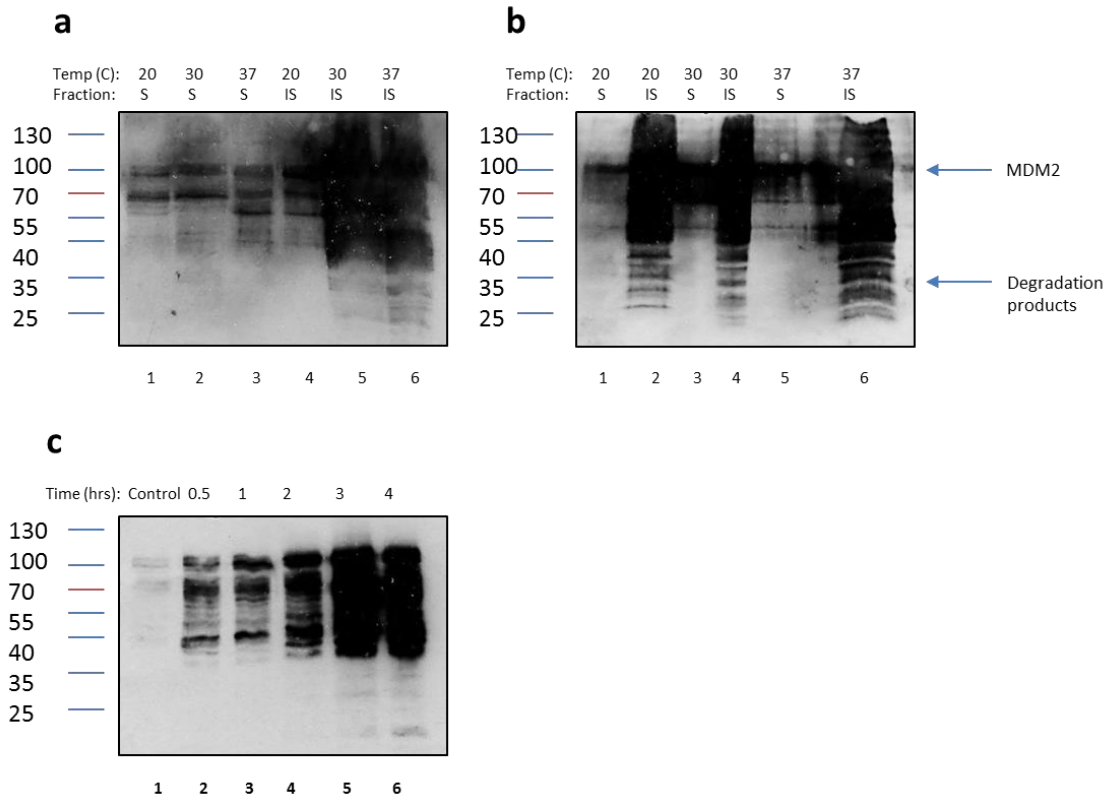

Figure 3.2: Cell expression trials for full length MDM2. a) BL21 (DE3) cells were grown in autoinduction media at 20, 30 and 37 ^{o}C until the OD ~0.4, they were then induced with IPTG for 3 hours. Western blot shows protein present in the soluble and insoluble fractions. b) BL21 (DE3) cells were grown in LB media at 20, 30 and 37 ^{o}C until the OD ~0.4, they were then induced with IPTG for 3 hours. Western blot shows protein present in the soluble and insoluble fractions. **c)** BL21 (DE3) cells were grown in LB media at 37 ^{o}C until the OD ~0.4, following induction by IPTG, samples (5ml) were taken at indicated time points. Western blot shows the time course of protein production. 16µl of each sample loaded onto all gels. All blots probed with 2A10 (1:1000). S- soluble, IS- insoluble. Fermentas PageRuler Prestained Protein Ladder used for molecular weight maker, all molecular weights displayed are in kDa.

With this in mind I carried out a time course to see where MDM2 fell on the induction time scale. Small samples (5ml) of the induced culture were removed at 30 minutes, 1, 2, 3 and 4 hours, the cells were then lysed and the soluble fraction analysed by SDS-PAGE and immune blotting **(figure 3.2c)**. MDM2 expression and protein levels continue to increase up to 3 hours after induction **(figure 3.2c, lanes 1-5)**, if left for 4 hours protein levels begin to fall and more degradation products begin to appear **(figure 3.2c, lane 6)**. For MDM2 3 hours is the optimum time for induction.
It is worth noting that the antibody used to probe the immunoblots shown in **figure 5.2** was 2A10. Whilst there is likely to be some degradation products of MDM2, it is unlikely
to be as much as the immunoblots imply. 2A10 has a high background, this could be because it recognises at least two short epitopes in MDM2[221]. If these blots were to be repeated a different antibody may well produce a cleaner outcome.

When cloning full length MDM2, or indeed any protein, certain consideration has to be given to the tag. A Post-doctoral colleague in the Ball lab was trying to purify untagged MDM2 and was encountering a number of problems, including very low protein expression and yield; bearing this in mind I cloned MDM2 with a cleavable tag.
When choosing between a His and GST-tag there are a number of factors to consider. The size of these two tags tag vary greatly, the His tag is ~1kDa compared to the ~26kDa of GST. The His tag can be advantageous as its small size means that his is unlikely to be contributing to affects seen in biochemical assays. The GST-tag does however have its own advantages, it is very soluble and can help keep a protein in solution if it is less than inclined to do so.
As the literature does not indicate that MDM2 is particularly insoluble, I chose to clone MDM2 with a His tag, primarily chosen due to its small size.

With expression trials complete the next step was to purify his-MDM2. The result of the purification was not as predicted (**figure 3.3a and b**) as the majority of the protein was in the flow through and washes (**figure 3.3a, lanes 2,3 and 5 and 3.3b, lanes 2-5**). There was some protein in the elution but the amount is not comparable to the protein levels seen in the flow through and washes.

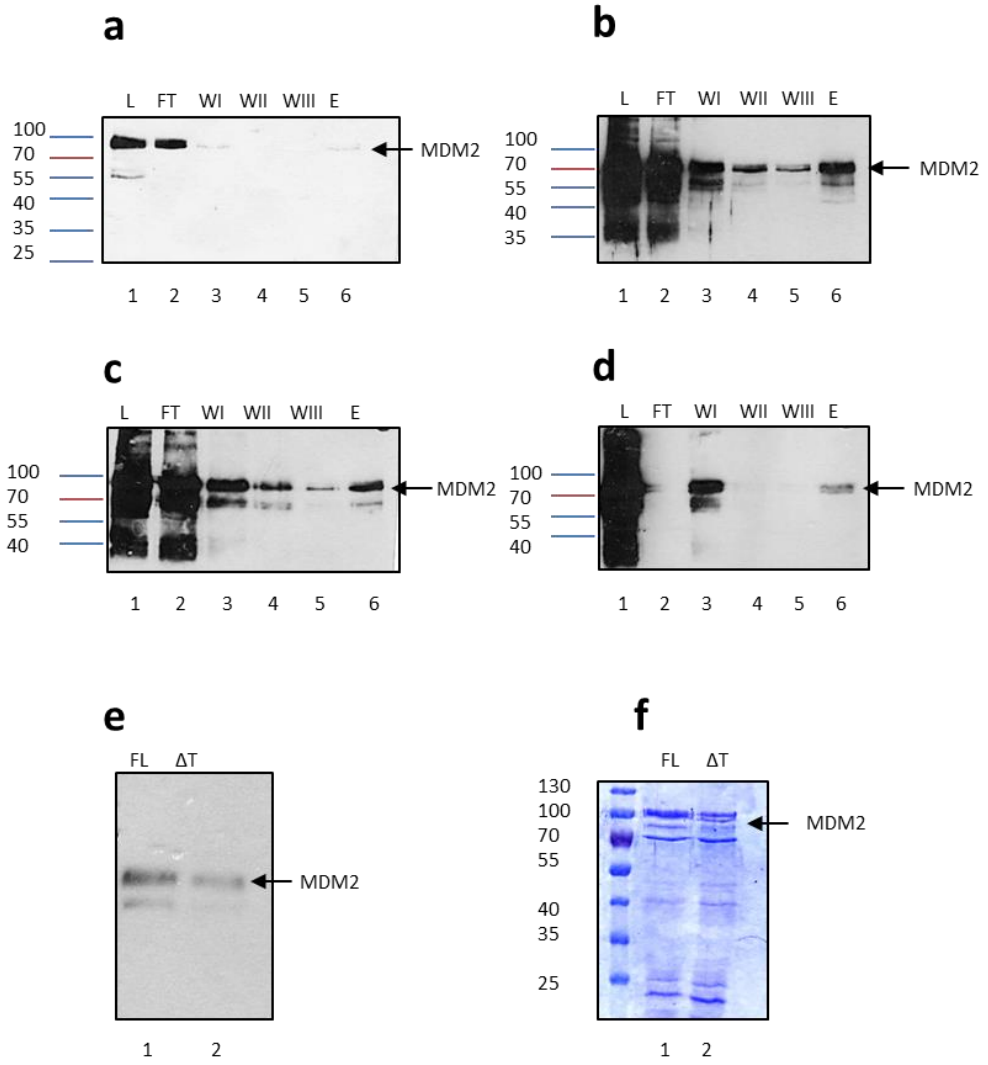

Figure 3.3: Purification of FL MDM2 and MDM2 ΔT. **a)** BL21 (DE3) cell pellet was lysed on ice, centrifuged and the resultant supernatant purified on a nickel column. Western Blot shows the mobility of His-tagged MDM2 **b)** BL21 (DE3) cell pellet was lysed on ice, centrifuged and the resultant supernatant purified on a nickel column. Western Blot shows the mobility of His-tagged MDM2 **c)** BL21 (DE3) cell pellet was lysed on ice, centrifuged and the resultant supernatant purified on a nickel column. The flow through was reloaded onto a second nickel column. Western Blot shows the mobility of His-tagged MDM2 eluted from the second nickel column **d)** BL21 (DE3) cell pellet was lysed on ice, centrifuged and the resultant supernatant denatured with 4M urea before being applied to a nickel column. Western Blot shows the mobility of His-tagged MDM2 **e)** BL21 (DE3) cell pellet was lysed on ice, centrifuged and the resultant supernatant purified on a Glutathione sepharose column. Western Blot shows the mobility of GST-tagged MDM2 **f)** Coomassie stained SDS-PAGE gel showing GST-tagged FL MDM2 and MDM2 ΔT following purification on glutathione sepharose beads. Blots 3a + e were probed with 3G5, blots 3b, c + d were probed with 2A10. L- load, FT- flow through, WI- wash I, WII- wash II, WIII- wash III, E- elution, FL- FL MDM2, ΔT- MDM2 ΔT. Fermentas PageRuler Prestained Protein Ladder used for molecular weight maker, all molecular weights displayed are in kDa.

It was possible that the amount of MDM2 protein was simply too high for it all to bind to the beads however reloading the flow through onto a fresh column did not result in increased protein binding, once again the majority of protein was in the flow through and the washes (**figure 3.3c**). These results indicate that the MDM2 protein is having some difficulty binding to the column. A possible explanation for this is that the His tag is cryptic i.e. the MDM2 protein has folded in such a way that it is obscuring the His tag and preventing it binding to the nickel. To test this the MDM2 was unfolded by pre-incubating the load with 4M urea (**figure 3.3d**), this urea treated protein was more capable of binding the column with minimal protein appearing in the flow through, although some is released in early washes, possibly due to weak interactions, and the rest was eluted in the presence of increased imidazole (**figure 3.3d, lane 2, 3 and 6**). As I wished to assay MDM2 activity I did not want to use renatured protein, I therefore re-cloned MDM2, this time with a cleavable GST-tag. Full expression trials were not carried out as before, instead the optimum conditions previously identified were used as a starting point with a view to changing them should there be a problem, which there was not (data not shown). The GST-tag was not cryptic and FL MDM2 and MDM2ΔT both purify well (**figure 3.3e and f)**.

Alongside cloning of full length constructs of MDM2 shorter constructs containing the RING domain of MDM2 were also cloned (**figure 3.1**). A former PhD student had cloned two RING constructs, containing 41 (438-479) or 53 (438-491) amino acids; however these constructs proved to be highly unstable. Researchers in a different laboratory, with whom the Ball group collaborate, had been having more success with a longer RING domain construct. Using this information two RING domain constructs were cloned that contained not only the RING domain but an extra 116 amino acids, beginning just after the zinc finger of MDM2 at residue 322. As with the full length MDM2 constructs the RING was cloned both with and without the 12 amino acid tail critical for E3 activity (FL RING and RING ΔT) (**figure 3.1c and d**).

To optimise expression of the RING constructs BL21 (DE3) cells were grown and induced in LB media at a range of temperatures (20, 30 and 37 ^{o}C). The greatest level of protein expression was seen at 37 ^{o}C (**figure 3.4a and b, lanes 7**).
The RING constructs were cloned with a His tag and unlike the full length constructs the tag was not cryptic, and purification by nickel beads proceeded as expected

(**figure 3.4c and d**). Some protein was seen in the flow through and washes but there was much higher amounts in the elution fractions. It is possible that there was simply too much protein to bind the nickel beads. For all subsequent purifications a greater volume of beads was used.

Protein is routinely rapidly frozen in liquid nitrogen and stored at -80 ^{o}C for biochemical research however when the RING was stored this way it rapidly formed higher order structures and aggregates (**figure 3.4e**). This affect was especially seen in FL RING (**figure 3.4f**) where the effect could be seen immediately. The RING constructs were therefore stored at -20 ^{o}C, no higher order structures or aggregates could be seen after storage at this temperature.

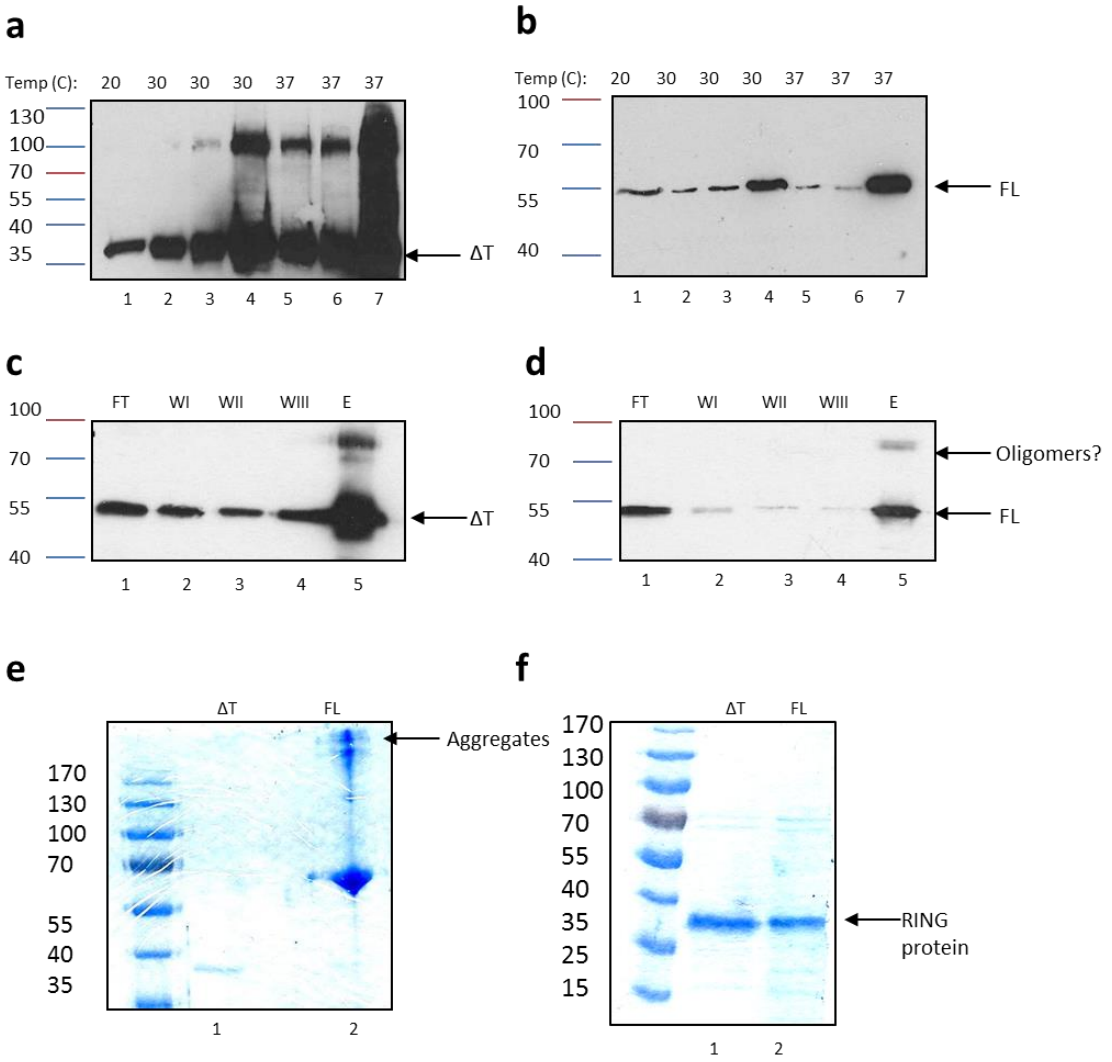

Figure 3.4: Expression and purification of MDM2 RING constructs. a) BL21 (DE3) cells were grown in LB media at 20, 30 and 37 ^{o}C until the OD ~0.4, they were then induced with IPTG for 3 hours. Western blot shows RING ΔT. **b)** BL21 (DE3) cells were grown in LB media at 20, 30 and 37 ^{o}C until the OD ~0.4, they were then induced with IPTG for 3 hours. Western blot shows FL RING. **c)** BL21 (DE3) cell pellet was lysed on ice, centrifuged and the resultant supernatant purified on a nickel column. Western Blot shows the mobility of His- tagged RING ΔT. **d)** BL21 (DE3) cell pellet was lysed on ice, centrifuged and the resultant supernatant purified on a nickel column. Western Blot shows the mobility of His-tagged FL RING. **e)** Coomassie stained SDS PAGE gel showing His-tagged RING ΔT ^{and} FL RING following storage at -80 ^{o}C. **f)** Coomassie stained SDS-PAGE gel showing His-tagged RING ΔT and FL RING following storage at -20 ^{o}C. Blots were probed with 2A10. FT- flow through, WI- wash I, WII- wash II, WIII- wash III, E- elution, ΔT- RING ΔT , FL- FL RING. Fermentas PageRuler Prestained Protein Ladder used for molecular weight maker, all molecular weights displayed are in kDa.

3.1.3 E3 ligase activity of MDM2

The literature states that MDM2 is an E3 ligase specific for p53 and that without the presence of the C-terminal 12 amino acid tail E3 ligase activity is lost[133]. The consensus is that the tail is crucial for the E3 ligase activity of MDM2; however the reason(s) as to why it is critical remain elusive.

I initially carried out activity assays to test that the purified proteins were folded correctly and working as predicted from the literature. The first assay used to test for protein activity was a substrate ubiquitination assay. In this assay all the components of the ubiquitination cascade are present and the reaction is started by the addition of E3 ligase. This ubiquitination assay has been optimised so that the E3 ligase is the rate limiting factor, if ubiquitination is not seen it is due to some property of the ligase and not any other component of the reaction. Contrary to what is seen in the literature my ubiquitination assay is a stopped enzyme assay, it is not permitted to run to completion. This is because I was interested in what factors could affect the rate of ubiquitination (V_{max}). Assuming that all components are active and are at the correct ratio to each other, the E3 ligase should ubiquitinate the target, this ubiquitination can be in the form of mono ubiquitination, multi monoubiquitination and/or polyubiquitination and can be detected by immunoblotting (**figure 3.5a**)

The results show that FL MDM2 was able to ubiquitinate p53 and is therefore active as an E3 ligase (**figure 3.5b, lanes 6-8**), conversely MDM2 ΔT was not able to ubiquitinate p53 and is inactive as an E3 ligase in his assay (**figure 3.5b, lanes 3-5**). This result was predicted based on the literature but does prove that the protein has been folded correctly. FL RING was able to ubiquitinate p53 and therefore is active as an E3 ligase (**figure 3.5c, lanes 6-8**), again this was predicted based on the literature but this result confirms that this specific RING construct behaves similarly to FL MDM2 in terms of E3 activity. RING ΔT was not able to ubiquitinate p53 and is inactive as an E3 ligase (**figure 3.5c, lanes 3-5)**; this construct behaves in a manner similar to MDM2 ΔT in terms of E3 ligase activity.

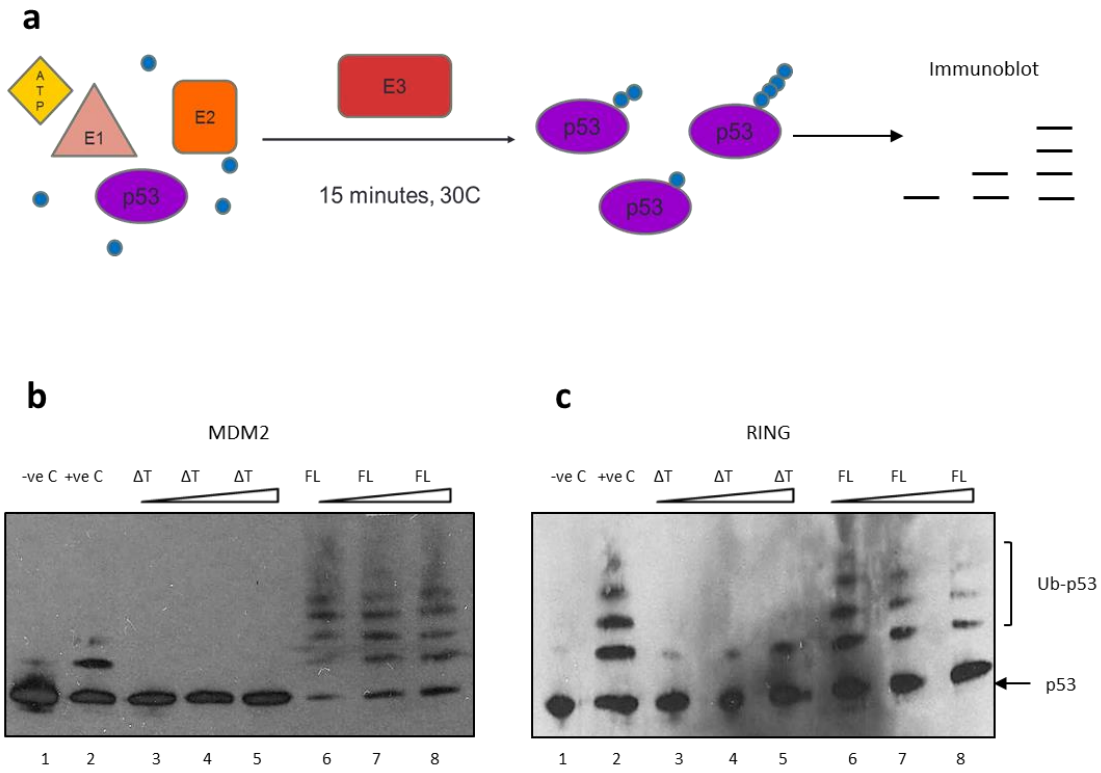

Figure 3.5: Ubiquitination of p53 by MDM2. **a)** Schematic diagram showing components and methods of a ubiquitination assay. The blue circles represent ubiquitin. **b)** Blot showing no ubiquitination of p53 by MDM2 ΔT (lanes 3-5) and ubiquitination of p53 by FL MDM2 (lanes 6-8). **c)** Blot showing no ubiquitination of p53 by RING ΔT (lanes 3-5) and ubiquitination of p53 by FL RING (lanes 6-8). UbcH5α is capable of monoubiquitinating p53 in the absence of an E3 ligase. This is the reason for the band seen in the negative control and ΔT lanes. In each blot the positive control protein is CHIP. Blots were probed by DO1. –ve C- negative control, +ve C- positive control.

It should be noted that a single monoubiquitination band can be seen in both the negative control lane (**figure 3.5b and c, lane 1**) and also in lanes where E3 ligase dead MDM2 ΔT and RING ΔT are present (**figures 3.5b and c, lanes 3-5)**. Different batches of E2 can sometimes be sufficient for monoubiquitination of the target protein without the E3 needing to be present. As this monoubiquination band can be seen in the negative control, as well as those proteins considered to be inactive, it can be assumed that this band is due to the E2 and not some minor E3 ligase activity of the MDM2 proteins missing the C-terminal tail.

Another activity assay used was the discharge assay. This assay was used to look at whether a protein can discharge ubiquitin from an E2. This is a very labile assay and as such it is important to have a control that tests for spontaneous discharge of the ubiquitin from the E2. It is also important to have a control containing a reducing agent. Two bonds can exist between an E2 and ubiquitin, the first, a labile thioester linkage, and the second a covalent isopeptide bond i.e. the E2 can become ubiquitinated. It is possible for both to be present in the same assay, the thioester bond is collapsible by DTT, and the isopeptide bond is not. This assay has been optimised to reduce the presence of isopeptide bonds.
This assay can only show that a protein discharges ubiquitin from the E2, it does not show whether the protein can then transfer the ubiquitin to a target protein. In theory it is possible that a protein may be able to discharge ubiquitin from an E2 without actually being able to transfer it to a ubiquitination target. In this assay an E2 was loaded with ubiquitin before being incubated with the protein of interest, whether or not the protein can discharge ubiquitin from the E2 was be detected by immunoblotting (**figure 3.6a**).

FL MDM2 facilitates discharge of ubiquitin from UbcH5α (**figure 3.6b. lanes 4-6)** this was expected as FL MDM2 was active as an E3 ligase. In this assay the discharge of ubiquitin is not complete. This could be due to the amount of FL M2M2 present. MDM2 ΔT was not able to discharge ubiquitin from UbcH5α (**figure 3.6b, lanes 7-9**) this is consistent with its inability to catalyse p53 ubiquitination.

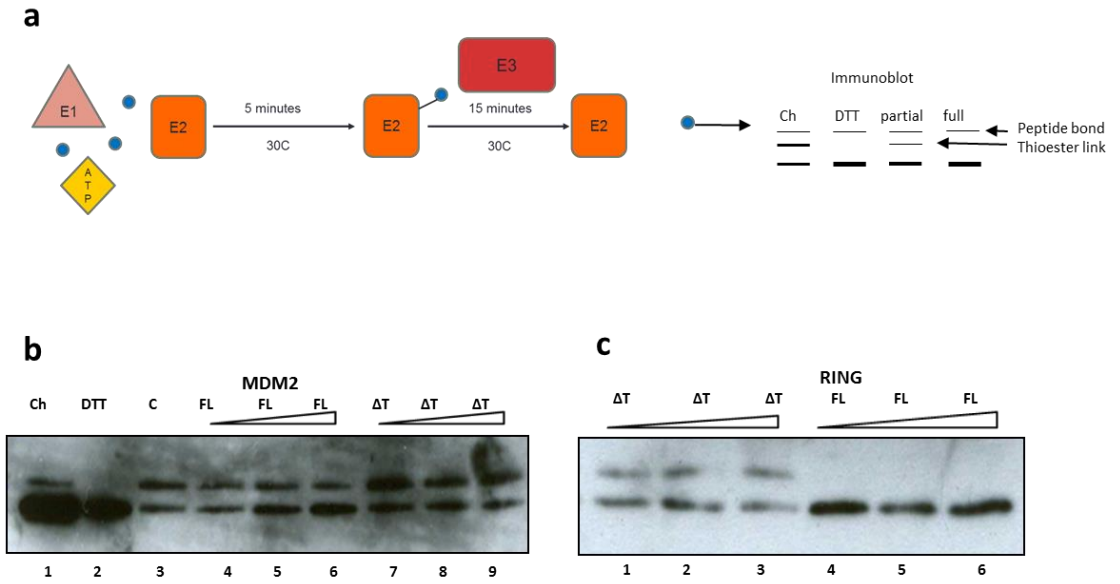

Figure 3.6: Discharge of ubiquitin from UbcH5α by MDM2. a) Schematic diagram showing components and methods of a discharge assay. The blue circles represent ubiquitin. **b)** Blot showing no discharge of ubiquitin from UbcH5α by MDM2 ΔT (lanes 7-9) and discharge of ubiquitin from UbcH5α by FL MDM2 (lanes 4-6). **c)** Blot showing no discharge of ubiquitin from UbcH5α by RING ΔT (lanes 1-3) and discharge of ubiquitin from UbcH5α by FL RING (lanes 4-6). Blots were probed by anti-his (Novagen).Ch- charged UcH5α, DTT- DTT control, C- control.

When I examined the associated RING domain constructs FL RING could discharge ubiquitin from UbcH5α (**figure 3.6c, lanes 4-6)** whereas RING ΔT was not able to discharge ubiquitin from the E2 (**figure 3.6c, lanes 1-3**). As in the ubiquitination assay the RING constructs exhibit the same activity as their full length counterparts. It should be noted that the FL RING is able to facilitate complete discharge of ubiquitin from the E2 compared to the partial discharge seen with FL MDM2, possible reasons for this are outlined in the discussion.

MDM2 ΔT and RING ΔT are both inactive as E3 ligases in the activity assays described previously, this supports cell based assays presented in the literature[141]. It could be argued however, that the reason for the differences between these proteins and FL MDM2 and FL RING is not solely down to the absent tail. These assays confirm no E3 ligase activity but they do not show that this is due to loss of tail function as it could be argued that these proteins have an aberrant or misfolded structure and that the role of the tail is structural rather than functional.

In order to differentiate between E3 inactivity and misfolded protein an assay was needed that compares an activity of the proteins other than E3 ligase activity; this could then prove that E3 loss is indeed down to absent tail and not aberrant conformation.

MDM2 is known to bind p53; the N-terminal hydrophobic pocket of MDM2 binds to the Box I domain of p53 and the acidic domain within MDM2 binds to the Box V domain of p53. Whilst MDM2 does exhibit allosteric behaviour between these two domains the tail has not been reported to be critical for p53 binding.

Due to possible allosteric activity, the binding of FL MDM2 vs MDM2 ΔT to box I and box V peptides may not be identical; still a binding assay may help confirm that the MDM2 ΔT can perform activities that are not reliant on the tail.

A peptide binding assay was carried out in which binding of FL MDM2 and MDM2 ΔT to the box I and box V peptides of p53 was measured. This is an assay that measures stable binding.

Both FL MDM2 and MDM2 ΔT bound Box I peptide with almost identical affinity (**figure 3.7a**), the loss of the tail does not affect the ability of the hydrophobic pocket of MDM2 to bind p53.

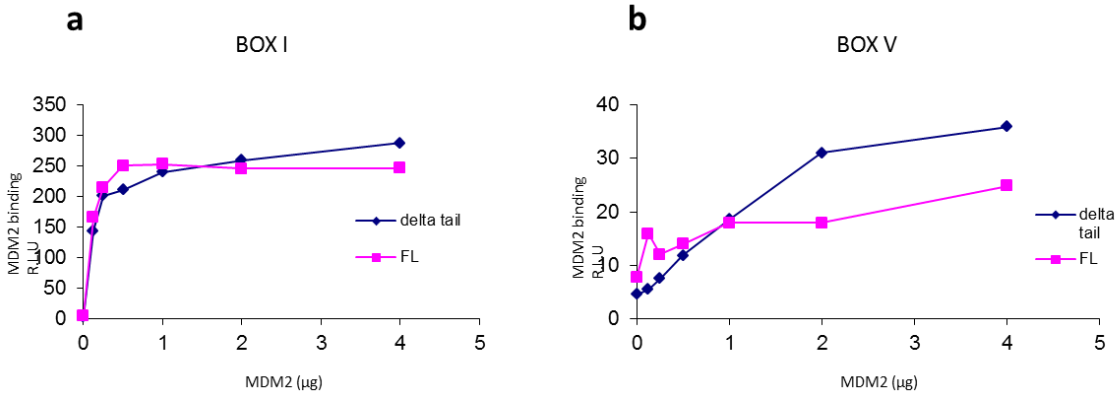

Figure 3.7: FL MDM2 and MDM2 ΔT binding to box I and box V peptides. a) Biotin labelled box 1 (SGSGPPLSQETFSDLWKLLP) (100 ng/well) was captured onto streptavidin coated microtitre wells, a titration of FL MDM2 or MDM2 ΔT was added and incubated for 1 hour at room temperature, unbound protein was removed by extensive washing and bound MDM2 was detected by using the monoclonal antibody 2A10. Graph shows protein binding as Relative Light Units (R.L.U) FL MDM2 and ΔT MDM2 bind to box I peptide. **b)** Biotin labelled box V peptide (100ng/well) was captured onto streptavidin coated microtitre wells, a titration of FL MDM2 or MDM2 ΔT was added in the mobile phase and incubated for 1 hour at room temperature, unbound protein was removed by extensive washing and bound protein was detected by 2A10. Graph shows protein binding as R.L.U. FL MDM2 and ΔT MDM2 bind to box V peptide.

In addition FL MDM2 and MDM2 ΔT bind to Box V peptide however, interestingly MDM2 ΔT binds the peptide with greater affinity than the wt protein (**figure 3.7b)**. It is unlikely that this reflects a difference in the amount of protein added as FL MDM2 and MDM2 ΔT were normalised by ELISA (data not shown) and no difference in binding of these two proteins to Box I was observed. Another explanation for the increased affinity for box V is that without the tail some conformational constraint of FL MDM2 is lost, allowing for a greater level of binding.

These results would suggest that MDM2 ΔT is folded correctly as it is behaving in a similar manner to FL MDM2 in binding assays and therefore retains some activities and selectively loses E3 function.

This assay can clearly not be used to test RING ΔT as the RING construct has no hydrophobic pocket or acidic domain. Different binding assays, discussed shortly, confirmed that RING ΔT behaved like FL RING in non E3 ligase activities, confirming RING ΔT is also purified and folded correctly.

3.1.4 MDM2 binds to UbcH5α

As previously outlined the general consensus for RING domain containing proteins is that they contact their E2 partner then catalyse the transfer of ubiquitin to the target protein, however no one has shown exactly how this mechanism may work.
There are crystal structures and models of other E2:E3 binding partners, and contact sites on both MDM2 and UbcH5α have been predicted, but no one has actively shown that they bind to each other in solution. In fact it has been stated that the E2:RING cannot form a complex that is stable enough to investigate[133]. To investigate the mechanism of ubiquitin transfer, first MDM2 and UbcH5α binding must be better understood.

A protein binding assay (**figure 3.8a**) was carried out between UbcH5α and MDM2. In this assay UbcH5α was immobilised onto a microtitre well and the MDM2 constructs were present in the mobile phase. MDM2 binding was detected using the MDM2 specific monoclonal antibody 2A10 which bind to a region in the RING and acidic domain of MDM2. FL MDM2 and MDM2 ΔT can both bind UbcH5α in a protein binding ELISA (**figure 3.8b**). This assay does not work if it is performed in the opposite orientation i.e. MDM2 immobilised onto the well and E2 in solution. This suggests that the conformational flexibility of MDM2 is an important determinant of E2 binding and may explain why crystallisation of the MDM2 RING and E2 has not been achieved. The result shows that MDM2 ΔT binds UbcH5α with greater affinity than FL MDM2; it is possible that MDM2 without the tail forms a conformation that allows for greater UbcH5α binding.

RING ΔT and FL RING can both bind to UbcH5α in a protein binding assay (**figure 3.8c**); unlike FL MDM2 they can bind to UbcH5α in either the immobile or solution phase. The results from this assay suggest that FL RING may be binding with marginally greater affinity than the ΔT construct.
This protein binding assay is also an example of an activity other than E3 ligase activity. The fact that RING ΔT can bind UbcH5α helps to confirm that the protein is folded correctly and that the missing tail is the cause of E3 ligase inactivity.

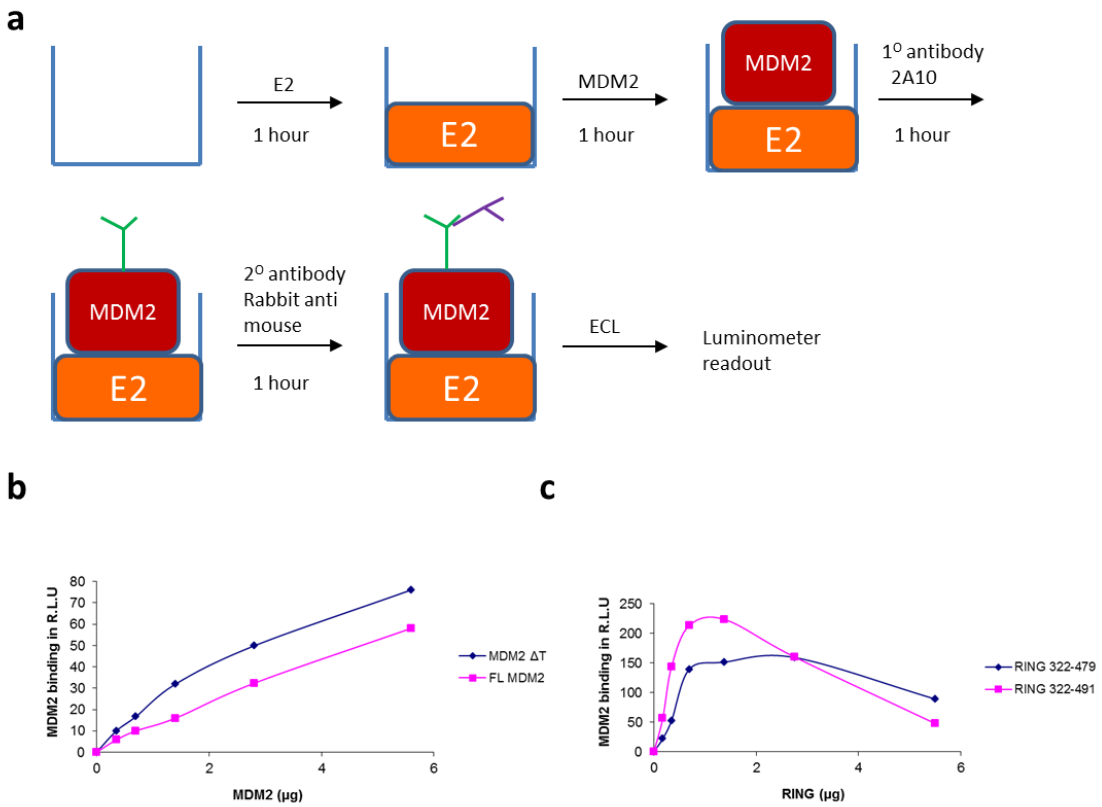

Figure 3.8: MDM2 binds to UbcH5α in solution. a) Schematic diagram showing the basic methodology of this protein binding assay. **b)** UbcH5α was captured onto microtitre wells (100 ng/well); a titration of FL MDM2 or MDM2 ΔT was added in the mobile phase and incubated for 1 hour at room temperature. Unbound protein was removed by extensive washing and bound protein was detected using monoclonal antibody 2A10. Graphs show UbcH5α binding expressed as relative light units (R.L.U). **c)** UbcH5α was captured onto microtitre wells (100ng/well), titrations of RING ΔT or FL RING was added and detected as above.

It is interesting that the proteins missing the tail can bind to UbcH5α with a similar affinity as the proteins with the tail. As the constructs without the tail are inactive as E3 ligases one hypothesis has been that they are not able to bind UbcH5α and therefore not able to catalyse the transfer of ubiquitin to the target protein, in this case p53, these results demonstrate that this is clearly not the case. This idea will be explored further in the discussion.

As the protein binding assay unexpectedly demonstrated readily detected interactions between MDM2 and UbcH5α I wished to confirm the data using a second solution based assay. An alpha screen (**figure 3.9a**) was therefore carried out with FL MDM2, MDM2 ΔT and UbcH5α. An alpha screen has a number of advantages over a protein binding ELISA where one component is immobilised on a charged plastic surface. it is very sensitive and can measure interactions at the picomole level with both the proteins being in solution, and presented in the same orientation, perhaps most importantly it is a real time assay that is carried out at equilibrium.

The assay was set up so that FL MDM2 or MDM2 ΔT was displayed on protein A acceptor beads preloaded with 4B2 and incubated with nickel coated donor beads displaying His-tagged UbcH5α. The beads were combined and preincubated for 1 hour before energy transfer measurements were carried out, by exciting the donor beads at 680 nm and measuring the emission from the acceptor beads at 520-620 nm. Energy transfer can only take place if the donor and acceptor beads are within 200 nm suggesting a direct protein:protein interaction has taken place.
FL MDM2 and MDM2 ΔT both bind to UbcH5α in an alpha screen (**figure 3.9b**), they bind with almost identical affinity. This confirms the protein binding assay, MDM2 can bind to UbcH5α in solution.

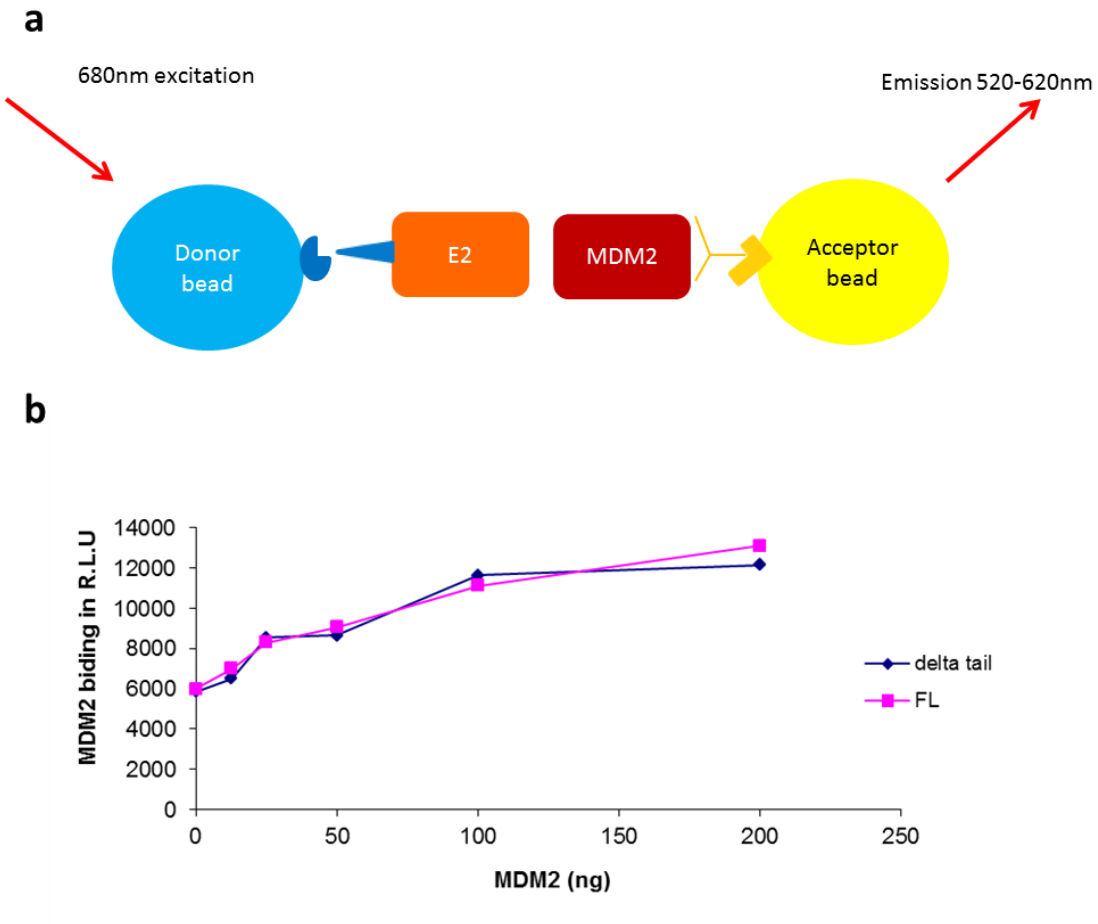

Figure 3.9: MDM2 binds to UbcH5α in solution, alpha screen. **a)** Schematic diagram showing the basic methodology of this alpha screen. **b)** Protein A acceptor beads (20 µl) preincubated with mouse monoclonal 4B2 then bound to FL MDM2 and MDM2 ΔT were incubated (in darkness) with nickel donor beads (20 µl) loaded with UbcH5α at room temperature for 1 hour. Graph shows the two proteins binding in solution expressed in relative light units (R.L.U).

3.1.5 MDM2 binds to ubiquitin

As discussed in the introduction, there are more than one class of E3 ligase. Those E3 ligases that contain a HECT domain accept ubiquitin from their partner E2, onto an active site cysteine, then transfer it to the target protein themselves. This is in contrast to E3 ligases containing a RING domain which are not considered to accept ubiquitin from their partner E2.

In order to determine whether, as recently suggested for RNF4 and ubiquitin[220], the RING of MDM2 can bind ubiquitin, a protein binding assay was carried out with ubiquitin and all four MDM2 constructs. In each case ubiquitin was captured onto the microtitre well and MDM2 was in the mobile phase (**figure 3.10a**).
FL MDM2 and MDM2 ΔT both bound to ubiquitin in a protein binding assay (**figure 3.10b**), this result is not seen if MDM2 is immobilised to the plate, again suggesting that the conformational flexibility of MDM2 is an important determinant of ubiquitin binding, just as for E2 binding.
This result is interesting for a couple of reasons; firstly given what is predicted about the E3 ligase mechanism, the question of why ubiquitin is binding is raised, possible explanations for binding are outlined in the discussion. Secondly this ELISA is very changeable, although binding is always seen the curves are variable, suggesting a low affinity but specific binding, Traditionally high affinity interactions have been thought to be more important physiologically, however it has been recently suggested that ubiquitin functions through many low affinity interactions[222], perhaps the interaction between ubiquitin and MDM2 is one of these low affinity interactions.
I next determined if the isolated RING domain was sufficient for ubiquitin binding.
RING ΔT and FL RING could both bind ubiquitin in a protein binding assay, unlike FL MDM2 they can bind ubiquitin regardless of whether they are immobilised or in the solution phase. The presence of the tail looks to have no effect on binding affinity. As with UbcH5α the tail is not necessary for binding ubiquitin.

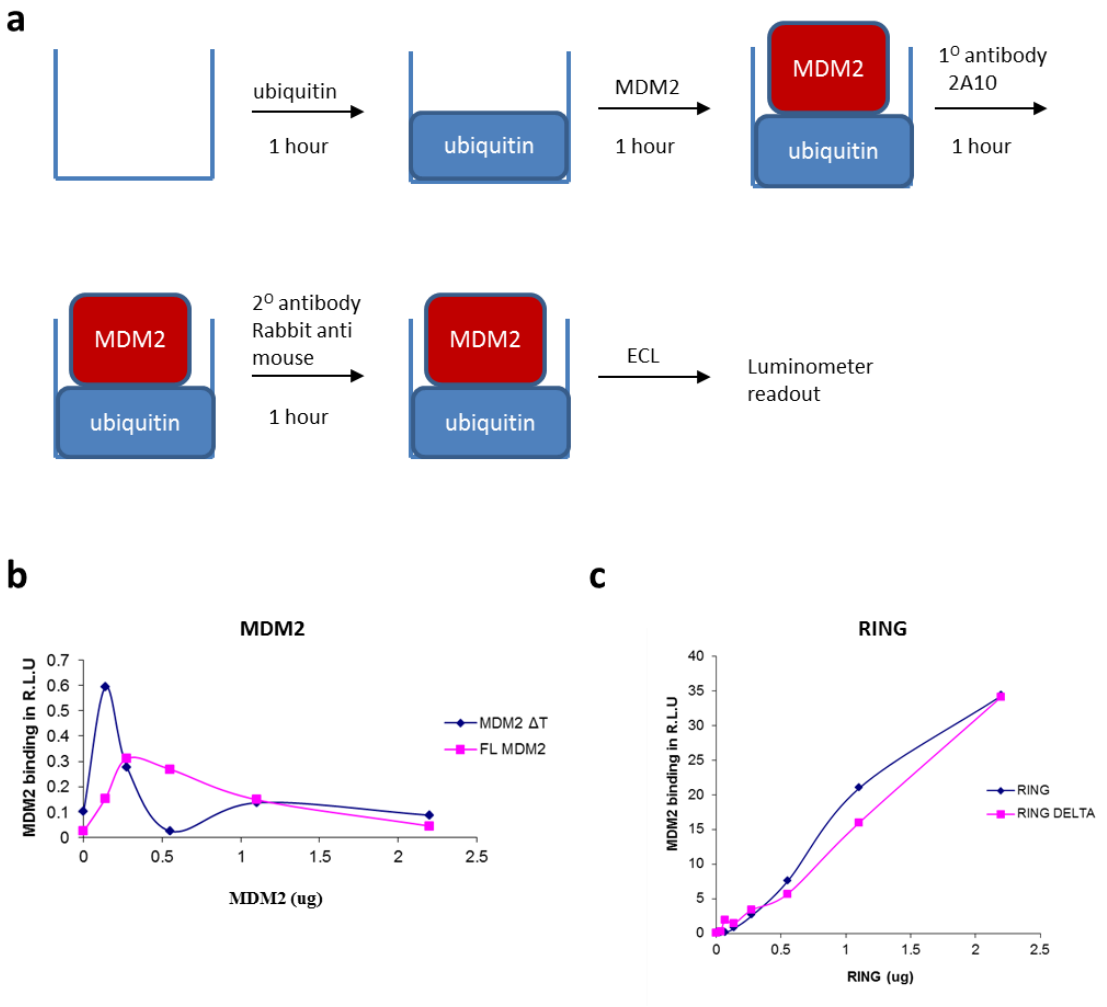

Figure 3.10: MDM2 binds ubiquitin in solution. a) Schematic diagram showing the basic methodology of this protein binding assay. **b)** Ubiquitin was captured onto microtitre wells (100 ng/well), a titration of FL MDM2 or MDM2 ΔT was added and incubated for 1 hour at room temperature. Unbound protein was removed by extensive washing and bound protein was detected using monoclonal antibody 2A10. Graphs show ubiquitin binding expressed as relative light units. **c)** Ubiquitin was captured onto microtitre wells (100ng/well), a titration of RING ΔT or FL RING was added and detected as above.

3.1.6 UbcH5α and ubiquitin bind to the same region of the RING domain

The previous experiments have shown that MDM2 can bind Ubch5α and ubiquitin, they further demonstrated that both proteins bind within the extended RING domain of MDM2 (i.e. residues 322-491). It is possible that one or both are binding to the unstructured region of outwith the RING domain i.e. amino acids 322-437. Based on what is known about other E2:E3 binding pairs however it is likely that UbcH5α, at least, is binding within the RING domain. Considering the link between UbcH5α, ubiquitin and the RING in the ubiquitination cascade it also appears possible that ubiquitin is binding within the RING domain.

The RING domain is 54 amino acids in length, assuming that both UbcH5α and ubiquitin bind within this domain the next point of investigation was to study where within the RING domain they bind. I first screened a RING-based peptide library. Each peptide is 20 amino acids in length and the peptides were highly degenerate with an overlap of 15 amino acids (16 in the case of peptide 8). There is one extra peptide (peptide 9) that is only 12 amino acids in length, this peptide represents the tail of MDM2. Each peptide has an N-terminal biotin tag with a Ser-Gly-Ser-Gly spacer (**figure 3.11a**).

A peptide binding assay was carried out with the RING peptides and UbcH5α (**figure 3.11b**). The aim was to first to confirm that UbcH5α bound within the RING domain of MDM2 and second to narrow down a specific area region(s) of the RING that are directly involved in UbcH5α binding. In each case the peptide was displayed on a streptavidin coated well before addition of UbcH5α in the mobile phase .

UbcH5α bound to peptide 8 to form a stable complex (**figure 3.11c**). This peptide contains the tail residues of MDM2 along with an extra 8 amino acids, it can be concluded therefore that one or more of these extra residues is important for binding as UbcH5α does not bind peptide 9, containing the tail residues in isolation.

There is some binding to peptide 7, this is unsurprising as it shares the 8 extra amino acids that may be important for binding, interestingly, although it does share these amino acids, UbcH5α binds with lower affinity. It is possible that the tail is involved in the binding of in UbcH5α as peptide 9 shows weak but reproducible binding. Taken with earlier data this suggests that the tail of MDM2 may play a positive role in MDM2 binding, but is not sufficient for binding. Furthermore residues present in

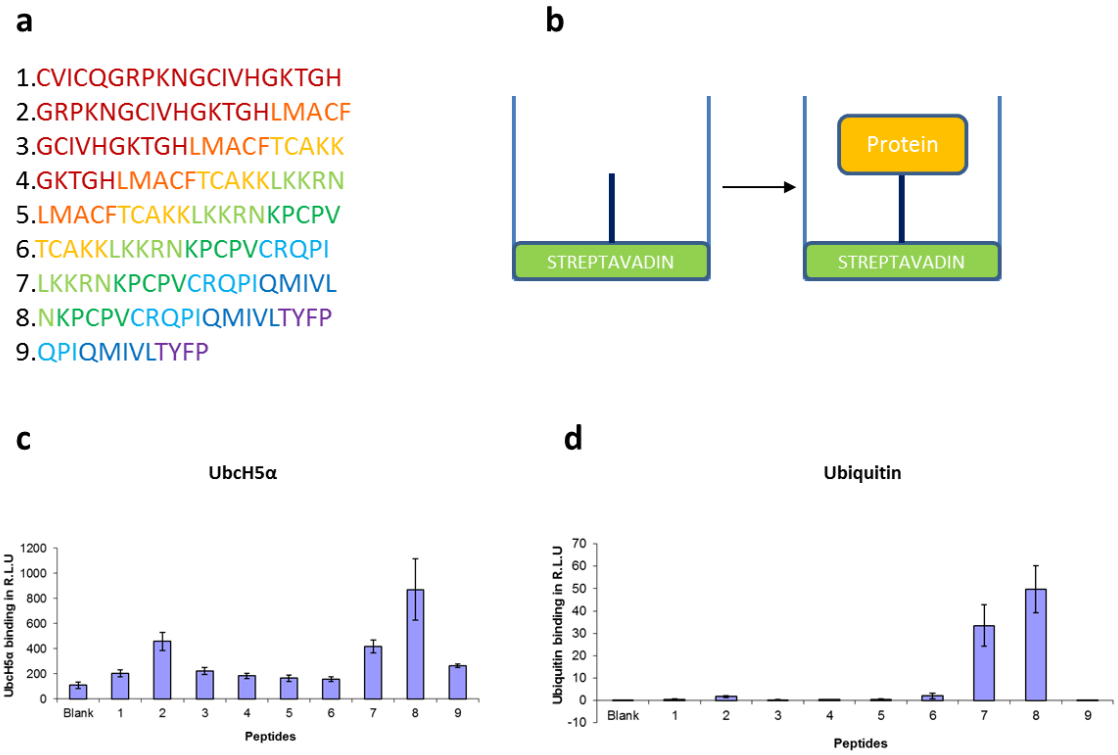

Figure 3.11: UbcH5α and ubiquitin bind to RING peptides. a) Diagram showing the amino acid sequences of the RING peptides. Colour sequence indicates overlapping residues. **b)** Schematic diagram showing the method of this peptide binding assay. The microtitre well is coated with streptavidin; biotinylated peptide is added and incubated, followed by the addition and incubation of protein. **c)** A series of biotin labelled RING peptides (100 ng/well) were captured onto streptavidin coated microtitre wells, UbcH5α (100 ng/well) was added and incubated for 1 hour at room temperature. Unbound UbcH5α was removed by extensive washing and bound protein was detected using anti-His antibody. Graph shows UbcH5α binding expressed as relative light units (R.L.U). **d)** A series of biotin labelled RING peptides (100 ng/well) were captured onto streptavidin coated microtitre wells, ubiquitin (100 ng/well) was added and binding was detected as above.

.

peptide 7 that are not present in peptide 8 could be having some sort of inhibitory affect, it is possible that they are partially blocking binding. There is also some binding to peptide 2, though it is weaker than peptide 8 binding this is consistent with data from other RING:E2 conformations which show a conserved point of contact in this reigon[37,223,224].

A second binding assay was carried out, this time with the RING peptides and ubiquitin. As before the RING peptides were displayed on a streptavidin coated well and ubiquitin was in the mobile phase.
Strikingly ubiquitin bound predominantly to peptide 8 and to a lesser extent peptide 7 (**figure 3.11d**), the ideas laid out above in relation to UbcH5α and peptide 7 binding may also apply here. The binding to peptide 7 and 8 is very similar to what is seen with Ubch5α however ubiquitin did not bind the tail peptide (peptide 9) as is seen with UbcH5α. This suggests that the tail by itself is not sufficient for ubiquitin to bind.

The results confirm that both UbcH5α and ubiquitin bind to MDM2, furthermore they imply that UbcH5α and ubiquitin bind to the same region of the RING domain though there are subtle differences in specificity.

3.1.7 Can the RING of MDM2, UbcH5α and ubiquitin form a trimeric complex?

Based on the data presented in the previous section the following question arises, can ubiquitin and UbcH5α bind the peptide 8 region of the RING to form a trimeric complex or is binding mutually exclusive (**figure 3.12a**)?

To answer this question a peptide binding assay was designed to determine which of these models was correct. It was known, from the results of a fellow student in the Ball group, that when UbcH5α is captured onto the plate and ubiquitin is in solution no ubiquitin binding is detected however when ubiquitin is captured onto the plate and UbcH5α is in solution UbcH5α binding can be detected. Knowing this an assay was carried out as follows, UbcH5α was captured onto the plate, peptide 8 was then added at a concentration high enough to saturate the binding sites of UbcH5α, unbound peptide 8 was subsequently washed away and a titration of ubiquitin was added. In theory if ubiquitin could bind to peptide 8 at the same time as UbcH5α, ubiquitin binding would be detected, if ubiquitin could not bind to peptide 8 at the same time as UbcH5α there would be no detection of ubiquitin binding (**figure 3.12b**). When ubiquitin was titrated into the assay an increase in ubiquitin binding was detected (**figure 3.13a**). The maximum concentration of ubiquitin was also added to a control well, with immobilised UbcH5α and no peptide 8, no ubiquitin binding was detected therefore it can be concluded that UbcH5α and ubiquitin can bind to peptide 8 simultaneously in this case

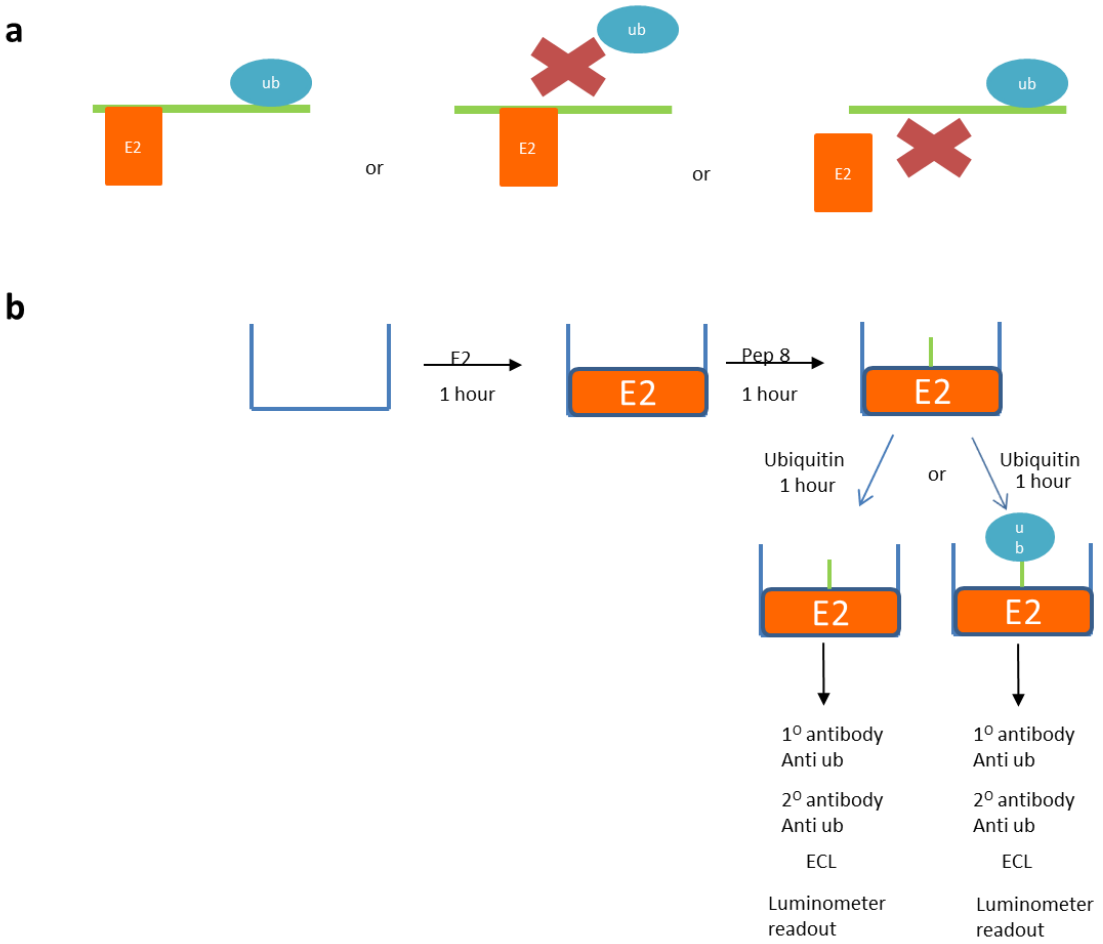

Figure 3.12: Can UbcH5α, ubiquitin and peptide 8 form a trimeric complex? a) Schematic diagram showing the possible models for UbcH5α and ubiquitin binding to the RING. They could form a trimeric complex or binding of the two proteins to a similar region of the RING could be mutually exclusive. **b)** Schematic diagram showing the basic methodology of the peptide binding assay designed to investigate which model was correct.

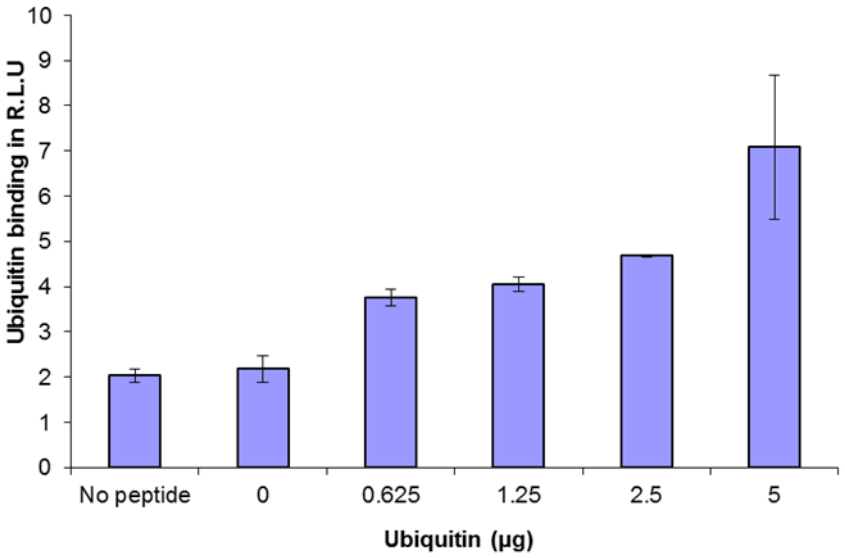

Figure 3.13: UbcH5α and ubiquitin bind to peptide 8 simultaneously. a) UbcH5α (100 ng/well) was coated onto microtitre wells, peptide 8 (100 ng/well) was added and incubated for 1 hour at room temperature. Unbound peptide 8 was removed by extensive washing. Ubiquitin was titrated in and incubated for 1 hour at room temperature. Unbound protein was removed by extensive washing and bound protein was detected by anti-ub antibody. Graph shows ubiquitin binding expressed as relative light units. The control had no peptide present and the maximum concentration of ubiquitin was titrated in. Ubiquitin, UbcH5α and peptide 8 form a trimeric complex in this assay.

3.1.8 Narrowing down residues important for UbcH5α and ubiquitin binding

What the previous result cannot confirm is the nature of binding of the two proteins, are they binding to completely different residues within the peptide or are they binding to opposing faces of the same peptide as has been described for PCNA and cyclin D binding to p2 [225] (**figure 3.14a**).
One possible way of identifying which one of the models of simultaneous binding is correct is to look in more detail at which specific residues in peptide 8 are important for UbcH5α and ubiquitin binding.

To do this an alanine scan of peptide 8 was used. An alanine scan of a peptide involves each residue being substituted for an alanine in turn. An alanine scan of peptide 8 for example resulted in 20 peptides that were all 20 amino acids in length and had an N-terminal biotin tag with ser-gly-ser-gly spacer (**figure 3.14b**). Using these peptides a peptide binding assay was carried out with the alanine scan peptides and UbcH5α, in each case the peptides were displayed on streptavidin coated wells with UbcH5α in solution. There was reduced binding to many of the alanine scan peptides (**figure 3.15a**), in particular when a tyrosine at position 489 of MDM2 was substituted for alanine (**figure 3.15a, peptide 28)** binding to both UbcH5α and ubiquitin was greatly reduced.

A second binding ELISA was carried out with the alanine scan peptides and ubiquitin. There was reduced binding to the majority of the alanine scan peptides (**figure 3.15b**), the binding trend is actually very similar to that of UbcH5α, once again substitution of the tyrosine at position 489 results in almost no binding of ubiquitin. The results suggest a broad interface is required for UbcH5α to bind. This binding interface does overlap with the binding interface for ubiquitin but there are residues which are specifically involved in ubiquitin binding. One such example is peptide 18, this peptide has an alanine in place of an arginine at position 479 of MDM2 and this substitution results in a significant decrease in ubiquitin binding, and only a marginal decrease for E2 binding.

a

b

11.AKPCPVCRQPIQMIVLTYFP
12.NAPCPVCRQPIQMIVLTYFP
13.NKACPVCRQPIQMIVLTYFP
14.NKPAPVCRQPIQMIVLTYFP
15.NKPCAVCRQPIQMIVLTYFP
16.NKPCPACRQPIQMIVLTYFP
17.NKPCPVARQPIQMIVLTYFP
18.NKPCPVCAQPIQMIVLTYFP
19.NKPCPVCRAPIQMIVLTYFP
20.NKPCPVCRQAIQMIVLTYFP
21.NKPCPVCRQPAQMIVLTYFP
22.NKPCPVCRQPIAMIVLTYFP
23.NKPCPVCRQPIQAIVLTYFP
24.NKPCPVCRQPIQMAVLTYFP
25.NKPCPVCRQPIQMIALTYFP
26.NKPCPVCRQPIQMIVATYFP
27.NKPCPVCRQPIQMIVLAYFP
28.NKPCPVCRQPIQMIVLTAFP
29.NKPCPVCRQPIQMIVLTYAP
30.NKPCPVCRQPIQMIVLTYFA

Figure 3.14: UbcH5α and ubiquitin bind the same region of the RING simultaneously, what is the nature of this binding? **a)** Schematic diagram showing two possible models for simultaneous binding of UbcH5α and ubiquitin to peptide 8. **b)** Diagram showing the amino acid sequences of the alanine scan peptides. Red indicates the residue that has been substituted for alanine.

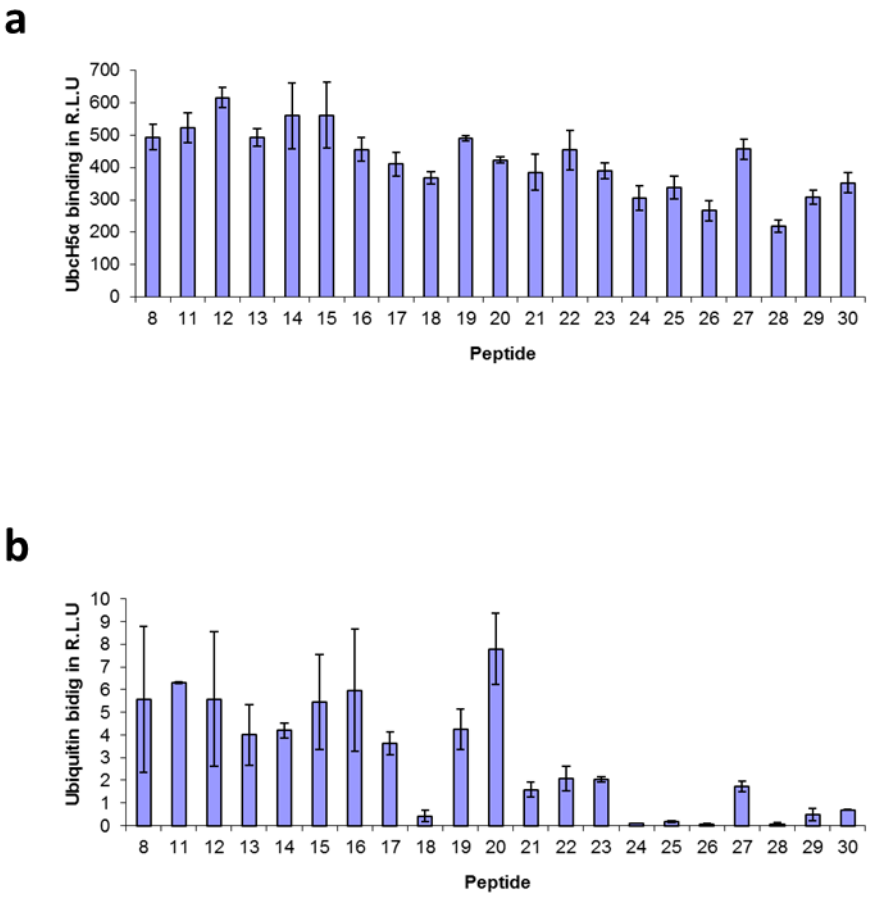

Figure 3.15: UbcH5α and ubiquitin binding to alanine scan peptides in comparison to peptide 8. A series of biotin labelled alanine scan peptides (100 ng/well) were captured onto streptavidin coated microtitre wells, UbcH5α (100 ng/well) **(a)** or ubiquitin (100 ng/well) **(b)** was added and incubated for 1 hour at room temperature, unbound protein was removed by extensive washing. UbcH5α was detected using anti-his antibody and ubiquitin was detected using anti-ub antibody. Graph shows binding expressed as relative light units (R.L.U).

As well as showing that there are differences in the binding interfaces of UbcH5α and ubiquitin this result also serves as quality control for the experiment. It cannot be argued that ubiquitin does not bind to peptide 18 because of some issue with peptide 18, i.e. none present in well, aggregated peptide, because UbcH5α does exhibit binding to peptide 18. This result is especially important in showing quality control as the binding interfaces between the two proteins are so similar.

The alanine scan has provided information regarding the residues involved in peptide 8 binding to UbcH5α and ubiquitin. It did not however help to decipher whether UbcH5α and ubiquitin bind to similar or distant residues (**figure 3.14a**). Substitution at 489 affects binding of both and this would suggest they bound similar residues, however a substitution at 479 only greatly affects ubiquitin, suggesting they bind distant residues. It is possible that both of them could have more than one point of contact with the RING and while they bind some residues that are distant from each other they also share a common point of contact too.

Reduced binding is seen for the most part when residues within the tail are substituted, when residues outside of the tail are substituted any change in binding affinity is slight. If this is considered along with all the previous results it suggests that the tail is not required for MDM2 to bind to UbcH5α and ubiquitin but conversely it important for this binding, these potentially conflicting ideas will be considered in the discussion.

3.1.9 Specific residues within the RING domain of MDM2 are important for UbcH5α and ubiquitin binding and for E3 ligase activity

Point mutations were introduced into the RING construct to replicate the data obtained using the alanine scan peptides. Peptides are useful tools for studying protein-protein interactions but it is important to consider that although the sequence is the same any tertiary structure that the protein has, any allosteric affect the domains exhibit towards each other, will not be replicated by the peptide. This is the reason for cloning the alanine substitutions into the protein. Thus an alanine was introduced at position 479, replacing an arginine, this protein shall be known as $RING^{R479A}$. In the other construct an alanine was introduced at position 489, replacing a tyrosine, this protein will be known as $RING^{Y489A}$. The point mutants were expressed, purified and stored in the same manner as RING ΔT and FL RING. The soluble protein yield of the point mutants is comparable and similar to RING ΔT and FL RING (**figure 3.16**).

In order to determine the properties of the RING point mutant proteins a protein binding assay was initially carried out to compare binding of the point mutants plus FL and ΔT RING domain protein constructs to UbcH5α. Both $RING^{R479A}$ and $RING^{Y489A}$ exhibit considerably less binding to UbcH5α than RING ΔT and FL RING (**figure 3.17a**) and $RING^{R479A}$ displays less binding than $RING^{Y489A}$, while the ability to form a stable complex is less both RING alanine mutants do still bind to UbcH5α.

Next the ability of the four RING domain protein constructs to bind to ubiquitin was compared using a protein binding assay. Ubiquitin was captured onto the well and the RING proteins were titrated in the mobile phase.
$RING^{Y489A}$ exhibited considerably less binding to ubiquitin than RING ΔT and FL RING, the ability of $RING^{R479A}$ to bind to ubiquitin was essentially abolished consistent with the effect of this substitution in peptide 8 (**Figure 3.17b**).
It is hard to reconcile the fact that when the entire tail is absent MDM2 can bind to UbcH5α and ubiquitin just as well as when the tail is present, yet one substitution in the tail can substantially decrease or near abolish binding. In the discussion the possible idea that the presence of the tail greatly influences the structure of MDM2 will be explored.

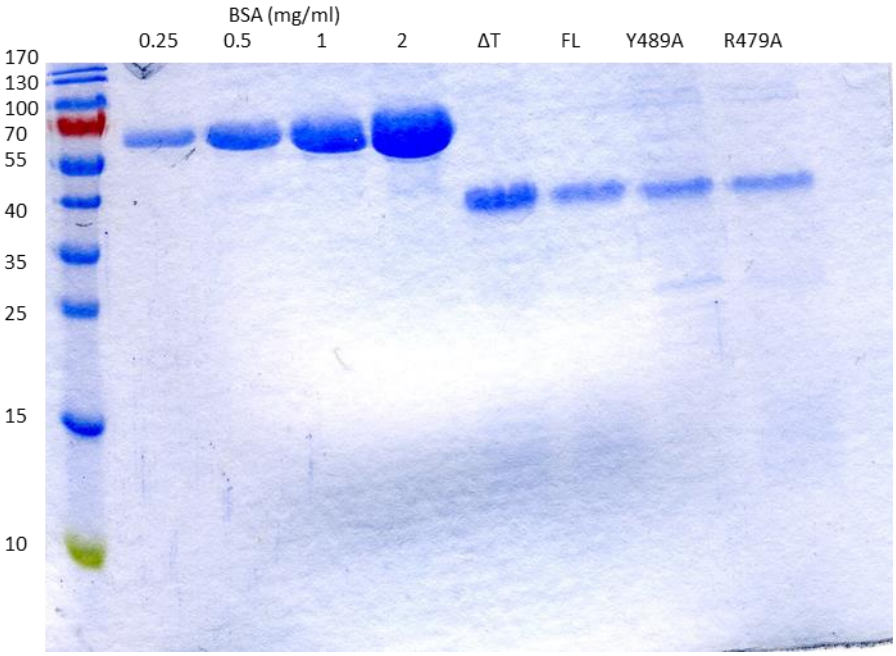

Figure 3.16: Purification of RING domain proteins. Coomassie stained 10 % polyacrylamide gel showing the purification of all four RING domain proteins in comparison to BSA protein standards. ΔT= RING ΔT, FL= FL RING, Y489A= $RING^{Y489A}$, R479A= $RING^{R479A}$. Fermentas PageRuler Prestained Protein Ladder used for molecular weight maker, all molecular weights displayed are in kDa.

Finally I asked how the decreased E2 and ubiquitin binding function of the RING mutants related to their activity in the E3 ligase assay. The four RING domain protein constructs were therefore compared in a ubiquitination assay to look for differences in E3 activity on p53 (**figure 3.17c**).

Interestingly the $RING^{Y489A}$ protein was not active as an E3 ligase (**figure 3.17c, lanes 6-7**). This RING could bind to UbcH5α and ubiquitin, albeit less than the wild type RING, suggesting that simply binding to Ubch5α and ubiquitin is not sufficient for E3 ligase activity, this is similar to RING ΔT which can bind UbcH5α and ubiquitin but is also inactive as an E3 ligase. The difference of course is that $RING^{Y489A}$ has the tail needed for E3 activity, but the tail has a mutation, these results suggest that the tyrosine at position 489 of MDM2 plays an important role in E3 ligase activity.

$RING^{R479A}$ was barely active as an E3 ligase (**figure 3.17c, lane 8-9**) there was a little activity but was far less than that of FL RING. $RING^{R479A}$ bound with much less affinity to UbcH5α and ubiquitin, a possible reason for its reduced E3 ligase activity.

These results show that both point substitutions result in decreased binding to UbcH5α and ubiquitin, this confirms the alanine scan peptide binding results. They also show that binding to UbcH5α and ubiquitin does not correlate precisely with E3 ligase activity and that binding is not sufficient for activity.

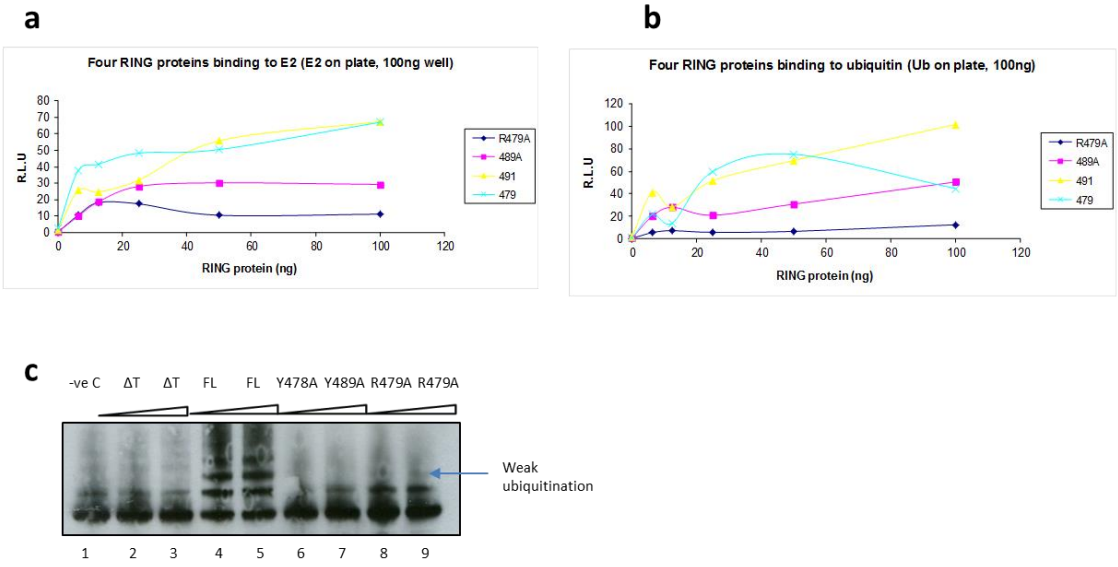

Figure 3.17: E3 ligase activity and Ubch5α and ubiquitin binding of all four RING domain protein constructs. UbcH5α **(a)** or ubiquitin **(b)** was captured onto microtitre wells (100 ng/well), a titration of FL RING or RING ΔT, RING^{Y489A} or RING^{R479A} was added and incubated for 1 hour at room temperature. Unbound protein was removed by extensive washing and bound protein was detected using monoclonal antibody 2A10. Graphs show binding expressed as relative light units (R.L.U). **c)** Blot showing no ubiquitination of p53 by RING ΔT (lanes 2-3), ubiquitination of p53 by FL RING (lanes 4-5), no ubiquitination of p53 by RING^{Y489A} (lanes 6-7) and ubiquitination of p53 by RING^{R479A} (lanes 8-9). Blot was probed by DO1. C-control, –ve negative control, ΔT- RING ΔT, FL- FL RING, Y489A- RING^{Y489A}, R479A- RING^{R479A}.

3.1.10 Discussion

The results presented in this chapter show that the 12 amino acid tail of MDM2 is necessary for E3 ligase activity. It is required for the discharge of ubiquitin from UbcH5α and also potentially the subsequent transfer of ubiquitin to the target p53. The obvious question arising from these results is 'Why is the tail critical for E3 activity?' Some research would suggest that the dimerization of MDM2 is key to answering this question.

Some RING domain containing proteins have been shown to dimerise, furthermore this dimerisation, either as a heterodimer such as BRCA1/BARD1[142] or a homodimer such as CHIP[143], is essential for E3 ligase activity. MDM2 can form homodimers[130] or heterodimers[140] with MDM4. Regardless of dimer type the tail has been implicated in dimer formation. One study showed that deletion of the 5 C-terminal amino acids of MDM2 resulted in no dimer formation[141]. In this study the last 5 or 7 C-terminal amino acids were deleted, and two new GST-tagged MDM2 proteins produced. They were analysed by gel filtration, and the two tail mutants eluted from the column in the same peak, they were resolved on a 12 % SDS page gel and both tail mutants present bands that correspond to monomeric protein. Conversely gel filtration studies of the RING by a former PhD student, working with Professors Walkinshaw and Ball, suggest that when the 12 amino acid tail was deleted the RING protein could still form a dimer. These results are at odds with each other but in the first study the entire tail was not deleted, just the last 5 amino acids. Maybe the structure of MDM2 changes less when the entire tail is deleted as opposed to just the five amino acids, and perhaps structure is just as important for dimer formation as contact residues. From the solution structure of the RING MDM2/MDM4 heterodimer a number of residues were implicated in the dimer interface, 5 were located within the tail (483, 485, 487, 488 and 489), but a further 6 were not[130]. It is possible that all these points of contact are important but it is also possible that some could be lost, such as in the tail, and a dimer would still be able to form. The solution structure shows that the tail is buried in the heterodimer with MDM4 (**Figure 3.18**), work from the Walkinshaw and Ball lab suggest the possibility that the tail is in a different position when E2 is bound, so now I ask, if the tail is in a different position, is it still involved in dimer formation?

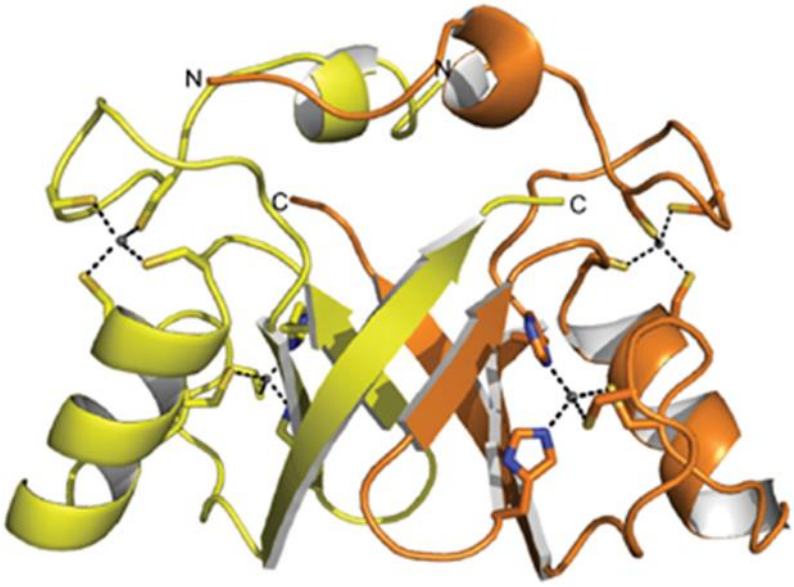

Figure 3.18: Structure of the MDM2/MDM4 RING domain heterodimer. a) Cartoon diagram of the MDM2l/MDMX RING domain heterodimer structure. MDM2 RING is shown in orange and MDMX RING in yellow, with the zinc ions and coordinating residues shown as spheres and sticks, respectively.

Figure from Linke K, Mace PD, Smith CA, Vaux DL, Silke J, Day CL. Structure of the MDM2/MDMX RING domain heterodimer reveals dimerization is required for their ubiquitylation in trans. Cell Death Differ 2008;15(5):841-8.

Secondly if the position of the tail, when E2 is bound, means that it is no longer involved in dimer formation can MDM2 still form a dimer or does it act as a monomer with E2 bound?

Research is conflicting as to whether MDM2 must be a dimer to be active as an E3 ligase, there are those that report E3 ligase activity regardless of whether MDM2 is in monomer or dimer form[141], others report that it must be a dimer to be active[102]. Looking at some dimer studies it is unclear whether a monomer was used as a control for activity. Research is still clearly ongoing regarding MDM2, dimerisation and activity. If however dimerisation is required for activity and the tail is required for this dimerisation then this would explain why MDM2 ΔT is inactive as an E3 ligase.

Another explanation for the necessity of the tail in E3 ligase activity is the role that the tail may play as an allosteric activator, this leads to the UbcH5α results. At the start of this chapter I set out to show that MDM2 could bind to UbcH5α in solution. The results show that FL MDM2 and MDM2 ΔT can both bind to UbcH5α and that the tail is not necessary for this binding. Clearly simply binding to UbcH5α is not sufficient for E3 ligase activity, as MDM2 ΔT is not active. The tail must have another role in E3 ligase activity other than binding to UbcH5α.

There is the view that proteins containing a RING domain act as a scaffold, orientating a substrate and ubiquitin conjugating enzyme in a manner optimum for ubiquitination[28,34]. This hypothesis is challenged by crystal structures of RING domain containing complexes which show the substrate and ubiquitin conjugating enzyme a distance apart[39] making it unclear whether the ubiquitin could be transferred from ubiquitin conjugating enzyme to the substrate. My results also challenge the orientation hypothesis, MDM2 ΔT can bind both p53 and UbcH5α and yet there is no ubiquitination of p53. Whilst not discounting orientation entirely, certainly it may play an important role in E3 ligase activity, there must be more to MDM2s E3 ligase activity than simply binding and orientating UbcH5α.

One idea is that E3 ligases can allosterically activate their partner E2s, and it has been suggested that UbcH5α has the potential to be allosterically activated[35].

If UbcH5α can be allosterically activated and MDM2 is the cause of the activation then it is possible that residues within the tail are responsible for the activation of UbcH5α and subsequent E3 ligase activity.

It has been suggested in the literature that MDM2 cannot form a stable interaction with UcbH5α *in vitro* and there is no published data for MDM2 bound to UbcH5α. In contrast I have shown that MDM2 can bind UbcH5α in solution, although this precise result had not been previously shown, the result was not totally unexpected, there are many examples of E3 ligases binding to their specific E2. However my results show that the RING and UbcH5α can form a stable complex in the absence of ubiquitin, data that has not been show until now. A much more unexpected result was that of MDM2 binding to ubiquitin. It was unexpected as E3 ligases containing a RING domain are traditionally thought to act as a scaffold protein bringing to together their E2, charged with ubiquitin and target substrate before catalysing the transfer of ubiquitin between the two, this does not involve the RING binding to ubiquitin.
It has been reported that RNF4, another E3 ligase that contains a RING domain, can bind to ubiquitin, there are however a number of difference between their experiments and my results. They report that ubiquitin alone has no detectable binding affinity for the RING of RNF4, they only show ubiquitin contacting the RING after it is linked via a thioester bond to E2[220]. It is also worth noting that this study describes the interaction between free UbcH5α and RNF4 as very weak, RNF4 only binds tightly to UbcH5α when it is charged with ubiquitin.

RNF4 and MDM2 both contain RING domains and UbcH5α is their E2 partner, but it is important to remember that they are different proteins, within the RING domain MDM2 has unique zinc coordination and also contains an integrated ATP binding site, the like of which is only found in MDM2 and MDM4. It is possible that MDM2 can bind to ubiquitin and UbcH5α alone, without the need for them to be linked to each other and equally possible that RNF4 can only bind to ubiquitin and, to some degree, UbcH5α once they have the thioester link to each other. Considering the data obtained from the RNF4 study it could also be that although MDM2 can bind to ubiquitin and UbcH5α alone, as my results show, it is possible that the RING will have higher affinity for ubiquitin once it is bound to UbcH5α and also likewise higher affinity for UbcH5α once it is bound to ubiquitin. In fact during the course of my PhD

I attempted to use the complex utilised in the Hay paper[220], in which the E2 was mutated so that it was constantly linked to ubiquitin. I wanted to use this E2-ubiquitin to test the affinity of MDM2 for the complex in contrast to the free E2 and ubiquitin. I was kindly sent the plasmid to work with, however I found this mutated E2-ubiquitin complex to be highly unstable, the ubiquitin would spontaneously discharge from the E2, students of the Hay lab had warned that it was very difficult to work with and in the end I decided that this mutated complex was not suitable for my experiments.

If MDM2 can bind to ubiquitin this could suggest that it is acting more like an E3 ligase that contains a HECT domain, and accepting ubiquitin from UbcH5α before transferring to the target. Or, more likely, MDM2 still catalyses the transfer of ubiquitin to targets via UbcH5α, with ubiquitin contact playing a different role altogether. As I have shown that free ubiquitin binds to MDM2 it is possible that MDM2 is acting as a ubiquitin binding domain protein.

I have shown that MDM2 binds to both UbcH5α and ubiquitin. My results from peptide binding ELISAs (**figure 3.11c and d**) indicate that UbcH5α and ubiquitin are binding to the same region of the MDM2 RING domain, they both interact with a residue or residues within peptide 8. There was some cause for hesitation in believing that this was a true result, there was always the possibility that some characteristic of the peptide resulted in it being 'sticky'. A closer look at the peptide binding ELISA profiles revealed that whilst they are very similar there a some distinct differences, for example UbcH5α shows some binding affinity for peptide 9, binding that ubiquitin does not exhibit. Some of the binding seen for certain peptides then is protein specific, and it is possible that UbcH5α and ubiquitin both have a genuine binding affinity for peptide 8.

At the time these peptide binding ELISA results were being obtained a fellow PhD student, Dr Vivien Landre, was studying the computer modelling of complexes, using programmes HADDOCK, that docks proteins onto one another, and molecular dynamic simulations, that predicted the most energetically favourable structure for a complex. Independently of my peptide ELISA results she produced a model of the MDM2 RING with UbcH5α and ubiquitin, showing the predicted location on the RING that they both may bind (**figure 3.19**).

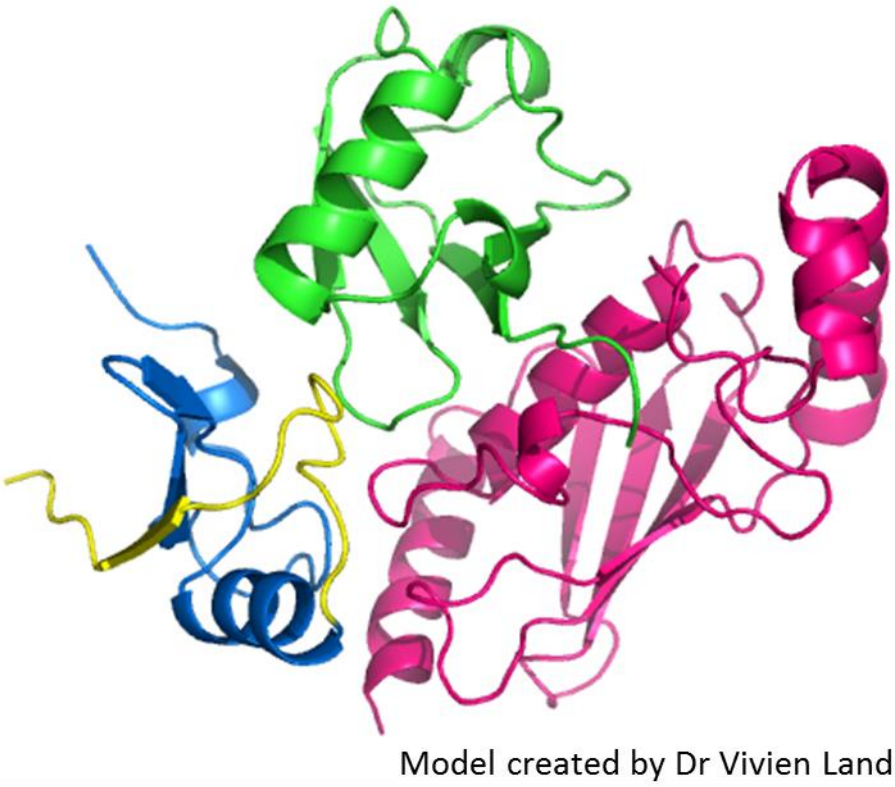

Figure 3.19: Predicted model of MDM2 RING:UbcH5α:ubiquitin complex. UbcH5α is represented by the pink molecule, ubiquitin is represented by the green molecule and MDM2 RING is represented by the blue and yellow molecule. The residues of peptide 8 have been highlighted in yellow. They form a free flexible loop that is in position to bind UbcH5α and ubiquitin.

In this model I have highlighted the residues that correspond to peptide 8 (**figure 3.19, residues highlighted in yellow**), these residues form a free flexile loop that leads on to the C-terminal tail. The program predicts that both UbcH5α and ubiquitin can bind to this region, orientating them close to the free flexible loop. The fact that **u**biquitin may possibly bind to this region is at odds with the literature, the majority of characterised ubiquitin binding domains are α helical[65]. If ubiquitin can truly bind to this region it would be very different to previously defined ubiquitin interactions. All the helical ubiquitin binding domains bind to the residue Ile 44, in the model this residue is far from the predicted ubiquitin:RING interface.
This model does help to confirm that my peptide binding ELISA results are showing true binding affinity and are likely not the result of a sticky peptide.

3.1.10.1 Comparison of MDM2 RING and RNF4 RING binding to UbCH5α and ubiquitin

Compiling all the data so far I was confident that UbcH5α and ubiquitin were binding to a similar region of the RING domain. What still remained unclear was whether they could bind to this same region simultaneously or if they could only bind one at a time, perhaps due to steric conformation or both proteins requiring the same residue for binding. At the start of my PhD there was no published data relating to a RING, E2, and ubiquitin model. The predicted model (**figure 3.19**) developed by Dr Vivien Landre, indicated that both UbcH5α and ubiquitin are binding the RING simultaneously, however this was only a prediction and needed to be validated experimentally.

At about this time the Hay lab brought out two sequential papers[37,220] discussing the RNF4 RING, E2, ubiquitin complex. I am going to discuss these two papers and the similarities and differences seen in my results.

The first study published contradicted the predicted model that I had, as the study with RNF4 reported that one subunit of the dimer contacted the E2 and the other subunit contacted ubiquitin, the same subunit did not contact both, as indicated in my model. They showed that one monomer of the RNF4 homodimer contacted the ubiquitin charged UbcH5α and that the thioester linked ubiquitin then reached across

the dimer to contact the second monomer. In this model Ile44 of ubiquitin is involved in RING contact, corresponding with what is known about ubiquitin binding, they reported that Ile 44 contacts a tyrosine within the RING, this tyrosine is involved in the dimer interface and is not involved in an α helix[220]. If this is true it is similar to my results in that I see ubiquitin binding to a region other than an α helix. This study presumes that the interaction of UbcH5α with one monomer and ubiquitin with the other alters the conformation of the active site of UbcH5α facilitating ubiquitin transfer, but there is no mechanism provided for this theory.

Considering the conflicting models from the computer simulation and from the RNF4 study I designed an ELISA that would confirm if MDM2 could bind to UbcH5α and ubiquitin simultaneously or separately. The ELISA showed that UbcH5α and ubiquitin could bind to peptide 8 simultaneously (**figure 3.13**). In this ELISA both UbcH5α and ubiquitin were free, they were not linked by a thioester, or amide, bond. In contrast to the RNF4 study my results show that as well as binding to the RING domain simultaneously, UbcH5α and ubiquitin also bind independently of one another. My ELISA does not provide information on the binding location of the two proteins, we do not know if they are binding completely different regions of the peptide or if they are binding different interfaces of the same residues with the peptide acting as a molecular glue (**figure 3.15a**).

The follow up study on RNF4, published a year later shows a complete turn of events. This study provides a crystal structure of the RNF4 homodimer linked to UbcH5α charged with ubiquitin. From the crystal structure they conclude that some residues of ubiquitin contact the same monomer as UbcH5α while others contact either the second monomer or even both subunits of the dimer[37]. Ile44 highlighted to be so important for contact in the first study was not mentioned in the second, in fact the previous model is not mentioned in this second study. If I take the crystal structure from this second study to be the correct model from the two published papers, then it does correspond well with my ELISA results and predicted model.

I overlaid the crystal structure of the RNF4 homodimer with the MDM2/MDM4 heterodimer, then inserted the MDM2/MDM4 heterodimer into the crystal structure of the RNF4:UbcH5α:ubiquitin protein complex (**figure 3.20**). The resulting structure is

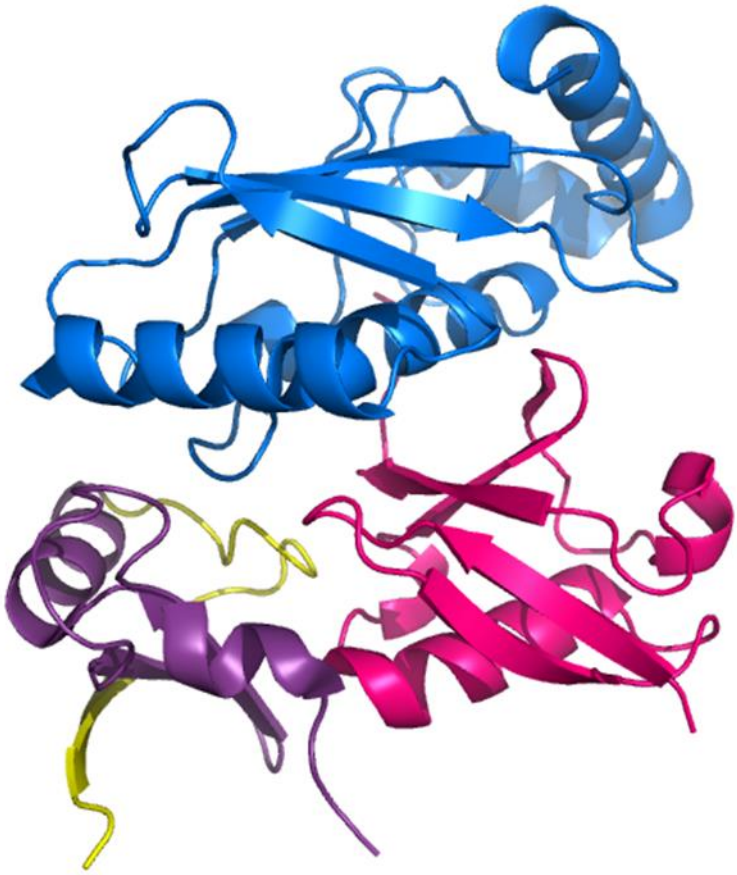

Figure 3.20: MDM2/MDM4 heterodimer inserted into the RNF4 RING:UbcH5α:ubiquitin complex. Only the MDM2 monomer half of the dimer is shown. UbcH5α is represented by the blue molecule, ubiquitin is represented by the pink molecule and MDM2 RING is represented by the purple and yellow molecule. The residues of peptide 8 have been highlighted in yellow. They form a free flexible loop that is still in position to bind UbcH5α and ubiquitin. This model from the crystal structure can be compared to the predicted model in **figure 3.19**.

actually very similar to the predicted model, peptide 8 still forms the free flexible loop and UbcH5α and ubiquitin are orientated so that they could contact this region.
This is a positive outcome for the validity of my results but there are a number of issues with the crystal structure that need to be considered. In the crystal structure the ubiquitin is linked to UbcH5α not by a thioester bond but instead an amide bond, it is possible that this could have an affect with the points of contact with the RING for one or both proteins. Also in this crystal structure the C-terminus of one monomer has been directly cloned onto the N-terminus of the other monomer, the tail, which is thought to be so important for E3 activity in MDM2, is not free. Not only might this compromise the true contact residues of UbcH5α and ubiquitin with the RING it also means that there is no indication for the role of the tail in E3 activity.

If I am to assume that UbcH5α and ubiquitin are binding to the same subunit of the RING then questions arise about the role of the tail. It may be involved in dimer formation, this information is not provided in the crystal structure, as the dimer is 'forced'. If the tail is involved in dimer formation then why is the dimer itself so important if both proteins are binding to the same subunit of the dimer? The tail could also be involved in the allosteric activation of UbcH5α and/or ubiquitin once they are bound to the RING, facilitating the transfer of ubiquitin to the target, again the crystal structure cannot provide any information regarding this as the tail is static, not free.

In conclusion the crystal structure in the second published study gives validity to the predicted computer model of the MDM2-E2-ubiquitin complex and also my ELISA results that show UbcH5α and ubiquitin can bind the same region of the RING simultaneously. The published structure does not however provide me with information regarding the oligomeric status of MDM2, nor does it offer a role of the tail of MDM2 in either dimer formation or activity.

3.1.10.2 Further dissecting UbcH5α and ubiquitin binding to the RING of MDM2

From the alanine scan binding results (**figure 3.15**) it looks as if multiple residues are important for both UbcH5α and ubiquitin binding to the MDM2 RING, no one residue is solely responsible for protein binding. The binding profiles of UbcH5α and

ubiquitin to the alanine scan peptides look fairly similar with the tail residues being important, especially the tyrosine at position 489 of MDM2. There are some differences, the ubiquitin interface is possibly more compact than the UbcH5α interface and one distinct difference in the profiles is that when an arginine at position 479 is substituted for alanine the impact on ubiquitin binding is much more severe than that on UbcH5α binding. These mutations impacted on E3 ligase activity as well as protein binding, $RING^{R479A}$ showed decreased E3 ligase activity whereas in $RING^{Y489A}$ E3 ligase activity was completely lost. The result with $RING^{Y489}$ corresponds to the result already published, in which the tyrosine at position 489 in FL MDM2 is mutated to alanine[133]. These results simply add to the questions surrounding the tail.

The tail is not necessary for MDM2 RING binding to UbcH5α or ubiquitin, from the model this makes sense as the tail is nowhere near these two proteins. When the tail is present however the results suggest that the integrity of the residues within the tail is very important, as one substitution significantly affects protein binding. It is possible that the tail is not necessary for the structure of the RING required to bind UbcH5α or ubiquitin, hence why MDM2 ΔT can bind to both, yet when the tail is present it greatly influences the structure hence why a substitution of a tail residue could cause such a decrease in protein binding. Some of these questions could be potentially addressed by using E2-linked ubiquitin. As the system outlined in the Hay studies[220] proved to be unstable I would investigate using a more stable E2-ubiquitin complex, for example a stable complex made using 'click chemistry'. Click chemistry has already been used to stably link ubiquitin to PCNA. In this technique artificial amino acids that carried an azide or alkyne side chain were incorporated into ubiquitin and PCNA respectively. The two proteins were then linked site specifically by the Cu (I)-catalysed azide-alkyne cycloaddition[226].

The alanine substitution at position 479 of MDM2 provides yet more puzzling information. MDM2 ΔT shows us that simply binding to UbcH5α and ubiquitin is not enough for E3 ligase activity. $RING^{R479A}$ shows decreased binding to both UbcH5α and ubiquitin and exhibits decreased E3 ligase activity, this result could imply that, in this case at least, binding is related to E3 ligase activity. Other explanations for this correlation include the arginine that is involved in protein binding is also involved in allosteric E3 ligase activity, and so substituting it results in decreased activity.

Alternatively, as well as protein binding, this residue could be involved in maintaining the correct structure of MDM2, and this structure could be important for E3 activity.
Lastly this mutant exhibits negligible ubiquitin binding, either this small amount of possible binding is enough for E3 ligase activity, or, although MDM2 can bind to ubiquitin, it does not actually need to for E3 ligase activity.

When the tyrosine at position 489 of MDM2 is substituted for alanine once again there are more questions are raised than answers. RING^{Y489} can still bind to UbcH5α and ubiquitin but is completely inactive as an E3 ligase. Binding alone is not sufficient for E3 ligase activity so this tyrosine must play a different role in activity.
It has been reported that an aromatic residue at this position is critical for E3 ligase activity[133]. A tyrosine or phenylalanine is often seen at the corresponding position in various RING E3 ligases.
RNF4 has a tyrosine at the corresponding position within its RING domain, in this case the tyrosine is implicated in dimer formation[220]. When this tyrosine is substituted for alanine in the MDM2 RING however, MDM2 can still homo-oligomerise or hetero-dimerise with wt MDM4[133]. Interestingly the homo-oligomer displayed no E3 ligase activity whereas the hetero-oligomer displayed the ability to target p53 for degradation in cells. This suggests that if MDM2 does function as a dimer that only one wt tail is required for activity. Perhaps one subunit binds to the proteins and the tail of the other allosterically activates them, facilitating ubiquitin discharge. MDM2 has also been shown to act as a monomer, it may be that it can act as a monomer or dimer as long as at least one wt tail is present. I have shown that RING^{Y489A} can bind to UbcH5α and ubiquitin, if I gave this protein the chance to oligomerise with wt RING it is possible that E3 ligase could be restored due to the wt tail present on the RING.

To summarise, the C-terminal tail of MDM2 is required for E3 ligase activity. The tail is not required for binding to UbcH5α or ubiquitin but when it is present residue integrity is important for binding. Binding to UbcH5α and ubiquitin is not sufficient for activity and certain residues within the tail are critical for E3 ligase activity. It is possible that residues within the tail are having an allosteric effect on either UbcH5α or ubiquitin, the mechanism of this possible activation and the subsequent ubiquitin

transfer to the target remains unclear. The next step in my investigation was to look at whether MDM2 could have an allosteric effect on either UbcH5α or ubiquitin.

Chapter 4: RESULTS

4.1 Allosteric activation of UbcH5α by MDM2

4.1.1 Introduction

Data in my previous chapter showed that the RING of MDM2 could bind to UbcH5α in solution. This was consistent with published data showing other RING proteins binding to an E2 partner[36-38]. My data also showed that the 20 C- terminal amino acids of the MDM2 RING were important for E2 binding.

The next question to address was the role that E2-E3 binding had in the mechanism of RING-dependant E3 ligase activity. The mechanism for how RING E3s transfer ubiquitin to a target protein remains unclear, though there are theories that hint at the role(s) that this binding may play in the overall mechanism of ubiquitination.

The first theory was that the RING E3s acted as scaffold proteins, bringing together ubiquitin bound E2 and the substrate and orientating them in such a position as to optimise ubiquitin transfer[28,34]. Later structural studies have revealed that this is unlikely to be the sole mechanism of RING E3 activity, though it may play a part, as the E3 binding site within E2 is ~15Å away from the active site cysteine[39,227]. Even in the correct orientation it is unclear whether ubiquitin could transfer from E2 to substrate at that distance. Structural studies also showed no clear structural difference between free E2 and E2 bound to E3 that would explain the enhanced activity of the E2[34].

More recent studies are now suggesting that E2s can be allosterically activated by their E3[35]. One such study looking at the interaction between the RING E3 ligases BRCA1/BARD and E4B with UbcH5c indicated an allosteric activation of the E2 by E3. Using NMR they showed that E2-ubiquitin conjugates favoured a more closed conformation upon E3 binding. The study also noted that leucine 104, a highly conserved residue throughout the E2 family was important for this closed conformation and that mutating it to glutamine decreased E3 ligase activity[228].

Questions

1) Is UbcH5α allosterically activated by MDM2

   a. Can peptide 8 be used as a tool to study potential allosteric regulation?
   b. Can biochemical and biophysical assays be used to detect allosteric changes and the residues of UbcH5α involved?

2) Can the areas of MDM2 responsible for activation be identified and is there a role for the tail?

4.1.2 Peptide 8 can be used to study the interaction between UbcH5α and ubiquitin

My previous data (see Chapter one) has shown that peptide 8 can bind to UbcH5α and ubiquitin in a manner similar to FL MDM2 and FL RING. I therefore wondered if peptide 8 could replace FL MDM2/FL RING in activating UbcH5α to discharge ubiquitin onto a ubiquitin acceptor (**figure 4.1a)**.

I carried out a discharge assay in which I added MDM2 peptide, as opposed to MDM2 protein, after the E2 had formed a thioester bond with ubiquitin. Peptide 8 was able to partially discharge ubiquitin from the E2 (**figure 4.1b, lane 10**). This result is similar to what is seen when FL MDM2 is used in this assay (**figure 3.6b**). Peptide 9 was also able to partially discharge ubiquitin from the E2 (**figure 4.1b, lane 11**). This is interesting as it implies that the tail of MDM2 has a role in facilitating the transfer of ubiquitin from the E2 to the target even though the tail itself does not bind to ubiquitin (**figure 3.11d**). Ubiquitination assays carried out with peptide 8 were inconclusive (data not shown). No discharge of ubiquitin is seen by peptide 1, and so I used peptide 1 as a control as it does not exhibit binding to the E2 or ubiquitin.

As peptide 8 and 9 were able to affect a partial discharge of ubiquitin from UbcH5α I next asked whether the ability of MDM2 to mediate p53 ubiquitination relied solely on its E2 activating activity or if this is only a part of its function in substrate ubiquitination. If activating the E2 was MDM2s only function than peptide 8 should be sufficient to ubiquitinate p53. Ubiquitination assays were inconclusive; this is likely due to the fact that MDM2 has other roles in substrate ubiquitination other than activating the E2. However this assay can be difficult to optimise and would have to be repeated before any definite conclusions were made. As low amounts of UbcH5α can bind to peptide 8 and peptide 8 is able to mimic the majority of activity displayed by FL MDM2 in E2 activation, I used peptide 8 as a tool to determine whether MDM2 could act as an allosteric regulator of UbcH5α.

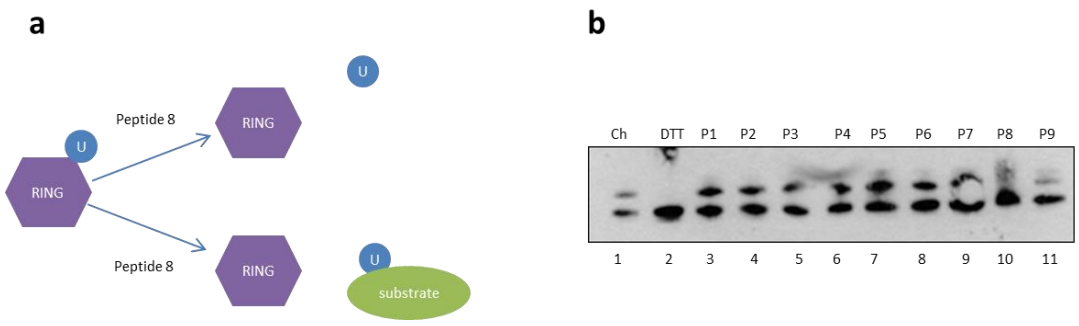

Figure 4.1: Peptide 8 can mimic FL MDM2 in an activity assay. a) Schematic diagram showing the possible activity of peptide 8 There is the possibility that peptide 8 is sufficient to discharge ubiquitin from the RING, or there is the possibility that peptide 8 is not only sufficient to discharge ubiquitin from the RING but also able to transfer ubiquitin to the target substrate. **b)** Blot showing discharge of ubiquitin from UbcH5α by peptide 8 and peptide 9 (**lanes 10 + 11**). Blot does not show discharge of ubiquitin by control peptide 1 (**lane 1**). Blot was probed by anti-His antibody. Ch- charged, DTT- DTT control, P1- P9= peptides 1 to 9.

4.1.3 Proteolysis of UbH5α

The precise mechanism of how RING E3s transfer ubiquitin from the E2 protein to the substrate remains unclear. It has been suggested that E2s can be allosterically activated by the RING[35,228]. I have shown that the MDM2 RING binds to UbcH5α and so my next question was could I determine if the MDM2 RING allosterically activated UbcH5α. I used partial proteolysis to determine if evidence could be found for a difference in conformation between free E2 and an E2:peptide 8 complex. If there is a conformational change it may be possible to see different digestion products on a gel (**figure 4.2**).

I set up a proteolysis assay in which UbcH5α (20 µg) was incubated at room temperature for 10 minutes with or without peptide 8 (5 µg). Following incubation a protease was added, this was either trypsin, Arg-C or Glu-C (0.5 µg/µl) at a ratio of 1:100 (W/W) with UbcH5α. The reaction was allowed to proceed for a set length of time (15 or 30 min) at a set temperature (4 or 30 ^{o}C). The reaction was terminated by the addition of sample buffer (1x) and incubation at 80 ^{o}C for 3 min. The entire digest reaction was run on an SDS polyacrylamide gel before staining with coomassie blue to detect digest products.

Trypsin cleaves at the C-terminus of lysine and arginine, except when followed by a proline and digests free UbcH5α (~15kDa) to form one primary product of molecular weight ~12kDa. On the other hand UbcH5α in complex with peptide 8 was relatively resistant to cleavage and a higher proportion of the E2 remained undigested (**figure 4.3a**). After 15 min at 30 ^{o}C free UbcH5α was almost completely digested (**figure 4.3a, lane 4**), when the reaction was allowed to proceed to 30 minutes digestion was complete (**figure 4.3a, lane 2**). In contrast, when in complex with peptide 8, the rate of digestion of UbcH5α was slowed (**figure 4.3a, lanes 1 and 3**). When the reaction was carried out at 4 ^{o}C the rate of digestion decreases but after 30 min free UbcH5α was still sensitive to cleavage. (**figure 4.3a, lanes 5 and 6)**. Arg-C cleaves at the C-terminus of arginine and also cleaved to produce an ~12kDa band however Arg-C was not as efficient at cleavage of UbcH5α as Trypsin under the conditions of the assay. Similar to the trypsin reactions the addition of peptide 8 increased the resistance of UbcH5α to cleavage by Arg-C. (**figure 4.3b**).

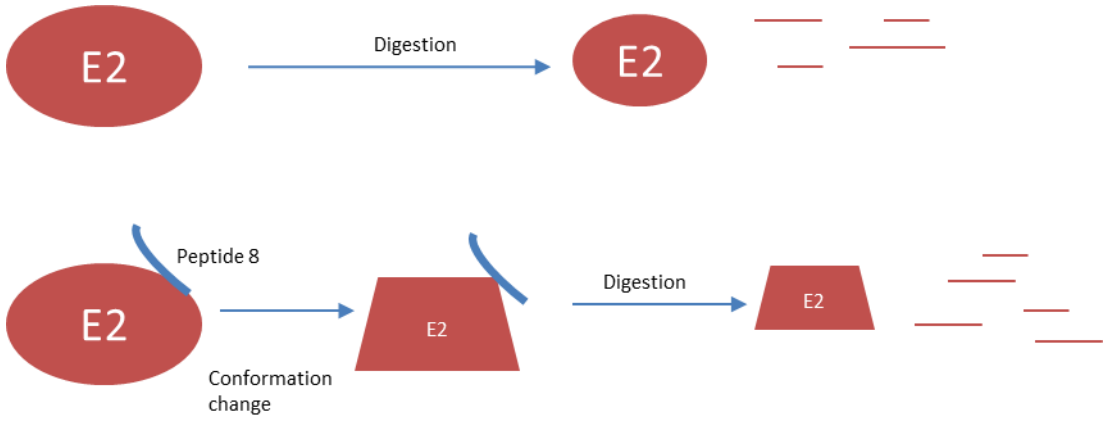

Figure 4.2: Model of how peptide 8 could result in a conformational change and different digestion products of UbcH5*α*. If the E2 contains exposed recognition sites for a protease it will give a certain digestion pattern. If peptide 8 binding results in a conformational change of E2 then there is the possibility of previously exposed recognition sites for a protease being buried and buried recognition sites being exposed. This will provide different size/shape fragments which will present differently on a coomassie stained gel.

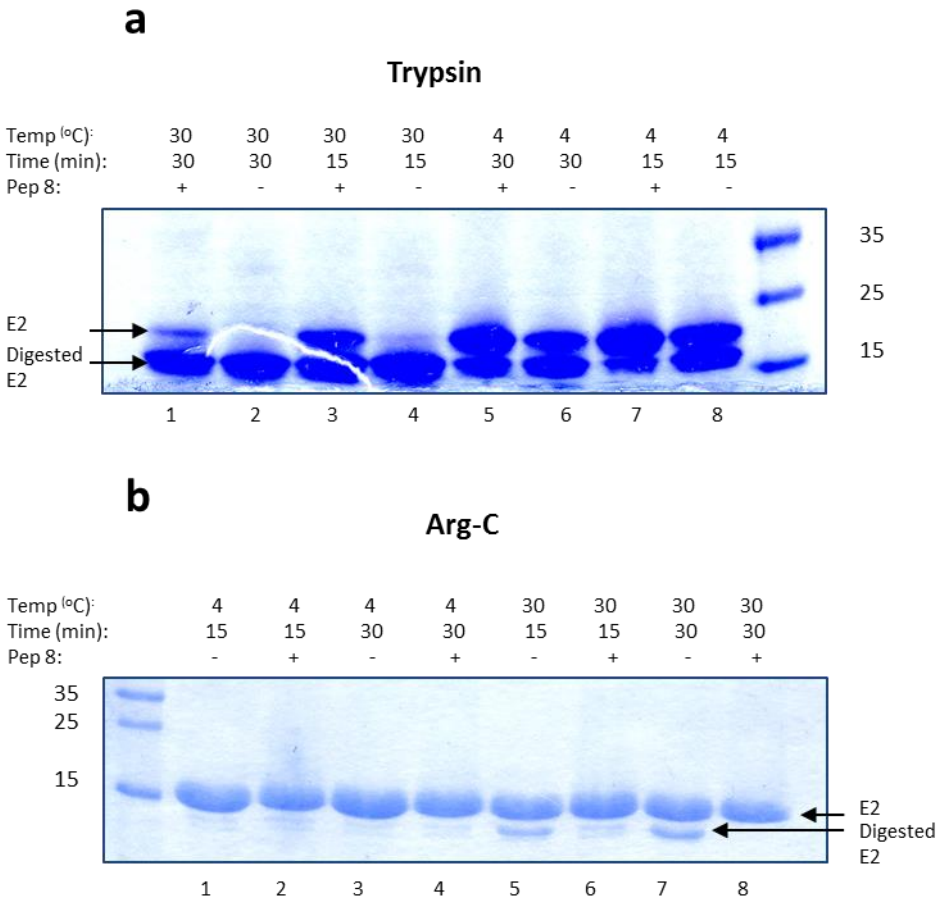

Figure 4.3: Trypsin and Arg-C digest of UbcH5α. UbcH5α (20 µg) with or without peptide 8 (5 µg) was pre-incubated for ten min at room temperature. Trypsin (**a)** or Arg –C (**b**) was added (1:100 W/W) and the digest reaction carried out at 4 ^{o}C or 30 ^{o}C. The reaction was terminated at certain time points by adding SDS sample buffer, containing DTT, and heating for 3 min at 80 ^{o}C. The samples were run on a 15 % agarose gel and the rate of digestion viewed by coomassie staining. Fermentas PageRuler Prestained Protein Ladder used for molecular weight maker, all molecular weights displayed are in kDa.

This result implies one of two things, either the peptide is a competitive substrate binding to and/or partially concealing the recognition site for the proteases, or alternatively, peptide 8 binding is resulting in a conformational change of UbcH5α that is partially burying the previously accessible recognition site (**figure 4.4 i and iii)**.

Strikingly when similar experiments were carried out using the protease Glu-c, which cleaves at the C-terminus of glutamic acid and aspartic acid, the results were reversed. Thus, in the presence of the peptide, UbcH5α was more sensitive to Glu-C cleavage whereas the unliganded protein was resistant to cleavage (**figure 4.5**). This difference in digestion was noticeable after 15 minutes (**figure 4.5, lanes 5 and 6**) when the reaction was incubated at 30 ^{o}C, and the difference clearly apparent after 30 minutes (**figure 4.6, lanes 7 and 8**).

This Glu-C proteolysis result implies that upon binding to peptide 8 UbcH5α undergoes a conformational change that opens up a previously buried recognition site for Glu-C (**figure 4.4 iv**).

Although the Trypsin and Arg-C data can be interpreted as a conformational change in UbcH5α on peptide binding, they are not definitive as it could also be argued that the peptide physically blocks cleavage. The results with Glu-C however lend strong support for the exposure of a previously buried recognition site, this could only happen should a conformational change take place within UbcH5α. If a conformational change is taking place upon peptide binding in this digest then it could suggest that conformation change in UbcH5α is the reason that digestion of the complex is slowed in the experiments with trypsin and Arg-C. These results are my first clear evidence that MDM2 may allosterically activate its E2 partner.

In the case of the limited proteolysis using trypsin the UbcH5α-peptide 8 complex was more resistant to digestion than free UbcH5α. Trypsin recognises and cuts at lysine and arginine at the carboxyl side except if either is followed by a proline. It could be argued that as peptide 8 contains one recognition site for trypsin (arginine at residue 8) that the rate of digestion of the complex is simply decreased because peptide 8 is also a substrate for trypsin (**figure 4.4 ii**).

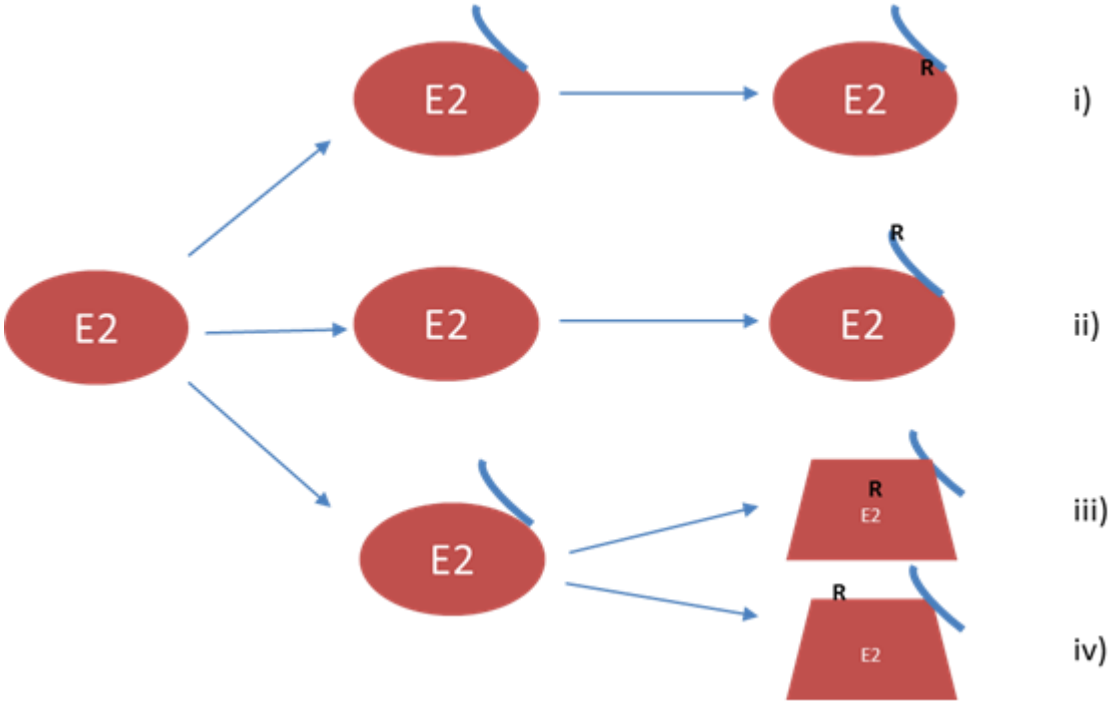

Figure 4.4: Model showing how peptide 8 binding to UbcH5α may affect its digestion. i) The peptide may physically block the recognition site of the protease protecting UbcH5α from digestion. **ii**) The peptide may contain a recognition site for the protease resulting in the appearance of slowed digestion or protection from digestion of UbcH5α. **iii**) Binding of the peptide results in a conformational change of UbcH5α that buries a previously exposed recognition site, protecting UbcH5α from digestion. **iv**) Binding of the peptide results in a conformational change of UbcH5α that exposes a previously buried recognition site, promoting UbcH5α for digestion.

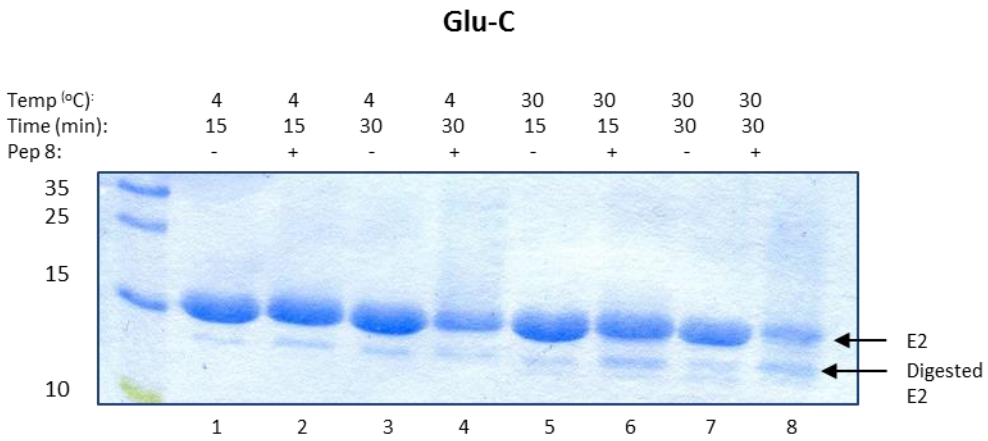

Figure 4.5: Glu-C digest of UbcH5α. UbcH5α (20 µg) with or without peptide 8 (5 µg) was pre-incubated for ten min at room temperature. Glu –C was added (1:100 W/W) and the digest reaction carried out at 4 ^{o}C or 30 ^{o}C. The reaction was terminated at certain time points by adding SDS sample buffer, containing DTT, and heating for 3 min at 80 ^{o}C. The samples were run on a 15 % agarose gel and the rate of digestion viewed by coomassie staining. Fermentas PageRuler Prestained Protein Ladder used for molecular weight maker, all molecular weights displayed are in kDa.

My idea was to create a control that would account for this. I needed a peptide that did not bind to UbcH5α and had one trypsin recognition site. Unfortunately none of the MDM2 RING peptides fitted this criteria, many of them contain numerous recognition sites for trypsin. The closest peptide matching my criteria was peptide 1. Peptide 1 does not bind to UbcH5α but it does have two recognition sites for trypsin, it was not an ideal scenario as this peptide was even more likely to compete than peptide 8 but I chose to proceed with this control.

This assay showed that in the control lane, containing peptide 1, the mere presence of the peptide slowed the rate of digestion of Ubch5α (**figure 4.6a, lane 11 compared to 10**), as was seen with peptide 8 (**figure 4.6a, lane 12**). I do not believe this result is a consequence of peptide 1 binding to UbcH5α, based on my earlier experiments, I believe that the result is due to the fact that peptide 1 contains two recognition sites for trypsin as opposed to the one that peptide 8 has.

I tried a second control using peptide 1 in the limited proteolysis assay using Glu-C. Glu-C recognises aspartic acid and glutamic acid, neither peptide 8 or peptide 1 contains these amino acids. With this control I aimed to prove that a change in digestion of the UbcH5α-peptide 8 complex was due to the peptide eliciting a change in conformation upon binding and not just presence of the peptide. The result shows that when UbcH5α was in complex with peptide 8 it was less resistant to digestion by Glu-C than free UbcH5α (**figure 4.6b, lane 12 compared to 10**). When peptide 1 was present in the assay no change in digestion of the UbcH5α was detected between this UbcH5α and free UbcH5α (**figure 4.6b, lane 11 compared to 10**). This result shows that it is the peptide in complex with UbcH5α that is facilitating the change in digestion of the E2 and not simply the presence of the peptide.

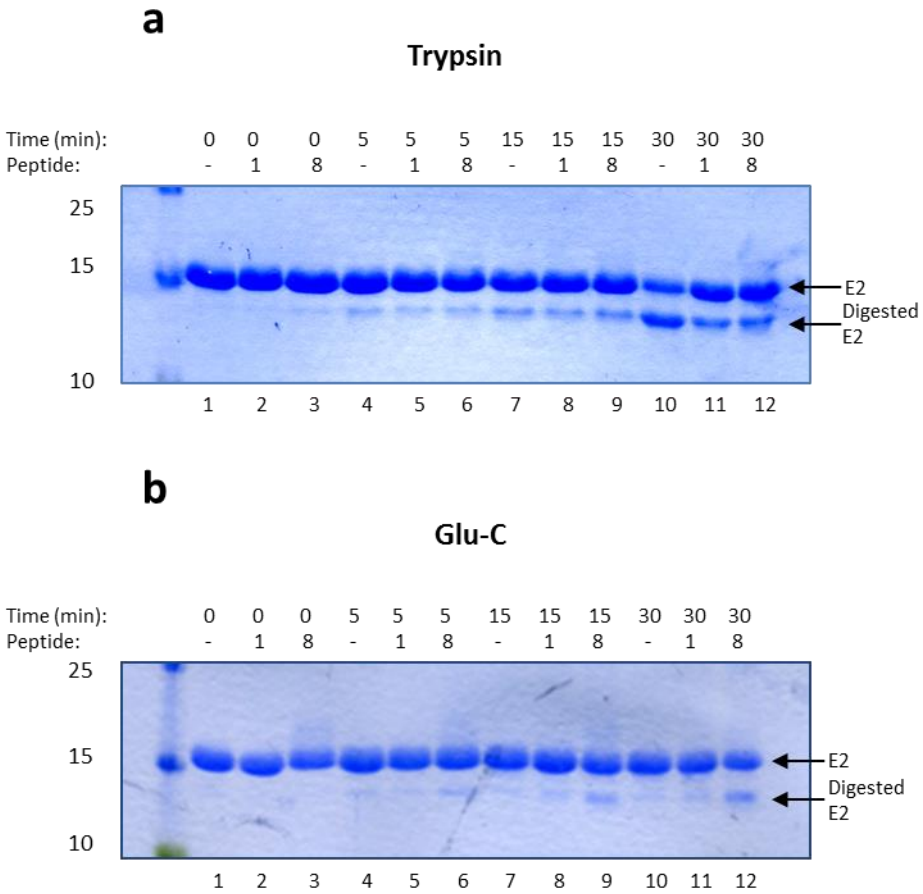

Figure 4.6: Controls for trypsin and Glu-C digests of UbcH5α. UbcH5α (20 µg) with either no peptide, peptide 1 or 8 (5 µg) was pre-incubated for ten min at room temperature. Trypsin (**a)** or Glu – C (**b**) was added (1:100 W/W) and the digest reaction carried out at 30 ^{o}C. The reaction was terminated at certain time points by adding SDS sample buffer, containing DTT, and heating for 3 min at 80 ^{o}C. The samples were run on a 15 % agarose gel and the rate of digestion viewed by coomassie staining. Fermentas PageRuler Prestained Protein Ladder used for molecular weight maker, all molecular weights displayed are in kDa.

4.1.4 Mass spectrometry of limited proteolysis

The results from the limited proteolysis suggest that UbcH5α undergoes a conformational change when bound to peptide 8. I wanted to investigate this further, limited proteolysis, although a useful tool for probing conformation differences, does not provide information regarding the area(s) undergoing the change. Richer data can be obtained from limited proteolysis when the results of this assay are combined with mass spectrometry, this is a novel method developed by us and Lenka Hernychova at the Masaryk Memorial Cancer Institute. The bands produced, when UbcH5α or UbcH5α in complex with peptide 8 are digested with Glu-C, undergo in-gel digestion by trypsin, the peptides are then purified and analysed using an Orbitrap elite mass spectrometer.

The Orbitrap elite (thermo scientific) is a member of the family of linear trap quadruple (LTQ) mass spectrometer hybrid instruments. It incorporates a dual cell linear trap and the orbitrap analyser (**figure 4.7a**). The linear ion trap is an independent MS detector which can store, isolate and fragment ions then send them to the orbitrap for further analysis. From the linear trap to the orbitrap analyser ions move through the gas free octapole into the gas filled curved linear trap (C-trap) (**figure 4.7b**). Ions entering the C-trap lose their kinetic energy through collisions with nitrogen gas and are collected in the middle of the C-trap. For ion extraction extracting voltage pulses are applied to the electrodes, pushing ions orthogonally to the curved axis and through a slot in the inner electrode. Ions of each mass-to-charge ratio arrive at the entrance to the orbitrap in short packets, when these packets enter the orbitrap at a position offset from its equator (**figure 4.7c**) they start coherent axial oscillations without the need for any additional excitation cycle. At the heart of the orbitrap is an axially- symmetrical mass analyser. It consists of a spindle shaped electrode surrounded by a pair of bell-shaped outer electrodes, it employs electrical fields to capture and confine ions (**figure 4.7d**).

The in-gel trypsin digest and subsequent peptide purification, using the FASP method, was carried out by myself. The programming and running of the Orbitrap Elite MS was carried out by Petra Dvorakova, in my presence, as was the interpretation of the resultant spectra.

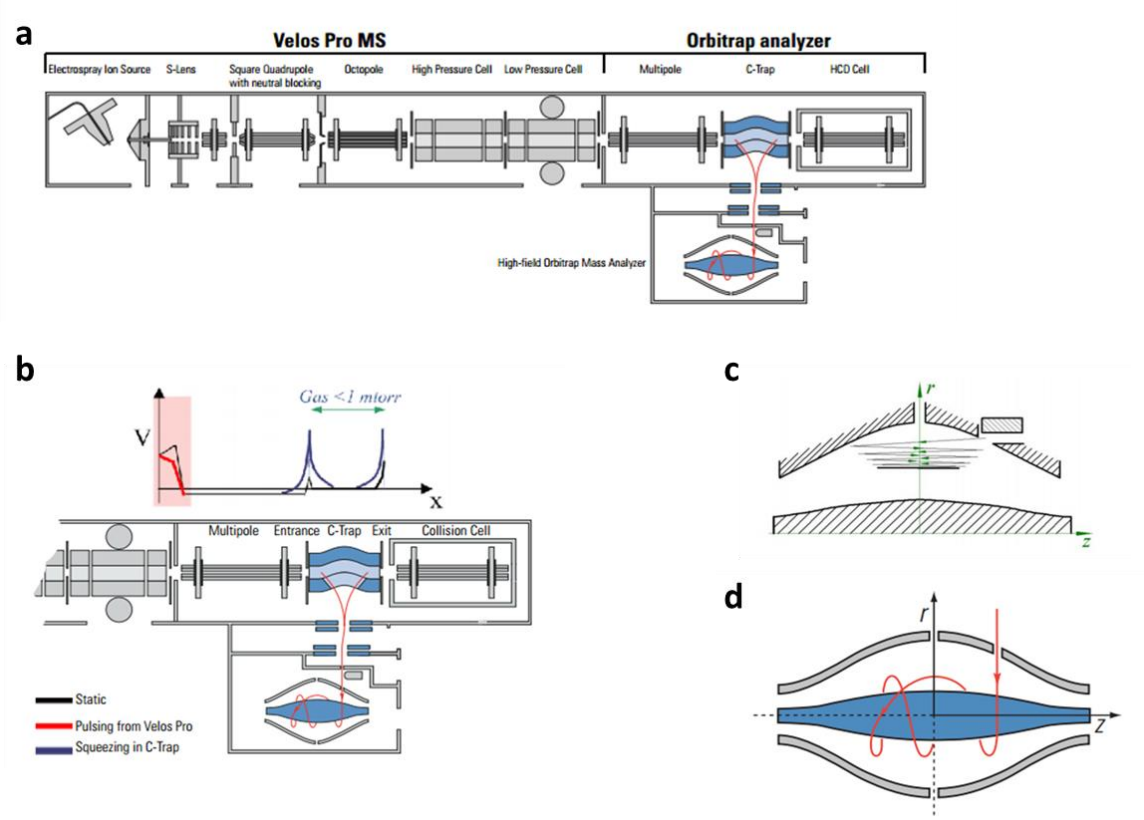

Figure 4.7: The Orbitrap Elite MS analyser. **a**) Schematic of the Orbitrap Elite mass spectrometer. **b**) Layout of the Orbitrap Elite MS, showing the applied voltages. **c)** Principle of electrodynamic squeezing of ion in the orbitrap analyser as field strength is increased. **d**) Schematic of the orbitrap cell and an example of stable ion trajectory.

Information and diagrams from Orbitrap Elite hardware manual (P/N 1288170, Revision A) Thermo Fisher Scientific.

I carried out one more proteolysis assay with Glu-C, using increased amounts of protein in order to produce sufficient material for MS, **figure 4.8a** shows the result of this assay. The image is not clear, this is due to the fact that the gel could not be imaged in the usual way for fear of contaminating the gel, which would in turn compromise the MS results, and as such this image is a photograph of the gel in destain hence the lack of clarity. **Figure 4.8b** shows a schematic of how the gel actually looked. I first reasoned that the lowest molecular weight band in the absence of peptide, band 3, represented the stable core domain of UbCh5α as any peptides that had been cleaved away from the core would have run off the gel or with the dye front. I then reasoned that band 4, which was unique to the E2 and peptide reaction, and ran with a lower apparent mass than band 3, would be the stable core for UbcH5α and peptide.

UbcH5c is an extremely close relation to UbcH5α both proteins are 147 amino acids in length with a highly homologous amino acid sequence, only differing at 16 single residues. The change in residue is often subtle, with the nature of the amino acid retained i.e. charged, small, hydrophobic. In **figure 4.9** I have overlaid the two structures showing that I can use the model for UbcH5c in my analysis of UbcH5α. Using the molecular model of UbcH5c generated by Dr Vivien Landre, as shown in the previous chapter the peptides generated by MS were mapped onto the model to analyse the stable cores. Firstly it can be seen that there is a change to the stable core of UbcH5α when it is in complex with peptide 8 compared to when it is free (**figure 4.10a and b**). When in complex with peptide 8 amino acids 16-42 of UbcH5α that form β-sheets are no longer part of the stable core. Interestingly amino acids 100-111 that form an α-helix become more stable when UbcH5α is in complex with peptide 8. Peptide 8 makes contact at sites distant from these changes seen (**figure 4.10c**), this provides further evidence for the allosteric activation of UbcH5α by peptide 8.

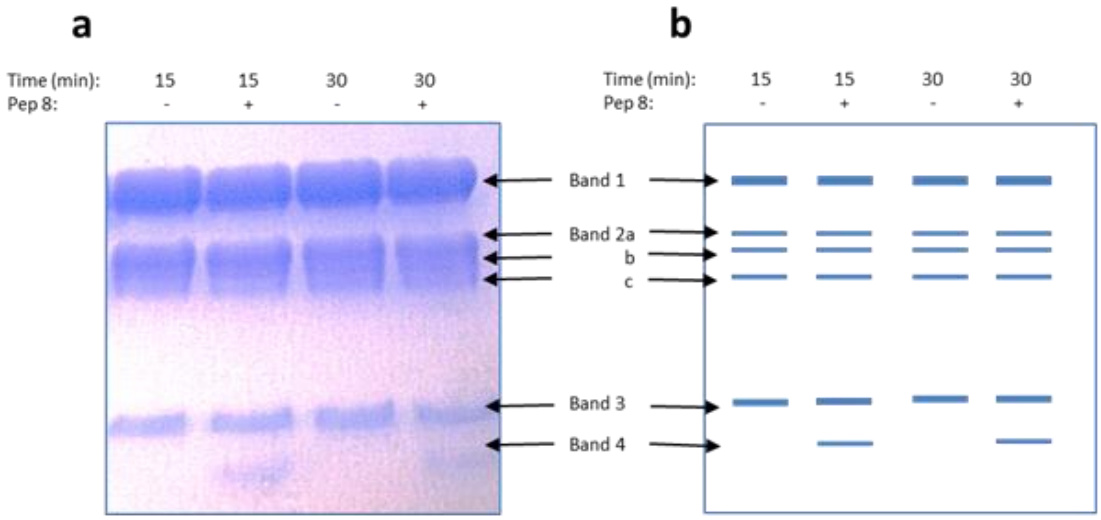

Figure 4.8: Proteolysis assay with Glu-C in preparation for MS analysis. a) Photo of coomassie stained 12 % SDS PAGE gel showing the results of proteolysis with Glu-C. **b**) Schematic diagram representing a clear image of the gel. All bands were excised and proteins underwent in-gel digestion with trypsin (0.5 µg), the results from bands 3 and 4 were used for modelling the stable core of UbcH5α.

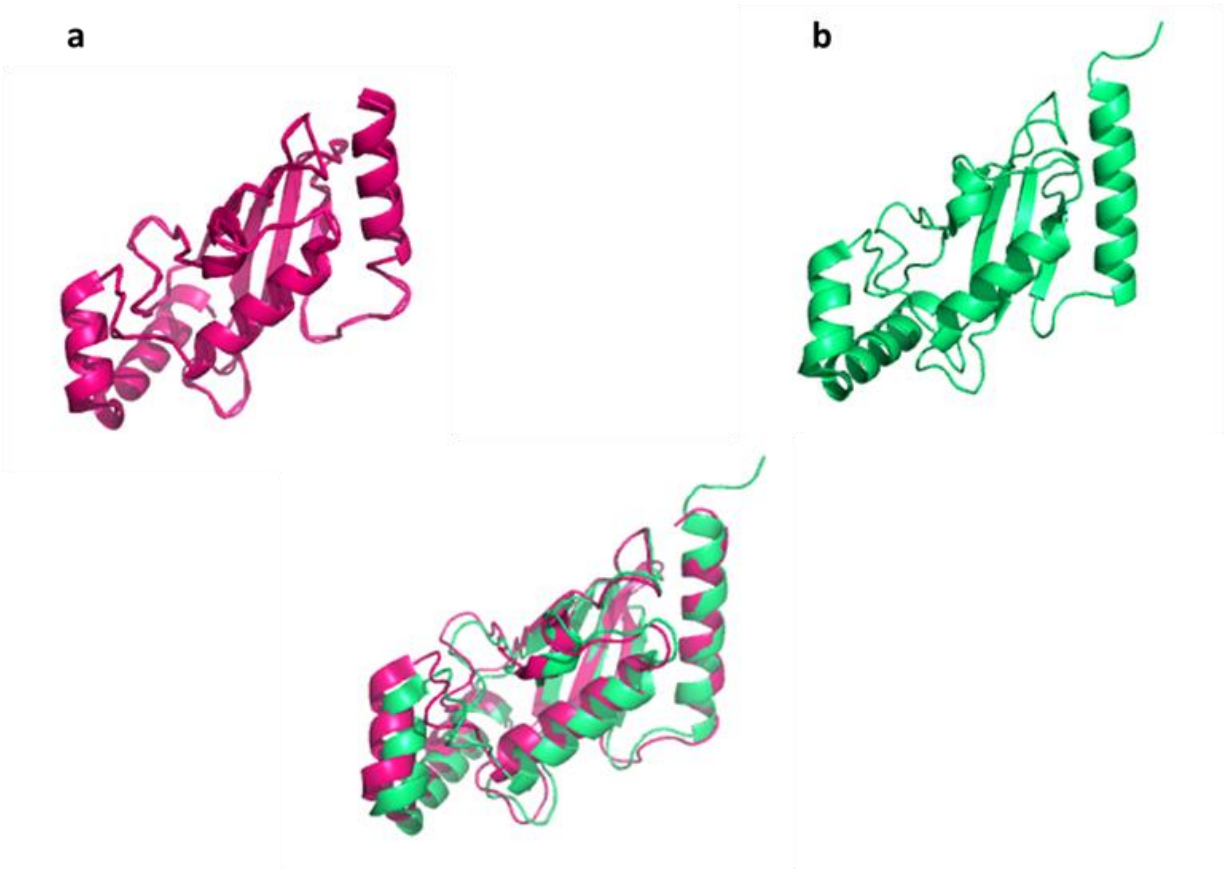

Figure 4.9: Comparing the crystal structures of UbcH5α and UbcH5c. a) Crystal structure of UbcH5α. **b**) Crystal structure of UbcH5c. **c**) Aligned crystal structures of UbcH5α and UbcH5c.

Allosteric activation of UbcH5α will have implications for its activity. Interestingly when ubiquitin is added to the model showing the stable core of UbCh5α, when in complex with peptide, clues to how this activation may affect its activity come to light. The α-helix within Ubch5α that becomes more stable following peptide 8 binding is the site of ubiquitin binding (**figure 4.11a and b**). Ubiquitin and peptide 8 bind to different sites of UbcH5α (**figure 4.11c and d**) so any change in the interaction between UbcH5α and ubiquitin is not due to competition from peptide 8, this is further evidence for peptide 8 allosterically activating UbcH5α resulting in the transfer of ubiquitin to a target protein.

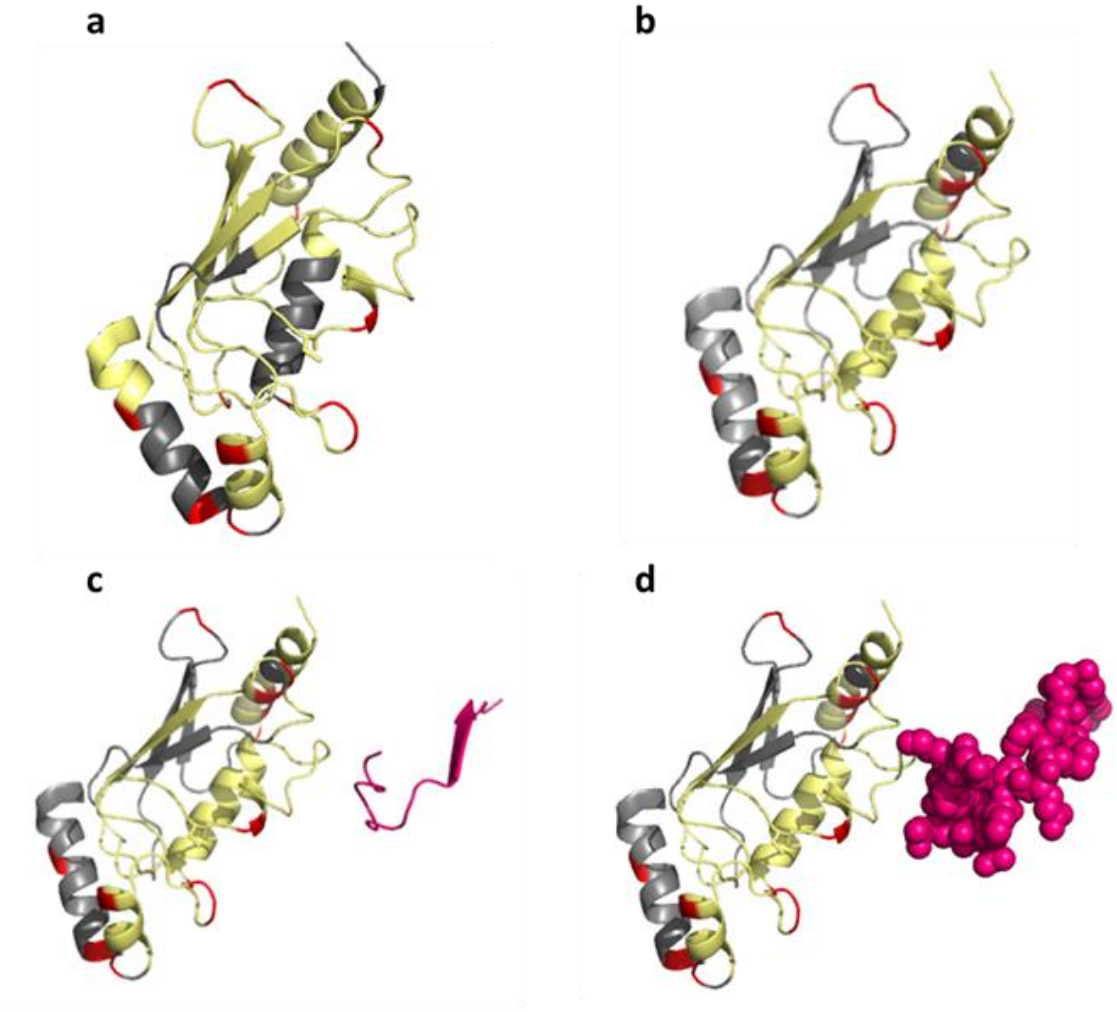

Figure 4.10: Stable core of UbcH5α. Grey residues indicate starting material, yellow residues indicate the stable core left after Glu-C digestion, red residues are sites of Glu-C recognition and pink residues represent peptide 8. **a**) Model showing the stable core of free UbcH5α. **b**) Model showing the stable core of UbcH5α when in complex with peptide 8. **c +d**) Model of the stable core of UbcH5α when in complex with peptide 8, showing the location of peptide 8.

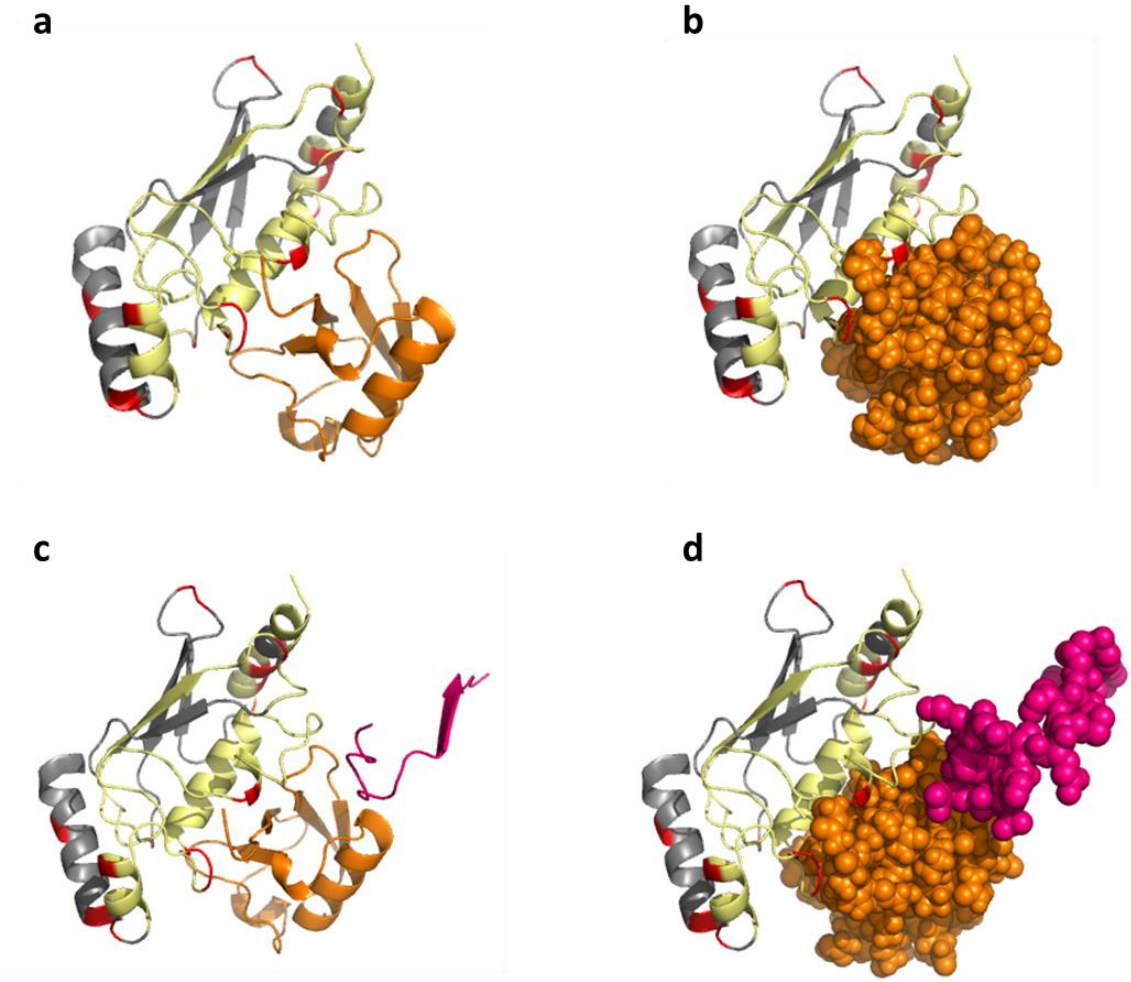

Figure 4.11: Interaction of UbcH5α, peptide 8 and ubiquitin. Grey residues indicate starting material, yellow residues indicate the stable core left after Glu-C digestion, red residues are sites of Glu-C recognition, pink residues represent peptide 8 and orange residues represent ubiquitin. **a +b**) Model shows the stable core of UbcH5α, when in complex with peptide 8, interacting with ubiquitin. **c +d**) Model showing the stable core of UbcH5α, when in complex with peptide 8, interacting with ubiquitin and peptide 8.

When the RING domain is added in its entirety to the model, the same result as with peptide 8 is seen. No part of the RING domain interacts with UbcH5α at the exact same point as ubiquitin (**figure 4.12**). The points of interaction are close though, this makes sense as my previous results show that the RING binds to UbcH5α and ubiquitin simultaneously, if the RING has to orientate itself to bind both simultaneously then it is not unexpected it binds UbcH5α close to ubiquitin.

Interestingly when the RING is added to the model a second point of contact between the RING and UbcH5α is seen. In earlier ELISA assays I had established a point of contact between peptide 8 and UbCh5α but the model shows a different point of contact made with a different area of the RING. This point of contact is between residues 9-10 that form an α-helix in UbcH5α and residues 441-442 in the RING (**figure 4.13a and b**). Perhaps even more interestingly this point of contact destabilises part of this α-helix when compared to the stability of the α-helix in free UbcH5α (**figure 4.13a and c**).

Combining limited proteolysis with mass spectrometry has confirmed that UbcH5α undergoes a conformational change upon peptide 8 binding. It has also highlighted regions of UbcH5α that become more or less stable including the increased stability of the ubiquitin binding interface.

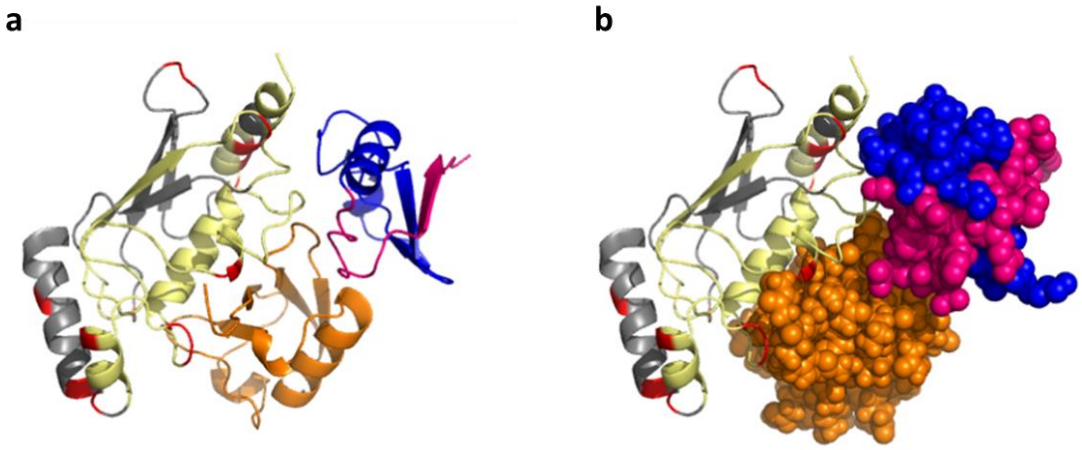

Figure 4.12: Interaction of UbcH5α, RING and ubiquitin. Grey residues indicate starting material, yellow residues indicate the stable core left after Glu-C digestion, red residues are sites of Glu-C recognition, pink residues represent peptide 8, blue residues are the rest of the RING domain and orange residues represent ubiquitin. **a +b**) Model showing the stable core of UbcH5α, when in complex with peptide 8, interacting with ubiquitin and peptide 8.

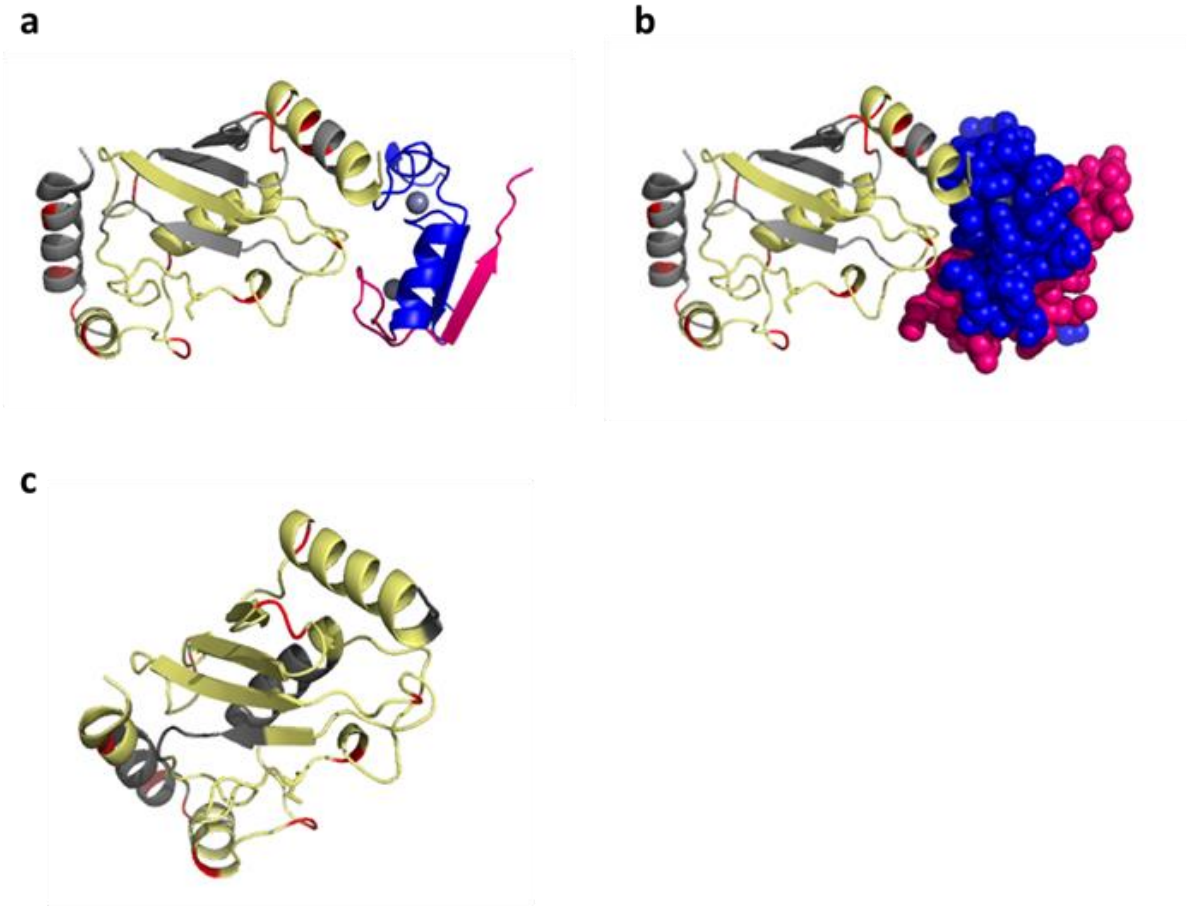

Figure 4.13: RING contact point on UbcH5α. Grey residues indicate starting material, yellow residues indicate the stable core left after Glu-C digestion, red residues are sites of Glu-C recognition, pink residues represent peptide 8 and blue residues are the rest of the RING domain. **a +b)** The RING domain contacts UbcH5α at its N-terminal α-helix. **a +c)** Residues 6-8 within this α-helix re destabilised upon RING binding.

4.1.5 Hydrogen deuterium exchange

My results up to this point had suggested a conformational change of UbcH5α, activated upon binding of the MDM2 RING domain peptide 8. I wanted to further investigate this change, to do this I used hydrogen deuterium exchange.

In 1954 Linderstrom-Lang developed hydrogen exchange with the goal of identifying hydrogen bonded structures in proteins. Using deuterated solvent he observed rapid exchange of amide protons for deuterium in short unstructured peptides. The exchange for folded proteins such as insulin were complex and took place slowly[229]. Exposed hydrogens exchanged quickly, partially exposed hydrogens exchanged at a slower rate.

Using mass spectrometry to determine the deuterium label content during hydrogen-deuterium (HD) exchange has a number of advantages including the need for less sample[230]. Monitoring the presence or absence of label sites in the protein after initial exposure gives an instantaneous snapshot of protein conformation. Folded conformations with more amides buried or involved in hydrogen bonding will be observed at a lighter mass than less folded conformations that take on more label in their exposed and non-hydrogen bonded reigons[229].

In order to localise incorporated label to specific positions in the sequence a protein must be fragmented following HD exchange. Application of proteolysis following HD exchange is the most common fragmenting method, known as bottom up HXMS[231,232]. Following incubation in label for different lengths of time, an aliquot is drawn and subjected to conditions (low pH, 0 ^{o}C) that drastically slow exchange. It is then treated with acid stable, broad specificity protease(s) such as pepsin, to generate a set of fragments to obtain good sequence coverage for the protein[229] (**figure 4.14**).

HD exchange provides insight into three dimensional structures of proteins and complexes that are too disordered/flexible to meet the traditional requirements of X-ray crystallography and NMR.

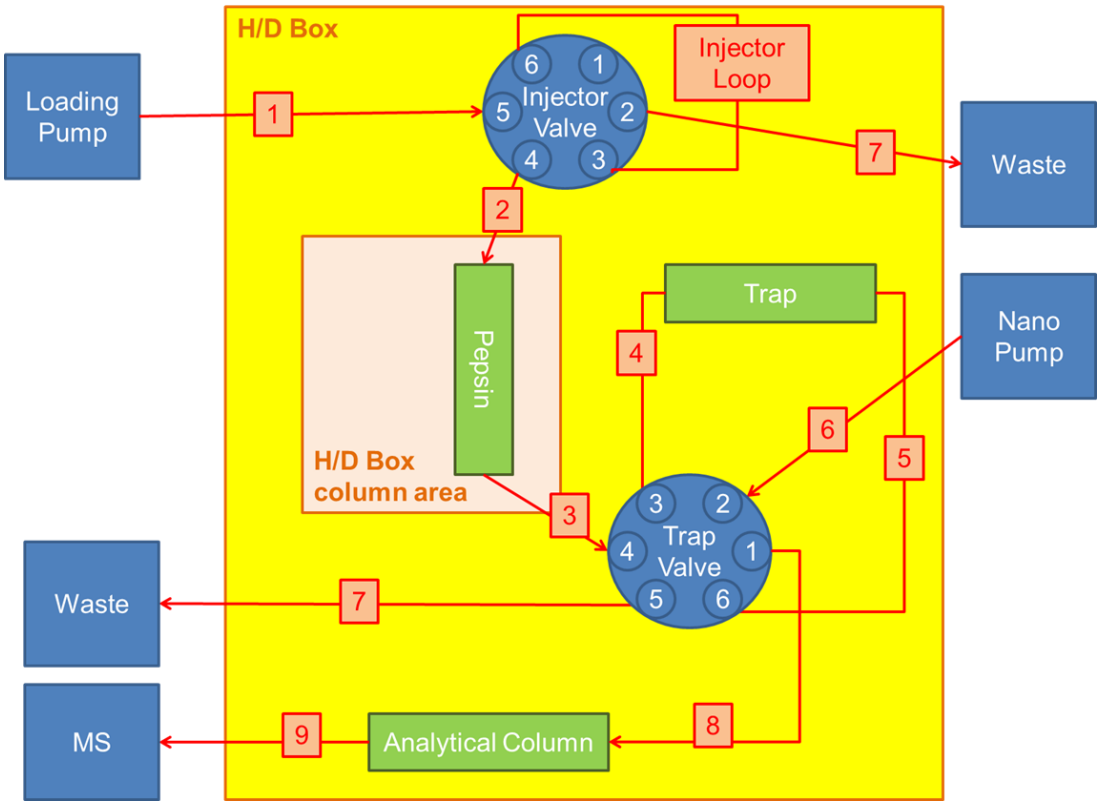

Figure 4.14: HD exchange linked to mass spectrometry. A schematic diagram showing the route that the deuterated sample takes, firstly they are digested on a pepsin column, followed by an analytical column to spate the peptides, and then into the mass spectrometer to be fragmented.

The HD exchange was carried out in collaboration with Dr Lenka Hernychova at RECAMO where I have made several visits to carry out experiments, observe procedures and learn the basics about MS sample preparation and instruments. The HD MS described in this thesis used an Orbitrap Elites MS combined with a robot from PALsystem. I wanted to use HD exchange to probe for a conformational change of UbcH5α upon the binding of peptide 8. To probe for a change in the complex first HD exchange had to be carried out on unliganded UbcH5α Initial experiment were carried out in the absence of deuterium in order to determine the coverage of the E2 structure. The coverage of UbcH5α is not 100 % (**figure 4.15**) i.e. peptides for certain sites were not found. Residue 1 (methionine), residue 87, (aspartic acid) and residues 106, 107 and 108 (isoleucine, cysteine and serine) of UbcH5α were not covered. Coverage of the His tag and linker were also not found, this is less of a concern. Although coverage of the E2 was not 100 % it was very good when compared to coverage seen of other proteins.

My primary purpose of HD exchange was to probe for a conformational change of UbcH5α upon the binding of peptide 8. However HD exchange can tell us a great deal about UbcH5α by itself, it can tell us about the areas of the proteins that are flexible and the areas that are very stable and resistant to exchange in solution. **Figures 4.16 and 4.17** show the percentage of deuterium exchange for peptides from different areas of the E2. The majority of α helices and β sheets are most stable and the hydrogens in these regions do not exchange readily with deuterium, with the exception of a β stand (aa 23-27, **figure 4.17**) leading into a flexible loop. Interestingly the loops show no pattern, with some exchanging rapidly and other very resistant to exchange. There is an area of the E2 starting at residue 51 that is dark blue, indicating very low levels of exchange, in actual fact this area showed no exchange at all. Other areas of very low exchange did not show 0 % as this result did. We will be repeating this analysis prior to publication to validate the data in an independent experiment.

With a baseline of HD exchange established for the unliganded UbcH5α and with coverage of the E2 sequence reasonably close to 100 % I was happy to go ahead with HD exchange on the complex of UbcH5α and peptide 8.

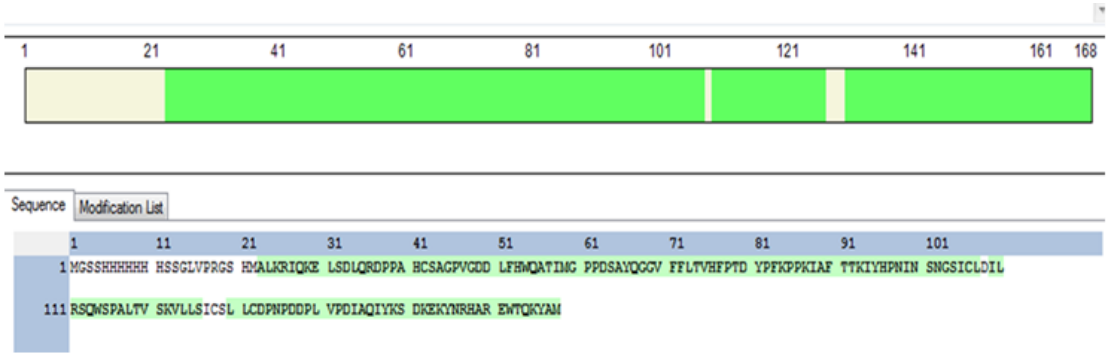

Figure 4.15: Screenshot showing the peptide coverage of UbcH5α. This screenshot shows the coverage of UbcH5α both as a schematic diagram and as a sequence. Residues highlighted in green are covered by the peptides, those in grey are not.

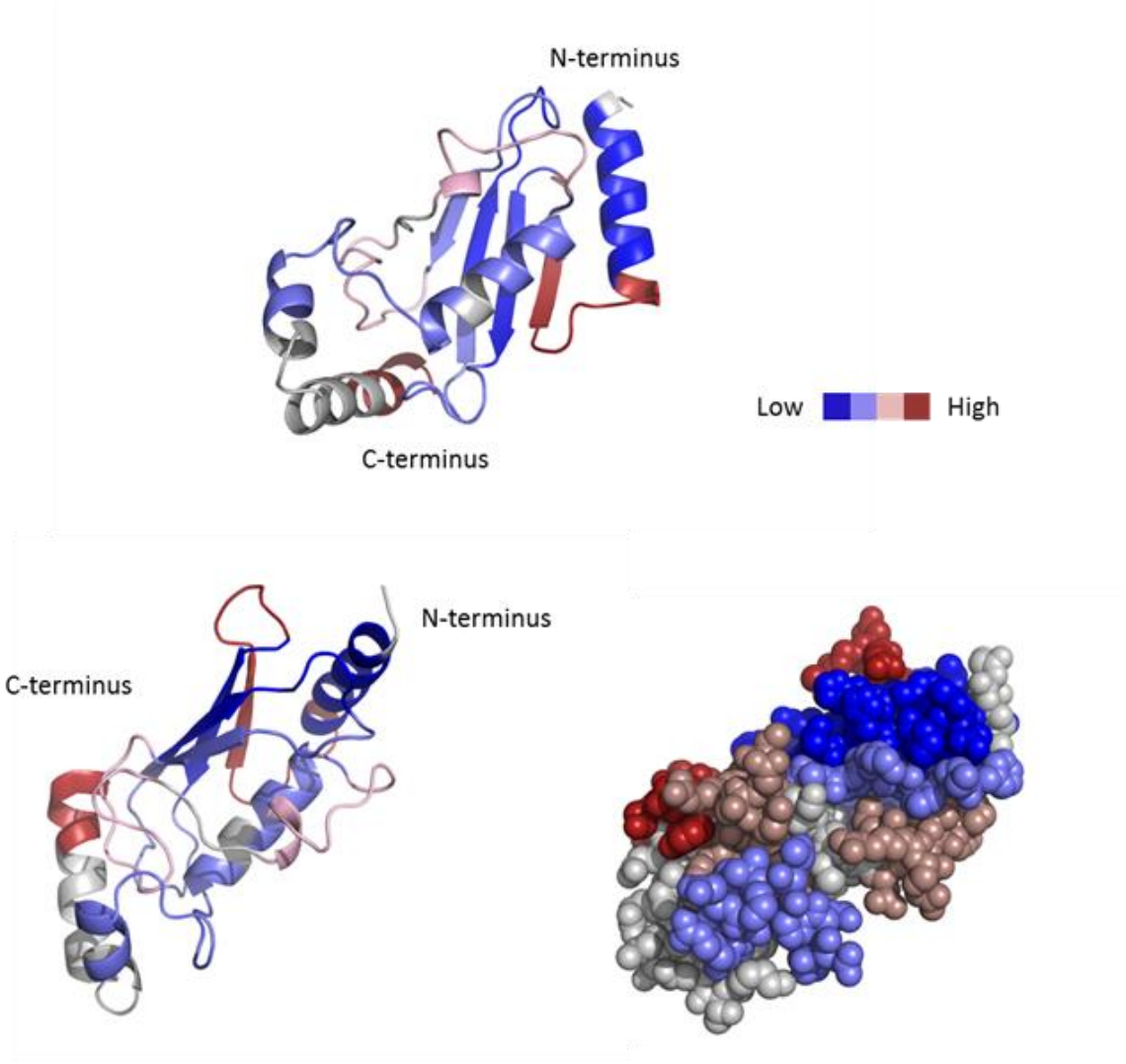

Figure 4.16: Model showing the level of HD exchange for free UbcH5α. These models show the level of hydrogen-deuterium exchange for different areas of UbCh5α. Dark blue indicates residues with <20 % HD exchange, light blue indicates residues with 21-35 % HD exchange, pink indicates residues with 36-50 % HD exchange and red indicates residues with >50 % HD exchange. These models indicate areas of greater flexibility and more stable areas resistant to exchange.

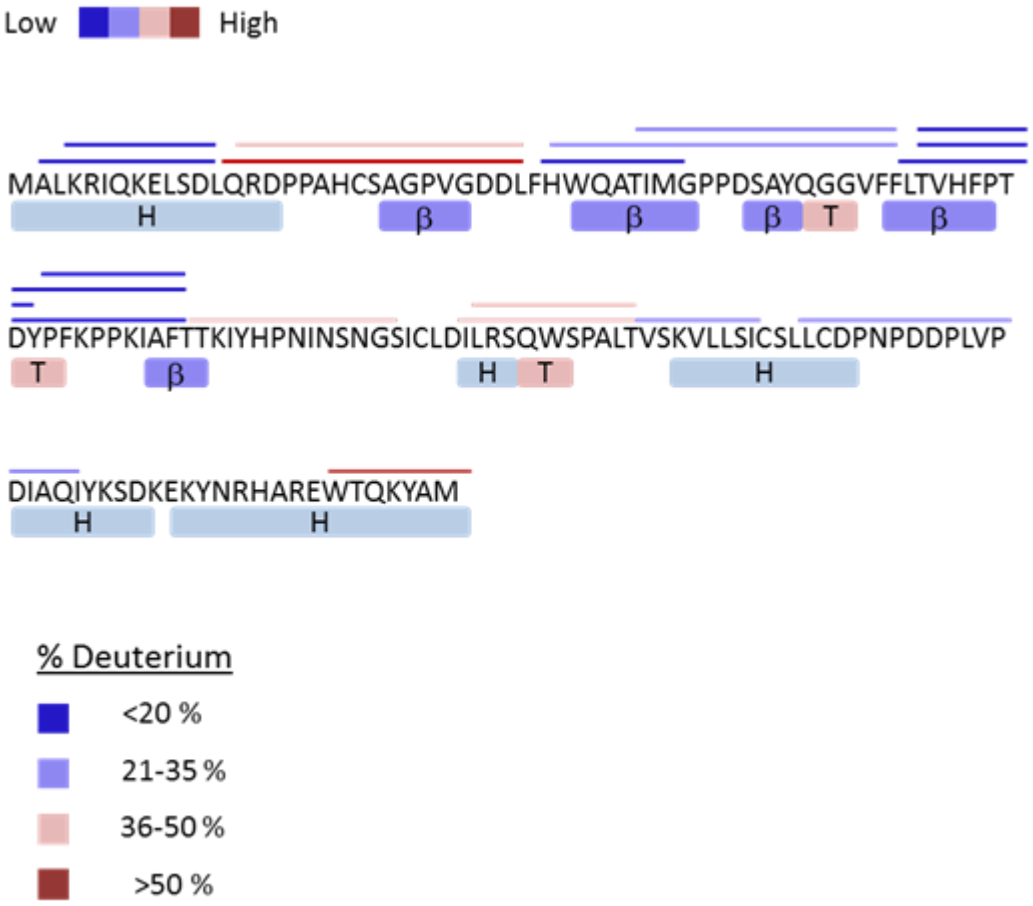

Figure 4.17: The sequence of UbcH5α showing the level of HD exchange for specific residues. This sequence shows the level of hydrogen-deuterium exchange for the different peptides of UbCh5α. The lines above the sequence are representative of the peptides obtained and analysed. The block areas under the sequence indicate secondary structures. H=α helix, β= β sheet and T= Turn. Dark blue indicates residues with <20 % HD exchange, light blue indicates residues with 21-35 % HD exchange, pink indicates residues with 36-50 % HD exchange and red indicates residues with >50 % HD exchange. This sequence indicates areas of greater flexibility and more stable areas resistant to exchange.

Different molar ratios of E2 to peptide 8 were used (1:1, 1:10 and 1:100) and E2 and peptide were incubated for 30 minutes at room temperature to accommodate complex formation. Proton exchange with deuterium was then allowed to proceed for set time intervals (1, 2, 5, 10, 30, 60 and 180 min) before samples were quenched with acid. Results for molar ratios 1:1 and 1:100 protein to peptide were not successful, with the 1:100 ratio leading to the precipitation of E2. Not long after HD exchange experiments had taken place a number of other experiments with peptide 8 did not proceed as expected. I discovered that the newly synthesised batch of peptide was not the concentration it should have been based on the information provided by mimotopes (commercial supplier), instead it was significantly (100x) less. I believe that this could explain the difficulty in obtaining significant information from some of the HD experiments. The hydrophobic nature of peptide 8 makes it very difficult to synthesis successfully. I have since had a new batch of peptide synthesised by peptide chemists who collaborate with RECAMO and a second round of HD MS experiments will take place to generate publishable HD MS data.

However there was some change seen in the HD experiment carried out at the molar ratio 1:10, with two overlapping peptides displaying a significant change in the rate of deuteriation (see p values in **figure 4.18**).

Peptide ALKRIQKELSDL shows supressed deuteriation after peptide 8 binding at early time intervals (**figure 4.18a**). The shorter version of this peptide KRIQKELSDL also displays supressed deuteriation after peptide 8 binding at early time intervals, as time progresses it shows increased deuteriation (**figure 4.18b**). The overlapping peptides correspond to the N-terminal α-helix of UbcH5α (**figure 4.20a and b**). My limited proteolysis linked to mass spectrometry indicated that part of the same α-helix is destabilised upon peptide 8 binding. Together the HD exchange and limited proteolysis suggest that the N-terminal helix of UbcH5αis initially stabilised following interaction with peptide 8 whereas prolonged binding may lead to an overall increase in flexibility.

The residues that become more stable are in the centre of the peptides identified above (**figure 4.20c and d**). As our modelling of the N-terminus suggests that the N-

terminus of UbcH5α is not directly involved in peptide 8 binding this is likely to represent allosteric changes in the N-terminal peptide.

a

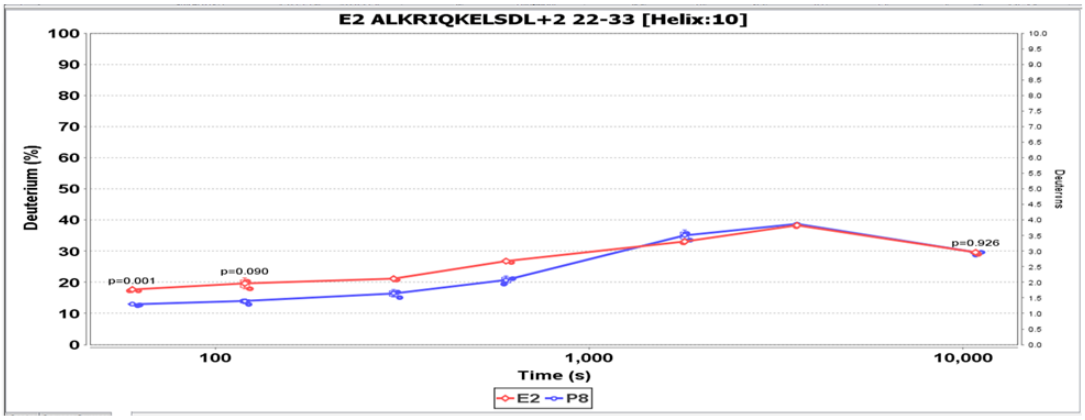

b

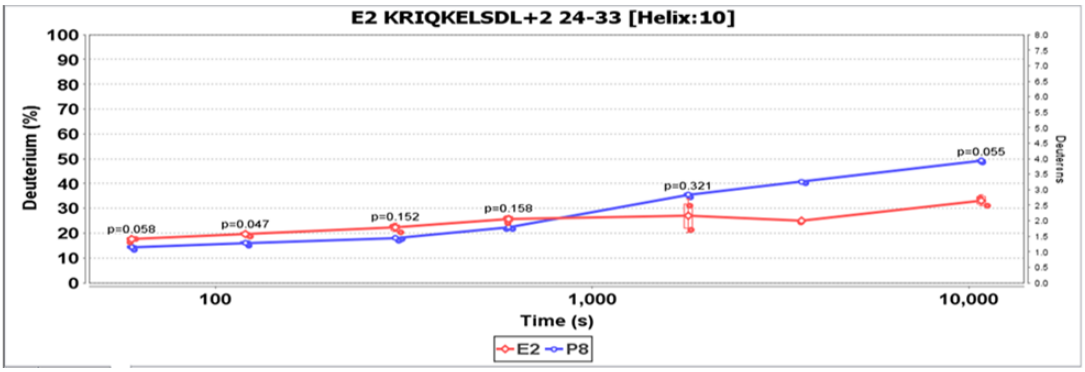

Figure 4.18: Screenshot showing UbcH5α peptides that display a change in HD exchange when UbcH5α is in complex with peptide 8. a) Peptide ALKRIQKELSDL shows supressed deuteriation after peptide 8 binding at early time intervals. **b)** Peptide KRIQKELSDL displays supressed deuteriation after peptide 8 binding at early time intervals, as time progresses it shows increased deuteriation. The red data points display deuteriation of the peptide from free UbcH5α, the blue data points display deuteriation of the peptide from the UbcH5:peptide 8 complex.

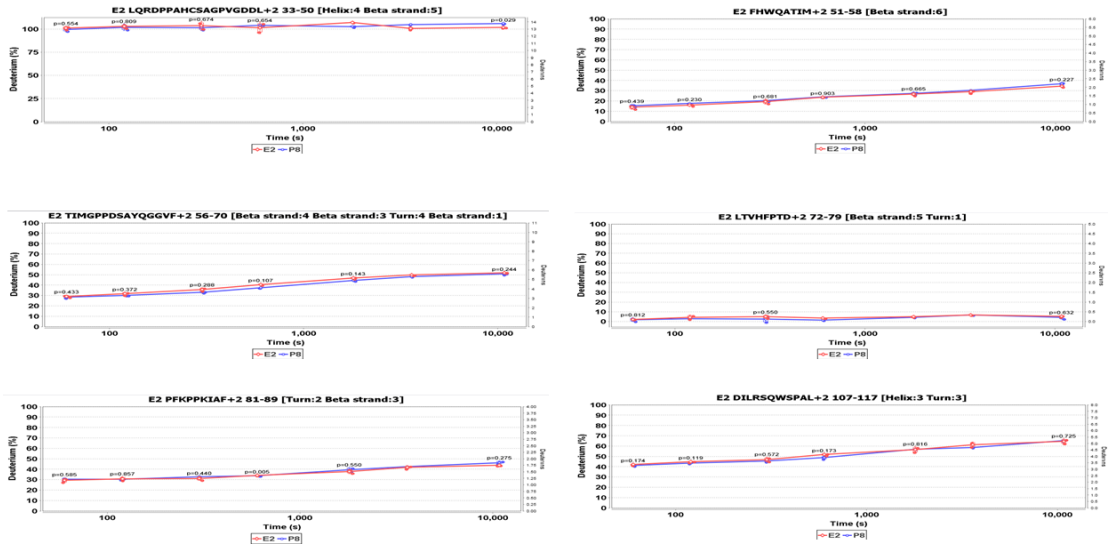

Figure 4.19: Screenshot showing examples of UbcH5α peptides that display no change in HD exchange when UbcH5α is in complex with peptide 8. This screenshot shows just some of the peptides that showed no change in HD exchange when from free UbcH5α or UbcH5α in complex with peptide 8. The red data points display deuteriation of the peptide from free UbcH5α, the blue data points display deuteriation of the peptide from the UbcH5:peptide 8 complex. The data from all the peptides can be viewed in appendix I.

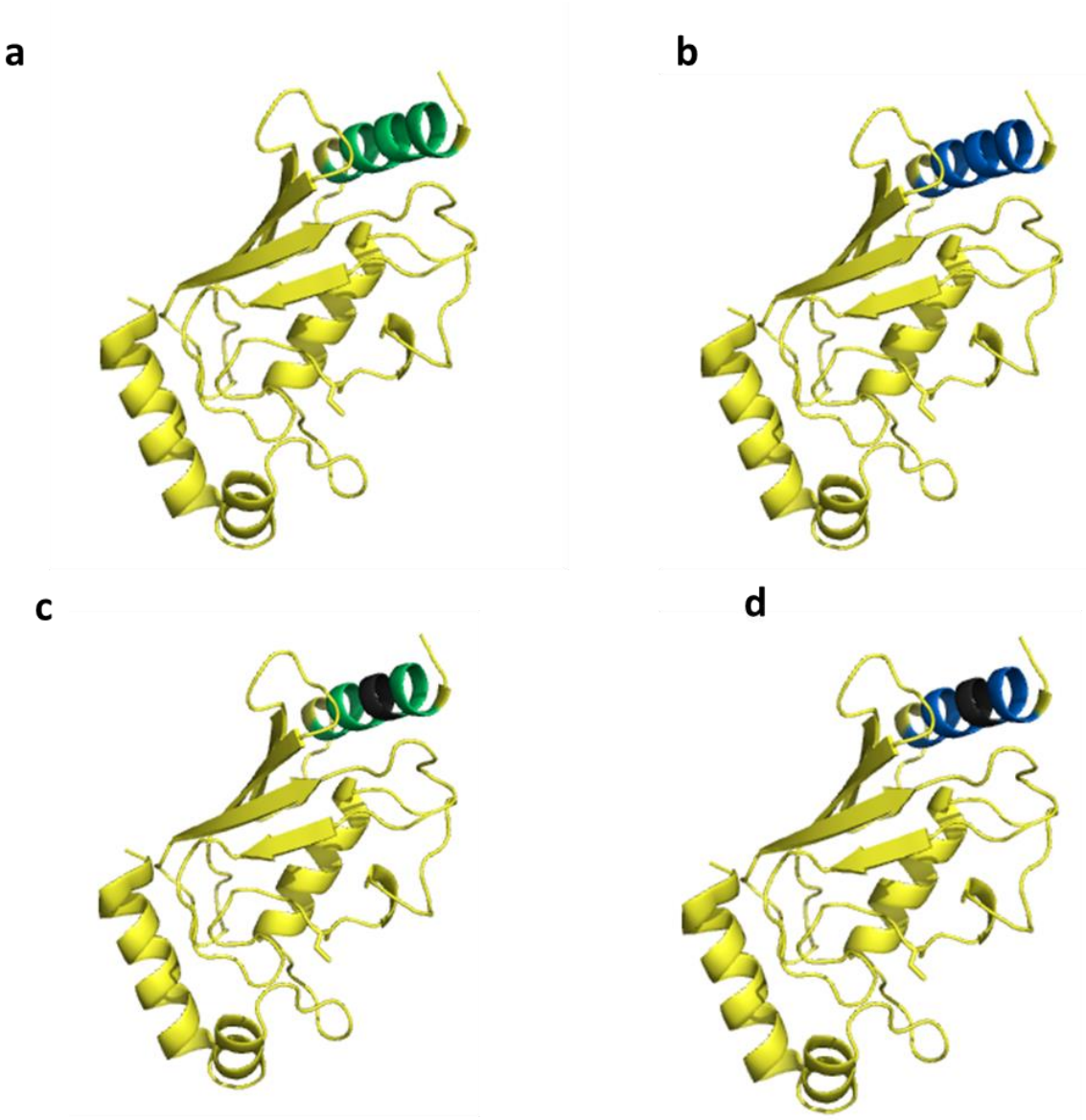

Figure 4.20: The overlapping peptides that display a difference in HD exchange correspond to the N-terminal α-helix of UbcH5α. a) Residues highlighted in turquoise correspond to peptide ALKRIQKELSDL that showed supressed deuteriation after peptide 8 binding at early time intervals. **b**) Residues highlighted in blue correspond to peptide KRIQKELSDL that displayed suppressed deuteriation after peptide 8 binding at early time intervals and as time progresses showed increased deuteriation. **c + d**) Residues in grey highlight the areas that limited proteolysis linked to MS showed to be less stable, the change in stabilisation suggests a conformational change. This correlates with the change in deuteriation of this N-terminal helical region.

Initial HD exchange experiments show some promising data that corresponds with earlier results using limited proteolysis. Repeating this with the correct concentration of peptide and different molar ratios could provide further information regarding the conformational changes of UbcH5α upon peptide 8 binding. In addition I plan to confirm the result obtained using peptide 8 by adding the entire RING domain.

4.1.6 Discussion

The experiments in this chapter were carried out with the aim of discovering if the RING domain of MDM2 could allosterically activate its partner E2, UbcH5α.

At the start of my PhD there was some evidence in the literature that E2s could be allosterically activated by their partner E3s[35]. If this is true then part of the mystery regarding how RING E3s facilitate the transfer of ubiquitin from the E2 to their target protein could be solved. Allosteric activation of the E2 has become the favoured hypothesis for ubiquitin transfer by RING domains, the simple orientation hypothesis[28,34] i.e. RING E3s acting as a scaffold, bringing together ubiquitin bound E2 and substrate and orientating them in optimum positions for transfer, having fallen out of favour[39,227] due to the distance between the E3 binding site and the active site cysteine on the E2. Should the RING be able to allosterically activate UbcH5α any conformational change is likely to be subtle as studies had shown no clear structural differences between free E2 and E2 in complex with E3 that would explain the enhanced activity of E2[34].

During the course of my PhD a study was published that suggested E2s could indeed be allosterically activated by their E3s[228]. Using NMR this study showed that some E2-ubiquitin conjugates (UbcH5c) favoured a more closed conformation upon E3 binding (Bmi/Ring1b). A change in conformation is linked to the mechanism, in this case it would appear that the RING docks to the nucleosome positioning UbcH5c for ubiquitin transfer, following transfer of a ubiquitin UbcH5c-ubiquitin is no longer able to access both the E2 binding site on the RING and the nucleosome at the same time leading to a termination of the cycle after a single ubiquitination event.

Based on this literature I wanted to test for a conformational change of UbcH5α, designing experiments to do so presented a number of considerations. There are a variety of spectroscopic techniques for monitoring conformational changes of proteins in solution. These include circular dichroism (CD), far-UV CD can evaluate the overall features of the secondary structure of the protein and near-UV CD can evaluate the tertiary structure. NMR spectroscopy is frequently used for the structural elucidation of proteins in solution. Disadvantages of NMR include the need for non-

aggregating protein and it is of limited success in the detailed analysis of fluctuating states of proteins due to resonance broadening and/or lack of chemical shift dispersion. X-ray crystallography is another commonly used technique to study the structure of proteins, however MDM2 is not a protein that crystallises easily, so much so that a crystal structure of MDM2 in its entirety does not exist. Also previous report suggest that it is not easy to obtain stable MDM2 RING/E2 binding[220] , this may have put others off attempting to crystallise this interaction. However I have shown a stable interaction using protein interaction assays and alpha screens (Chapter 1) suggesting crystallisation may be worth a second look. As well as protein suitability another disadvantage of X-ray crystallography is that subtle allosteric change may not be visible in a crystal. No one technique for structural analysis is superior, they all have their advantages and disadvantages.

We also considered the fact that my earlier results showed that UbcH5α binds to peptide 8 (See Chapter 1) and that peptide 8 is able to mimic the majority of activity displayed by FL MDM2. It was therefore decided that I would use peptide 8 as a tool to study the activation of UbcH5α. Using peptide 8 instead of the RING domain or FL MDM2 opens up a range of biophysical techniques and allows the optimisation of assay conditions before potentially introducing full length protein. In an ideal situation I would want to use FL MDM2 as, by using just peptide, I cannot account for any reciprocal changes in the conformation of MDM2 itself upon interaction with UbCh5α.

Limited proteolysis can provide important information on the structure and dynamics of a protein. An advantage of using limited proteolysis is that the technique is simple and modest amounts of sample are required. Another advantage is that it can provide data on the solution structure of a protein, even if the data does not provide the high resolution offered by NMR and X-ray crystallography[233]. This lack of resolution was solved here by development of a novel approach where I coupled limited proteolysis to MS in order to provide information of the topology of the proteases sensitive sites and how they changed on peptide binding. Limited proteolysis has been used for structural analysis of wild type and mutant proteins[234], analysis of overall structure and structural domains of proteins[235] and analysis of the stability of domains[236].

I used limited proteolysis to probe for conformational differences between free UbcH5α and UbcH5α in complex with peptide 8. My results using trypsin showed that the Ubch5α:peptide 8 complex was protected from digestion by trypsin (**figure 4.3**). One hypothesis for this result is that binding of peptide 8 to UbcH5α induces a conformation change of UbcH5α that results in the burial of a previously exposed trypsin recognition site. However this result cannot be used to definitively suggest a conformational change in UbcH5α as there is a second possible theory for the protection from digestion. It is possible that the trypsin recognition site is within the peptide 8 binding site, and that peptide 8 simply blocks the recognition site without inducing a conformational change. I therefore used a second protease to see if this provided a clearer picture. The theory was that if other proteases also protected Ubch5α from digestion then it would be unlikely that the peptide would block the digestion sites for all of them, suggesting that UbcH5α was undergoing a conformational change.

The actual result seen when limited proteolysis was carried out by Glu-C was surprising, UbcH5α in complex with peptide 8 was not protected from digestion, instead the complex promoted digestion when compared to free UbcH5α (**figure 4.5**). This result suggests that binding of peptide 8 to UbCh5α results in a conformational change that exposes a previously buried recognition site for Glu-C.

My limited proteolysis results show that a conformational change of UbcH5α upon peptide 8 binding is highly likely. Although allosteric activation of E2s by RING E3s has been suggested for certain pairings[228] there is a lack of strong experimental evidence, especially in the case of MDM2, and my study is probably the first direct evidence that MDM2 allosterically activates its E2, UbcH5α. Interestingly during a time course, in which digestion with Glu-C was allowed to proceed for up to 8 hours, no further digestion of either free UbcH5α or UbcH5α in complex was seen than the amount of digestion seen after 30 minutes. This suggests that UbcH5α has a stable core whether it is free or in complex, as my results suggest a conformational change, upon peptide 8 binding this stable core may be different in each scenario.

My proteolysis results suggest that there is a conformational change of UbcH5α upon peptide 8 binding and that UbcH5α has a stable core, it cannot however provide

answers regarding the precise residues involved in these conformational changes or stable cores. For this reason I chose to combine limited proteolysis with mass spectrometry, this combination has been used previously to examine the dynamics of protein domains[236] but not full length proteins like UbcH5α.

Models were produced from the mass spectrometry data showing that UbcH5α and UbcH5α in complex with peptide 8 both had a stable core, interestingly the stable core for each differed. One main difference is that the site of ubiquitin binding appears to become much more stable when peptide 8 is bound.

The stabilisation of the ubiquitin binding site could help to explain why the RING domain of MDM2 facilitates discharge of ubiquitin from UbcH5α (**figure 3.6c**). The stabilisation of the ubiquitin binding helix could result in it becoming less flexible and/or more rigid in such a way that it facilitates ubiquitin transfer by 'ejecting' the ubiquitin moiety. The RING without the tail is still able to bind UcH5α (**figure 3.8c**) but cannot facilitate the discharge of ubiquitin from UbcH5α (**figure 3.6c**). It would therefore be interesting to see if the RING without the tail affects the stability of UbcH5α in the same way as peptide 8. If the result is different it would imply that the tail of MDM2 plays a role in this allosteric change of UbcH5α.

A study published in 2012 states that UbcH5c conjugated to ubiquitin is a highly dynamic structure that prefers an open conformation. It goes on to say that binding of the RINGS BRCA/BARD or E4B to this conjugate shifts the conjugate towards a closed conformation and it shows that this closed conformation is linked to E3 enhancement of E2-ub reactivity (**figure 4.21**). The study also noted that leucine 104, a highly conserved residue throughout the E2 family was important for this closed conformation and that mutating it to glutamine decreased E3 ligase activity[228]. There is a leucine at position 104 in UbcH5α. If this study is correct then perhaps the stabilisation of the ubiquitin binding domain that I show in my results could facilitate a closed formation of the UbcH5α and ubiquitin conjugate, the stabilisation of the domain could correspond to the decreased flexibility of the conjugate. It would be very interesting to repeat this experiment with a UbcH5α ubiquitin conjugate and then look at the affect that peptide 8 has on conformation and stability of the conjugate.

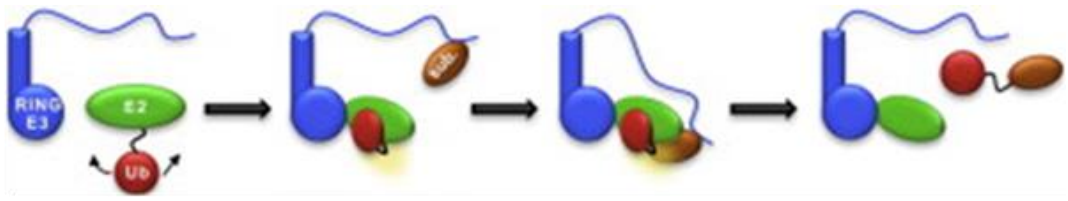

Figure 4.21: Schematic diagram showing how a 'closed conformation' of the E2-ubiquitin conjugate upon RING binding contributes to the overall mechanism. When the RING binds to the E2 the E2-ubiquitin conjugate adopts a 'closed' formation. This orientates the conjugate in such a way that is optimum for transfer of ubiquitin to the substrate.

Figure adapted from Pruneda JN, Littlefield PJ, Soss SE, Nordquist KA, Chazin WJ, Brzovic PS, Klevit RE. Structure of an E3:E2~Ub complex reveals an allosteric mechanism shared among RING/U-box ligases. Mol Cell 2012;47(6):933-42.

I did not carry this out, as previously discussed in Chapter 1 creating a stable E2-ubiquitin conjugate is an extremely tricky task. I describe the new method of click chemistry as an alternative way to create a stable E2-ubiquitin conjugate. If this method were to produce a stable conjugate then this would certainly be an experiment worth repeating.

My previous results show that the RING binds to UbcH5α (**figure 3.8c**) and that of all the RING peptides, peptide 8 has the greatest affinity for UbcH5α though Peptide 2 also showed some affinity for UbcH5α (**figure 3.1c**). From the model (**figure 4.13**) it looks like residues in peptide 1 and 2 contact the N-terminal helix of UbcH5α, other RING E3 have also been shown to contact this α helix[228], part of this very same helix changes upon peptide 8 binding to UbcH5α as demonstrated by HD exchange and limited proteolysis. Therefore it is likely that the change in flexibility of the N-terminal helix on peptide 8 binding contributes to the binding of the E to the FL RING and that binding of the peptide 8 region of the RING then facilitates (or potentially disfavours) subsequent formation of additional interfaces.

The limited proteolysis and mass spectrometry experiments could be developed further; it could potentially be used to study the change of UbcH5α, upon peptide 8 binding, over time. As mentioned above it could also be used to look at the affect that peptide 8 has on the UbcH5α:ubiquitin conjugate.

I used HD exchange as it is a very useful tool for studying three dimensional protein structure and allosteric changes that may not be detected by X-ray crystallography. I thought that using HD exchange would complement my limited proteolysis and mass spectrometry results and possibly provide more information regarding the allosteric activation of UbcH5α upon peptide 8 binding.

For the most part my HD exchange assays were unsuccessful. Although I had nearly 100 % primary amino acid coverage the main problem lay in the concentration of the peptide. Initially the concentration of the peptide was 5 mg/ml, and this was used in all earlier experiments. We carried out calculations and the HD exchange based on this. However a couple of later experiments using the peptide did not proceed as planned and so I re-tested the peptide concentration and found that it was 100x less

concentrated than suggested by the manufactures. Consequently the molar ratios of 1:1 , 1:10 and 1:100 (E2 to peptide) that we thought we used for HD exchange were actually molar ratios 100:1, 10:1, 1:1 (E2 to peptide). It is highly unlikely that complexes would have formed at this molar ratio and any complexes that did form would not be detected by the mass spectrometer due to the excess of protein not in complex. This explains the minimal change or no complex formation that is seen in the results. I aim to repeat this with new peptide at the original molar concentration planned (1:1, 1:10, 1:100, E2 to peptide), the hope is that one or more of these ratios is optimal for complex formation and that we therefore may be able to detect conformational changes of UbcH5α due to this complex formation.

The HD exchange did provide one result; there was a change in the rate of deuteriation of two peptides (**figure 4.18**) that correspond to the N-terminal α-helix of UbcH5α. This is the same α-helix that is destabilised upon peptide 8 binding in my limited proteolysis assay (**figure 4.20**). It is a promising sign that the results from these two approaches reach complimentary conclusions and it provides hope that repeating the HD exchange may provide us with further information.

In conclusion my results show that peptide 8 binding to UbcH5α induces an allosteric change and that this activation may play a part in the transfer of ubiquitin from the E2 to the target.

Chapter 5: Results

5.1 Peptide phage display

5.1.1 Introduction

A bacteriophage is a DNA containing virus that infects bacteria and produces many copies within a short space of time. In 1985 it was reported that a 'foreign' peptide could be displayed on the surface of a filamentous bacteriophage[237], following this phage display technology was developed.

Peptide phage display describes a selection technique in which a library of peptides are expressed on the outside of phage, while the genetic material encoding the peptide is contained within the phage. This physical linkage between the peptide and genetic material encoding it allows rapid partitioning based on a binding affinity to a given target molecule by an *in vitro* process known as panning. Panning is carried out by incubating a library of phage displayed peptides on a plate, or bead, coated with the target, washing away the unbound phage and eluting the specifically bound phage. The eluted phage are then amplified and put through additional binding and amplification cycles to enrich the phage pool in favour of binding sequences (**figure 5.1**). After multiple rounds the individual clones are characterised by DNA sequencing. Next generation sequencing (NGS) is a novel technique developed by the Hupp/Ball labs, with NGS it is possible to sequence millions of inserts in parallel, previously peptide phage display data was limited by conventional DNA sequencing and only obtained 20-50 sequences.

Commercially available phage display systems can be obtained from New England Biolabs, their Ph.D.™ system is based on a simple M13 phage vector , modified for pentavalent display of peptides as N-terminal fusions to the minor coat protein pIII. The phage-peptide combination has been optimised so that there is no effect on the infectivity of the phage[238-240].

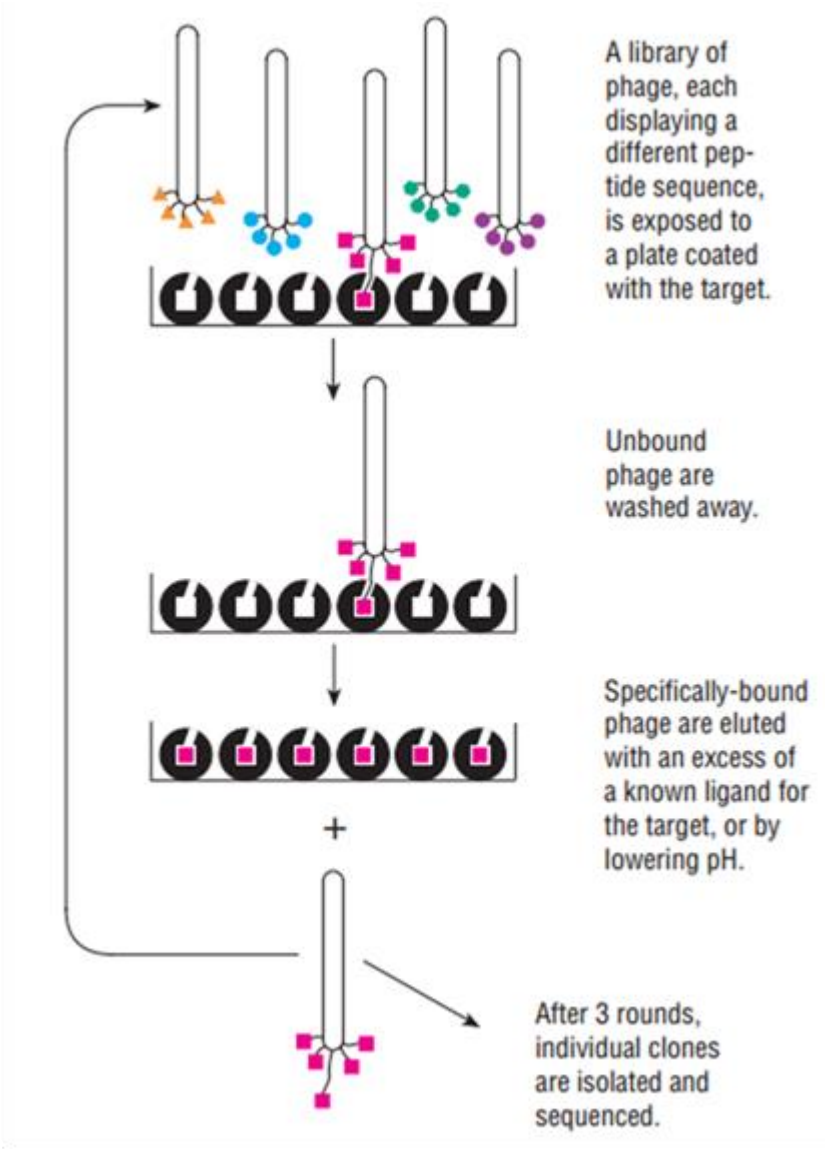

Figure 5.1: Schematic diagram showing simplistic phage display method. Panning is carried out by incubating a library of phage-displayed peptides on a plate (or bead) coated with the target, washing away the unbound phage, and eluting the specifically bound phage. The eluted phage are amplified and taken through additional binding/elution/amplification cycles to enrich the pool in favour of binding sequences. Individual clones are characterised by DNA sequencing.

Figure from NEB Ph.D.™ Phage Display Libraries, Introduction manual

NEB currently provide three premade random peptide libraries, all the libraries are claimed to have complexities in the order of 10^9 independent clones. I used the linear dodecapeptide (Ph.D.-12) library.

Advantages of peptide phage display technology over other methods include its relative inexpensiveness and the short time required for the selection and amplification process.

This system can be used in a diverse range of applications including the identification of small molecule binders, novel enzyme substrates, cell targeting peptides and epitope mapping. A dramatic application of peptide phage display involved the Ph.D.-12 library being panned against taxol to identify the natural target for the drug, Bcl-2[241]. This application demonstrated that short peptides from an unstructured peptide library can mimic a 3-dimensional ligand binding site, greatly increasing the potential for peptide phage display applications.

I am involved in the developing of a novel use for phage display to use it to probe protein conformation. My goal was to determine if peptide phage display could provide a tool to probe the UbcH5α conformations defined in Chapter 2.

Questions

1) Can I confirm the biophysical data?

- **a.** Is there a conformational change in UbcH5α plus peptide 8 compared to free UbcH5α that can be detected as a difference in binding activity?
- **b.** If there is a difference in peptide binding than what implications could this hold for the activity of UbCh5α in ubiquitination?

2) Can I identify peptide motifs that bind UbcH5α that could be important for

- **a.** activity?
- **b.** designing of therapeutics towards UbcH5α?

5.1.2 Peptide phage display utilising NGS for a novel application

As described in the introduction peptide phage display has been utilised for a number of different applications. I wanted to use it to probe for a conformational change of UbcH5α upon binding of peptide 8. My hypothesis was, if UbcH5α were to undergo a conformational change upon peptide 8 binding this may be accompanied by a change in the binding specificity of the E2. As such I set up the peptide phage display assay to isolate those phage peptides that bound to UbcH5α and those that bound to UbcH5α in complex with peptide 8. I also used an empty well as a control to assay whether any of the phage were particularly sticky.

It should be noted for my results that using peptide phage display to probe for conformational change is a novel idea and as such the assay protocol and interpretation of the results are still emerging methods. Further experimental work would have to be carried out in order to establish standard experimental methods and result analysis.

The first thing to consider when carrying out peptide phage display, for any application, is the diversity, the proportion of possible sequence present in the library, of the peptide library. The more diverse the peptide library is the higher the quality of the library. Should a peptide library be less diverse the final results may be biased in favour of certain peptides and other valid peptides could be incorrectly discounted.

Prior to the availability of NGS it was hard to determine the diversity of a commercial peptide library in the laboratory and we were obliged to go with the quality control of NEB. However with the advent of NGS we are now able to make or own assessment of library quality and diversity. **Figure 5.2a** is an example of a poorly diverse library, there are a number of clone with an exceedingly high copy number (234301) and a large number of clones with copy numbers in the hundreds. In a more diverse library there would be more clones with a lower copy number, ideally one, and no clones with exceedingly high copy numbers as in this library. **Figure 5.2b** shows the peptide library that I used, this has much better diversity than the library displayed in **figure 5.2a**.

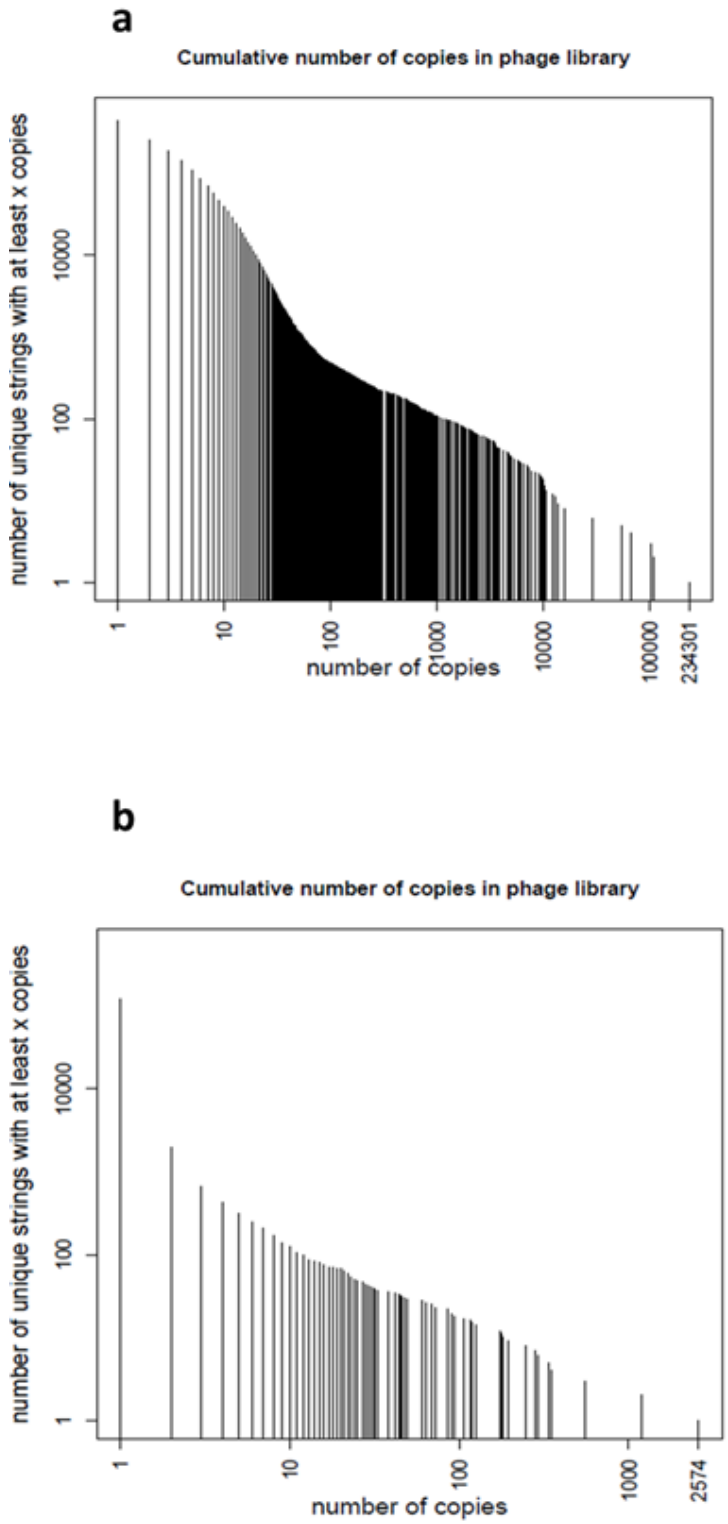

Figure 5.2: The diversity of phage libraries. a) Graph showing the diversity of a commercial peptide library, the diversity of this library is poor. **b**) Graph showing the diversity of a commercial peptide library, the diversity of this library is good. The Y axis represents the number of unique peptides with at least the number of copies displayed on the X axis. NGS makes it possible to test the diversity of commercial peptide libraries.

A large number of the clones have only one copy, there are much fewer clones with multiple copies and the highest copy number is (2574), this is 100x times less than the highest copy number of the less diverse library.

I followed the peptide phage display protocol as described in detail in the methods section of this thesis. Briefly, free and ligand bound UbcH5α were captured onto a microtitre well, they were incubated with the phage library followed by the removal of unbound phage via washing, either 10 fast washes of 6 slow washes. The bound phage was eluted and the process was repeated again, this time adding the eluted phage from round one as opposed to the entire phage library. Subsequently the amplified and eluted phage for free and ligand bound E2 in rounds one and two, were sent for deep sequencing. In this method the peptide sequences are mixed prior to sequencing, each set of peptides from each sample are identified by a 'bar-code' introduced to the peptides during the PCR step (**figure 5.3**).

For demultiplexing of sample, barcodes located upstream of the sequencing primer were read independently through Illumina sequencing (Otogenetics, GA, USA) and provided as *fastq* files. Fastq files were then captured using a custom tool programmed in Java language that was used to extract amino acid sequences from raw NGS reads. Only forward reads were processed (as reverse reads do not capture the bar code). Barcode and mimotope DNA sequences were extracted from reads that passed quality control. All sequences having nonsense (not in list) bar code were filtered out. Mimotope sequences having inappropriate length or containing nonsense codons (stop codons as well as some other "forbidden" codons that should not be present according to New England BioLabs phage library manual) were filtered out. Sequences passing these filters were translated, grouped by resulting peptide sequence and sorted as indicated in the tables.

Figure 5.3: PCR primers for peptide phage display. The PCR step incorporates a bar code to the PHAGE peptides. The bar code differes for each of the conditions e.g the peptides that bind to free UbcH5α in round 1. This bar code allows the peptides for each condition to be seperated after NGS. NNN represent sthe bar code, where N= A,C,G or T.

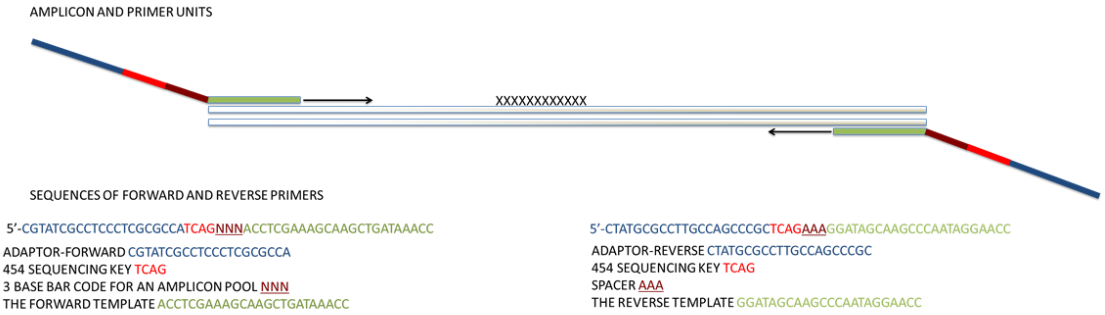

The general flow of the custom Java tool is as follows- for each read in .fastq file: (i)) check quality (no "N" signs for unknown nucleotides etc.) and discard reads with low quality; (ii) read first 3 nucleotides which is the barcode; (iii) if nucleotides (X)n + 1 to (X)n + 36 this is a insert sequence. Nucleotides 1 to 36 are taken as peptide sequence, and translated to 12 AAs. If none of these two conditions is satisfied, read is discarded; (v) Sequences with barcodes are sorted so that for each unique sequence one line contains counts with all barcodes. Lines are sorted and top 50,000 (in terms of sum of all barcodes) are outputted.

5.1.3 Analysis of raw data

The list of peptides provided by Adam Krejci at RECAMO contains hundreds of thousands of peptides and so I had to try and find the best way to sort them. As previously mentioned this is an emerging method, therefore there was no standard analysis route to follow.

I first sorted the results to analyse those peptides that bound preferentially to free UbcH5α. To do this I selected peptides that were found to bind to free UbcH5α at least 4x more than UbcH5α in complex. I also introduced a cut off point for analysing peptides, I did not analyse any peptides that were found to bind to free UbcH5α less than 8 times in the sample. Following this analysis I ended up with four tables that show the peptides that preferentially bind to free UbcH5α in round 1, for the quick wash (**table 5.1**) and slow wash (**table 5.2**) method and round 2, for the quick (**table 5.3**) and slow wash (**table 5.4**) method.

The data shows that there are a large number of peptides that bind preferentially to free UbcH5α. It could also be argued that when peptide 8 is present in the complex it physically blocks the binding of peptides that bind to the same site of UbcH5α as peptide 8. Whilst this argument may be valid for a number of the differences it seems unlikely that it would account for all the differences seen in the tables leading to the conclusion that there is a conformational change of UbcH5α upon peptide binding.

seq	sum	QW C	QW E2	QW E2 + 8
DSDIGPTRNHRV	393	28	28	6
HTWHEDVNVQRP	470	21	26	6
DLVTVSRMVVNR	169	10	25	4
RTPEMTSLMAWG	1060	15	21	5
VFSLTPDWRISL	54	11	19	5
LEGDTETIVRKI	270	13	18	5
YDSSLTMPPQAT	19	10	15	4
SAYVRHVSGGPR	189	7	15	4
ATSSDRHNRYVS	16	15	15	3
TWTYDSSTMQLV	105	13	14	4
VLSRVGHFNIPS	33	13	14	4
GSNNVSWSTNLH	218	13	14	2
KPQPHGIDVWLT	34	8	13	3
DYKVTRTQVWTF	63	10	13	3
SHSIRWDPQGAC	32	8	13	3
KIMSQGQEPQGY	66	16	13	2
TETFGSGLNFRG	43	3	13	1
VSHSRAFIVSGG	84	14	12	3
TSSIVHKIVHAR	38	9	12	3
EVHSGRPWLRTG	52	15	12	2
TMKPSMTRTHLL	43	11	12	2
GNFSDTHRGLPV	47	10	12	2
GGHFAVTVRSEL	5	10	12	2
EGRLLWYGSPAT	23	6	12	1
QVAVLDEKTFLR	74	12	11	3
GFAAALAANNAQ	30	6	11	3
DVDHSADSSLMS	56	5	11	3
YPPYFTPPFQLM	34	8	11	3
MPSMSTNHLNTR	373	8	11	2
TQMRLNSYFYDS	6	11	11	2
TLRIRCLADHTK	8	5	11	2
SEPRAIQNLDRW	4	5	11	1
DDFRVWWPNFPR	1546	7	10	2
IDGNGGVQQRGL	49	7	10	2
LTCCHVDLSANS	4	1	10	1
SLGQSNNVSPIV	97	9	10	0
KYATPIPYDRLA	73	4	10	0
HGTAYSFHGPAV	100	9	9	2
IHRYTPNEIDRA	18	6	9	2
GKAADLAPFTRA	78	11	9	2
RAFYSDPMLYDA	30	8	9	2
ETLIQHIQVFAV	5	6	9	2
TPTHYSDDGPNN	87	7	9	2
SYIPTFPPGLSR	30	3	9	2
DDLRPVSRIFVT	5	8	9	2
RPEINFTQSLSS	19	3	9	2
IDSPSLTPMKLM	7	3	9	2
KLLHVTPSSASK	6	7	9	1
TRRILDQGLGTT	60	7	9	1
TTRILDQVLGTT	208	5	9	1
SVHGTKHLSSEL	688	4	8	2
YDAEAAAVSRRN	9	7	8	2

KAPPDAEPNFRH	28	3	8	2
GQAVDLAPFIRA	3	3	8	2
KSYNPTDYHASR	4	7	8	2
SVNTTVTLMPTT	35	8	8	2
GCCGPSRALLPI	16	8	8	2
SQGPVRTHIARL	11	7	8	2
GKHGTEKVPAHQ	3	4	8	2
YGTRDHSVLIRQ	14	4	8	2
YSQPDGPLWYIR	11	3	8	2
FAFPVIPYFTHT	60	6	8	2
GIGASPNTFRLP	23	5	8	2
YPWLDAARHLMR	55	3	8	2
AGAWNRDATPEP	15	8	8	2
GSYAVVVPEGVD	4	6	8	2
WKAADLAPFIRA	429	6	8	1
ELGEVNTLGRVT	33	5	8	1
GMASDGRVDSAS	15	1	8	1
YNTHLIVSESAH	26	8	8	1
ADANTWFPGRTK	44	5	8	1
ALPANMGRLMEL	81	6	8	0
NPSRVAGVNLAF	150	2	8	0
SGILNPSQRQDL	32	3	8	0

Table 5.1: Peptides that preferentially bind to free UbcH5α compared to UbcH5α in complex, in round one with the quick wash method. Seq= peptide sequence, sum= number of times peptide was identified in sequencing. QW= quick wash, C= Control, E2= free UbcH5α, E2+8= UbcH5α in complex

seq	sum	SW C	SW E2	SW E2 + 8
NYKVTRSQVWTF	281	27	34	5
NYKVTRIQVWTF	133	10	17	4
QSSHSARLIQYG	371	5	16	4
SAPPDAVPGYVH	354	20	16	4
QSGMLRLDENHD	107	3	15	3
GDGNSVLKPGNW	901	2	14	3
LSIGASNISLVQ	567	11	13	3
QGSWSPSSSHSL	169	7	13	3
AYITKRDPHASP	108	10	12	3
SHGEMSNIAIAS	109	8	12	2
FSELPKQSGYFL	199	10	11	3
STLAPTPEELHT	157	7	11	3
STDSHYGRWVND	113	6	11	2
SVFPKPGYNSNL	103	4	11	2
NSVHDLMLSPPP	99	6	11	2
DALEESNVNSAH	63	2	11	2
TFNMKAFGTNAM	115	4	11	1
SFHPMGLPSTSF	123	6	11	0
FDMYPTNRNPGR	66	1	11	0
SQSGPPMWSTFW	104	8	10	2
TTRIFDQGLGTT	80	6	10	2
QPDVCSIRGCTY	78	10	10	2
YTKHLIVSESAH	49	3	10	2
INNVPNEMPLGL	44	2	10	2
TNSPKTFTNTSS	40	1	10	2
DSERNTLNPYRS	82	6	10	0
SPLLMPRMPGIG	91	4	9	2
TLGSPSDLPISE	59	1	9	2
EVHSGRPWLRTG	52	3	9	2
TDTSAALSFSAR	614	2	9	1
SLASEDTPNVLA	144	2	9	1
LPRGTYLIYPDQ	78	5	9	1
NKVGLVPHMSAI	65	2	9	1
LPAWSGWGYRVL	310	5	8	2
SIWDRYGAVSHG	72	1	8	2
EVHSWSPWLRTG	62	7	8	2
TFAERNVLPDLQ	59	0	8	2
WEGSYGNAARHR	59	2	8	2
TRITNGIDVALT	49	0	8	2
HDTLPRASVTRQ	44	3	8	2
HPHEMRTDGLRR	41	2	8	2
DIASHSSQMTAL	39	0	8	2
HHRNYLPTSGTK	36	4	8	2
NANSSVDTATIL	68	3	8	1
AVHADHMCSIHI	55	2	8	1
DLKQSILSPAPG	54	2	8	1
TELLQIDSLKGQ	54	5	8	0

Table 5.2: Peptides that preferentially bind to free UbcH5α compared to UbcH5α in complex, in round one with the slow wash method. Seq= peptide sequence, sum= number of times peptide was identified in sequencing. SW= slow wash, C= Control, E2= free UbcH5α, E2+8= UbcH5α in complex.

seq	sum	QW C 2	QW E2 2	QW E2 + 82
SVPPSTNSPFSH	681	30	218	36
KVPTVCANPEWC	769	120	205	35
LPYKIPSTFFNI	414	12	133	11
AVGIYHAAEHPY	264	11	118	12
CFAIAPTRLMYS	276	25	107	6
ALKPWDLSSNLS	284	22	100	23
DSDIGPTRNHRV	393	26	93	20
DSQFNKYSIATV	552	10	89	11
DLQLPRSGPRAS	453	46	88	17
RILPMVDTQILT	130	0	80	1
HVADTGSLISKR	253	9	76	8
ARSASNPSWIAP	242	14	66	7
TDLYFESWRMTG	100	1	55	2
MQPRSVNTIDIL	187	10	49	8
LTAGYDHRFRQP	131	1	46	11
HPDAEDITNTLQ	105	0	42	0
DWSIREGHQTYP	46	3	39	0
HIHVRTTSALVA	78	0	38	1
VTVTDMNHDRDF	47	0	38	0
VWAMENSIRMTL	140	6	37	7
TDNYGGRSTQAA	483	14	37	4
TYTSRMFIEHVR	180	10	37	2
VPGALSKANTLG	177	9	36	5
WAYDGDQKFRRL	183	5	35	4
GEVAQLRSAEPY	99	44	35	1
SSHPSNATLKTN	45	0	35	1
ASSSLCCTRGLM	114	3	34	5
FSLSRYPSSASI	59	0	34	0
NYHLSEQVPRHR	325	19	32	5
DRNLPSNQFQRS	103	0	32	0
VKDIRGTAMRWA	37	0	32	0
SATFPGPYHSTP	175	3	30	1
IGSRNAPSFLLH	120	1	30	1
RKAPETSLSIPL	101	7	29	6
GSEPAQRLEDRK	108	6	29	4
GGTVTNQVVTLR	134	1	29	3
YLPYDALRKAWG	74	1	29	3
GFARPDGSLLTS	199	6	28	7
FPLREGHHWDAG	189	41	28	6
NSVAWWGDFSSS	57	0	28	6
DVVSSGHTIASI	113	8	27	6
SSILDYIDSYPF	84	16	27	6

AGTHHPLYFRQV	80	18	27	3
VHCKMPMRLLYG	44	1	27	3
RKQHAIPLIWPA	59	4	27	2
RIDFLSNSWSAR	61	0	26	5
SPVSAGARNLPY	57	1	26	1
NSSPFTTPGSSK	77	15	26	0
AEIVPMSHRGFS	43	4	26	0
SHAEWAMASTSS	335	12	25	6
HHPLGWNDTVEA	107	8	25	5
SQFATVWERMRN	158	15	25	2
NTYIPANLHHMP	264	18	24	6
HDSPNALTTKLN	63	1	24	0
SLINFLAHPTQN	37	7	24	0
AFNMTRFPERYA	30	0	24	0
SGPSNYGASHRN	27	0	24	0
GQSEHHMRVASF	87	0	23	6
SHTAYSISSGGH	382	18	23	5
ASYVKAASAVFD	129	8	23	4
VAAAGCSRCHSG	133	7	23	1
YSCPSSGLYSGC	92	0	22	1
SLQWTVDLGMPP	56	4	21	5
ASVLDYKGFFQR	79	1	21	3
RPAVLDFHWAKI	64	0	21	1
GGFHVSDPVMSY	55	0	20	0
VRFPDPQVTHRL	62	2	19	4
TVSMVNYGGSTV	276	7	19	3
SQSGLPPATGLE	117	0	19	3
ATARFSLTMVGF	287	4	19	2
IVGEPRMSRSYS	138	1	19	2
YVEPGTPLSYTH	60	0	19	1
YPWLDAARHLMR	55	0	19	1
TTIVQPPSKDST	80	0	19	0
QYYGAWWHTPAA	35	0	19	0
HTHLRDALWVHS	30	0	19	0
KTPFNHVNQFSL	21	0	19	0
TYITGPYRSSAP	292	25	18	3
SPNPLPWSSRVP	191	9	18	3
GYCMNKQHSTLD	91	1	18	2
HESWLPAYVLGS	42	0	18	2
GTDLYNAFKTFS	121	1	18	0
VPSGLPSTGHRI	59	4	18	0
EYQRSVAWLKEH	27	0	18	0
FPTSLWSPEQDV	23	1	18	0
SGVYKVAYYWQH	92	13	17	4

EPYSKRVFDPVP	70	0	17	4
IALPNESNIHLP	175	7	17	2
YTPSSIATPLRL	144	13	17	2
VRSADRPNVVFE	46	0	17	1
IAHDAVPWPASP	111	9	17	0
GKAAGLAPFIRA	277	11	16	4
NTNYVTWSPSSR	64	0	16	4
ALVTSLMENEST	107	3	16	3
QLNPTRFTPLAW	79	0	16	3
EHWYSLVKAIPF	209	21	16	1
GALLPSMNKGHW	192	3	16	0
YHVPRSVFYAMH	31	1	16	0
RAYESVSVYRAW	28	1	15	4
DSTAKVSTLKDT	198	18	15	3
SYAERPIQKFST	123	8	15	3
NGPASLLQLWVA	34	0	15	3
IPHESNALSHDE	129	1	15	1
YSRHPSSQPVHY	82	1	15	1
GASAVPWRTINH	70	1	15	1
IGRQGTTDFLFS	34	0	15	1
TVQRTDFYGSQY	17	0	15	1
GDVMDKRNQFLF	52	0	15	0
QQRPYVQDLRLI	48	1	15	0
WVLSPNSFPRAK	38	1	15	0
INTDFEKAPTPH	19	0	15	0
NYKVTGTQVWTF	155	4	14	2
GPSFSMLDDPSG	65	0	14	2
TITWMWTGTPRG	187	10	14	1
WNAPSVANGPRM	176	1	14	1
HKLDRTWFHHTP	106	29	14	1
FQNKVSGDSGVR	51	5	14	1
AGTHLLNIPIDG	35	0	14	1
AMIGNQRAWEPN	19	1	14	1
SVAVLSKTFEVY	58	0	14	0
SIRMSYFEFAGN	45	0	14	0
LTVNHNLRNDSR	35	1	14	0
VSAGERTLLLMP	34	1	14	0
SLRSVSYNPSTL	128	11	13	3
HPHRLWDIHQGT	69	3	13	3
DRVHDASKLYGH	77	10	13	2
MDENVATNQLMI	71	1	13	2
GWNDMSSNDSNG	52	0	13	1
GHIDHSRALGAR	17	0	13	1
TVTSAQPSSHTR	95	11	13	0

FPTLSVHASAST	57	2	13	0
RLPFSFGAPHMP	20	0	13	0
VNNESWSWSADS	20	1	13	0
SLPDTLNMLMLA	17	0	13	0
QVSNSEYMRITQ	14	0	13	0
GKAADLGPFIRA	179	8	12	4
KLARNNDWSYMQ	124	1	12	4
GNVHENVNTTRS	78	4	12	4
SGNTTVTLIPTT	40	4	12	4
SMLRVFSELREP	327	20	12	3
STNGAVIANSKP	246	4	12	3
GKSADLAPFIRA	181	6	12	3
DYVSAITRIRMV	173	12	12	3
GKAADLATFIRA	165	3	12	3
SFWLPPQPYHPV	147	32	12	2
DFTLLSSNGRSK	98	2	12	2
FVDPETDLFLDD	48	10	12	0
ASPQCCDWQAIG	41	1	12	0
EAAYTTLDPRNQ	35	0	12	0
QNDMLNLRVSQV	35	14	12	0
VEASSQDERNTQ	34	0	12	0
AADAGTQDHTLV	22	0	12	0
SDPCGRCSITFD	16	0	12	0
GVATGSRVETFL	12	0	12	0
VGQLSWYTPQKT	175	9	11	2
SSLWSELYGGSM	167	0	11	2
SLHTSFFRTPEF	158	13	11	2
MSGLKPVKGDLS	59	0	11	2
NLITQAPNPSRS	242	9	11	1
GYEDFAERVSHG	161	2	11	1
YLVPSPPWSQTF	100	7	11	1
GMLQHALVPKVW	18	0	11	1
WMATTTEQLVVR	86	5	11	0
NADPAMVTRLSA	78	1	11	0
SPRMAAEEHSHG	60	0	11	0
KWWSAAEGALLS	29	1	11	0
VIAKSSPVMDYH	22	0	11	0
TPRMAQDRAVHQ	191	27	10	2
NSVFIPLTKPDT	154	4	10	2
ARSTEVLFLSSS	136	12	10	2
LLSSPRQPAMPG	133	5	10	2
TTMRMDSMTRNP	131	7	10	2
STIWGWSNNSHF	129	5	10	2
DRDEGFASGWSL	59	11	10	2

GAETTPLSLSPP	136	7	10	1
SGDNDTQLEYIA	117	9	10	1
SNMHLLQPTKPR	68	4	10	1
AMFHTRPLTSQT	58	2	10	1
HEMDGFIVVSSY	167	1	10	0
VFSLTPDWRISL	54	1	10	0
LTTEVAQIMRYE	50	0	10	0
ASLTPLVRTPSA	25	0	10	0
ATFRPTGVPVVH	23	0	10	0
GHRHHTIHNMNL	23	0	10	0
SSYRPTHDTWML	22	0	10	0
KTLNGLSLDRPY	20	0	10	0
YAKSAQQISPMY	19	0	10	0
TPDQSRRIGSVW	15	0	10	0
SHPRAISAASVG	14	2	10	0
HQVGLVPHRSMP	13	0	10	0
SLPHPINSTYNN	10	0	10	0
TTRILDQVLGTT	208	10	9	2
YAIVPQRHDKHH	180	0	9	2
KGGLEVHSRNLQ	118	12	9	2
ASSLPQGNFARA	95	8	9	2
TLSLDCTSHPNN	86	8	9	2
TPIRPLESVVRH	424	19	9	1
FPHASTLNSYGG	131	4	9	1
FSSRASSAPHTD	95	3	9	1
GGLQMSRHTTYT	77	0	9	1
VHNSGLDSVIRV	66	4	9	1
FSDDWLVNTSLK	65	3	9	1
LVAQRTPEVEKL	61	13	9	1
ICSSCFVQKSIV	56	1	9	1
LTHTQHGRSATL	48	0	9	1
GATQIQSTNRIG	26	2	9	1
HVTSAFRFGLSA	24	0	9	1
NPSNVHRSSANN	158	3	9	0
TDLPIPASFGKF	105	10	9	0
MFGPSQSIRTKV	64	8	9	0
TMWSAHFGPLVR	57	0	9	0
TFTAPHYPVILA	43	19	9	0
FVERSTDNKLVG	29	2	9	0
VASLHIPMTDHP	10	0	9	0
NLMTASTISLWG	9	0	9	0
AFHADHMGSIHI	185	3	8	2
DSALPSRGFRIS	182	24	8	2
NVARDMYRNGAD	149	8	8	2

SWLGLTGSGTLF	95	17	8	2
GKAADLASFIRA	84	6	8	2
ASATVSKPWPTG	63	1	8	2
FAFPVIPYFTHT	60	4	8	2
SNGSSYLFATNS	55	0	8	2
FSDPDMRAWAFS	49	9	8	2
ACNGRDCIPKGH	46	2	8	2
NYPMKSLRGVHS	39	12	8	2
ATEERSRIWMFL	34	0	8	2
HSTHDYGTFLTR	23	0	8	2
DLVTVSRMVVNR	169	4	8	1
GFYQHWRVGASA	128	0	8	1
YYPAYAHGPRGT	50	8	8	1
SGVYKGAYDWQH	39	5	8	1
SDAWPTKNLLIS	13	0	8	1
GPESAMQKQMAG	111	0	8	0
FNTVNSPNVQNN	74	17	8	0
SDEASKTFSLGH	69	0	8	0
QHAQRHITLGSE	62	5	8	0
TNEPIRGTMRLS	60	1	8	0
LTPNASRSLTSD	55	7	8	0
APARVVTDCSRC	54	0	8	0
SLADAGHPKGSL	49	0	8	0
GYNLYPVVGPDE	48	7	8	0
QAPTEIREQGLQ	35	1	8	0
HYKQDYDWRPGK	30	0	8	0
SHALQGPEGTAT	26	0	8	0
SVWQGASILWRL	22	1	8	0
NLWSYSMPNRDI	17	0	8	0
GRIDEQARGPVM	14	0	8	0
WTWPLPAAKMKR	13	0	8	0
QFHHWRQNNAHQ	10	0	8	0
NSCWVGDCERLR	9	0	8	0

Table 5.3: Peptides that preferentially bind to free UbcH5α compared to UbcH5α in complex, in round two with the quick wash method. Seq= peptide sequence, sum= number of times peptide was identified in sequencing. QW= quick wash, 2= Round two C= Control, E2= free UbcH5α, E2+8= UbcH5α in complex

seq	sum	SW C 2	SW E2 2	SW E2+ 8 2
TSIQISNAHPKS	1082	48	165	40
GSGASYQVWRPM	183	5	58	3
GLMESRPVSTPV	213	32	40	9
ARSASNPSWIAP	242	18	36	9
DRNLPSNQFQRS	103	1	36	2
NYKVTRTQAWTF	336	17	35	7
VVASAKGHIQVT	165	21	35	7
SSVMTAAQEAWS	68	2	34	7
NTHREVRYLTEM	148	10	31	4
GGLHTDHFKPIL	101	15	31	1
NHLSTPVWSITG	212	31	29	6
GNKHVSGLDIHW	133	6	29	7
VQFPQGRQFGAL	314	17	28	4
HPTNVSIASTKK	87	7	28	5
GTDTRWELLYRP	79	2	28	2
ADPLGISYLRSS	112	28	27	6
DVIVPPIAQTAD	100	18	27	7
NWSHNVRLNYTY	46	0	26	2
HYSWSWIAYSPG	186	0	25	4
TQGYDNRVVSSK	198	13	24	4
ALADSIHHYRFI	158	11	24	5
SWYRPSDGPGPQ	45	2	23	4
SVDSRVAPRLLS	135	5	22	5
YSAAIPNWLSNW	121	8	22	5
DRMPPFTSLELQ	62	1	22	1
VTLHTPAPSTRA	61	2	22	2
APLHQVSSIWQS	47	1	22	1
SLHTSFFRTPEF	158	2	21	3
GHDFGGKPMIWW	111	46	21	3
AKPTAMLYPSAT	31	0	21	0
ALKSNAWGPWMT	167	28	20	4
FSISLIDSESHT	152	5	20	3
YISPWHSLDLKG	107	10	20	1
HTFHGENSHPTS	78	0	20	2
CFAYDIVSDEMW	72	2	20	1
VETSNGFGWPNG	25	0	20	0
ALKPWDLSSNLS	284	47	19	1
VSIPKNSQHHLL	165	20	19	4
TVGLPMTYYMDT	115	0	19	2
TLTSETPWSLNR	50	0	19	0
GTVTGHIMRLDQ	33	1	19	1

GYFRVSVSEDSR	30	0	19	0
VFAYDLPIYSKV	137	26	18	4
GHSARTMGVLTP	41	2	18	2
IDAHFGLRLVND	221	3	17	2
ASTSHVSSGGSN	146	26	17	3
QWNWPVRSVANV	130	1	17	0
SSILDYIDSYPF	84	0	17	3
QSVDSAPLDLRR	65	0	17	3
DMTNVPPQRVSL	62	25	17	2
VPWPVGSLWWDH	24	0	17	2
QRTLSSDSTSVV	214	6	16	3
SLGPYGLAAPIS	168	53	16	2
KVPVGVLPLSHS	117	7	16	4
FGPPYWSSNGQN	70	1	16	3
WDSSDFHWIDTQ	22	0	16	0
HIPNNGVQTYLP	21	0	16	0
IPQIALDAQRWV	20	0	16	0
TVFPNTQAVSMT	117	24	15	3
LHTSIAPTDGWQ	71	14	15	3
GTLSRDHNIVGW	70	8	15	3
FGNRATPSSYPG	58	10	15	1
LGLPDRRPNLLH	58	2	15	1
AVARVLYTDDPG	53	0	15	0
SEGHAPPVQHRI	44	0	15	0
SALTDARTENKL	27	3	15	0
DNGQHLWSTTTV	22	0	15	1
TRPPVISMHSWH	22	0	15	2
QLPFYTQRNAAS	166	11	14	3
AQHNITAYSTTF	124	1	14	3
LPADPVQKHRIN	105	2	14	3
YWRPHPGHSTVG	103	9	14	1
KLAVTTHDTSSM	74	2	14	2
DNGHFKLSEVWA	60	0	14	2
TNHQMSNHTEKP	55	0	14	2
SPNLIKRMPSLS	37	0	14	1
NGDGCRYNACAT	219	7	13	3
SLASEDTPNVLA	144	9	13	3
IPHESNALSHDE	129	2	13	1
DVVSSGHTIASI	113	4	13	1
AHDILHAMKTPR	86	2	13	1
YVTTWTPDQRVV	57	3	13	0
QGMGYGSNWPSI	51	10	13	1

ELVRTTPRMLYL	34	0	13	0
TMPRHGSAVTTM	33	1	13	2
IRFDTPSHLPPP	112	7	12	2
SAVFNSYDQDVT	107	20	12	3
HTAHVQADRPTQ	75	1	12	1
HVANRGLTENTL	74	0	12	2
SFADPFAQMRFV	53	1	12	2
HAGQAHMADLTQ	40	1	12	3
DYLRDRMSHSRP	32	0	12	1
GFPRLSTLPAPN	30	0	12	2
HGPTHGYFLHLR	30	2	12	2
KPIYDGMRNSFY	28	0	12	0
SVPTNWHTLDSL	27	0	12	0
DSSIYYNWWMVG	26	0	12	3
RLDFIDVFRSSF	26	0	12	0
DWSPLANLQQNK	25	0	12	1
VSSSEFPHRAVL	25	2	12	0
LPPPAPWGHARE	16	0	12	0
LLSSPRQPAMPG	133	6	11	1
DMRALHQGTTLD	109	7	11	1
ITGLKATDYKDW	101	10	11	2
AKAQLMSQTWYL	86	29	11	2
AGTHHPLYFRQV	80	2	11	2
FGLSTENRGQYR	80	0	11	1
VADLGAYNYPVP	76	11	11	2
GHDLTRNTGRIS	73	1	11	2
YPHTYSPSSWSL	65	2	11	1
GGAVYFGQVKVA	54	0	11	1
AHFSLKYTFTRT	53	2	11	3
GSSSLMNPASVM	49	2	11	0
SSDFLWNYRLLG	40	1	11	1
ATEERSRIWMFL	34	2	11	0
SPTYTFISTSVA	29	0	11	3
SEMNNFSWLTVI	25	0	11	0
SNGHSLGIKADT	22	0	11	0
GLHDMTRPPHHG	21	1	11	0
SQTPTTSPSTSF	21	1	11	0
SHQFLPMGGPLP	14	0	11	0
WTTQSTGSAARF	11	0	11	0
AYITKRDPHASP	108	2	10	2
DGPKYTPPIQGQ	64	0	10	0
SLTAWKTNEMAY	63	2	10	1

WNDTMSHYHTRP	58	1	10	2
SPQMWITNPGNI	55	1	10	0
HVSWKITTIDSI	52	0	10	2
RLDAPLNTGEYS	52	7	10	2
NPDWFVFYDKGR	51	0	10	2
VADSENRYKEPQ	49	0	10	0
VNASNGESLGRR	39	2	10	0
AFNSKIEKLDLA	36	3	10	0
EAAYTTLDPRNQ	35	1	10	0
WQDFGAVRSTRS	35	5	10	1
DVWEPKFREDRT	34	0	10	0
HHNMVPVMYSVR	34	0	10	1
SSSHLISAEMYG	33	0	10	2
HSVANTYPYARS	27	0	10	0
NWHRLDGFQTLV	25	0	10	1
VPNMRDEPAINN	18	0	10	0
SVIQTVPMSLGL	17	0	10	2
HVDFRRDTNSFN	13	0	10	0
SSHLMLVESKEF	11	0	10	0
LVGNHYGFQGGW	123	21	9	1
CVASARGAQIGM	115	4	9	2
LPRAPERASLAS	99	6	9	1
TTGILDQGLGTT	97	4	9	2
FPHDSTLNSYGA	89	4	9	0
HSGLARNSAYWY	86	1	9	2
GQDRMPKWPANS	81	2	9	0
WPQRLEMGRSSA	73	1	9	0
SAMTMNQVQTKV	69	0	9	2
SGGAQMVASSNH	69	5	9	1
THAKDNREPFAG	69	0	9	2
SHEGRYIVSTVV	58	6	9	2
GFDVRNPPRDDR	56	0	9	0
AQFERQTQPAYE	55	3	9	1
DRNWAYNLLQDI	50	3	9	1
VVSPDINLLLTN	42	5	9	2
HFDYIRLAMVSN	38	1	9	1
VPLTGRPLSPLT	36	0	9	2
YRLPHVPYNYAE	35	0	9	1
GPTAYPQALTNR	30	0	9	1
ALNSLAPSSVMT	29	1	9	1
ANLTHHSSHLIF	29	0	9	0
DLRFQPRMASYV	29	3	9	0

RPLDSPDRLNAR	28	0	9	1
VNRDPYAGNWQM	28	9	9	0
RCVETHVLCADM	25	0	9	1
SVRPPSDIRSPT	24	1	9	0
NHQTAMLGVVGD	22	0	9	1
DSENGDSIRRFI	17	0	9	1
YTPNAVNNVGSD	15	0	9	2
APHPADSMMNLP	14	3	9	0
TDVHVHPNHNHG	14	0	9	0
NPLVHRHATLKV	9	0	9	0
STSTFEIYRLRG	9	0	9	0
ISMPEMLLSPLL	221	1	8	1
SVWEPGVGNQHW	152	4	8	1
SLDRKILRAYEE	140	9	8	0
SNTQSERHPLSM	126	0	8	1
KPLVGYGQMPEQ	122	3	8	1
SHRPVEMWVAAV	110	4	8	2
NYKFTRTQVWTF	100	2	8	2
AGSSHYAALGWT	94	1	8	1
VSHEGAFSGFAI	92	8	8	0
TQPAATAIMWLQ	88	1	8	1
LCTDPSPYCPRF	86	5	8	2
TWRDSVHPIWRD	84	7	8	1
YEPVGIGNMMAM	68	18	8	2
DTHQYVHSTSIN	56	4	8	2
YQAANTMGHVKT	56	5	8	1
QVSVSVQNVLHR	54	7	8	2
TAYWTTAYQQGY	54	7	8	1
TVNSEEEIHQRI	53	0	8	1
AVMHQSYNYYHR	52	0	8	2
NDMTPRRAIAMS	51	0	8	1
YIFKPDHRTNNV	49	3	8	0
CYAGHDLYVAAD	46	0	8	2
VGPNLEFHFDKG	45	0	8	0
VPMQDLSTNHVT	42	0	8	2
IPVKSWPIRPSS	41	0	8	2
EHGTLSNIFHAR	39	12	8	2
DLFGSVQLVRGA	35	2	8	1
WNDYSSRPGHFD	35	1	8	2
GSVASLSSLRGL	34	0	8	2
NAVLPAWVPRVV	34	0	8	0
GPPTSTPTSRNA	25	0	8	1

SEIGYGLMASEL	25	0	8	1
QSHMTRGSMAPS	24	0	8	0
QDEEFKEFAKYY	21	0	8	1
GAGVTVTNDRDV	19	0	8	0
SLAHDPNRFTLT	19	0	8	0
YLNKVYPSPILL	19	1	8	0
TWRVGHDQAYTR	18	0	8	0
GTDKGSTYWKYN	16	0	8	0
SYKNLSLPGAPY	14	0	8	0
TFVFNPSITPLI	14	0	8	1
NLDTNSDHLFMK	11	1	8	0
YSQPDGPLWYIR	11	0	8	0
GPFMLSYHRHPY	10	0	8	0
SESSLVRSQTFH	10	0	8	0
GVLISDTTYLDT	9	0	8	0

Table 5.4: Peptides that preferentially bind to free UbcH5α compared to UbcH5α in complex, in round two with the slow wash method. Seq= peptide sequence, sum= number of times peptide was identified in sequencing. SW= slow wash, 2= Round two C= Control, E2= free UbcH5α, E2+8= UbcH5α in complex

I then sorted the results to analyse those peptides that bound preferentially to ligand bound UbcH5α. As before I selected peptides that were found to bind to ligand bound UbcH5α at least 4x more than free UbcH5α and I did not analyse any peptides that were found to bind to ligand bound UbcH5α less than 8 times in the sample. Following this analysis I ended up with four tables that show the peptides that preferentially bind to ligand bound UbcH5α in round 1, for the quick (**table 5.5**) and slow wash (**table 5.6**) method and round 2, for the quick (**table 5.7**) and slow wash (**table 5.8**) method.

The data shows that there are peptides that bind preferentially to UbcH5α in a ligand bound conformation. It could also be argued that when peptide 8 is present it itself attracts peptide binding partners and that some of the differences are simply due to its presence in the assay. Whilst this argument may be valid for a number of the differences it seems unlikely that it would account for all the differences seen in **tables**, also if this were the case I would think that this would give more not fewer overall binders, leading to the conclusion that there is a conformational change of UbcH5α upon peptide 8 binding. Interestingly there are many less peptides that preferentially bind to ligand bound UbcH5α compared to the amount that preferentially bind to free UbcH5α. This could be due to the nature of the conformational change, if UbcH5α were to become more ridged/less flexible upon peptide 8 binding, then it could be that it is less receptive to interactions with peptide small linear motifs in the assay.

seq	sum	QW C	QW E2	QW E2 + 8
NRDFLNLKPWDI	71	11	2	10
TFNMKAFGTNAM	115	5	0	9
NYKVTRIQVWTF	133	9	2	8

Table 5.5: Peptides that preferentially bind to UbcH5α in complex compared to free UbcH5α, in round one with the quick wash method. Seq= peptide sequence, sum= number of times peptide was identified in sequencing. QW= quick wash, C= Control, E2= free UbcH5α, E2+8= UbcH5α in complex

seq	sum	SW C	SW E2	SW E2 + 8
NPSRVAGVNLAF	150	5	4	14
AHVKLYHRNGAT	101	6	4	14
TRRILDQGLGTT	60	5	2	11
DRMASTVLSMGS	90	3	2	10
KNLRDDRFEMSA	73	1	2	10
DSSIVYKPLHSP	97	5	2	9
QKVEYSRWHQPL	65	3	2	9
SSVAVAHSMRDN	102	13	2	8

Table 5.6: Peptides that preferentially bind to UbcH5α in complex compared to free UbcH5α, in round one with the slow wash method. Seq= peptide sequence, sum= number of times peptide was identified in sequencing. SW= slow wash, C= Control, E2= free UbcH5α, E2+8= UbcH5α in complex

seq	sum	QW C 2	QW E2 2	E2 + 8 2
IGLPHSANSTKP	428	102	14	58
EDLRKESSRLVD	298	3	9	55
VTSPIDSGARQL	344	2	5	54
GDGNSVLKPGNW	901	6	6	48
SSAFDSRMNVHW	57	0	0	47
VFAYDLPIYSKV	137	1	6	33
WNLDYAPSGVPT	191	16	5	30
TNDPSHRYEMLM	203	6	3	30
SLASEDTPNVLA	144	1	6	25
SPSWVPSAPNER	142	0	3	22
YSLPYQMYAYHT	218	7	2	21
KMPKENPSSWLS	64	1	0	21
FVTHASANPWIP	45	1	0	21
LSVSGGNSYVTT	81	0	4	19
LQTTTNSLSELV	101	1	2	19
LRLDSHVNMSRD	89	8	0	18
TVISSVSTPANS	138	25	3	17
WTEGWRWINFHP	103	19	2	17
SHGELMQGLAMQ	119	4	1	17
WSAKDVINFIRV	19	0	0	17
SIQLERVSKWSL	18	0	0	17
NLHDASSFPYHW	535	3	4	16
ELLAYDSPPAVG	92	3	4	16
VSPAKYKPLILA	247	63	2	16
HSGQPFTKVVSH	51	0	2	16
MYPTNPNPFNTR	40	0	0	16
TVGLPMTYYMDT	115	23	1	15
HHSNTWTGPLRS	39	1	0	15
SNTQSERHPLSM	126	4	4	14
LVPDVHLLLSYA	75	0	2	14
SSRDAAFSWTMT	31	0	1	14
HYAQMSIVGRTS	121	41	1	13
TLGGLYQFEYAL	25	0	0	13
TIYTSGLAAFNR	183	69	3	12
DRMPPFTSLELQ	62	1	2	12
IPLNTALFATRN	47	0	2	12
AGESFEGAAEPF	44	1	2	12
SPLQLDVGGPKP	37	12	2	12
HTPLAWHWAVQN	52	27	1	12
HSSIALEAQTDS	74	2	0	12
ASHVLWSTVTYM	16	0	0	12

SHYFPPSNQTSR	25	0	3	11
DNGHFKLSEVWA	60	15	2	11
LVGNHYGFQGGW	123	31	1	11
DYDRIPDIPMLG	109	21	1	11
LGHSGGPTRPSW	45	11	1	11
YEGRWAELDSLK	16	0	1	11
HPTNVSIASTKK	87	11	0	11
CFAYDIVSDEMW	72	1	0	11
TNMPSPSLTNHY	39	2	0	11
QFDSQGYVSYNP	36	0	0	11
GGARTMYQAIGI	14	0	0	11
IETSHYRGYPPN	14	0	0	11
STVSRDFMHMHG	14	0	0	11
TTPDGSPEPNSL	14	0	1	10
YGEVMDAMQANG	81	1	0	10
FTVARPLQWSLT	52	0	0	10
SWSLPSVWRLHA	47	17	0	10
ELVRTTPRMLYL	34	1	0	10
LQPSGSSPVAPF	26	0	0	10
TSSWQEVIRMSV	23	0	0	10
STYHSTRDSLPQ	15	0	0	10
NYKVTRTQVLTF	228	4	2	9
LSVHLPVVDSPN	205	7	2	9
TLSWYDSTYAHH	191	62	2	9
FTADVLSERSEY	154	1	2	9
CVASARGAQIGM	115	6	2	9
KVLPPLWVQAYE	74	1	2	9
KVPVGVLPLSHS	117	0	1	9
SMEEAVVSPTST	71	1	1	9
RIQELSPIRTWA	43	4	1	9
SEVSNSVAGNWR	12	0	1	9
GEHMHAVLMIEG	23	0	0	9
FCLDRSHCVIGG	16	4	0	9
MADARMTGEHIL	12	0	0	9
YIWPFSAVWETP	126	59	2	8
VIGKGHPMIVTV	95	0	2	8
MHEGILIEPMTA	93	0	2	8
FAASDMAGFKWV	79	0	1	8
FNMTGRGLFPPF	71	0	1	8
STTANEVAKITT	60	1	1	8
QIAGGSPSKVER	134	1	0	8
SPNLLFPISTRN	69	17	0	8

SSVMTAAQEAWS	68	2	0	8
GLPSEHQMLPAR	46	0	0	8
TIRLNKAPSPDV	29	1	0	8
SWVPMSQIVELR	12	0	0	8
AEMGALVTHFSL	11	0	0	8
HHPRLSMDAMDH	8	0	0	8

Table 5.7: Peptides that preferentially bind to UbcH5α in complex compared to free UbcH5α, in round two with the quick wash method. Seq= peptide sequence, sum= number of times peptide was identified in sequencing. QW= quick wash, 2= Round two C= Control, E2= free UbcH5α, E2+8= UbcH5α in complex

seq	sum	SW C 2	SW E2 2	SW E2 +8 2
TPAGGWLAWLSH	183	9	11	55
ELFTTNNVRPEN	393	34	9	41
HSDATVRFAHRE	428	49	5	28
WNKPLSDRDAPI	89	6	5	28
FTADVLSERSEY	154	2	5	25
IGTLPLKIENRR	98	2	2	24
YIWPFSAVWETP	126	11	0	20
ASTAGYPGGALS	30	0	1	20
GFIHDYSGSHRS	29	0	1	19
ALLANHEELFQT	117	43	1	18
MLSKLPVSIDET	23	0	1	18
GHLTVVGTNYHR	188	14	6	17
SPSWVPSAPNER	142	27	3	17
GHYHKSRDQLLL	79	1	0	17
MDNKTTRWRDPL	36	1	0	17
STQSAVCMNCHD	76	0	1	15
VSLSGVSSNSRV	222	15	1	14
DSSIVYKPLHSP	97	6	1	14
NNANPHLPKQWL	94	13	2	14
SGDVPVTSTYTS	91	1	2	14
EHPNTSGNSVVD	46	0	1	14
WNAPSVANGPRM	176	29	3	13
SLFNPLQMLPYP	95	3	3	12
ELLAYDSPPAVG	92	1	2	12
ALAADTPQSARR	90	7	1	12
LGVREYGMRGLG	84	22	2	12
FPALSEFGSSLR	73	4	2	12
FGVERDDAAHRW	37	3	0	12
SQFATVWERMRN	158	39	2	11
FSWSMVMPWPTA	143	1	2	11
LVPGAMKLLSDT	115	0	3	11
STDSHYGRWVND	113	4	3	11
NSVHDLMLSPPP	99	1	1	11
HDLTSYVTLKAQ	74	5	0	11
VARATSHGPSTT	74	2	1	11
NTNYVTWSPSSR	64	0	0	11
GPSWLFIHSWQS	55	0	0	11
NDAAEMTWASLV	37	0	0	11
HDASWRDVTAMV	24	0	1	11
TVPRSSSVPTQW	153	7	1	10
VAPVSFQPWVHS	112	1	2	10

HMRFDHMRPQTG	63	6	2	10
MGLESTSLMADS	59	0	0	10
GDVMDKRNQFLF	52	0	0	10
NYPATNTHRYTP	32	7	0	10
GYHTTYSAGPKW	12	0	0	10
VEHMAYWDQVLD	148	4	1	9
FPFTFAHATGAS	113	15	2	9
GKAADLTPFIRA	110	8	6	9
TDLYFESWRMTG	100	8	0	9
YQKYDPAMVSVT	74	11	0	9
LQVGTLNIQLTN	54	1	0	9
RLDLATSNWPSR	36	0	1	9
YGHAGARPATAT	34	1	0	9
YSYPPTKLALAN	31	4	0	9
SKFMDSQSRMWR	27	0	0	9
TLQGYAIDSDYL	18	2	1	9
AVPTPFAHGSNL	17	0	0	9
NLPIPPHIPLPQ	12	0	0	9
SLLSSGQASITG	154	2	1	8
VIGKGHPMIVTV	95	1	1	8
DSYTRATNWSPH	65	2	2	8
YTTHLIVSEPAH	65	1	2	8
TLSLDWTIHPNN	58	1	2	8
HHLPFVRDGLRP	50	0	1	8
YPAVNLRTPVYF	50	5	5	8
AVWRTQASPQSL	48	1	0	8
EYWSLGSHQTIY	48	11	2	8
SPGHAHLRLDKR	40	0	0	8
DSTNSSMSLTGM	31	0	1	8
KNLYSEHYRGPA	31	2	0	8
DMGLHYVQFDHV	30	0	1	8
APYHPLDSLTPN	21	0	0	8
FPTPLTETSFED	19	0	0	8
GVTHNSTNWLYR	19	4	0	8
SQPHMQNAPSKT	17	0	1	8
TGTMPNSFPQSG	11	0	0	8
FSISYFPQYPVQ	8	0	0	8

Table 5.8: Peptides that preferentially bind to UbcH5α in complex compared to free UbcH5α, in round two with the slow wash method. Seq= peptide sequence, sum= number of times peptide was identified in sequencing. SW= slow wash, 2= Round two C= Control, E2= free UbcH5α, E2+8= UbcH5α in complex

I have used peptide phage display to demonstrate a likely conformational change of UbcH5α upon peptide 8 binding. I came to this conclusion based on the fact that different peptides bind to free UbcH5α than to UbcH5α in complex with peptide 8.

The results gathered are what I had primarily set out to achieve, however this is just one way to analyse that data that I have obtained. There are a number of ways that the peptides could be analysed to provide various information, such as consensus sites in the binding peptides, protein binding partners of UbcH5α, families of proteins that bind UbcH5α and the roles binding proteins may play in UbcH5α function. I have not analysed my data in this much detail, this is something I would like to pursue and is highlighted in 'Further Work'. I have however provided examples of how my data could be analysed to obtain further information.

The peptides listed in the previous tables could be analysed to identify consensus sequences. A consensus sequence is a genetic sequence found with minor variations and similar functions in different genetic locations. The consensus sequence may consist of DNA nucleotides or amino acids. In a consensus sequence some residues are absolute and others can be variable, with either any other residue viable or only a certain subset viable. Software can be used to identify consensus sequence within peptides, one of these programs is MEME. In **figure 5.4** is the consensus sequences identified by MEME from the list of peptides that preferentially bind to free UbcH5α or ligand bound UbcH5α after two rounds of panning, using the slow wash method. Each sequence was identified twice within the list of peptides. Further analysis would be required to assess whether these sequences.

Although computer software is an extremely useful tool for the analysis of peptide phage display data any peptides that appear to be interesting need to be validated. It would be an extremely time consuming and expensive task to validate all the peptides displayed in the above tables. I would further narrow down the peptides for validation by sorting the round 2 fast and slow wash tables into a top ten, based on the difference of a peptide binding to UbcH5α over UbcH5α in complex (**figure 5.5**). I would then do the same for peptides that bind UbcH5α in complex over free UbcH5α (**figure 5.6)**.

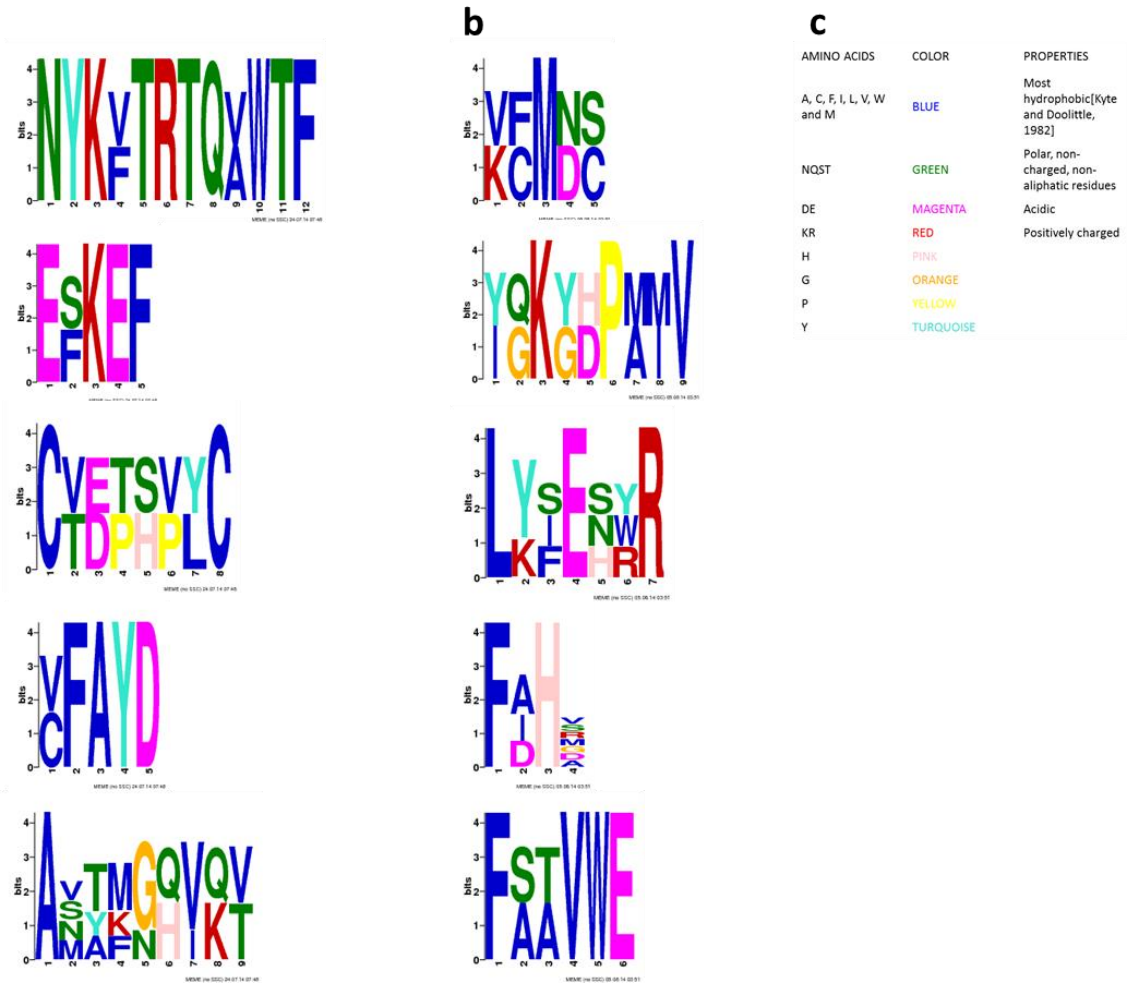

Figure 5.4: Peptides that preferentially bind to free UbcH5α or ligand bound Ubch5α, in round two of panning with slow wash method, analysed by MEME. a) The top five consensus sites in peptides that preferentially bind free UbcH5α as determined by MEME, each site was identified twice. **b**) The top five consensus sites in peptides that preferentially bind ligand bound UbcH5α **c)** Key showing the amino acids, their properties and colour.

a

seq	sum	QW C	QW E2	QW E2 + 8
TETFGSGLNFRG	43	3	13	1
EGRLLWYGSPAT	23	6	12	1
SEPRAIQNLDRW	4	5	11	1
LTCCHVDLSANS	4	1	10	1
SLGQSNNVSPIV	97	9	10	0
KYATPIPYDRLA	73	4	10	0
KLLHVTPSSASK	6	7	9	1
TRRILDQGLGTT	60	7	9	1
TTRILDQVLGTT	208	5	9	1
WKAADLAPFIRA	429	6	8	1

b

seq	sum	SW C	SW E2	SW E2 + 8
TFNMKAFGTNAM	115	4	11	1
SFHPMGLPSTSF	123	6	11	0
FDMYPTNRNPGR	66	1	11	0
DSERNTLNPYRS	82	6	10	0
TDTSAALSFSAR	614	2	9	1
SLASEDTPNVLA	144	2	9	1
LPRGTYLIYPDQ	78	5	9	1
NKVGLVPHMSAI	65	2	9	1
NANSSVDTATIL	68	3	8	1
AVHADHMCSIHI	55	2	8	1

c

seq	sum	QW C 2	QW E2	QW E2 + 8 2
RILPMVDTQILT	130	0	80	1
HPDAEDITNTLQ	105	0	42	0
DWSIREGHQTYP	46	3	39	0
HIHVRTTSALVA	78	0	38	1
VTVTDMNHDRDF	47	0	38	0
GEVAQLRSAEPY	99	44	35	1
SSHPSNATLKTN	45	0	35	1
FSLSRYPSSASI	59	0	34	0
DRNLPSNQFQRS	103	0	32	0
VKDIRGTAMRWA	37	0	32	0

d

seq	sum	SW C 2	SW E2 2	SW E2+ 8 2
GGLHTDHFKPIL	101	15	31	1
DRMPPFTSLELQ	62	1	22	1
APLHQVSSIWQS	47	1	22	1
AKPTAMLYPSAT	31	0	21	0
YISPWHSLDLKG	107	10	20	1
CFAYDIVSDEMW	72	2	20	1
VETSNGFGWPNG	25	0	20	0
GSGASYQVWRPM	183	5	58	3
ALKPWDLSSNLS	284	47	19	1
TLTSETPWSLNR	50	0	19	0

Figure 5.5: Top Ten peptides that preferentially bind to free UbcH5α in varied conditions. a) Round one, quick wash method **b)** Round one, slow wash method, **c)** Round two, quick wash method **d)** Round two slow wash method. Seq= peptide sequence, sum= number of times peptide was detected in sequencing, QW= quick wash, SW= slow wash, 2= round two, E2= free Ubch5α, E2+8= UbcH5α in complex with peptide 8.

a

seq	sum	QW C	QW E2	QW E2 + 8
TFNMKAFGTNAM	115	5	0	9
NRDFLNLKPWDI	71	11	2	10
NYKVTRIQVWTF	133	9	2	8

b

seq	sum	SW C	SW E2	SW E2 + 8
TRRILDQGLGTT	60	5	2	11
DRMASTVLSMGS	90	3	2	10
KNLRDDRFEMSA	73	1	2	10
DSSIVYKPLHSP	97	5	2	9
QKVEYSRWHQPL	65	3	2	9
SSVAVAHSMRDN	102	13	2	8
NPSRVAGVNLAF	150	5	4	14
AHVKLYHRNGAT	101	6	4	14

c

seq	sum	QW C 2	QW E2	E2 + 8 2
SSAFDSRMNVHW	57	0	0	47
KMPKENPSSWLS	64	1	0	21
FVTHASANPWIP	45	1	0	21
LRLDSHVNMSRD	89	8	0	18
SHGELMQGLAMQ	119	4	1	17
WSAKDVINFIRV	19	0	0	17
SIQLERVSKWSL	18	0	0	17
MYPTNPNPFNTR	40	0	0	16
TVGLPMTYYMDT	115	23	1	15
HHSNTWTGPLRS	39	1	0	15

d

seq	sum	SW C 2	SW E2 2	SW E2 +8 2
YIWPFSAVWETP	126	11	0	20
ASTAGYPGGALS	30	0	1	20
GFIHDYSGSHRS	29	0	1	19
ALLANHEELFQT	117	43	1	18
MLSKLPVSIDET	23	0	1	18
GHYHKSRDQLLL	79	1	0	17
MDNKTTRWRDPL	36	1	0	17
STQSAVCMNCHD	76	0	1	15
VSLSGVSSNSRV	222	15	1	14
DSSIVYKPLHSP	97	6	1	14

Figure 5.6: Top Ten peptides that preferentially bind to UbcH5α in complex with peptide 8 in varied conditions. a) Round one, quick wash method, it should be noted there is not 10 peptides that bind hence the reduced top ten **b)** Round one, slow wash method, **c)** Round two, quick wash method **d)** Round two slow wash method. Seq= peptide sequence, sum= number of times peptide was detected in sequencing, QW= quick wash, SW= slow wash, 2= round two, E2= free Ubch5α, E2+8= UbcH5α in complex with peptide 8.

Forty is still a large number of peptides to validate and so I would probably narrow it down further and validate the top 5 peptides in each of these tables. There are instances in which I may not select one of the peptides should the control be very high, I would be suspicious of the result if the peptide bound with high affinity to the empty control well, an example of this can be seen below:

	SUM	C	E2	E2 + 8
ALLANHEELFQT	117	43	1	18

A second way of narrowing down the peptides to validate is to take the peptides obtained in the 'top ten' tables above or alternatively the consensus sites identified by MEME and BLAST them. Basic Local Alignment Search Tool (BLAST) is an algorithm that compares primary biological sequence information. During a BLAST search a query sequence is compared with a database of known sequences and database sequences that resemble the query sequence are identified. BLAST could be used on the peptides in the top ten tables or MEME consensus sites to see if the peptides are present in any proteins that may be important in relation to UbcH5α, then these peptides could be chosen for validation. For example I ran the top consensus motif, identified by MEME, for peptides that bind to free UBCh5α and the top hit was a deubiquitinating enzyme. It is very interesting that a deubiquitinating enzyme would bind to UbcH5α only when it is not bound to the RING. This peptide is one that I would choose to validate.

Once selected there are a number of ways in which the peptides could be validated to bind to UbcH5α or UbcH5α in complex, these include ELISAs, α screens and pull down assays.

Finally BLAST could be used on all the peptides generated in **tables 5.1-5.4,** they could be run through BLAST and the protein hits gained from this could be put into a program such as Cytoscape. In Cytoscape the proteins could be analysed and sorted into groups of proteins that have similar functions e.g. chaperone, DNA repair.

In conclusion peptide phage display has further provided evidence for a conformational change of UbcH5α upon peptide 8 binding and yet has also shown that I have only touched the surface of the information that this data can provide.

5.1.4 Discussion

We now appreciate that proteins can be regulated through their interaction with short linear peptide motifs in binding partners. Such peptide motifs are predominantly found in disordered regions, and are characterised by low binding affinities which are crucial for reversible signal transduction events. These linear motifs are typically very short and their specificity, on average, can be determined by as few as 3-4 residues[242]. Peptide phage display is a relatively new technique which exploits short linear interaction motifs and which can be applied to many experimental situations to analyse large numbers of linear motifs in a high-throughput format. The applications of peptide phage display are constantly evolving and developing. It has previously been used in a diverse range of applications including the identification of novel enzyme substrates and cell targeting peptides as well as epitope mapping. I used peptide phage display in an attempt to further confirm the conformational change of UbcH5α upon peptide 8 binding that I had previously identified using limited proteolysis and mass spectrometry (Chapter 2). My hypothesis reasoned that if there was a conformational difference between free UbcH5α and UbcH5α in complex then there would be a difference in the peptides that it could bind i.e. the unliganded form of the UbcH5 may have a different binding specificity than the E2 in its bond conformation.

There are certain drawbacks when using an emerging method for a novel function. Firstly I had issues with the method itself; I used two methods which were for the most part identical apart from the wash step. In one method the washes were quick and in the other method they were slow, by this I mean that the unbound ligand was either washed away from the well 10x, with the wash immediately discarded or 6x with the wash left on the well for 5 minutes. The length of the washes clearly makes a difference as when examining the results there are differences in the peptides obtained depending on the length of the wash. It should be noted that not all the peptides are different just that there are some differences. I do not know which results I should use, as of yet I am analysing both. I currently do not know if one method holds more advantages than the other; it would take further experimental work and validation to work this out.

I am also not entirely sure if the controls that I have used are relevant or used correctly. I used a blank well to test for 'stickiness' of any of the peptides. In some cases the number of copies of peptide eluted from the control, free UbcH5α and UbcH5α in complex were all of a similar value and very high, in these cases I assumed that the peptide was sticky. There are other results however that show a high value for the control and then a lower value for binding UbcH5α, an example of such a result is displayed below:

seq	sum	SW C AMP 2	SW E2 AMP 2	SW E2+ 8 AMP 2
ALKPWDLSSNLS	284	47	19	1

In a case such as this I am uncertain if it is a true result, the peptide does not appear to be sticky as the result value with protein is low but I am still unsure as to why the control is so high.

The results of the peptide phage display are generated as a numerical value. When a result is numerical the natural questions that follow are regarding statistics. Statistics do not apply to the results of peptide phage display, just because there are numbers present does not mean that a p value can be applied to them. The peptides in this assay are not neutral and so they could potentially provide the bacteria with a growth advantage or disadvantage and as such the actual number is not significant. I look at the peptide phage display as an enrichment assay and therefore analyse the results as such. I chose to analyse results that were 4x higher than that of their counterpart, I do not know if this is significant until I validate my results by carrying out further experiments. As mentioned previously I could validate the peptides by ELISA, α-screen or pull down assays. If this assay were repeated and enough validations were confirmed then it may in the future be possible to make statistical rules for analysing peptide phage display data for conformational changes of a protein.

I wanted to use peptide phage display to confirm a conformational change in UbcH5α upon binding to peptide 8. My results show that there is a difference in peptides that bind to free UbcH5α and UbcH5α in complex with peptide 8, this difference may

suggest a conformational change, though there are other arguments for this difference. For example it could be argued that when peptide 8 is present in the complex it physically blocks the binding of peptides that were previously able to bind free UbcH5α. Secondly it could be argued that when peptide 8 is present it can bind some peptide phage. These are two valid arguments and it is likely that some of the differences in peptide binding are simply down to the presence of the peptide. It does however seem unlikely that all the differences a simply due to the presence of the peptide.

My previous limited proteolysis and mass spectrometry data indicated a conformational change of UbcH5α upon peptide 8 binding and in combination with the peptide phage display data I believe that there is a strong argument for the conformational change of UbcH5α upon peptide 8 binding.

The mass spectrometry data suggested that upon peptide 8 binding a very stable core of UbcH5α was formed. It is possible that when peptide 8 binds to UbcH5α the complex is very ridged and less flexible than free UbcH5α. In the peptide phage display data less peptides bind preferentially to UbcH5α in complex than free UbcH5α, this could be because the complex is less flexible and less receptive to binding partners than free UbcH5α.

As well as being used to probe for changes in E2 specificity and conformation the data I have obtained using phage display can also be analysed in other ways to extend its utility. For example to identify lead molecules or to define novel members of the E2-interactome.

I have outlined how next generation sequencing data from phage peptide display can be analysed by MEME to provide consensus sequences. An application of the MEME sequences is to use them as the basis of a bioinformatics screen for open reading frames which contain similar motifs. For example, when I BLAST the top two consensus sequences provide by MEME analysis for peptides which bind to unliganded UbcH5α I can identify consensus sequences in proteins which are known to be involved in ubiquitination, such as and TRABID/ZRANBI and UCHL5/UCH37

(**Figure 5.7**). The next step in this type of approach would be to synthesise both the MEME peptides and the homologues region from TRABID/ZRANBI and UCHL5/UCH37 to see if the sequences bind to UbcH5α. Following on from this you could begin by determining if the two proteins interact in cells, for example using proximity ligation assays and/or co-immunoprecipitation analysis. Based on the output from this type of experimental approach you could subsequently undertake a detailed molecular analysis on the role of complex formation on the function of the E2 partner proteins. This type of approach could therefore help to further decipher the role and mechanism of UbcH5α in ubiquitin mediated signalling.

UbcH5α was originally thought to be an undruggable target of the ubiquitination pathway, as it was characterised as very 'flat' protein with no obvious binding pockets or crevices. However, a recent study has suggested that small molecules can be identified which bind to the E2 and inhibit its function. Using this study as a proof of concept peptides identified using phage display may provide binding motifs that can be utilised as a lead biologic molecule for use in structure based drug design strategies[243].

`

SEARCH: NYKXTRTQXWTF

TRABID: NKLNTRTQHWTC

MSERGIKWACEYCTYENWPSAIKCTMCRAQRPSGTIITEDPFKSGSSDVGRDWDPSSTEG
GSSPLICPDSSARPRVKSSYSMENANKWSCHMCTYLNWPRAIRCTQCLSQRRTRSPTESP
QSSGSGSRPVAFSVDPCEEYNDRNKLNTRTQHWTCSVCTYENWAKAKRCVVCDHPRPNNI
EAIELAETEEASSIINEQDRARWRGSCSSGNSQRRSPPATKRDSEVKMDFQRIELAGAVG
SKEELEVDFKKLKQIKNRMKKTDWLFLNACVGVVEGDLAAIEAYKSSGGDIARQLTADEV
RLLNRPSAFDVGYTLVHLAIRFQRQDMLAILLTEVSQQAAKCIPAMVCPELTEQIRREIA
ASLHQRKGDFACYFLTDLVTFTLPADIEDLPPTVQEKLFDEVLDRDVQKELEEESPIINW
SLELATRLDSRLYALWNRTAGDCLLDSVLQATWGIYDKDSVLRKALHDSLHDCSHWFYTR
WKDWESWYSQSFGLHFSLREEQWQEDWAFILSLASQPGASLEQTHIFVLAHILRRPIIVY
GVKYYKSFRGETLGYTRFQGVYLPLLWEQSFCWKSPIALGYTRGHFSALVAMENDGYGNR
GAGANLNTDDDVTITFLPLVDSERKLLHVHFLSAQELGNEEQQEKLLREWLDCCVTEGGV
LVAMQKSSRRRNHPLVTQMVEKWLDRYRQIRPCTSLSDGEEDEDDEDE

TRABID/ZRANB1 – OUT domain deubiquitinatase

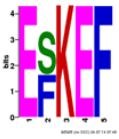

SEARCH: EFKEF

UCHL5: EFKEF

MTGNAGEWCLMESDPGVFTELIKGFGCRGAQVEEIWSLEPENFEKLKPVHGLIFLFKWQP
GEEPAGSVVQDSRLDTIFFAKQVINNACATQAIVSVLLNCTHQDVHLGETLSEFKEFSQS
FDAAMKGLALSNSDVIRQVHNSFARQQMFEFDTKTSAKEEDAFHFVSYVPVNGRLYELDG
LREGPIDLGACNQDDWISAVRPVIEKRIQKYSEGEIRFNLMAIVSDRKMIYEQKIAELQR
QLAEEEPMDTDQGNSMLSAIQSEVAKNQMLIEEEVQKLKRYKIENIRRKHNYLPFIMELL
KTLAEHQQLIPLVEKAKEKQNAKKAQETK

UCHL5/UCH37 – Proteasome associated deubiquitinatase

Figure 59: BLAST of MEME consensus sites. BLAST data of the top two consensus sequences provided by MEME analysis of peptides which bind to unliganded UbcH5a identify consensus sequences in proteins which are known to be involved in ubiquitination, such as the deubiquitinating enzymes TRABID/ZRANBI and UCHL5/UCH37.

Chapter 6: RESULTS

6.1 Investigating the role of the tail in the dimerisation of MDM2

6.1.1 Introduction

At the start of this project information regarding the dimerisation of MDM2 provided more questions than answers. It is true that MDM2 is able to form a dimer, the solution structure shows that MDM2 can form a stable homodimer[130,139] or heterodimer with its homologue MDM4[130], it might be that the heterodimer is the preferential form[139].

The solution structure shows that the homodimer interface primarily includes residues Val451, Lys453, Thr455, Gly456, Leu458, Met459, Val486, Leu487, Thr488, Tyr489, Phe490, Pro491[130]. Six of these residues reside within the C-terminal 12 amino acid tail of MDM2. The tail of MDM2 has been implicated as necessary for dimer formation with tail mutants running on an polyacrylamide gel at a size depicting monomeric structure[141]. Conversely a student with Professor Malcolm Walkinshaw, working on MDM2 prior to my PhD had shown, via gel filtration, that MDM2 without the tail could still form a dimer ('Biochemical and Biophysical studies of MDM2-ligand interactions.'). So the first question raised was 'Is the tail of MDM2 involved in dimer formation?'

There is also controversy regarding whether MDM2 must be present as a monomer or dimer to be active as an E3 ligase. There are *in vitro* studies that report that MDM2 is active as an E3 ligase towards p53 regardless of whether it is in monomeric or dimeric form[141] and there are opposing *in vivo* studies that report that MDM2 must be dimeric to be active as an E3 ligase[102]. This raises the questions 'Is MDM2 active as an E3 ligase as a monomer, dimer or both?' and 'If active as both is there a preferred form?'.

If we assume that MDM2 is active as an E3 ligase when a dimer, whether or not it is also active as an E3 ligase when a monomer, then the questions arise of whether or not it is active as a homodimer, heterodimer or both, and if both, is one preferred.

Heterodimers of MDM4 and MDM2 have been shown to be highly stable [130,139] this does not necessarily mean that in the cells the heterodimer is the preferred dimer required for E3 activity of MDM2. There are functions other than E3 ligase activity that could be the sole reasons that MDM2 and MDM4 form a dimer. Experiments show that when MDM4 is not present in cells MDM2 is inefficient at down regulating p53 due to its very short half-life. Association of MDM2 with MDM4 leads to an increase in steady state levels of MDM2[185]. MDM4 is present in the cytoplasm and requires MDM2 to locate to the nucleus where it can inactivate p53 by blocking its transactivation[184].

My results so far would suggest that MDM2 is active as an E3 ligase, independent of its association with MDM4 *in vitro*, as my ubiquitination assays contain no MDM4 and ubiquitination of p53 is seen. This of course does not mean the heterodimer is inactive as an E3 ligase or that it is not the preferred dimer for E3 activity, the results simply show that MDM2 can be active without the presence of MDM4.

Questions

1) Does MDM2 form a homodimer in solution?

2) Is the C-terminal 12 amino acid tail of MDM2 required for dimer formation?

6.1.2 Full length MDM2 dimerises in solution as detected by SERS.

During my PhD I had the opportunity to contribute to a publication investigating how surface-enhanced Raman scattering could be used to study protein interactions, and in particular MDM2.

Current techniques used to probe interactions in biological systems commonly use read out tools such as fluorescence[244]. Disadvantages of these methods include a high background from biological media, limitations due to broad emission bands and the inability to probe interactions over distances greater than 10nm. Surface-enhanced Raman scattering (SERS) is a vibrational spectroscopy that provides a similar sensitivity to fluorescent methods but narrower spectral peaks allow for the detection of multiple species simultaneously[245]. SERS interrogates an analyte adsorbed onto a roughened metal surface and can be enhanced by the aggregation of nanoparticles (NP). NP and SERS have been used for proteomic investigation[246] and a number of SERS based immunoassays have been developed[247,248].

Our collaborative study with the group of Professor Duncan Graham (Strathclyde) and Professor Ted Hupp (Edinburgh) began with a solution based approach to investigate the interaction of full length MDM2 with a p53 peptide mimic using the selectivity and sensitivity of SERS. Cell based studies suggest that MDM2 is dimeric in solution[141]. So the theory behind this investigation was that putative dimerisation of FL MDM2 , through its RING domain would present two N-terminal hydrophobic pockets, per dimer, to interact with ligands, in this case the p53 Box-1 mimic peptide, 12.1. N-terminal interactions of 12.1 would therefore bring together two peptide 12.1 functionalised nanoparticles (PSN-12.1) in solution. PSN aggregation from MDM2 dimerisation could then be measured over time by excitation spectroscopy[249] (**figure 6.1**).

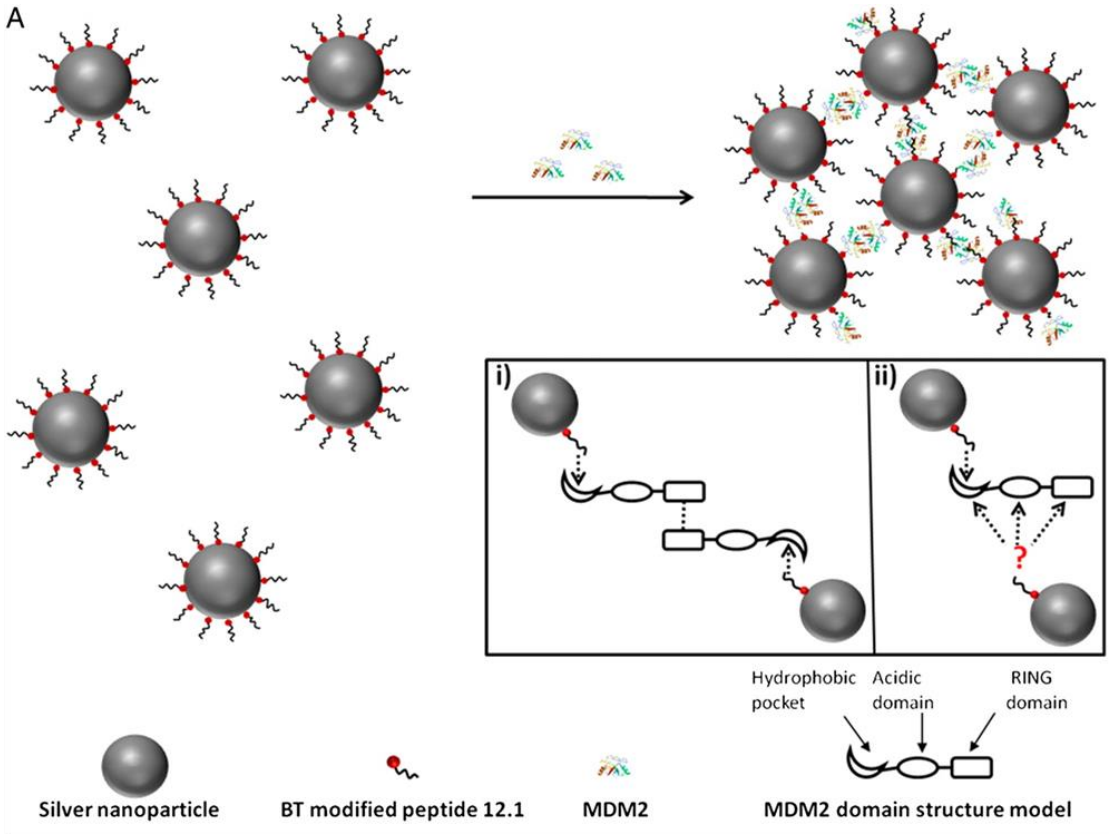

B

Resin- NLGEWYDMFRPM-GSGS

Figure 6.1: a) Schematic of the proposed assemble of PSN through specific interactions between peptide 1.1 and MDM2. Inset **i)** and **ii)** show two proposed models for MDM2 binding resulting in PSN aggregation from MDM2 dimerisation. **b)** Sequence (C-N) of peptide 12.1

Figure adapted from Robson AF, Hupp TR, Lickiss F, Ball KL, Faulds K, Graham D. Nanosensing protein allostery using a bivalent mouse double minute two (MDM2) assay. Proc Natl Acad Sci U S A 2012;109(21):8073-8.

Peptide 12.1 and the negative control mutant, $12.1_{W\Delta A}$, were modified with benzotriazole and directly conjugated to EDTA reduced silver NP in a one-step reaction. I showed that benzotriazole modified peptide 12.1 and mutant peptide 12.1 displayed high level and low level binding, respectively to MDM2 protein, in peptide competition assays. I carried out a competition assay in which biotinylated p53 Box-1 peptide was adsorbed onto a streptavidin coated microtitre well and fixed levels of MDM2 (100ng) were titrated in with increasing amounts of indicated peptide, 12.1, $12.1_{W\Delta A}$ and Nutlin-3. Nutlin-3 is a small molecule that binds to the hydrophobic pocket of MDM2 and competes with p53, or biotinylated p53 Box-1 peptide for MDM2 binding. Unbound protein and or peptide were removed by extensive washing and binding of MDM2 was quantified by monoclonal antibody 4B2. My result shows that peptide 12.1 is almost as potent as Nutlin-3 in displacing MDM2 from p53 (**figure 6.3**)

Unlabelled MDM2 was added to PSN solutions at various concentrations based on molar excess of protein to PSN and was shown to induce PSN aggregation (**figure 6.2**). There is the remote possibility that 12.1 can bind elsewhere in MDM2 other than the N-terminal hydrophobic pocket, and that this is causing the aggregation of the PSN. There is no evidence for this model in the literature so it is assumed that the aggregation is the result of the dimerisation of MDM2.

This study showed that full length MDM2 was able to aggregate PSN-12.1, suggesting that FL MDM2 is dimeric in solution and maintains the biological activity of the hydrophobic pocket. It would be interesting to repeat this experiment with MDM2 ΔT and to see if the same level, diminished levels or no level of aggregation, when compared to MDM2 is seen. Repeating this experiment in this manner could provide answers regarding the tail of MDM2 and dimer formation.

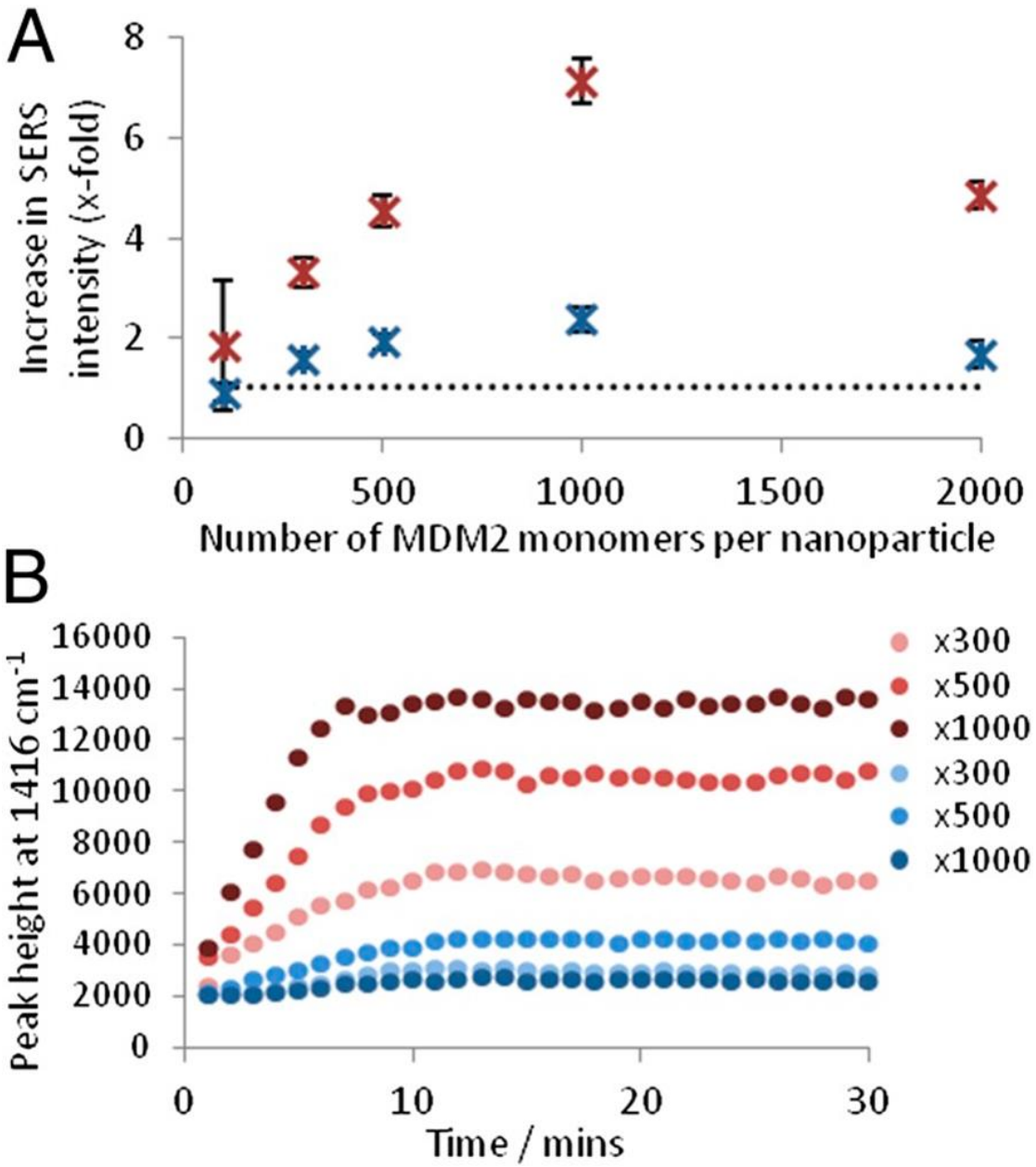

Figure 6.2: SERS analysis of PSN aggregation. **a)** Calculated x-fold increase in SERS intensity following MDM2 addition to PSN-12.1 (red) and PSN-12.1$_{W\Delta A}$ (blue). **b)** Peak height at 1416 cm^{-1} monitored every 60 seconds for 30 min following addition of varying amounts of MDM2 to PSN-12.1 (red) and PSN-12.1$_{W\Delta A}$ (blue). X-value represents the excess of MDM2 monomers per PSN. Dotted line indicates PSN samples when MDM2 is absent. Error bars illustrate the SD.

Figure from Robson AF, Hupp TR, Lickiss F, Ball KL, Faulds K, Graham D. Nanosensing protein allostery using a bivalent mouse double minute two (MDM2) assay. Proc Natl Acad Sci U S A 2012;109(21):8073-8.

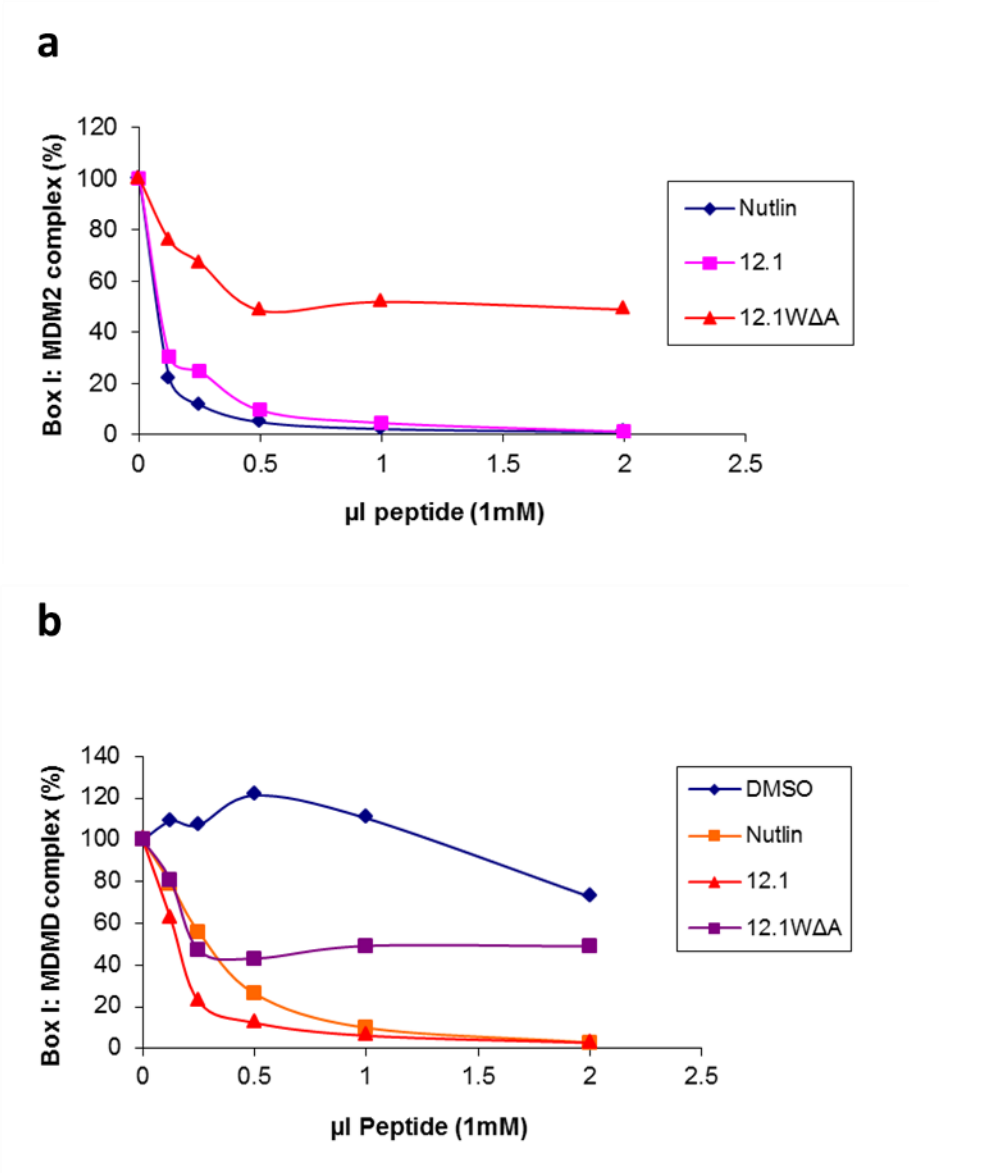

Figure 6.3: Competitive inhibition of MDM2 binding to p53 derived BOX-1 peptides by ligand. a) and b) Biotinylated p53 BOX-1 peptide was adsorbed onto a streptavidin coasted ELISA well. Fixed levels of MDM2 were added into a buffer with increasing amounts of indicated ligand. Reaction solutions were added to the ELISA well and incubated from 1 hour at room temperature. MDM2 binding was quantified using monoclonal antibody, 2A10 and secondary antibody coupled with horseradish peroxidase.

Figure adapted from Robson AF, Hupp TR, Lickiss F, Ball KL, Faulds K, Graham D. Nanosensing protein allostery using a bivalent mouse double minute two (MDM2) assay. Proc Natl Acad Sci U S A 2012;109(21):8073-8.

6.1.3 Gel filtration chromatography

Having established using SERS that FL MDM2 has a dimeric or oligomeric structure in solution I wanted to look in more detail at the structure of the RING domain. A size exclusion column contains hydrated beads made from cross-linked polymers such as dextran, agarose or polyacrylamide. The migration of a protein through the column is governed by its partitioning between the two solvent spaces, the solvent space surrounding the packed beads and the solvent within the packed beads, the smaller the proteins the more they interact with the solvent in the packed beads and they require a greater volume of buffer to pass through the column before they are eluted[250]. In principle therefore large proteins elute from the column first followed by proteins of decreasing size.

Proteins fractions eluted from the column are collected and are examined by spectroscopic techniques such as ultraviolet (UV) or refractive index (RI). Aromatic amino acids absorb UV light at 280 nm. Tryptophan absorbs the greatest amount followed by tyrosine and to a lesser extent phenylalanine. Using the absorption trace of a protein with unknown size and a set of protein standards of a known size it is possible to calculate the size of the unknown protein.

Advantages of size exclusion chromatography include the recovery of the protein, the ability to separate a protein from contaminants to obtain a clean sample and the ability to determine the oligomeric state of a protein. Disadvantages include the inability to separate proteins of similar sizes, the dilution of the protein sample and the need for a protein to contain aromatic residues.

I wanted to use size exclusion chromatography to analyse the oligomeric state of my MDM2 RING protein with the tail ($RING^{322-491}$) and without the tail ($RING^{322-479}$). The theory was that I would be able to use this method to ascertain if the RING was a monomer or a homodimer in solution and, if the homodimer was the preferred species, if the tail was necessary for his dimer formation. I used a Superdex 200 10/300 (GE Healthcare) column to separate out RING species.

There were problems encountered with this method that we had not anticipated. The RING proteins did not provide a change in UV readout. $RING^{322-491}$ contains one tryptophan, two tyrosines and three phenylalanines, $RING^{322-479}$ contains one tryptophan, one tyrosine and two phenylalanines. From this limited number of aromatic amino acids I would perhaps expect to see a much smaller peak than for other proteins but I would expect a peak. However it appears that a property of RING structure is a lack of absorbance (similar results were obtained previously by the Walkinshaw biophysics unit). Any slight peak in the trace was negligible and could not be assigned with any degree of certainty to protein.

In theory, even if a UV readout is not given, the protein should still travel through the column as expected, with larger complexes eluted from the column earlier than smaller ones. So I decided to see if I could still utilise size exclusion chromatography to analyse the oligomeric state of the RING. I collected fractions eluted from the column straight onto a microtitre plate, the idea being that I could detect the protein this way, using antibody detection instead of UV.

Unfortunately this result is not easy to interpret, the antibody detected protein in the majority of the fractions indicating a broad elution, this result was seen for FL RING (**figure 6.4a**), RING ΔT (**figure 6.4b**), $RING^{Y849A}$ (**figure 6.4c**), $RING^{R479A}$ (**figure 6.4d**).

From these ELISAs I would predict that there are different oligomeric forms of the RING present in solution, i.e. monomer, dimer, tetramer etc. Interestingly although protein oligomeristaion state cannot be determined from the ELISAs when the ELISA for FL RING and RING ΔT are overlaid they appear to be behaving in a very similar way (**figure 6.5a**), this hints that perhaps the tail is not necessary for whatever structures the RING is forming. $RING^{R479A}$ and $RING^{Y489A}$ show different elution profiles to FL RING and RING ΔT, interestingly though their elution profiles are similar to each other (**figure 6.5b**).

The RING proteins all elute in the included volume, there is no significant elution in the void volume. This suggests that although their elution ranges are broad and

multiple oligomeric states are likely, they are not forming aggregates as has been suggested previously in the literature[141].

Although this result did not provide oligomeric status for the RING, it did suggest that there are multiple states, this result was enough to warrant further investigation.

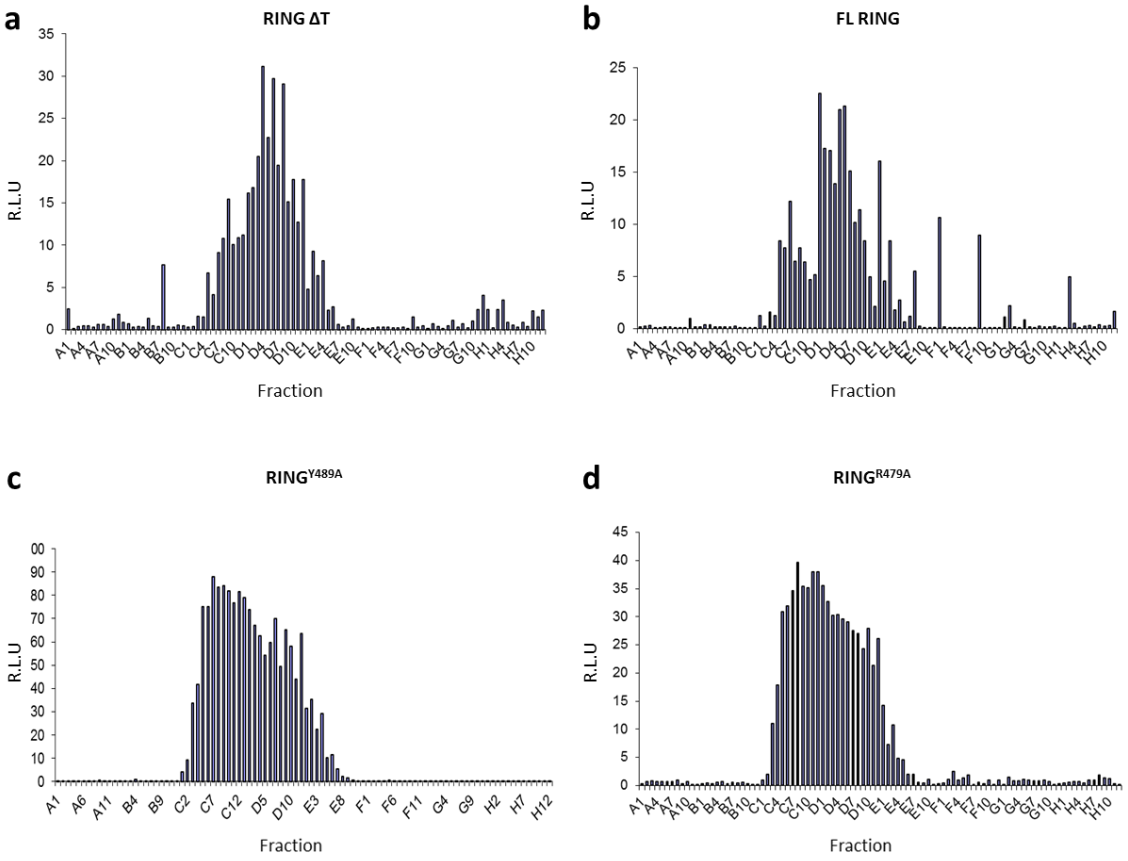

Figure 6.4: Elution profiles of RING proteins as detected by ELISA. a-d) All protein fractions were eluted into a microtitre well and incubated overnight at 4 ^{o}C. Protein was detected using monoclonal antibody 2A10.

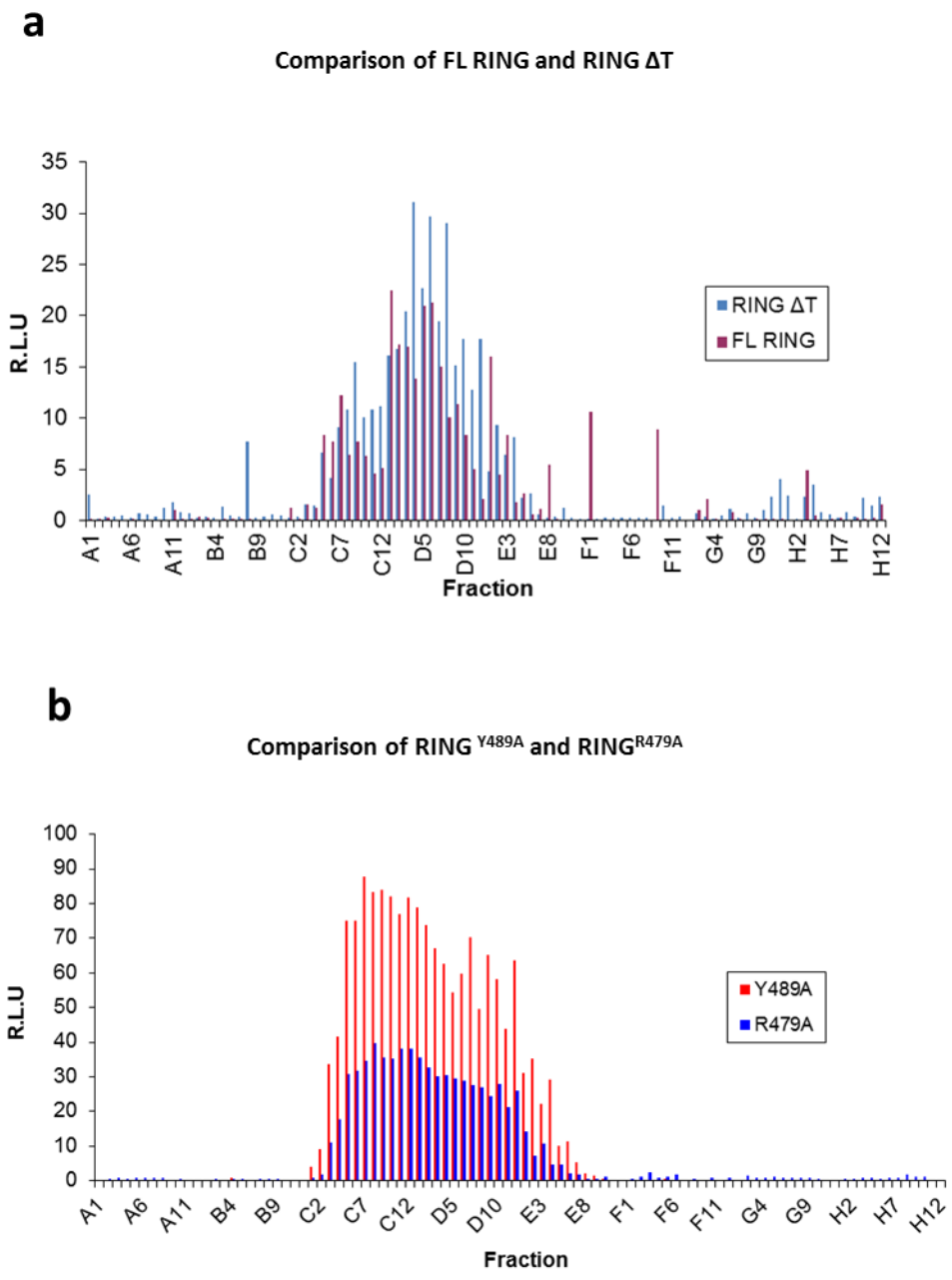

Figure 6.5: Comparison of elution profiles of RING proteins as detected by ELISA a) A comparison of the elution profiles of FL RING and RING ΔT, the elution profiles for both the proteins is highly similar. **b**) A comparison of the elution profiles of RING^{Y489A} and RING^{R479A}, the elution profiles for both the proteins is highly similar. The elution profiles in **a** are different to those in **b.**.

6.1.4 Size exclusion chromatography with multi angle light scattering

As the results from gel filtration were inconclusive a second, more specialised, method commonly used to determine the molecular weight of a protein was tried. Size exclusion chromatography coupled with multi angle light scattering (SECMALS) is widely used for determining the absolute molecular weight and average molecular weight of a protein[251]. However the instrumentation is expensive and therefore not widely available. The Edinburgh Protein Interaction Facility has recently been successful in obtaining this machine and so I was fortunate enough to run my samples.

The main advantage of this technique is that it can provide an absolute measurement of molecular weight without requiring any calibration standards. Another advantage is multi angle light scattering is the determination of molecular dimensions of a protein, this combined with a molecular weight provides information on the size, shape and conformation of the protein in solution. An advantage for us using this technique, and the reason we tried it, is the fact that a visible UV absorbance is not strictly necessary for SECMALS, the RING will have a refractive index and this will allow us to detect its elution from the column. In theory SECMALS should produce a size and we can use this to determine oligomeric structure.

RING ΔT gives a surprising and inconclusive result. Firstly there is a small UV peak which had not been seen previously, there was also a refractive index peak that aligned with the UV peak, therefore the peak we see on the UV trace is due to RING ΔT (**figure 6.6a**). These peaks however are extremely small, so much so that an absolute size of RING ΔT cannot be determined from this data. The data suggests that we are only recovering 30 % of the protein that was loaded onto the column, this would explain the small data peaks (**figure 6.6b**). This either means that the actual protein concentration was much lower than detected using the nanodrop or that the protein is ‘sticking’ to the column.

The small peak that can be seen correlates with RING ΔT being a monomer in solution. However this peak also has a shoulder (**figure 6.6b**), and this shoulder correlates with a size that would indicate that RING ΔT is also capable of forming a dimer in solution. If this result proves to be reproducible then it would suggest that RING ΔT prefers to be a monomer in solution yet is able to form a homodimer, this would further suggest that the tail is not necessary for dimer formation at least in some conformational sates. There is likely to be at last two distinct conformational states for the RING. This experiment would have to be repeated to test this hypothesis.

FL RING did not provide a result for SECMALS. There was no visible UV or refractive index peak and the data retrieved suggested that we recovered less than 5 % of the protein. Like the RING ΔT either the actual protein concentration was much less than measured or the protein is sticking to the column.

Based on the results that this technique could provide it would be worth repeating with more freshly purified protein.

a

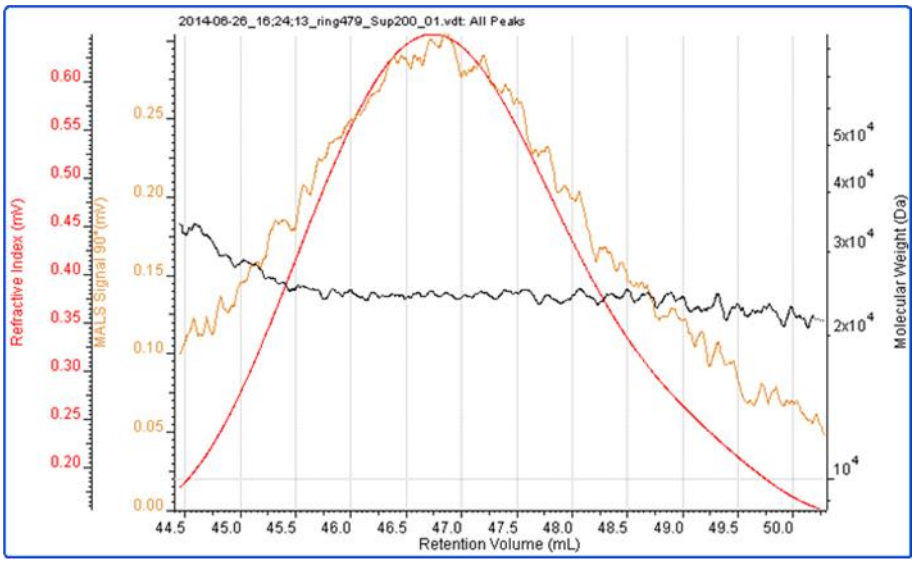

b

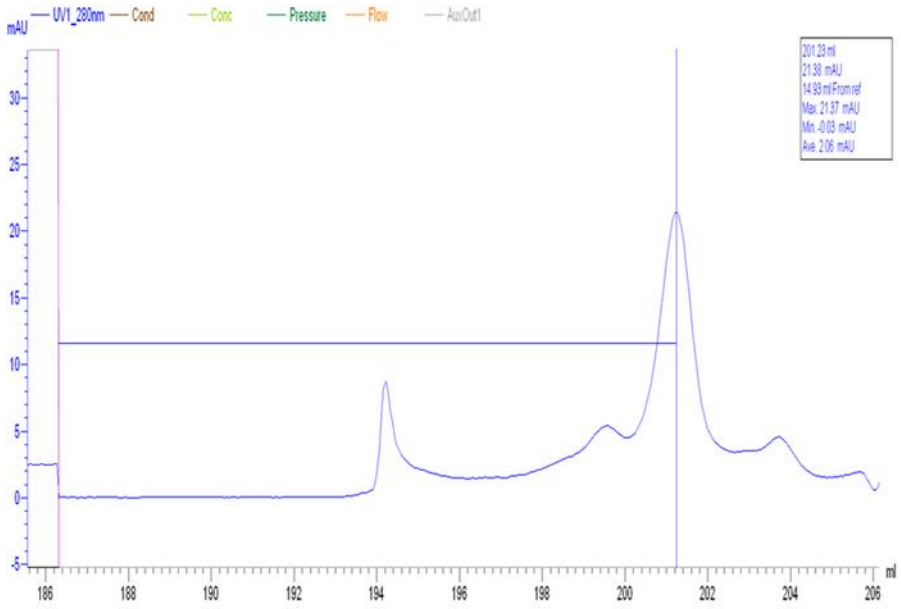

Figure 6.6: SECMALS data for RING ΔT. a) Trace shows that the refractive index of the protein corresponds with the peak obtained by MALS. **b)** Traces show the UV peak of RING ΔT, a shoulder can be seen to the left of the main peak, suggesting multiple oligomeric states.

Data File: 2014-06-26_16;24;13_ring479_Sup200_01.vdt Method: 2 mg ml BSA stnd Sup200 260514-0001.vcm

Peak RV - (ml)	46.721
Mn - (Daltons)	24,332
Mw - (Daltons)	24,455
Mz - (Daltons)	24,599
Mp - (Daltons)	24,559
Mw / Mn	1.005
Percent Above Mw: 0	100.000
Percent Below Mw: 0	0.000
IV - (dl/g)	0.0000
Rh(w) - (nm)	0.000
Rg(w) - (nm)	No Calc
Wt Fr (Peak)	1.000
Mark-Houwink a	0.000
Mark-Houwink logK	0.000
Branches	0.000
Branch Freq.	0.000
RI Area - (mvml)	2.31
UV Area - (mvml)	0.00
RALS Area - (mvml)	0.00
LALS Area - (mvml)	0.00
IVDP Area - (mvml)	0.00

Sample Parameters	Input	Calculated
Sample Conc - (mg/ml)	0.500	0.159
Sample Recovery (%)	0.000	31.785
dn/dc - (ml/g)	0.1850	0.0000
dA/dc - (ml/g)	0.8300	0.0000

Annotation	
Method File	Unsaved Method (2 mg ml BSA stnd Sup200 260514-0001.vcm)
Limits File	
Date Acquired	Jun 26, 2014 - 16:24:13
Solvent	PBS
Acquisition Operator	admin : Administrator
Calculation Operator	admin : Administrator
Column Set	Superdex200
System	EPPF SEC MALS
Flow Rate - (ml/min)	0.500
Inj Volume - (ul)	100.0
Volume Increment - (ml)	0.00498
Detector Temp. - (deg C)	22.0
Column Temp. - (deg C)	22.0
OmniSEC Build Number	438

6.1.5 Discussion

As described in the introduction to this chapter, whether dimerization of MDM2 is absolutely required for its E3-ligase activity and precisely how the dimer facilitates the transfer of ubiquitin from the MDM2-E2-partner to its substrate remains unclear. There is agreement that MDM2 is able to form dimeric (and oligomeric) structures, either as homodimers or heterodimers with MDM4[130], what remains a point of contention is the type of dimer that MDM2 preferentially forms *in vivo*[139] and the role of MDM2 homodimers verses MDM2:MDM4 heterodimers in the ubiquitination of p53. Structural studies have not shown significant differences between MDM2 homodimers and MDM2:MDM4 heterodimers[130,137,139]. However it is possible that the heterodimer is more thermodynamically stable than the homodimer and that this is important in cells.

Another contentious point is whether MDM2 needs to be a dimer for E3 ligase activity *in vivo* as it has been shown to be active as both a monomer and dimer[141], although some reports differ by claiming that the dimer is essential for its activity [102]. These studies are complicated by the fact that many of them are performed using cell based assays where it is difficult to determine whether monomers, dimers or oligomers are being studied and how additional cellular factors may be affecting the outcome[102,133,141]. It is of course possible that MDM2 is active in both its monomeric and dimeric/oligomeric forms, though it seems likely that one form would be preferential *in vivo*, or that different forms would perform distinct tasks, for example mono- vs polyubiquitination.

Lastly, the available crystal structures for the RING of MDM2 as either a homodimer or heterodimer[137] suggest that the tail is necessary for dimer formation[130], as in these structures it sits at the dimer interface where it is buried. While it may certainly be important based on the residues implicated in dimer formation, NMR experiments from a former PhD student in the Walkinshaw group ('Biochemical and Biophysical studies of MDM2-Ligand interactions.') suggest that it may not be necessary for all forms of dimerization. Also unknown at the current time is the effect of E2 binding on the dimer interface and whether regions outside of the RING domain normally contribute to the formation of full-length MDM2 dimers. For example studies on the

role of ATM dependent phosphorylation on the structure and function of MDM2 suggest that phosphorylation sites N-terminal to the RING inhibit MDM2 dimer formation[252].

The aim of the experiments in this chapter was therefore to further elucidate the role of the tail and investigate whether or not it was necessary for dimer formation

6.1.5.1 Exploring the ability of full-length MDM2 and the RING domain to dimerize

The theory behind using surface enhanced Raman scattering was that the N-terminal domain of MDM2 would bind a peptide 12.1 functionalised nanoparticle and if MDM2 dimerised this would bring more than one functionalised nanoparticle together. This aggregation could then be measured over time by extinction spectroscopy[249].

The results did show an aggregation of the nanoparticles and it was concluded that MDM2 was dimerising through its RING domain[249]. There is the possibility that MDM2 is dimerising through a different area but there is no evidence to support this. However, it can't be ruled out as we know for example as stated above that regions out-with the RING, such as the tail and the linker region between the Zn finger and the RING[252] can regulate dimerization.

The study we performed in collaboration to develop a nanoparticle assay for MDM2 oligomer formation supports the view that FL MDM2 can form a dimer in solution, however it does not provide information regarding the role of the tail of MDM2. There is the potential to repeat this experiment using MDM2 ΔT, as although missing the tail this protein can still bind peptide 12.1. Aggregation of the functionalised nanoparticles would imply that the tail is not necessary for dimer formation and no aggregation would imply that the tail was necessary. The process of conjugating the peptide to the nanoparticle is complicated, even though it is a one-step reaction and this could be the limiting factor for repeating this experiment.

Size exclusion chromatography is commonly used to determine protein size. Our theory was that if we could examine the size of FL RING and RING ΔT in solution this would indicate whether the proteins were monomer or dimer. The size of RING ΔT compared to FL RING could indicate whether the tail was involved in dimer formation i.e. if RING ΔT was monomer sized and FL Ring was dimer sized this was indicate that the tail was necessary for dimer formation.

Gel filtration did not provide a result for these two protein constructs as they do not give a UV absorption peak at 280 nm. Capturing and detecting the eluted fractions onto an ELISA plate hinted at different oligomeric forms of each protein in solution but they were not conclusive.

This experiment could be repeated measuring UV absorbance at different wavelengths to see if the RING constructs give a peak. For example disulphide bonds that form between the two cysteines show an absorbance at 260 nm and peptide bonds show an absorbance at 230 nm. It is likely that this method is not suitable for the RING constructs and that investigation into other methods for sizing proteins may be beneficial.

As size exclusion chromatography was not successful we decided to try SECMALS, which measures the absolute mass of a protein. Interestingly, RING ΔT did give a UV absorption peak at 280 nm, and this peak corresponded with the peak produced by the refractive index of the protein, however the two peaks were so small that no absolute mass could be calculated. However results hinted that RING ΔT was preferentially a monomer in solution though there was also the possibility of some dimer formation.

The main issue that was highlighted when using this technique is that the concentration of protein recovered from the column was much less than the concentration of protein that was loaded. This may be due to the protein sticking to the column and if this is the case then this technique is not suitable for these RING constructs. However if it is due to the actual concentration of protein loaded being much lower than calculated then this need to be addressed for two reasons, firstly a higher concentration is need to measure the absolute mass and secondly the low concentration of the solution could impact on dimer formation and the ratio of

monomer and dimer in solution. Thus, SECMALS may be more suitable for sizing FL MDM2 and MDM2 ΔT, especially if the RING constructs are sticking to the column.

The experiments in this chapter have not provided the information I was hoping for. However, in collaboration I have shown that the FL MDM2 forms a dimer/oligomer in solution and there are hints that the isolated RING can form a dimer even in the absence of the tail although this appears to be only a low percentage of total protein.

6.1.5.2 Previous studies on the role of the tail in dimerization

If we look at previous studies reported in the literature loss of E3-activity due to removal of the MDM2 tail, the introduction of point mutations in the tail and C-terminal tail extensions, are almost always equated with the loss of dimer structure[102]. However, both in vitro assays and cell based studies exist that suggest that the MDM2 monomer can have similar levels of E3-activity as dimers and homo-oligomers[141]. Further, E3-inactive MDM2 tail point mutant proteins can still form a dimer when mixed with MDM4 and the mixed dimer can be active as an E3-ligase even though MDM4 itself has no intrinsic E3-activity[133]. These studies suggest that, i) the monomer can be an active functional E3-ligase under some conditions, and, ii) that tail integrity is not a prerequisite for dimer formation. Some of this confusion might be made more clear if we had more structural information on the position of the MDM2 tail and the role of the dimer in binding to the E2. For example, although the tail is burried in the homo- and hetrodimer structures[130] does it remain burried once the RING is bound to the E2~Ub complex. My data (chapter 3 and 4) suggests that E2 access to the tail is critical for MDM2 mediated allosteric activation of UbcH5 and therefore for transfer of Ub to a substrate.

If we compare MDM2 to other RING domain E3-ligases where more detailed mechanistic information has been obtained the picture remains somewhat confused. The Hay lab have carried out studies on the mechanism of RNF4 and have published two papers on the RNF4 dimer in complex with the E2~Ub complex. The first of these[220] puts forward a mechanism where the dimer is required for ubiquitin transfer by offering two distinct binding interfaces such that one RING would interact with the E2 and the second RING would interact with the ubiquitin. However this study relied

heavily on the introduction of multiple point mutations into the E2 which made interpretation of the data complex. Subsequently the same group published a second model[37] where both the E2 and ubiquitin could bind to a single RING domain. This is in good agreement with my studies showing that peptide 8 can bind to ubiquitin and UbcH5 simultaniously and with MD simulations carried out in collaboration with Dr Chandra Verma (see Chapter 3).

However the second RNF4 study[37] also argues that contact of ubiquitin with both RING domains was essential for ubiquitin transfer and that therefore a RING dimer is required. However, this contrasts with biochemical studies on the MDM2 RING showing an active monomer[141]. The difference could be in the tail structure of MDM2 (that is not shared with RNF4) and the role played by the tail in activating the E2 as demonstrated in this thesis.

In my reading of the literature I have observed that the majority of studies on the MDM2 dimer and its role in the reaction mechanism of ubiquitination have been carried out using cell based assays and pulldowns which makes the claims about structure hard to validate. There are many inconsistencies in the literature and many of the studies are contradictory. The structural studies that have been carried out on the mechanism of MDM2 mediated ubiquitination have concentrated on using the isolated RING domain, however these have been carried out in the absence of the E2 or ubiquitin and therefore can not be used to inform us about the structure of the RING in relation to other ubiquitination pathway components or within the context of the full-length protein. As such it would add greatly to our understanding of MDM2 mechansim if biochemical, biophysical and structural studies could be carried out that are designed to study the properties of full-length MDM2 and its binding interactions.

Chapter 7: FURTHER WORK

7.1 Investigation of MDM2 and dimer formation

My results show that MDM2 can form a dimer, specifically a homodimer, in solution. My results so far have not provided concrete evidence that the C-terminal tail of MDM2 is or is not absolutely required for dimer formation, however previous unpublished studies from the Walkinshaw group using NMR agree with my preliminary data (**Figure 6.6**) a portion of MDM2 ΔT in a dimer peak as determined by SECMALS.

Surface-enhanced Raman scattering (SERS) data showed that full length MDM2 oligomerised in solution (Chapter 4). The conclusion was that MDM2 was forming a homodimer through its RING domains as this is the mechanism that the current literature suggests. This experiment has the potential to be repeated with MDM2 ΔT. I predict that if the tail is not required for dimer formation aggregation of the functionalised nanoparticles should be seen, as was for FL MDM2 although this could give a reduced signal compared to FL MDM2 protein as SECMALS suggests that only a portion of MDM2 ΔT is in a dimer. If the tail is required then no aggregation should be seen. The only issue with repeating this experiment is that the process of conjugating the peptide to the nanoparticle is difficult and time intensive.

Although I obtained some intriguing preliminary data by SECMALS (Chapter 4), suggesting as mentioned above that a portion of the MDM2 ΔT protein was dimeric the data was not of high enough quality for publication. The RING ΔT protein product appeared to be monomeric yet there was a shoulder present in the trace that suggested that dimer formation was still an option as a minor secondary product. I would like to retry SECMALS with more RING protein to see if a clearer answer can be obtained. There may be an intrinsic problem with the RING and SECMALS if the RING is sticking to the column (Chapter 4). If this is the case then I would like to try SECMALS with FL MDM2 and MDM2 ΔT, as the full length proteins are less prone to aggregation and therefore may be more suitable for SECMALS analysis.

I previously used HD exchange to analyse UbcH5α (Chapter 2), I would also like to use HD exchange to look at the RING proteins in solution. HD exchange could tell us more about the oligomeric state of the RINGS. Should a dimer be formed I would expect to see a lower rate, of or no exchange at the dimer interface.

If answers can be found as to whether or not the RING is a dimer and whether or not the tail is necessary for dimer formation, then this could have implications for the mechanism of MDM2 E3 ligase activity. A study says that dimer formation is necessary for E3 ligase activity as when the tail is removed MDM2 is inactive as an E3 ligase because dimer formation can no longer occur[253]. My results also show that MDM2 ΔT is inactive as an E3 ligase (Chapter 1), however it is not clear whether this is because dimer formation is no longer an option. There are also studies showing MDM2 active as an E3 ligase when it is present as a monomer. It is possible that he tail may have another role in E3 ligase activity that is of yet unknown. Knowing the role of the tail in dimer formation could help probe the role of the tail in E3 ligase activity.

7.2 MDM2 and the allosteric activation of UbcH5α

My results show that UbcH5α binds with relatively high affinity to the RING of MDM2 and specifically somewhere in the region of the 20 most C-terminal amino acids (peptide 8) with a second lower affinity interaction between UbcH5α and peptide 2 of the RING, an area that maps to previous E2 binding sites (Chapter 1). I also found that when peptide 8 binds to UbcH5α, Ubch5α undergoes an allosteric change (Chapter 3). This is the first solid evidence that MDM2 allosterically activates its E2 partner. Good results were achieved using limited proteolysis linked with MS and promising results were achieved with the first round of HD exchange.

I am going to repeat the HD exchange experiment using UbcH5α and a newly synthesised batch of peptide 8 in order to achieve publishable data. I would also like to repeat the HD exchange using the RING domain and UbcH5α, HD exchange on two proteins or protein domains is more tricky than using a protein and a peptide and less examples exist but successful application of this technique could provide additional insight into the interacting residues that are important for ubiquitin transfer.

I have written throughout my thesis about E2-ubiquitin conjugates (Chapter 1,2). Stable ubiquitin conjugates have not been successfully created and in order to increase the stability many mutations are being carried out on the UbcH5α[220]. These mutations may hide the true mechanism of E2 function and so another technique would be much better suited for my purpose. One such technique I would like to investigate further is 'Click' chemistry. Click chemistry has already been used to stably link ubiquitin to PCNA. In this technique artificial amino acids that carried an azide or alkyne side chain were incorporated into ubiquitin and PCNA respectively. The two proteins were then linked site specifically by Cu (I)- catalysed azide-alkyne cycloaddition[226]. It should be possible incorporate an artificial amino acid into UbcH5α and ubiquitin in order to link them and form a stable conjugate with minimal mutation, and we have set up a collaboration with chemists to achieve this.

If click chemistry is a viable option and it is possible to create the E2-ubiquitin conjugate I would like to use it to repeat some experiments already carried out with free UbcH5α Limited proteolysis suggested that the ubiquitin binding helix of UbcH5α increased in stability upon peptide 8 binding. I would like to see what happens when peptide 8 binds to the conjugate. I would investigate this using both limited proteolysis linked with MS and HD exchange.

I carried out peptide phage display in order to confirm a conformational change of E2. As explained in Chapter 3 my peptide phage display assay has provided a wealth of information that I have not investigated. It would be worth using some of the programs outlined, such as MEME and BLAST, in order to investigate the difference in the interactome of free UbcH5α and UbcH5α in complex with peptide 8/MDM2 RING.

7.3 MDM2 and ubiquitin

Throughout the course of my PhD I have focussed on the RING of MDM2 and its interaction with ubiquitin and UbcH5α and I have shown that the RING domain of MDM2 can bind both ubiquitin and UbcH5α. I then continued to focus on the

allosteric regulation of UbcH5α by MDM2, studying the activation of UbcH5α was the natural route to follow as the literature had already hinted that E2s had the potential to be allosterically activated by their partner E3s[35]. This led me to wonder about ubiquitin, could it too be undergoing some conformational change upon RING binding? The literature would perhaps suggest not as ubiquitin is unanimously described as a compact and extremely stable protein.

7.3.1 Electrochemistry

During my time collaborating with the Masaryk Memorial Cancer Institute I was able to use electrochemistry to carry out preliminary investigations looking at free ubiquitin and ubiquitin in complex with peptide 8.

For this work I used the Hanging Mercury Drop Electrode (HDME). The HDME produces a mercury drop, of a controlled, constant surface area, at the end of a capillary. An advantage of the HDME is that unlike solid electrodes it does not have to be cleaned and polished between each experiment, instead the HDME can release the contaminated drop and produce a new one between each experiment.

Studies had already shown that using Constant Current Chronopotentiometric Stripping Analysis (CPSA) and a HDME that proteins and peptides, at negative potentials, gave distinctive peaks at nanomolar and subnanomolar concentrations. These peaks were denominated as peak H as they were due to catalytic hydrogen evolution.

Peak H has been shown to be sensitive to global and local conformational changes of proteins[254].

I decided to try this technique to look for potential differences in the structure of free and ligand (peptide 8) bound ubiquitin. Cysteine, along with the other basic residues, is important for this method in producing the peak, as these residues adsorb to the mercury electrode. Ubiquitin contains no cysteines and limited numbers of other basic residues however at the right conditions it does produce a small reproducible peak

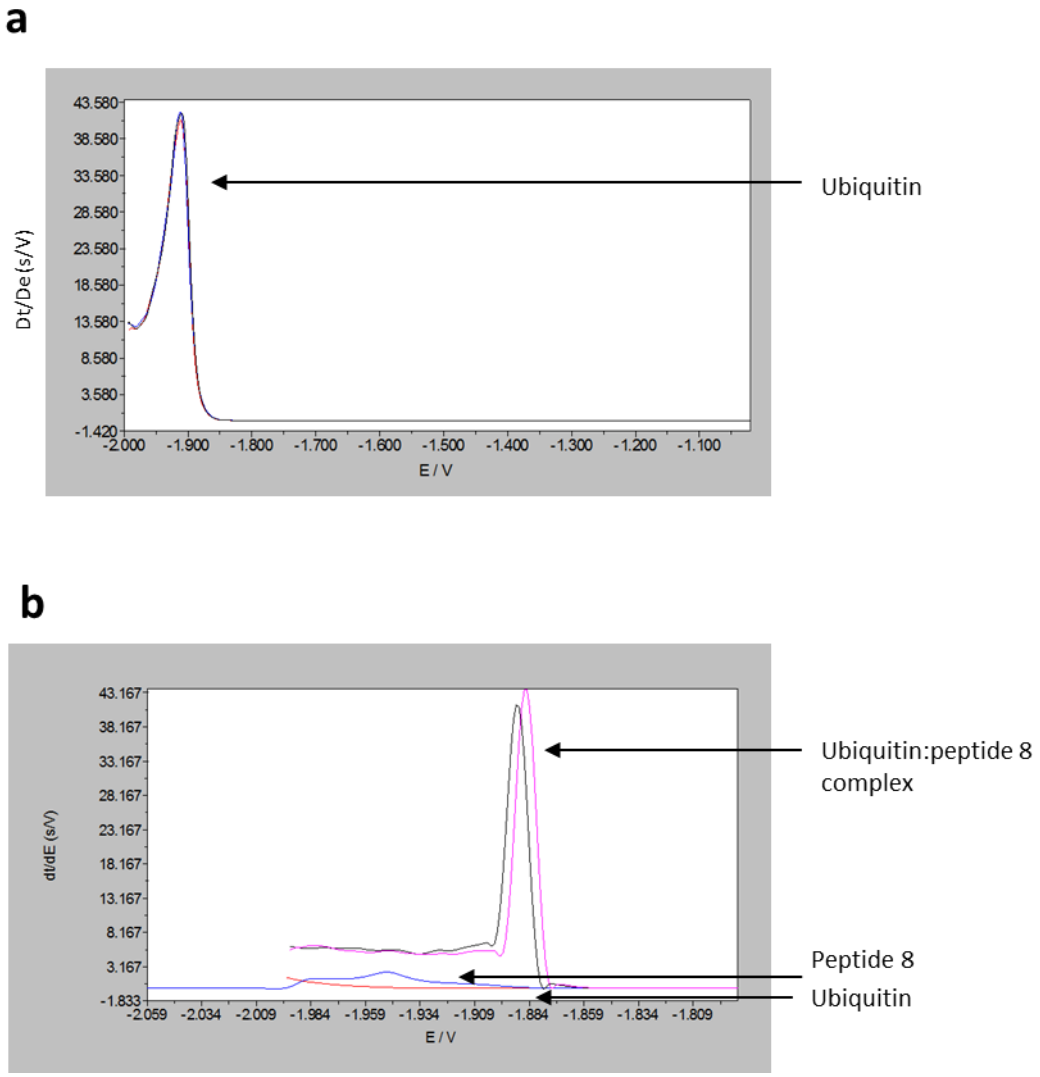

(**figure 7.1**). Using the exact same conditions ubiquitin in complex with peptide 8 produces a peak that was too great to measure.

Figure 7.1: Electrochemistry data from free and ligand bound ubiquitin. a) Graph showing the peak of free ubiquitin, the peak is reproducible. **b)** Graph showing the peak of ligand bound ubiquitin, peptide 8 and free ubiquitin. Ligand bound ubiquitin produces a much greater signal than free ubiquitin and peptide 8.

Changing the stripping current, the current at which the protein is stripped from the electrode, meant that the peak from ubiquitin alone was too small to be seen but the peak produced by ubiquitin in complex with peptide 8 can be measured.

The peptide by itself did not produce a peak under these conditions, even though it contains two cysteines; this indicates the change in peak intensity is due to the complex and not due to the mere presence of the peptide.

A number of events could be taking place that account for this increased peak. Firstly, the cysteines within the peptide may be responsible for increased adsorption of ubiquitin onto the electrode, i.e. peptide 8 binds to ubiquitin, peptide 8 adsorbs to the electrode, facilitating greater ubiquitin adsorption onto the electrode resulting in an increased signal. Secondly, the peptide binding to ubiquitin could result in a conformational change within ubiquitin that exposes a greater number of basic residues, allowing for increased adsorption of ubiquitin onto the electrode and an increase in signal. The increase in signal could also be due to a combination of these two events.

The electrochemistry data has indicated that there might be a change in the conformation of ubiquitin when it is in complex with peptide 8, unfortunately it cannot be used to confirm this change. To do this further biophysical assays would have to be carried out.

One such biophysical approach I would like to use is NMR. The structure of ubiquitin has already been extensively mapped by NMR and so experiments would be relatively simple. I would like to compare the spectra of ubiquitin to that of ubiquitin in complex with peptide 8. This could provide information regarding the binding interface of peptide 8 and ubiquitin and also any conformational change in ubiquitin upon peptide 8 binding. I have already tried preliminary NMR experiments, ubiquitin itself provided a good NMR spectra, however when I added peptide no change was seen. As previously described I realised the peptide was not the concentration I thought based on information provided by mimotopes, the company that synthesised it. I am going to repeat this experiment with a newly synthesised batch of peptide.

7.4 MDM2 and gankyrin

My PhD has focussed on the RING domain of MDM2 and its role in ubiquitination. Specifically I have focussed on the interaction of the RING with other ubiquitination cascade elements, UbcH5α and ubiquitin. The RING however can bind to other factors that are not part of the ubiquitination cascade, these other binding partners may or may not have an effect on the E3 activity of MDM2. One such binding partner is gankyrin. The Ball lab has begun a collaboration that is investigating the interaction of gankyrin with MDM2. This is of particular interest to me as gankyrin is one of the few proteins shown to activate, rather than inhibit, MDM2 E3 ligase activity[255].

Gankyrin is a small oncoprotein, ~25kDa and 226 amino acids in length, made up of seven ankryin repeats. It is a subunit of the 26s proteasome that specifically interacts with the S6b ATPase of the 19s regulator. Gankyrin is highly conserved across eukaryotes and overexpressed in the majority of hepatocellular carcinomas[256]. Gankyrin binds to retinoblastoma (pRb) protein and the 6s subunit of the 26s proteasome and increases the rate of degradation of pRb. Gankyrin also binds to CDK4 counteracting the inhibitory functions of tumours suppressors $p16^{ink4a}$ and $p18^{ink4c}$, gankyrin is clearly an important regulator of the cell cycle and tumourgenesis[257].

A study has shown that gankyrin has an effect on the E3 activity of MDM2 towards p53. This study showed that gankyrin could bind to MDM2 and facilitate the binding of p53 to MDM2 as well as increasing the ubiquitination and degradation of p53[255]. The mechanism by which gankyrin facilitates p53 binding to MDM2 and increases the E3 activity of MDM2 is currently unknown.

We are interested in investigating the interaction between gankyrin and MDM2 in an attempt to discover where on MDM2 Gankyrin makes contact and how the binding site(s) could have an effect on the E3 ligase activity of MDM2. I have already carried out some preliminary experiments on this interaction as described below.

7.4.1 Gankyrin binds to MDM2

I first tested two anti-gankyrin antibodies, a rabbit polyclonal and a mouse monoclonal, in order to identify reagents that can be used to study this protein. I designed an ELISA in which gankyrin (100 ng) was immobilised onto a microtitre well before detecting with the antibodies. The mouse monoclonal antibody had a higher binding capacity for gankyrin than the rabbit polyclonal (**figure 7.2a**), this is the antibody I therefore used routinely.

In cell based assays MDM2 immunoprecipitated with gankyrin leading to the conclusion that gankyrin binds to MDM2[255]. I carried out a protein binding assay to see if I was able to confirm the interaction and if the interaction was direct or required other cellular factors. In this particular protein biding assay MDM2 was immobilised on a microtitre well and gankyrin titrated in the mobile phase before being detected by the mouse anti-gankyrin MAb. Gankyrin bound to MDM2, confirming the interaction seen in the cell based assay. This assay does not work if it is performed in the opposite orientation i.e. gankyrin immobilised onto the well and MDM2 in solution, suggesting that the conformational flexibility of gankyrin may be an important determinant of MDM2 binding (**figure 7.2b**).

Gankyrin is reported to increase the E3 ligase activity of MDM2 towards p53, I was curious therefore to see if gankyrins point(s) of contact with MDM2 were within the RING. I carried out a protein binding assay similar to that described above; though this time I used my FL RING instead of FL MDM2. In this assay gankyrin bound to MDM2, unlike in the assay with FL MDM2 gankyrin can bind to FL RING in either the immobile or solution phase (**figure 7.3a and b**). As the RING can bind to gankyrin in either phase it may not be as I thought, the flexibility of gankyrin may not be an important determinant of MDM2 binding instead it could be that the binding site of gankyrin is cryptic when FL MDM2 is in the mobile phase and by capturing it to the plate the site is exposed.

Using a set of overlapping MDM2 peptides I carried out a peptide binding assay with gankyrin (**figure 7.4**). Having already shown that gankyrin binds to the RING of MDM2 it is of interest that gankyrin bound to several overlapping C-terminal MDM2

peptides. Strikingly gankyrin also bound to a number of N-terminal MDM2 peptides, suggesting that MDM2 and gankyrin have a complex extended interface involving both the N-terminal and C-terminal domains of MDM2. I would like to repeat this assay to test for consistent results and to confirm the peptide binding results using protein domains. In addition I plan to immobilise the MDM2 peptide library onto beads and use them to pull-down gankyrin from cell lysates to confirm and complement the *in vitro* peptide binding assay. As gankyrin binds to the RING domain of MDM2 and gankyrin has been shown to affect the ubiquitination activity of MDM2 I would like to carry out a peptide binding assay using the overlapping RING domain peptides. Ascertaining where in the RING gankyrin binds could help determine the mechanism of its activating effect on MDM2 E3 ligase activity.

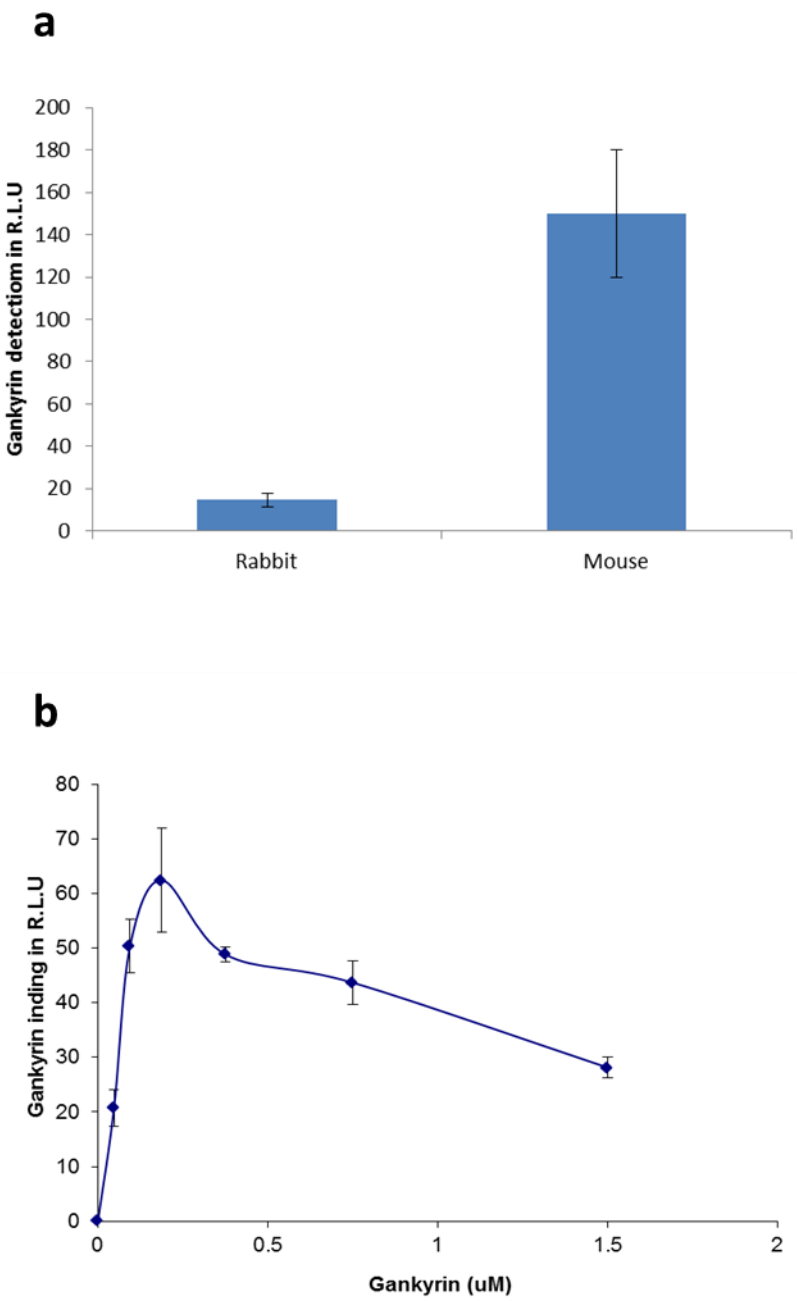

Figure 7.2: Gankyrin binds to MDM2. a) Rabbit polyclonal and mouse monoclonal antibodies detect gankyrin. **b)** MDM2 was captured onto microtitre wells (100 ng/well), a titration of gankyrin was added in the mobile phase and incubated for 1 hour at room temperature. Unbound protein was removed by extensive washing and bound protein was detected using mouse monoclonal antibody. Graphs show gankyrin binding expressed as relative light units (R.L.U).

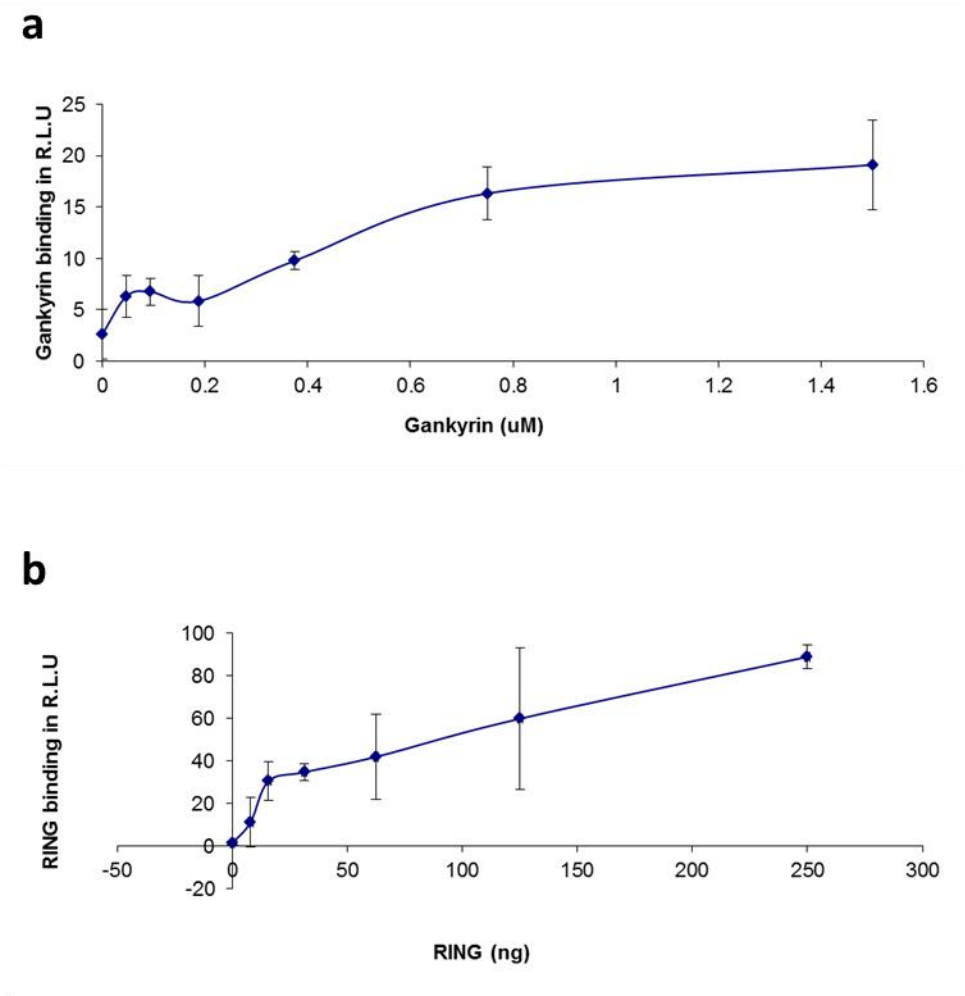

Figure 7.3: Gankyrin binds to the RING domain of MDM2. a) FL RING was captured onto microtitre wells (100 ng/well), a titration of gankyrin was added in the mobile phase and incubated for 1 hour at room temperature. Unbound protein was removed by extensive washing and bound protein was detected using mouse monoclonal antibody. Graphs show gankyrin binding expressed as relative light units (R.L.U). **b)** Gankyrin was captured onto microtitre wells (100 ng/well), a titration of FL RING was added in the mobile phase and incubated for 1 hour at room temperature. Unbound protein was removed by extensive washing and bound protein was detected using monoclonal antibody 2A10. Graphs show FL RING binding expressed as relative light units (R.L.U).

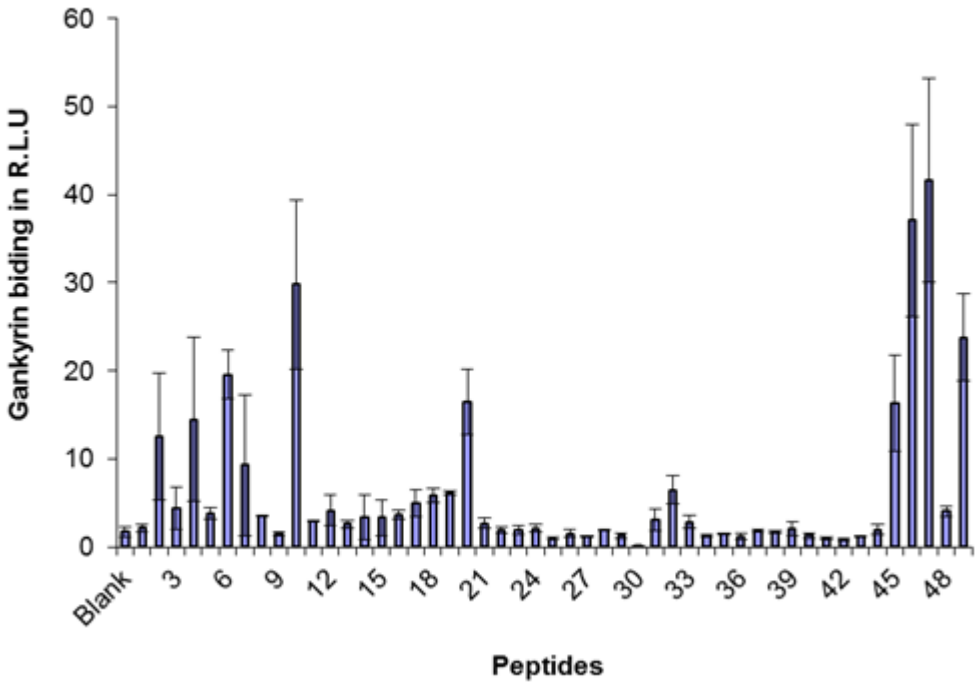

Figure 7.4: Gankyrin binding to MDM2 peptides. a) A series of biotin labelled MDM2 peptides (100 ng/well) were captured onto streptavidin coated microtitre wells, gankyrin (100 ng/well) was added and incubated for 1 hour at room temperature. Unbound gankyrin was removed by extensive washing and bound protein was detected using mouse monoclonal antibody. Graph shows gankyrin binding expressed as relative light units (R.L.U).

Chapter 8: REFERENCES

1. Ciechanover A, Elias S, Heller H, Ferber S, Hershko A. Characterization of the heat-stable polypeptide of the ATP-dependent proteolytic system from reticulocytes. J Biol Chem 1980;255(16):7525-8.
2. Hershko A, Ciechanover A, Heller H, Haas AL, Rose IA. Proposed role of ATP in protein breakdown: conjugation of protein with multiple chains of the polypeptide of ATP-dependent proteolysis. Proc Natl Acad Sci U S A 1980;77(4):1783-6.
3. Finley D. Recognition and processing of ubiquitin-protein conjugates by the proteasome. Annu Rev Biochem 2009;78:477-513.
4. Hicke L, Dunn R. Regulation of membrane protein transport by ubiquitin and ubiquitin-binding proteins. Annu Rev Cell Dev Biol 2003;19:141-72.
5. Hoege C, Pfander B, Moldovan GL, Pyrowolakis G, Jentsch S. RAD6-dependent DNA repair is linked to modification of PCNA by ubiquitin and SUMO. Nature 2002;419(6903):135-41.
6. Schnell JD, Hicke L. Non-traditional functions of ubiquitin and ubiquitin-binding proteins. J Biol Chem 2003;278(38):35857-60.
7. Bloom J, Amador V, Bartolini F, DeMartino G, Pagano M. Proteasome-mediated degradation of p21 via N-terminal ubiquitinylation. Cell 2003;115(1):71-82.
8. Xu P, Duong DM, Seyfried NT, Cheng D, Xie Y, Robert J, Rush J, Hochstrasser M, Finley D, Peng J. Quantitative proteomics reveals the function of unconventional ubiquitin chains in proteasomal degradation. Cell 2009;137(1):133-45.
9. Kim HT, Kim KP, Lledias F, Kisselev AF, Scaglione KM, Skowyra D, Gygi SP, Goldberg AL. Certain pairs of ubiquitin-conjugating enzymes (E2s) and ubiquitin-protein ligases (E3s) synthesize nondegradable forked ubiquitin chains containing all possible isopeptide linkages. J Biol Chem 2007;282(24):17375-86.
10. Pickart CM, Eddins MJ. Ubiquitin: structures, functions, mechanisms. Biochim Biophys Acta 2004;1695(1-3):55-72.
11. Ross CA, Pickart CM. The ubiquitin-proteasome pathway in Parkinson's disease and other neurodegenerative diseases. Trends Cell Biol 2004;14(12):703-11.
12. Schwartz AL, Ciechanover A. Targeting proteins for destruction by the ubiquitin system: implications for human pathobiology. Annu Rev Pharmacol Toxicol 2009;49:73-96.
13. Vijay-Kumar S, Bugg CE, Cook WJ. Structure of ubiquitin refined at 1.8 A resolution. J Mol Biol 1987;194(3):531-44.
14. Dikic I, Wakatsuki S, Walters KJ. Ubiquitin-binding domains - from structures to functions. Nat Rev Mol Cell Biol 2009;10(10):659-71.
15. Sloper-Mould KE, Jemc JC, Pickart CM, Hicke L. Distinct functional surface regions on ubiquitin. J Biol Chem 2001;276(32):30483-9.
16. Kamadurai HB, Souphron J, Scott DC, Duda DM, Miller DJ, Stringer D, Piper RC, Schulman BA. Insights into ubiquitin transfer cascades from a structure of a UbcH5B approximately ubiquitin-HECT(NEDD4L) complex. Mol Cell 2009;36(6):1095-102.

17. Hu M, Li P, Li M, Li W, Yao T, Wu JW, Gu W, Cohen RE, Shi Y. Crystal structure of a UBP-family deubiquitinating enzyme in isolation and in complex with ubiquitin aldehyde. Cell 2002;111(7):1041-54.
18. Kulathu Y, Komander D. Atypical ubiquitylation - the unexplored world of polyubiquitin beyond Lys48 and Lys63 linkages. Nat Rev Mol Cell Biol 2012;13(8):508-23.
19. Chen ZJ, Fuchs SY. Ubiquitin-dependent activation of NF-kappaB: K63-linked ubiquitin chains: a link to cancer? Cancer Biol Ther 2004;3(3):286-8.
20. Wu-Baer F, Lagrazon K, Yuan W, Baer R. The BRCA1/BARD1 heterodimer assembles polyubiquitin chains through an unconventional linkage involving lysine residue K6 of ubiquitin. J Biol Chem 2003;278(37):34743-6.
21. Geisler S, Holmström KM, Treis A, Skujat D, Weber SS, Fiesel FC, Kahle PJ, Springer W. The PINK1/Parkin-mediated mitophagy is compromised by PD-associated mutations. Autophagy 2010;6(7):871-8.
22. Baboshina OV, Haas AL. Novel multiubiquitin chain linkages catalyzed by the conjugating enzymes E2EPF and RAD6 are recognized by 26 S proteasome subunit 5. J Biol Chem 1996;271(5):2823-31.
23. Haas AL, Warms JV, Hershko A, Rose IA. Ubiquitin-activating enzyme. Mechanism and role in protein-ubiquitin conjugation. J Biol Chem 1982;257(5):2543-8.
24. Ohsumi Y. Molecular dissection of autophagy: two ubiquitin-like systems. Nat Rev Mol Cell Biol 2001;2(3):211-6.
25. Lake MW, Wuebbens MM, Rajagopalan KV, Schindelin H. Mechanism of ubiquitin activation revealed by the structure of a bacterial MoeB-MoaD complex. Nature 2001;414(6861):325-9.
26. Pickart CM. Mechanisms underlying ubiquitination. Annu Rev Biochem 2001;70:503-33.
27. Haas AL, Bright PM. The resolution and characterization of putative ubiquitin carrier protein isozymes from rabbit reticulocytes. J Biol Chem 1988;263(26):13258-67.
28. Pickart CM. Back to the future with ubiquitin. Cell 2004;116(2):181-90.
29. Hershko A, Ciechanover A. The ubiquitin system. Annu Rev Biochem 1998;67:425-79.
30. Behrends C, Harper JW. Constructing and decoding unconventional ubiquitin chains. Nat Struct Mol Biol 2011;18(5):520-8.
31. Christensen DE, Brzovic PS, Klevit RE. E2-BRCA1 RING interactions dictate synthesis of mono- or specific polyubiquitin chain linkages. Nat Struct Mol Biol 2007;14(10):941-8.
32. Seeler JS, Dejean A. Nuclear and unclear functions of SUMO. Nat Rev Mol Cell Biol 2003;4(9):690-9.
33. Hershko A, Heller H, Elias S, Ciechanover A. Components of ubiquitin-protein ligase system. Resolution, affinity purification, and role in protein breakdown. J Biol Chem 1983;258(13):8206-14.
34. Zheng N, Wang P, Jeffrey PD, Pavletich NP. Structure of a c-Cbl-UbcH7 complex: RING domain function in ubiquitin-protein ligases. Cell 2000;102(4):533-9.
35. Ozkan E, Yu H, Deisenhofer J. Mechanistic insight into the allosteric activation of a ubiquitin-conjugating enzyme by RING-type ubiquitin ligases. Proc Natl Acad Sci U S A 2005;102(52):18890-5.

36. Brzovic PS, Keeffe JR, Nishikawa H, Miyamoto K, Fox D, Fukuda M, Ohta T, Klevit R. Binding and recognition in the assembly of an active BRCA1/BARD1 ubiquitin-ligase complex. Proc Natl Acad Sci U S A 2003;100(10):5646-51.
37. Plechanovová A, Jaffray EG, Tatham MH, Naismith JH, Hay RT. Structure of a RING E3 ligase and ubiquitin-loaded E2 primed for catalysis. Nature 2012;489(7414):115-20.
38. Xu Z, Kohli E, Devlin KI, Bold M, Nix JC, Misra S. Interactions between the quality control ubiquitin ligase CHIP and ubiquitin conjugating enzymes. BMC Struct Biol 2008;8:26.
39. Zheng N, Schulman BA, Song L, Miller JJ, Jeffrey PD, Wang P, Chu C, Koepp DM, Elledge SJ, Pagano M and others. Structure of the Cul1-Rbx1-Skp1-F boxSkp2 SCF ubiquitin ligase complex. Nature 2002;416(6882):703-9.
40. Freemont PS, Hanson IM, Trowsdale J. A novel cysteine-rich sequence motif. Cell 1991;64(3):483-4.
41. Pintard L, Willems A, Peter M. Cullin-based ubiquitin ligases: Cul3-BTB complexes join the family. EMBO J 2004;23(8):1681-7.
42. Deshaies RJ, Joazeiro CA. RING domain E3 ubiquitin ligases. Annu Rev Biochem 2009;78:399-434.
43. Petroski MD, Deshaies RJ. Function and regulation of cullin-RING ubiquitin ligases. Nat Rev Mol Cell Biol 2005;6(1):9-20.
44. Aravind L, Koonin EV. The U box is a modified RING finger - a common domain in ubiquitination. Curr Biol 2000;10(4):R132-4.
45. Ohi MD, Vander Kooi CW, Rosenberg JA, Chazin WJ, Gould KL. Structural insights into the U-box, a domain associated with multi-ubiquitination. Nat Struct Biol 2003;10(4):250-5.
46. Murata S, Minami Y, Minami M, Chiba T, Tanaka K. CHIP is a chaperone-dependent E3 ligase that ubiquitylates unfolded protein. EMBO Rep 2001;2(12):1133-8.
47. Pringa E, Martinez-Noel G, Muller U, Harbers K. Interaction of the ring finger-related U-box motif of a nuclear dot protein with ubiquitin-conjugating enzymes. J Biol Chem 2001;276(22):19617-23.
48. Cyr DM, Höhfeld J, Patterson C. Protein quality control: U-box-containing E3 ubiquitin ligases join the fold. Trends Biochem Sci 2002;27(7):368-75.
49. Narayan V, Pion E, Landré V, Müller P, Ball KL. Docking-dependent ubiquitination of the interferon regulatory factor-1 tumor suppressor protein by the ubiquitin ligase CHIP. J Biol Chem 2011;286(1):607-19.
50. Scheffner M, Nuber U, Huibregtse JM. Protein ubiquitination involving an E1-E2-E3 enzyme ubiquitin thioester cascade. Nature 1995;373(6509):81-3.
51. Huibregtse JM, Scheffner M, Howley PM. E6-AP directs the HPV E6-dependent inactivation of p53 and is representative of a family of structurally and functionally related proteins. Cold Spring Harb Symp Quant Biol 1994;59:237-45.
52. Scheffner M, Kumar S. Mammalian HECT ubiquitin-protein ligases: biological and pathophysiological aspects. Biochim Biophys Acta 2014;1843(1):61-74.
53. Verdecia MA, Joazeiro CA, Wells NJ, Ferrer JL, Bowman ME, Hunter T, Noel JP. Conformational flexibility underlies ubiquitin ligation mediated by the WWP1 HECT domain E3 ligase. Mol Cell 2003;11(1):249-59.

54. Eisenhaber B, Chumak N, Eisenhaber F, Hauser MT. The ring between ring fingers (RBR) protein family. Genome Biol 2007;8(3):209.
55. Wenzel DM, Klevit RE. Following Ariadne's thread: a new perspective on RBR ubiquitin ligases. BMC Biol 2012;10:24.
56. Tan NG, Ardley HC, Scott GB, Rose SA, Markham AF, Robinson PA. Human homologue of ariadne promotes the ubiquitylation of translation initiation factor 4E homologous protein, 4EHP. FEBS Lett 2003;554(3):501-4.
57. Tokunaga F, Sakata S, Saeki Y, Satomi Y, Kirisako T, Kamei K, Nakagawa T, Kato M, Murata S, Yamaoka S and others. Involvement of linear polyubiquitylation of NEMO in NF-kappaB activation. Nat Cell Biol 2009;11(2):123-32.
58. Shimura H, Hattori N, Kubo S, Mizuno Y, Asakawa S, Minoshima S, Shimizu N, Iwai K, Chiba T, Tanaka K and others. Familial Parkinson disease gene product, parkin, is a ubiquitin-protein ligase. Nat Genet 2000;25(3):302-5.
59. Imai Y, Soda M, Inoue H, Hattori N, Mizuno Y, Takahashi R. An unfolded putative transmembrane polypeptide, which can lead to endoplasmic reticulum stress, is a substrate of Parkin. Cell 2001;105(7):891-902.
60. Ye Y, Rape M. Building ubiquitin chains: E2 enzymes at work. Nat Rev Mol Cell Biol 2009;10(11):755-64.
61. Koegl M, Hoppe T, Schlenker S, Ulrich HD, Mayer TU, Jentsch S. A novel ubiquitination factor, E4, is involved in multiubiquitin chain assembly. Cell 1999;96(5):635-44.
62. Matsumoto M, Yada M, Hatakeyama S, Ishimoto H, Tanimura T, Tsuji S, Kakizuka A, Kitagawa M, Nakayama KI. Molecular clearance of ataxin-3 is regulated by a mammalian E4. EMBO J 2004;23(3):659-69.
63. Imai Y, Soda M, Hatakeyama S, Akagi T, Hashikawa T, Nakayama KI, Takahashi R. CHIP is associated with Parkin, a gene responsible for familial Parkinson's disease, and enhances its ubiquitin ligase activity. Mol Cell 2002;10(1):55-67.
64. Grossman SR, Deato ME, Brignone C, Chan HM, Kung AL, Tagami H, Nakatani Y, Livingston DM. Polyubiquitination of p53 by a ubiquitin ligase activity of p300. Science 2003;300(5617):342-4.
65. Hurley JH, Lee S, Prag G. Ubiquitin-binding domains. Biochem J 2006;399(3):361-72.
66. Penengo L, Mapelli M, Murachelli AG, Confalonieri S, Magri L, Musacchio A, Di Fiore PP, Polo S, Schneider TR. Crystal structure of the ubiquitin binding domains of rabex-5 reveals two modes of interaction with ubiquitin. Cell 2006;124(6):1183-95.
67. Reyes-Turcu FE, Horton JR, Mullally JE, Heroux A, Cheng X, Wilkinson KD. The ubiquitin binding domain ZnF UBP recognizes the C-terminal diglycine motif of unanchored ubiquitin. Cell 2006;124(6):1197-208.
68. Sims JJ, Cohen RE. Linkage-specific avidity defines the lysine 63-linked polyubiquitin-binding preference of rap80. Mol Cell 2009;33(6):775-83.
69. Vucic D, Dixit VM, Wertz IE. Ubiquitylation in apoptosis: a post-translational modification at the edge of life and death. Nat Rev Mol Cell Biol 2011;12(7):439-52.
70. Reyes-Turcu FE, Ventii KH, Wilkinson KD. Regulation and cellular roles of ubiquitin-specific deubiquitinating enzymes. Annu Rev Biochem 2009;78:363-97.

71. Shih SC, Sloper-Mould KE, Hicke L. Monoubiquitin carries a novel internalization signal that is appended to activated receptors. EMBO J 2000;19(2):187-98.
72. Eletr ZM, Wilkinson KD. Regulation of proteolysis by human deubiquitinating enzymes. Biochim Biophys Acta 2014;1843(1):114-28.
73. Lin SC, Chung JY, Lamothe B, Rajashankar K, Lu M, Lo YC, Lam AY, Darnay BG, Wu H. Molecular basis for the unique deubiquitinating activity of the NF-kappaB inhibitor A20. J Mol Biol 2008;376(2):526-40.
74. Jacobson AD, Zhang NY, Xu P, Han KJ, Noone S, Peng J, Liu CW. The lysine 48 and lysine 63 ubiquitin conjugates are processed differently by the 26 s proteasome. J Biol Chem 2009;284(51):35485-94.
75. Xie Y, Varshavsky A. Physical association of ubiquitin ligases and the 26S proteasome. Proc Natl Acad Sci U S A 2000;97(6):2497-502.
76. Elsasser S, Finley D. Delivery of ubiquitinated substrates to protein-unfolding machines. Nat Cell Biol 2005;7(8):742-9.
77. Miller J, Gordon C. The regulation of proteasome degradation by multi-ubiquitin chain binding proteins. FEBS Lett 2005;579(15):3224-30.
78. Pion E, Narayan V, Eckert M, Ball KL. Role of the IRF-1 enhancer domain in signalling polyubiquitination and degradation. Cell Signal 2009;21(10):1479-87.
79. Verma R, Oania R, Graumann J, Deshaies RJ. Multiubiquitin chain receptors define a layer of substrate selectivity in the ubiquitin-proteasome system. Cell 2004;118(1):99-110.
80. Lauwers E, Jacob C, André B. K63-linked ubiquitin chains as a specific signal for protein sorting into the multivesicular body pathway. J Cell Biol 2009;185(3):493-502.
81. Kirkin V, Lamark T, Sou YS, Bjørkøy G, Nunn JL, Bruun JA, Shvets E, McEwan DG, Clausen TH, Wild P and others. A role for NBR1 in autophagosomal degradation of ubiquitinated substrates. Mol Cell 2009;33(4):505-16.
82. Bachmair A, Finley D, Varshavsky A. In vivo half-life of a protein is a function of its amino-terminal residue. Science 1986;234(4773):179-86.
83. Piatkov KI, Brower CS, Varshavsky A. The N-end rule pathway counteracts cell death by destroying proapoptotic protein fragments. Proc Natl Acad Sci U S A 2012;109(27):E1839-47.
84. Winston JT, Strack P, Beer-Romero P, Chu CY, Elledge SJ, Harper JW. The SCFbeta-TRCP-ubiquitin ligase complex associates specifically with phosphorylated destruction motifs in IkappaBalpha and beta-catenin and stimulates IkappaBalpha ubiquitination in vitro. Genes Dev 1999;13(3):270-83.
85. Ravid T, Hochstrasser M. Diversity of degradation signals in the ubiquitin-proteasome system. Nat Rev Mol Cell Biol 2008;9(9):679-90.
86. Rogers S, Wells R, Rechsteiner M. Amino acid sequences common to rapidly degraded proteins: the PEST hypothesis. Science 1986;234(4774):364-8.
87. Rechsteiner M, Rogers SW. PEST sequences and regulation by proteolysis. Trends Biochem Sci 1996;21(7):267-71.
88. Kravtsova-Ivantsiv Y, Ciechanover A. Non-canonical ubiquitin-based signals for proteasomal degradation. J Cell Sci 2012;125(Pt 3):539-48.
89. Hochstrasser M. Origin and function of ubiquitin-like proteins. Nature 2009;458(7237):422-9.

90. Fakharzadeh SS, Trusko SP, George DL. Tumorigenic potential associated with enhanced expression of a gene that is amplified in a mouse tumor cell line. EMBO J 1991;10(6):1565-9.
91. Michalovitz D, Halevy O, Oren M. Conditional inhibition of transformation and of cell proliferation by a temperature-sensitive mutant of p53. Cell 1990;62(4):671-80.
92. Hinds PW, Finlay CA, Quartin RS, Baker SJ, Fearon ER, Vogelstein B, Levine AJ. Mutant p53 DNA clones from human colon carcinomas cooperate with ras in transforming primary rat cells: a comparison of the "hot spot" mutant phenotypes. Cell Growth Differ 1990;1(12):571-80.
93. Oliner JD, Kinzler KW, Meltzer PS, George DL, Vogelstein B. Amplification of a gene encoding a p53-associated protein in human sarcomas. Nature 1992;358(6381):80-3.
94. Momand J, Zambetti GP, Olson DC, George D, Levine AJ. The mdm-2 oncogene product forms a complex with the p53 protein and inhibits p53-mediated transactivation. Cell 1992;69(7):1237-45.
95. Montes de Oca Luna R, Wagner DS, Lozano G. Rescue of early embryonic lethality in mdm2-deficient mice by deletion of p53. Nature 1995;378(6553):203-6.
96. Jones SN, Roe AE, Donehower LA, Bradley A. Rescue of embryonic lethality in Mdm2-deficient mice by absence of p53. Nature 1995;378(6553):206-8.
97. Fang S, Jensen JP, Ludwig RL, Vousden KH, Weissman AM. Mdm2 is a RING finger-dependent ubiquitin protein ligase for itself and p53. J Biol Chem 2000;275(12):8945-51.
98. Yin Y, Stephen CW, Luciani MG, Fåhraeus R. p53 Stability and activity is regulated by Mdm2-mediated induction of alternative p53 translation products. Nat Cell Biol 2002;4(6):462-7.
99. Wawrzynow B, Zylicz A, Wallace M, Hupp T, Zylicz M. MDM2 chaperones the p53 tumor suppressor. J Biol Chem 2007;282(45):32603-12.
100. Shvarts A, Steegenga WT, Riteco N, van Laar T, Dekker P, Bazuine M, van Ham RC, van der Houven van Oordt W, Hateboer G, van der Eb AJ and others. MDMX: a novel p53-binding protein with some functional properties of MDM2. EMBO J 1996;15(19):5349-57.
101. Shvarts A, Bazuine M, Dekker P, Ramos YF, Steegenga WT, Merckx G, van Ham RC, van der Houven van Oordt W, van der Eb AJ, Jochemsen AG. Isolation and identification of the human homolog of a new p53-binding protein, Mdmx. Genomics 1997;43(1):34-42.
102. Kawai H, Lopez-Pajares V, Kim MM, Wiederschain D, Yuan ZM. RING domain-mediated interaction is a requirement for MDM2's E3 ligase activity. Cancer Res 2007;67(13):6026-30.
103. Momand J, Jung D, Wilczynski S, Niland J. The MDM2 gene amplification database. Nucleic Acids Res 1998;26(15):3453-9.
104. Harris LC. MDM2 splice variants and their therapeutic implications. Curr Cancer Drug Targets 2005;5(1):21-6.
105. Wade M, Li YC, Wahl GM. MDM2, MDMX and p53 in oncogenesis and cancer therapy. Nat Rev Cancer 2013;13(2):83-96.
106. Lane DP, Cheok CF, Brown C, Madhumalar A, Ghadessy FJ, Verma C. Mdm2 and p53 are highly conserved from placozoans to man. Cell Cycle 2010;9(3):540-7.

107. Nicholson J, Hupp TR. The molecular dynamics of MDM2. Cell Cycle 2010;9(10):1878-81.
108. Chen J, Marechal V, Levine AJ. Mapping of the p53 and mdm-2 interaction domains. Mol Cell Biol 1993;13(7):4107-14.
109. Freedman DA, Epstein CB, Roth JC, Levine AJ. A genetic approach to mapping the p53 binding site in the MDM2 protein. Mol Med 1997;3(4):248-59.
110. Oliner JD, Pietenpol JA, Thiagalingam S, Gyuris J, Kinzler KW, Vogelstein B. Oncoprotein MDM2 conceals the activation domain of tumour suppressor p53. Nature 1993;362(6423):857-60.
111. Kussie PH, Gorina S, Marechal V, Elenbaas B, Moreau J, Levine AJ, Pavletich NP. Structure of the MDM2 oncoprotein bound to the p53 tumor suppressor transactivation domain. Science 1996;274(5289):948-53.
112. Thut CJ, Goodrich JA, Tjian R. Repression of p53-mediated transcription by MDM2: a dual mechanism. Genes Dev 1997;11(15):1974-86.
113. Shimizu H, Burch LR, Smith AJ, Dornan D, Wallace M, Ball KL, Hupp TR. The conformationally flexible S9-S10 linker region in the core domain of p53 contains a novel MDM2 binding site whose mutation increases ubiquitination of p53 in vivo. J Biol Chem 2002;277(32):28446-58.
114. Arva NC, Gopen TR, Talbott KE, Campbell LE, Chicas A, White DE, Bond GL, Levine AJ, Bargonetti J. A chromatin-associated and transcriptionally inactive p53-Mdm2 complex occurs in mdm2 SNP309 homozygous cells. J Biol Chem 2005;280(29):26776-87.
115. Worrall EG, Wawrzynow B, Worrall L, Walkinshaw M, Ball KL, Hupp TR. Regulation of the E3 ubiquitin ligase activity of MDM2 by an N-terminal pseudo-substrate motif. J Chem Biol 2009;2(3):113-29.
116. Wallace M, Worrall E, Pettersson S, Hupp TR, Ball KL. Dual-site regulation of MDM2 E3-ubiquitin ligase activity. Mol Cell 2006;23(2):251-63.
117. Schon O, Friedler A, Freund S, Fersht AR. Binding of p53-derived ligands to MDM2 induces a variety of long range conformational changes. J Mol Biol 2004;336(1):197-202.
118. McCoy MA, Gesell JJ, Senior MM, Wyss DF. Flexible lid to the p53-binding domain of human Mdm2: implications for p53 regulation. Proc Natl Acad Sci U S A 2003;100(4):1645-8.
119. Brzozowski AM, Derewenda U, Derewenda ZS, Dodson GG, Lawson DM, Turkenburg JP, Bjorkling F, Huge-Jensen B, Patkar SA, Thim L. A model for interfacial activation in lipases from the structure of a fungal lipase-inhibitor complex. Nature 1991;351(6326):491-4.
120. Worrall EG, Worrall L, Blackburn E, Walkinshaw M, Hupp TR. The effects of phosphomimetic lid mutation on the thermostability of the N-terminal domain of MDM2. J Mol Biol 2010;398(3):414-28.
121. Palmero I, Pantoja C, Serrano M. p19ARF links the tumour suppressor p53 to Ras. Nature 1998;395(6698):125-6.
122. Zindy F, Eischen CM, Randle DH, Kamijo T, Cleveland JL, Sherr CJ, Roussel MF. Myc signaling via the ARF tumor suppressor regulates p53-dependent apoptosis and immortalization. Genes Dev 1998;12(15):2424-33.
123. Weber JD, Kuo ML, Bothner B, DiGiammarino EL, Kriwacki RW, Roussel MF, Sherr CJ. Cooperative signals governing ARF-mdm2 interaction and nucleolar localization of the complex. Mol Cell Biol 2000;20(7):2517-28.

124. Ma J, Martin JD, Zhang H, Auger KR, Ho TF, Kirkpatrick RB, Grooms MH, Johanson KO, Tummino PJ, Copeland RA and others. A second p53 binding site in the central domain of Mdm2 is essential for p53 ubiquitination. Biochemistry 2006;45(30):9238-45.
125. Falquet L, Pagni M, Bucher P, Hulo N, Sigrist CJ, Hofmann K, Bairoch A. The PROSITE database, its status in 2002. Nucleic Acids Res 2002;30(1):235-8.
126. Yu GW, Allen MD, Andreeva A, Fersht AR, Bycroft M. Solution structure of the C4 zinc finger domain of HDM2. Protein Sci 2006;15(2):384-9.
127. Schlott T, Reimer S, Jahns A, Ohlenbusch A, Ruschenburg I, Nagel H, Droese M. Point mutations and nucleotide insertions in the MDM2 zinc finger structure of human tumours. J Pathol 1997;182(1):54-61.
128. Lindström MS, Jin A, Deisenroth C, White Wolf G, Zhang Y. Cancer-associated mutations in the MDM2 zinc finger domain disrupt ribosomal protein interaction and attenuate MDM2-induced p53 degradation. Mol Cell Biol 2007;27(3):1056-68.
129. Lai Z, Freedman DA, Levine AJ, McLendon GL. Metal and RNA binding properties of the hdm2 RING finger domain. Biochemistry 1998;37(48):17005-15.
130. Kostic M, Matt T, Martinez-Yamout MA, Dyson HJ, Wright PE. Solution structure of the Hdm2 C2H2C4 RING, a domain critical for ubiquitination of p53. J Mol Biol 2006;363(2):433-50.
131. Honda R, Tanaka H, Yasuda H. Oncoprotein MDM2 is a ubiquitin ligase E3 for tumor suppressor p53. FEBS Lett 1997;420(1):25-7.
132. Honda R, Yasuda H. Activity of MDM2, a ubiquitin ligase, toward p53 or itself is dependent on the RING finger domain of the ligase. Oncogene 2000;19(11):1473-6.
133. Uldrijan S, Pannekoek WJ, Vousden KH. An essential function of the extreme C-terminus of MDM2 can be provided by MDMX. EMBO J 2007;26(1):102-12.
134. Elenbaas B, Dobbelstein M, Roth J, Shenk T, Levine AJ. The MDM2 oncoprotein binds specifically to RNA through its RING finger domain. Mol Med 1996;2(4):439-51.
135. Lohrum MA, Ashcroft M, Kubbutat MH, Vousden KH. Identification of a cryptic nucleolar-localization signal in MDM2. Nat Cell Biol 2000;2(3):179-81.
136. Poyurovsky MV, Jacq X, Ma C, Karni-Schmidt O, Parker PJ, Chalfie M, Manley JL, Prives C. Nucleotide binding by the Mdm2 RING domain facilitates Arf-independent Mdm2 nucleolar localization. Mol Cell 2003;12(4):875-87.
137. Linke K, Mace PD, Smith CA, Vaux DL, Silke J, Day CL. Structure of the MDM2/MDMX RING domain heterodimer reveals dimerization is required for their ubiquitylation in trans. Cell Death Differ 2008;15(5):841-8.
138. Wawrzynow B, Pettersson S, Zylicz A, Bramham J, Worrall E, Hupp TR, Ball KL. A function for the RING finger domain in the allosteric control of MDM2 conformation and activity. J Biol Chem 2009;284(17):11517-30.
139. Boddy MN, Freemont PS, Borden KL. The p53-associated protein MDM2 contains a newly characterized zinc-binding domain called the RING finger. Trends Biochem Sci 1994;19(5):198-9.

140. Tanimura S, Ohtsuka S, Mitsui K, Shirouzu K, Yoshimura A, Ohtsubo M. MDM2 interacts with MDMX through their RING finger domains. FEBS Lett 1999;447(1):5-9.
141. Poyurovsky MV, Priest C, Kentsis A, Borden KL, Pan ZQ, Pavletich N, Prives C. The Mdm2 RING domain C-terminus is required for supramolecular assembly and ubiquitin ligase activity. EMBO J 2007;26(1):90-101.
142. Kentsis A, Gordon RE, Borden KL. Control of biochemical reactions through supramolecular RING domain self-assembly. Proc Natl Acad Sci U S A 2002;99(24):15404-9.
143. Nikolay R, Wiederkehr T, Rist W, Kramer G, Mayer MP, Bukau B. Dimerization of the human E3 ligase CHIP via a coiled-coil domain is essential for its activity. J Biol Chem 2004;279(4):2673-8.
144. Vander Kooi CW, Ohi MD, Rosenberg JA, Oldham ML, Newcomer ME, Gould KL, Chazin WJ. The Prp19 U-box crystal structure suggests a common dimeric architecture for a class of oligomeric E3 ubiquitin ligases. Biochemistry 2006;45(1):121-30.
145. Shadfan M, Lopez-Pajares V, Yuan ZM. MDM2 and MDMX: Alone and together in regulation of p53. Transl Cancer Res 2012;1(2):88-89.
146. Linzer DI, Levine AJ. Characterization of a 54K dalton cellular SV40 tumor antigen present in SV40-transformed cells and uninfected embryonal carcinoma cells. Cell 1979;17(1):43-52.
147. Eliyahu D, Raz A, Gruss P, Givol D, Oren M. Participation of p53 cellular tumour antigen in transformation of normal embryonic cells. Nature 1984;312(5995):646-9.
148. Pavletich NP, Chambers KA, Pabo CO. The DNA-binding domain of p53 contains the four conserved regions and the major mutation hot spots. Genes Dev 1993;7(12B):2556-64.
149. Stürzbecher HW, Brain R, Addison C, Rudge K, Remm M, Grimaldi M, Keenan E, Jenkins JR. A C-terminal alpha-helix plus basic region motif is the major structural determinant of p53 tetramerization. Oncogene 1992;7(8):1513-23.
150. Davison TS, Yin P, Nie E, Kay C, Arrowsmith CH. Characterization of the oligomerization defects of two p53 mutants found in families with Li-Fraumeni and Li-Fraumeni-like syndrome. Oncogene 1998;17(5):651-6.
151. Ribeiro RC, Sandrini F, Figueiredo B, Zambetti GP, Michalkiewicz E, Lafferty AR, DeLacerda L, Rabin M, Cadwell C, Sampaio G and others. An inherited p53 mutation that contributes in a tissue-specific manner to pediatric adrenal cortical carcinoma. Proc Natl Acad Sci U S A 2001;98(16):9330-5.
152. Vogelstein B, Lane D, Levine AJ. Surfing the p53 network. Nature 2000;408(6810):307-10.
153. Oren M. Decision making by p53: life, death and cancer. Cell Death Differ 2003;10(4):431-42.
154. Appella E, Anderson CW. Post-translational modifications and activation of p53 by genotoxic stresses. Eur J Biochem 2001;268(10):2764-72.
155. DiGiammarino EL, Lee AS, Cadwell C, Zhang W, Bothner B, Ribeiro RC, Zambetti G, Kriwacki RW. A novel mechanism of tumorigenesis involving pH-dependent destabilization of a mutant p53 tetramer. Nat Struct Biol 2002;9(1):12-6.
156. Harris SL, Levine AJ. The p53 pathway: positive and negative feedback loops. Oncogene 2005;24(17):2899-908.

157. Bates S, Phillips AC, Clark PA, Stott F, Peters G, Ludwig RL, Vousden KH. p14ARF links the tumour suppressors RB and p53. Nature 1998;395(6698):124-5.
158. Komarova EA, Diatchenko L, Rokhlin OW, Hill JE, Wang ZJ, Krivokrysenko VI, Feinstein E, Gudkov AV. Stress-induced secretion of growth inhibitors: a novel tumor suppressor function of p53. Oncogene 1998;17(9):1089-96.
159. Vousden KH, Lu X. Live or let die: the cell's response to p53. Nat Rev Cancer 2002;2(8):594-604.
160. Yew PR, Liu X, Berk AJ. Adenovirus E1B oncoprotein tethers a transcriptional repression domain to p53. Genes Dev 1994;8(2):190-202.
161. Weintraub SJ, Chow KN, Luo RX, Zhang SH, He S, Dean DC. Mechanism of active transcriptional repression by the retinoblastoma protein. Nature 1995;375(6534):812-5.
162. Venot C, Maratrat M, Sierra V, Conseiller E, Debussche L. Definition of a p53 transactivation function-deficient mutant and characterization of two independent p53 transactivation subdomains. Oncogene 1999;18(14):2405-10.
163. Maier B, Gluba W, Bernier B, Turner T, Mohammad K, Guise T, Sutherland A, Thorner M, Scrable H. Modulation of mammalian life span by the short isoform of p53. Genes Dev 2004;18(3):306-19.
164. Candeias MM, Powell DJ, Roubalova E, Apcher S, Bourougaa K, Vojtesek B, Bruzzoni-Giovanelli H, Fåhraeus R. Expression of p53 and p53/47 are controlled by alternative mechanisms of messenger RNA translation initiation. Oncogene 2006;25(52):6936-47.
165. Hartl FU, Hayer-Hartl M. Molecular chaperones in the cytosol: from nascent chain to folded protein. Science 2002;295(5561):1852-8.
166. Ongkeko WM, Wang XQ, Siu WY, Lau AW, Yamashita K, Harris AL, Cox LS, Poon RY. MDM2 and MDMX bind and stabilize the p53-related protein p73. Curr Biol 1999;9(15):829-32.
167. Asahara H, Li Y, Fuss J, Haines DS, Vlatkovic N, Boyd MT, Linn S. Stimulation of human DNA polymerase epsilon by MDM2. Nucleic Acids Res 2003;31(9):2451-9.
168. Marechal V, Elenbaas B, Piette J, Nicolas JC, Levine AJ. The ribosomal L5 protein is associated with mdm-2 and mdm-2-p53 complexes. Mol Cell Biol 1994;14(11):7414-20.
169. White DE, Talbott KE, Arva NC, Bargonetti J. Mouse double minute 2 associates with chromatin in the presence of p53 and is released to facilitate activation of transcription. Cancer Res 2006;66(7):3463-70.
170. Lai Z, Ferry KV, Diamond MA, Wee KE, Kim YB, Ma J, Yang T, Benfield PA, Copeland RA, Auger KR. Human mdm2 mediates multiple mono-ubiquitination of p53 by a mechanism requiring enzyme isomerization. J Biol Chem 2001;276(33):31357-67.
171. Hinds PW, Mittnacht S, Dulic V, Arnold A, Reed SI, Weinberg RA. Regulation of retinoblastoma protein functions by ectopic expression of human cyclins. Cell 1992;70(6):993-1006.
172. Zhu JW, DeRyckere D, Li FX, Wan YY, DeGregori J. A role for E2F1 in the induction of ARF, p53, and apoptosis during thymic negative selection. Cell Growth Differ 1999;10(12):829-38.
173. Damalas A, Kahan S, Shtutman M, Ben-Ze'ev A, Oren M. Deregulated beta-catenin induces a p53- and ARF-dependent growth arrest and cooperates with Ras in transformation. EMBO J 2001;20(17):4912-22.

174. Fiucci G, Beaucourt S, Duflaut D, Lespagnol A, Stumptner-Cuvelette P, Géant A, Buchwalter G, Tuynder M, Susini L, Lassalle JM and others. Siah-1b is a direct transcriptional target of p53: identification of the functional p53 responsive element in the siah-1b promoter. Proc Natl Acad Sci U S A 2004;101(10):3510-5.
175. Matsuzawa SI, Reed JC. Siah-1, SIP, and Ebi collaborate in a novel pathway for beta-catenin degradation linked to p53 responses. Mol Cell 2001;7(5):915-26.
176. Okamoto K, Beach D. Cyclin G is a transcriptional target of the p53 tumor suppressor protein. EMBO J 1994;13(20):4816-22.
177. Bates S, Rowan S, Vousden KH. Characterisation of human cyclin G1 and G2: DNA damage inducible genes. Oncogene 1996;13(5):1103-9.
178. Yardley G, Zauberman A, Oren M, Jackson P. Individual promoter and intron p53-binding motifs from the rat Cyclin G1 promoter region support transcriptional activation by p53 but do not show co-operative activation. FEBS Lett 1998;430(3):171-5.
179. Okamoto K, Li H, Jensen MR, Zhang T, Taya Y, Thorgeirsson SS, Prives C. Cyclin G recruits PP2A to dephosphorylate Mdm2. Mol Cell 2002;9(4):761-71.
180. Weinburg RA. the biology of CANCER. United States of America: Garland Science, Taylor & Francis Group, LLC.; 2007. 796 p.
181. Momand J, Wu HH, Dasgupta G. MDM2--master regulator of the p53 tumor suppressor protein. Gene 2000;242(1-2):15-29.
182. Böttger V, Böttger A, Garcia-Echeverria C, Ramos YF, van der Eb AJ, Jochemsen AG, Lane DP. Comparative study of the p53-mdm2 and p53-MDMX interfaces. Oncogene 1999;18(1):189-99.
183. Jackson MW, Berberich SJ. MdmX protects p53 from Mdm2-mediated degradation. Mol Cell Biol 2000;20(3):1001-7.
184. Gu J, Kawai H, Nie L, Kitao H, Wiederschain D, Jochemsen AG, Parant J, Lozano G, Yuan ZM. Mutual dependence of MDM2 and MDMX in their functional inactivation of p53. J Biol Chem 2002;277(22):19251-4.
185. Sharp DA, Kratowicz SA, Sank MJ, George DL. Stabilization of the MDM2 oncoprotein by interaction with the structurally related MDMX protein. J Biol Chem 1999;274(53):38189-96.
186. de Graaf P, Little NA, Ramos YF, Meulmeester E, Letteboer SJ, Jochemsen AG. Hdmx protein stability is regulated by the ubiquitin ligase activity of Mdm2. J Biol Chem 2003;278(40):38315-24.
187. Danovi D, Meulmeester E, Pasini D, Migliorini D, Capra M, Frenk R, de Graaf P, Francoz S, Gasparini P, Gobbi A and others. Amplification of Mdmx (or Mdm4) directly contributes to tumor formation by inhibiting p53 tumor suppressor activity. Mol Cell Biol 2004;24(13):5835-43.
188. Zak K, Pecak A, Rys B, Wladyka B, Dömling A, Weber L, Holak TA, Dubin G. Mdm2 and MdmX inhibitors for the treatment of cancer: a patent review (2011-present). Expert Opin Ther Pat 2013;23(4):425-48.
189. Lehman JA, Mayo LD. Integration of DNA damage and repair with murine double-minute 2 (mdm2) in tumorigenesis. Int J Mol Sci 2012;13(12):16373-86.
190. David SS, O'Shea VL, Kundu S. Base-excision repair of oxidative DNA damage. Nature 2007;447(7147):941-50.

191. Xanthoudakis S, Smeyne RJ, Wallace JD, Curran T. The redox/DNA repair protein, Ref-1, is essential for early embryonic development in mice. Proc Natl Acad Sci U S A 1996;93(17):8919-23.
192. Fung H, Demple B. A vital role for Ape1/Ref1 protein in repairing spontaneous DNA damage in human cells. Mol Cell 2005;17(3):463-70.
193. Izumi T, Brown DB, Naidu CV, Bhakat KK, Macinnes MA, Saito H, Chen DJ, Mitra S. Two essential but distinct functions of the mammalian abasic endonuclease. Proc Natl Acad Sci U S A 2005;102(16):5739-43.
194. Busso CS, Iwakuma T, Izumi T. Ubiquitination of mammalian AP endonuclease (APE1) regulated by the p53-MDM2 signaling pathway. Oncogene 2009;28(13):1616-25.
195. Alt JR, Bouska A, Fernandez MR, Cerny RL, Xiao H, Eischen CM. Mdm2 binds to Nbs1 at sites of DNA damage and regulates double strand break repair. J Biol Chem 2005;280(19):18771-81.
196. Bouska A, Lushnikova T, Plaza S, Eischen CM. Mdm2 promotes genetic instability and transformation independent of p53. Mol Cell Biol 2008;28(15):4862-74.
197. Nouspikel T. DNA repair in mammalian cells : Nucleotide excision repair: variations on versatility. Cell Mol Life Sci 2009;66(6):994-1009.
198. Sugasawa K, Ng JM, Masutani C, Iwai S, van der Spek PJ, Eker AP, Hanaoka F, Bootsma D, Hoeijmakers JH. Xeroderma pigmentosum group C protein complex is the initiator of global genome nucleotide excision repair. Mol Cell 1998;2(2):223-32.
199. Wang QE, Zhu Q, Wani G, El-Mahdy MA, Li J, Wani AA. DNA repair factor XPC is modified by SUMO-1 and ubiquitin following UV irradiation. Nucleic Acids Res 2005;33(13):4023-34.
200. Kamijo T, Weber JD, Zambetti G, Zindy F, Roussel MF, Sherr CJ. Functional and physical interactions of the ARF tumor suppressor with p53 and Mdm2. Proc Natl Acad Sci U S A 1998;95(14):8292-7.
201. Pomerantz J, Schreiber-Agus N, Liégeois NJ, Silverman A, Alland L, Chin L, Potes J, Chen K, Orlow I, Lee HW and others. The Ink4a tumor suppressor gene product, p19Arf, interacts with MDM2 and neutralizes MDM2's inhibition of p53. Cell 1998;92(6):713-23.
202. Zhang Y, Xiong Y, Yarbrough WG. ARF promotes MDM2 degradation and stabilizes p53: ARF-INK4a locus deletion impairs both the Rb and p53 tumor suppression pathways. Cell 1998;92(6):725-34.
203. Stoyanova T, Roy N, Kopanja D, Raychaudhuri P, Bagchi S. DDB2 (damaged-DNA binding protein 2) in nucleotide excision repair and DNA damage response. Cell Cycle 2009;8(24):4067-71.
204. Stoyanova T, Roy N, Kopanja D, Bagchi S, Raychaudhuri P. DDB2 decides cell fate following DNA damage. Proc Natl Acad Sci U S A 2009;106(26):10690-5.
205. Lieber MR. The mechanism of double-strand DNA break repair by the nonhomologous DNA end-joining pathway. Annu Rev Biochem 2010;79:181-211.
206. Gama V, Gomez JA, Mayo LD, Jackson MW, Danielpour D, Song K, Haas AL, Laughlin MJ, Matsuyama S. Hdm2 is a ubiquitin ligase of Ku70-Akt promotes cell survival by inhibiting Hdm2-dependent Ku70 destabilization. Cell Death Differ 2009;16(5):758-69.

207. Ganguli G, Wasylyk B. p53-independent functions of MDM2. Mol Cancer Res 2003;1(14):1027-35.
208. Vlatkovic N, Guerrera S, Li Y, Linn S, Haines DS, Boyd MT. MDM2 interacts with the C-terminus of the catalytic subunit of DNA polymerase epsilon. Nucleic Acids Res 2000;28(18):3581-6.
209. Dai MS, Lu H. Inhibition of MDM2-mediated p53 ubiquitination and degradation by ribosomal protein L5. J Biol Chem 2004;279(43):44475-82.
210. Dai MS, Zeng SX, Jin Y, Sun XX, David L, Lu H. Ribosomal protein L23 activates p53 by inhibiting MDM2 function in response to ribosomal perturbation but not to translation inhibition. Mol Cell Biol 2004;24(17):7654-68.
211. Zhang Y, Wolf GW, Bhat K, Jin A, Allio T, Burkhart WA, Xiong Y. Ribosomal protein L11 negatively regulates oncoprotein MDM2 and mediates a p53-dependent ribosomal-stress checkpoint pathway. Mol Cell Biol 2003;23(23):8902-12.
212. Zhang Z, Zhang R. p53-independent activities of MDM2 and their relevance to cancer therapy. Curr Cancer Drug Targets 2005;5(1):9-20.
213. Gu L, Findley HW, Zhou M. MDM2 induces NF-kappaB/p65 expression transcriptionally through Sp1-binding sites: a novel, p53-independent role of MDM2 in doxorubicin resistance in acute lymphoblastic leukemia. Blood 2002;99(9):3367-75.
214. Lu ML, Wikman F, Orntoft TF, Charytonowicz E, Rabbani F, Zhang Z, Dalbagni G, Pohar KS, Yu G, Cordon-Cardo C. Impact of alterations affecting the p53 pathway in bladder cancer on clinical outcome, assessed by conventional and array-based methods. Clin Cancer Res 2002;8(1):171-9.
215. Boyd MT, Vlatkovic N, Haines DS. A novel cellular protein (MTBP) binds to MDM2 and induces a G1 arrest that is suppressed by MDM2. J Biol Chem 2000;275(41):31883-90.
216. Iwakuma T, Agarwal N. MDM2 binding protein, a novel metastasis suppressor. Cancer Metastasis Rev 2012;31(3-4):633-40.
217. Scheffner M, Huibregtse JM, Howley PM. Identification of a human ubiquitin-conjugating enzyme that mediates the E6-AP-dependent ubiquitination of p53. Proc Natl Acad Sci U S A 1994;91(19):8797-801.
218. Jensen JP, Bates PW, Yang M, Vierstra RD, Weissman AM. Identification of a family of closely related human ubiquitin conjugating enzymes. J Biol Chem 1995;270(51):30408-14.
219. Jentsch S. The ubiquitin-conjugation system. Annu Rev Genet 1992;26:179-207.
220. Plechanovová A, Jaffray EG, McMahon SA, Johnson KA, Navrátilová I, Naismith JH, Hay RT. Mechanism of ubiquitylation by dimeric RING ligase RNF4. Nat Struct Mol Biol 2011;18(9):1052-9.
221. Maya R, Balass M, Kim ST, Shkedy D, Leal JF, Shifman O, Moas M, Buschmann T, Ronai Z, Shiloh Y and others. ATM-dependent phosphorylation of Mdm2 on serine 395: role in p53 activation by DNA damage. Genes Dev 2001;15(9):1067-77.
222. Huang H, Ceccarelli DF, Orlicky S, St-Cyr DJ, Ziemba A, Garg P, Plamondon S, Auer M, Sidhu S, Marinier A and others. E2 enzyme inhibition by stabilization of a low-affinity interface with ubiquitin. Nat Chem Biol 2014;10(2):156-63.

223. Mace PD, Linke K, Feltham R, Schumacher FR, Smith CA, Vaux DL, Silke J, Day CL. Structures of the cIAP2 RING domain reveal conformational changes associated with ubiquitin-conjugating enzyme (E2) recruitment. J Biol Chem 2008;283(46):31633-40.
224. Bentley ML, Corn JE, Dong KC, Phung Q, Cheung TK, Cochran AG. Recognition of UbcH5c and the nucleosome by the Bmi1/Ring1b ubiquitin ligase complex. EMBO J 2011;30(16):3285-97.
225. Jahn SC, Law ME, Corsino PE, Rowe TC, Davis BJ, Law BK. Assembly, activation, and substrate specificity of cyclin D1/Cdk2 complexes. Biochemistry 2013;52(20):3489-501.
226. Eger S, Castrec B, Hübscher U, Scheffner M, Rubini M, Marx A. Generation of a mono-ubiquitinated PCNA mimic by click chemistry. Chembiochem 2011;12(18):2807-12.
227. Yin Q, Lin SC, Lamothe B, Lu M, Lo YC, Hura G, Zheng L, Rich RL, Campos AD, Myszka DG and others. E2 interaction and dimerization in the crystal structure of TRAF6. Nat Struct Mol Biol 2009;16(6):658-66.
228. Pruneda JN, Littlefield PJ, Soss SE, Nordquist KA, Chazin WJ, Brzovic PS, Klevit RE. Structure of an E3:E2~Ub complex reveals an allosteric mechanism shared among RING/U-box ligases. Mol Cell 2012;47(6):933-42.
229. Jaswal SS. Biological insights from hydrogen exchange mass spectrometry. Biochim Biophys Acta 2013;1834(6):1188-201.
230. Miranker A, Robinson CV, Radford SE, Dobson CM. Investigation of protein folding by mass spectrometry. FASEB J 1996;10(1):93-101.
231. Landgraf RR, Chalmers MJ, Griffin PR. Automated hydrogen/deuterium exchange electron transfer dissociation high resolution mass spectrometry measured at single-amide resolution. J Am Soc Mass Spectrom 2012;23(2):301-9.
232. Percy AJ, Rey M, Burns KM, Schriemer DC. Probing protein interactions with hydrogen/deuterium exchange and mass spectrometry-a review. Anal Chim Acta 2012;721:7-21.
233. Fontana A, de Laureto PP, Spolaore B, Frare E, Picotti P, Zambonin M. Probing protein structure by limited proteolysis. Acta Biochim Pol 2004;51(2):299-321.
234. Brockerhoff SE, Edmonds CG, Davis TN. Structural analysis of wild-type and mutant yeast calmodulins by limited proteolysis and electrospray ionization mass spectrometry. Protein Sci 1992;1(4):504-16.
235. Coburger I, Dahms SO, Roeser D, Gührs KH, Hortschansky P, Than ME. Analysis of the overall structure of the multi-domain amyloid precursor protein (APP). PLoS One 2013;8(12):e81926.
236. Wilson C, Ramai D, Serjanov D, Lama N, Levinger L, Chang EJ. Tethered domains and flexible regions in tRNase Z(L), the long form of tRNase Z. PLoS One 2013;8(7):e66942.
237. Smith GP. Filamentous fusion phage: novel expression vectors that display cloned antigens on the virion surface. Science 1985;228(4705):1315-7.
238. Cwirla SE, Peters EA, Barrett RW, Dower WJ. Peptides on phage: a vast library of peptides for identifying ligands. Proc Natl Acad Sci U S A 1990;87(16):6378-82.
239. Devlin JJ, Panganiban LC, Devlin PE. Random peptide libraries: a source of specific protein binding molecules. Science 1990;249(4967):404-6.

240. Scott JK, Smith GP. Searching for peptide ligands with an epitope library. Science 1990;249(4967):386-90.
241. Rodi DJ, Janes RW, Sanganee HJ, Holton RA, Wallace BA, Makowski L. Screening of a library of phage-displayed peptides identifies human bcl-2 as a taxol-binding protein. J Mol Biol 1999;285(1):197-203.
242. Neduva V, Russell RB. Linear motifs: evolutionary interaction switches. FEBS Lett 2005;579(15):3342-5.
243. Scognamiglio PL, Di Natale C, Perretta G, Marasco D. From peptides to small molecules: an intriguing but intricated way to new drugs. Curr Med Chem 2013;20(31):3803-17.
244. Tang L, Dong C, Ren J. Highly sensitive homogenous immunoassay of cancer biomarker using silver nanoparticles enhanced fluorescence correlation spectroscopy. Talanta 2010;81(4-5):1560-7.
245. Faulds K, Jarvis R, Smith WE, Graham D, Goodacre R. Multiplexed detection of six labelled oligonucleotides using surface enhanced resonance Raman scattering (SERRS). Analyst 2008;133(11):1505-12.
246. Rohr TE, Cotton T, Fan N, Tarcha PJ. Immunoassay employing surface-enhanced Raman spectroscopy. Anal Biochem 1989;182(2):388-98.
247. Campbell FM, Ingram A, Monaghan P, Cooper J, Sattar N, Eckersall PD, Graham D. SERRS immunoassay for quantitative human CRP analysis. Analyst 2008;133(10):1355-7.
248. Douglas P, Stokes RJ, Graham D, Smith WE. Immunoassay for P38 MAPK using surface enhanced resonance Raman spectroscopy (SERRS). Analyst 2008;133(6):791-6.
249. Robson AF, Hupp TR, Lickiss F, Ball KL, Faulds K, Graham D. Nanosensing protein allostery using a bivalent mouse double minute two (MDM2) assay. Proc Natl Acad Sci U S A 2012;109(21):8073-8.
250. Gell DA, Grant RP, Mackay JP. The Detection and Quantitation of Protein Oligermerization. 2012.
251. Tarazona MP, Saiz E. Combination of SEC/MALS experimental procedures and theoretical analysis for studying the solution properties of macromolecules. J Biochem Biophys Methods 2003;56(1-3):95-116.
252. Cheng Q, Cross B, Li B, Chen L, Li Z, Chen J. Regulation of MDM2 E3 ligase activity by phosphorylation after DNA damage. Mol Cell Biol 2011;31(24):4951-63.
253. Poyurovsky MV, Priest C, Kentsis A, Borden KL, Pan ZQ, Pavletich N, Prives C. The Mdm2 RING domain C-terminus is required for supramolecular assembly and ubiquitin ligase activity. EMBO J 2007;26(1):90-101.
254. Bartosík M, Ostatná V, Palecek E. Electrochemistry of riboflavin-binding protein and its interaction with riboflavin. Bioelectrochemistry 2009;76(1-2):70-5.
255. Higashitsuji H, Itoh K, Sakurai T, Nagao T, Sumitomo Y, Sumitomo H, Masuda T, Dawson S, Shimada Y, Mayer RJ and others. The oncoprotein gankyrin binds to MDM2/HDM2, enhancing ubiquitylation and degradation of p53. Cancer Cell 2005;8(1):75-87.
256. Dawson S, Higashitsuji H, Wilkinson AJ, Fujita J, Mayer RJ. Gankyrin: a new oncoprotein and regulator of pRb and p53. Trends Cell Biol 2006;16(5):229-33.
257. Dawson S, Apcher S, Mee M, Higashitsuji H, Baker R, Uhle S, Dubiel W, Fujita J, Mayer RJ. Gankyrin is an ankyrin-repeat oncoprotein that interacts

with CDK4 kinase and the S6 ATPase of the 26 S proteasome. J Biol Chem 2002;277(13):10893-902.

Chapter 9: APPENDICIES

9.1 **Appendix I –** Mass spectrometry data

9.2 **Appendix 1I –** HD exchange peptide data

9.3 **Appendix III -** Nanosensing protein allostery using a bivalent mouse double minute (MDM2) assay

9.1 Appendix I

Sequence	# PSMs	# Proteins	# Protein Groups	Protein Group Accessions	Modifications	MH+ [Da]	1_NoPEP_0min*	XCorr 1_NoPEP_0min	1_NoPEP_5min*	XCorr 1_NoPEP_5min	1_NoPEP_10min*	XCorr 1_NoPEP_10min	1_NoPEP_15min*	XCorr 1_NoPEP_15min	1_NoPEP_30min*	XCorr 1_NoPEP_30min	1_PEP_0min*	XCorr 1_PEP_0min	1_PEP_5min*	Xcorr 1_PEP_5min	1_PEP_10min*	XCorr 1_PEP_10min	1_PEP_15min*	Xcorr 1_PEP_15min
GSSHHHHHHSSGLVPR	1554	1	1	1193890404		1768.850207	**High**	**4.66**	**High**	**5.01**	**High**	**5.02**	**High**	**5.03**	**High**	**4.87**	**High**	**5.13**	**High**	**4.55**	**High**	**5.13**	**High**	**5.04**
VLLSICSLLCDPNPDDPLVPDIAQIYK	65	1	1	1193890404		2954.527001	**High**	**4.56**	**Medium**	**2.59**	**High**	**4.68**	**High**	**5.19**	**High**	**4.99**	**High**	**4.39**	**High**	**4.28**	**High**	**4.72**	**High**	**5.35**
IYHPNINSNGSICLDILR	55	1	1	1193890404		2042.049977	**High**	**4.14**	**High**	**2.96**	**High**	**3.18**	**High**	**3.51**	**High**	**3.92**	**High**	**3.59**	**High**	**2.05**	**Medium**	**2.20**	**High**	**3.63**
SAYQGGVFFLTVHFPTDYPFKPPK	36	1	1	1193890404		2743.393936	**High**	**3.55**	**High**	**3.37**	**High**	**3.85**	**High**	**2.77**	**High**	**3.16**	**High**	**3.15**	**High**	**3.64**	**Medium**	**2.22**	**High**	**3.60**
SQWSPALTVSK	665	1	1	1193890404		1203.637999	**High**	**3.46**	**High**	**3.44**	**High**	**3.59**	**High**	**3.56**	**High**	**3.47**	**High**	**3.77**	**High**	**3.63**	**High**	**3.55**	**High**	**3.61**
IYHPNINSNGSICLDILRSQWSPALTVSK	30	1	1	1193890404		3226.666977	**High**	**3.30**	**High**	**3.67**	**High**	**4.82**	**High**	**3.75**	**High**	**4.13**	**High**	**3.42**	**High**	**2.93**	**High**	**3.58**	**High**	**4.35**
GSHMALKRIQK	40	1	1	1193890404		1268.726377	**High**	**3.09**	**High**	**2.81**	**Low**	**1.02**	**Low**	**1.10**	**High**	**3.29**	**High**	**2.75**	**High**	**3.46**	**High**	**2.71**	**High**	**3.41**
DPLVPDIAQIYK	43	1	1	1193890404		1371.751888	**High**	**2.85**	**Medium**	**1.40**	**Low**	**0.69**	**Medium**	**1.88**	**Medium**	**1.57**	**Medium**	**1.01**	**High**	**2.12**	**Medium**	**1.78**	**High**	**2.31**
ELSDLQR	593	1	1	1193890404		860.44719	**High**	**2.64**	**High**	**2.13**	**Medium**	**1.96**	**High**	**2.25**	**High**	**2.52**	**High**	**2.40**	**High**	**2.41**	**High**	**2.40**	**High**	**2.28**
GSHMALKR	314	1	1	1193890404		899.488151	**High**	**2.44**	**High**	**2.19**	**High**	**2.31**	**High**	**2.40**	**High**	**2.15**	**High**	**2.38**	**High**	**2.06**	**High**	**2.33**	**High**	**2.32**

GSSHHHHHHSSGLVPRGSHMALK	69	1	1	11938904		2493.22043	**Medium**	**2.05**	**Low**	**0.52**	**High**	**3.35**	**High**	**3.72**	**High**	**3.27**	**High**	**3.66**	**High**	**3.66**	**Medium**	**1.89**	**High**	**3.06**
EWTQKYAM	11	1	1	11938904		1056.48259	**High**	**2.01**	**High**	**2.34**	**High**	**2.13**	**High**	**2.17**	**High**	**2.41**	**High**	**2.21**	**High**	**2.41**	**High**	**2.23**	**High**	**2.27**
GSSHHHHHHSSGLVPRGSHMALKR	14	1	1	11938904		2649.31623	**Medium**	**1.43**	**Medium**	**2.00**	**Low**	**1.22**	**High**	**3.62**			**Low**	**0.33**	**Medium**	**2.82**	**Medium**	**2.08**	**Medium**	**2.86**
YNRHAR	47	1	1	11938904		816.42229	**Medium**	**1.39**	**Medium**	**1.77**	**Medium**	**1.26**	**Low**	**0.75**	**Medium**	**1.18**	**Medium**	**1.35**	**Medium**	**1.04**	**Medium**	**1.30**	**Medium**	**1.31**
YPFKPPK	16	1	1	11938904		876.49791	**Medium**	**1.35**	**Medium**	**1.62**	**Medium**	**1.94**	**Medium**	**1.28**	**Medium**	**1.82**	**Medium**	**1.46**			**Medium**	**1.78**	**Medium**	**1.52**
KYNRHAR	1	1	1	11938904		944.51744	**Low**	**0.84**																
IYHPNINSNGSICLD	9	1	1	11938904		1659.76938	**Low**	**0.20**							**Low**	**0.16**	**Low**	**0.41**	**Low**	**0.63**	**Low**	**0.86**	**Low**	**0.67**
IAFTTKIYHPNINSNGSICLD	1	1	1	11938904		2321.15312	**Low**	**0.07**																
HAREWTQK	11	1	1	11938904		1055.53850	**Low**	**0.05**	**High**	**2.61**	**Low**	**0.11**	**Low**	**0.08**			**High**	**2.54**			**Medium**	**1.54**	**Medium**	**1.91**
LFHWQATIMGPPDSAYQGGVFFLTVHFPTDYPFKPPK	6	1	1	11938904		4237.09731			**Medium**	**3.00**	**High**	**4.21**	**High**	**4.00**			**High**	**4.25**			**High**	**3.90**	**High**	**3.61**
IAQIYKSD	10	1	1	11938904		937.50078			**Low**	**0.61**	**Low**	**0.30**	**Low**	**0.49**	**Low**	**0.48**	**Low**	**0.46**	**Low**	**0.46**	**Low**	**0.65**	**Low**	**0.58**
DPLVPDIAQIYKSD	1	1	1	11938904		1573.82610			**Low**	**0.09**														
LFHWQATIMGPPD	2	1	1	11938904		1512.74529					**Medium**	**1.12**			**Low**	**0.02**								
IQKELSD	3	1	1	11938904		832.44170					**Low**	**0.40**	**Low**	**0.34**										

LSDLQRDPPAHCSAGPVGD	1	1	1	1193890444		1934.883770							**Low**	**0.65**										
SAYQGGVFFLTVHFPTD	2	1	1	1193890444		1885.917999											**Low**	**0.20**					**Low**	**0.12**
LQRDPPAHCSAGPVGDD	1	1	1	1193890444		1734.803244													**Low**	**0.53**				
YPFKPPKIAFTTK	1	1	1	1193890444		1537.864188															**Medium**	**0.91**		
ILRSQWSPALTVSKVLLSICSLLCDPNPD	1	1	1	1193890444		3168.661722															**Low**	**0.38**		
WTQKYAM	1	1	1	1193890444		927.44249															**Low**	**0.09**		
IAFTTKIYHPNINSNGSICLDILR	1	1	1	1193890444		2703.437223																	**High**	**3.73**

***Presence probability of peptide in this sample**

Sequence	# PSMs	# Proteins	# Protein Groups	Protein Group Accessions	MH+ [Da]	2A_NoPEP_0min	XCorr 2A_NoPEP_0min	2A_NoPEP_5min	Xcorr 2A_NoPEP_0min	2A_NoPEP_10min	XCorr 2A_NoPEP_10min	2A_NoPEP_15min	XCorr 2A_NoPEP_15min	2A_NoPEP_30min	XCorr 2A_NoPEP_30min	2A_PEP_0min	XCorr 2A_PEP_0min	2A_PEP_5min	Xcorr 2A_PEP_5min	2A_PEP_10min	Xcorr 2A_PEP_10min	2A_PEP_15min	Xcorr 2A_PEP_15min
GSSHHHHHHSSGLVPR	302	1	1	119389044	1768.85076	High	3.80	High	5.20	High	3.93	High	4.90	High	4.52	High	4.26	High	3.83	High	4.01	High	4.09
HAREWTQK	65	1	1	119389044	1055.53862	High	2.13	High	2.64	High	2.19	High	2.44	High	2.66	High	2.71	High	2.71	High	2.48	High	2.27
SQWSPALTVSK	667	1	1	119389044	1203.63762	High	3.56	High	3.58	High	3.59	High	3.34	High	3.54	High	3.25	High	3.55	High	3.27	High	3.48
EWTQKYAM	20	1	1	119389044	1056.48296	High	2.07	High	2.15	High	2.00	High	2.13	High	2.13	Medium	1.87	High	2.15	Medium	1.95	Medium	1.97
IYHPNINSNGSICLDILR	31	1	1	119389044	2042.05303	High	2.64	High	4.84	High	2.77	High	2.64	High	3.73	High	4.06			High	3.15	High	4.59
VLLSICSLLCDPNPDDPLVPDIAQIYK	41	1	1	119389044	2954.51419	High	5.46	High	4.72	High	5.79			High	4.07	High	4.77	Medium	2.68	High	4.45	High	3.61
SAYQGGVFFLTVHFPTDYPFKPPK	25	1	1	119389044	2743.39029	High	2.80	High	2.93	High	2.78	High	3.25	High	2.86	High	3.18	High	3.13	High	2.87	High	3.65
ELSDLQR	80	1	1	119389044	860.44756	Medium	1.75	High	2.12	High	2.20	Medium	1.83	Medium	1.86	High	2.03	Medium	1.85	Medium	1.87	High	2.05
YPFKPPK	10	1	1	119389044	876.49816	Medium	1.93	High	2.05	Medium	1.75	Medium	1.71	Medium	1.82	Medium	1.01	Medium	1.31	Medium	1.66	Medium	1.74
DPLVPDIAQIYK	41	1	1	119389044	1371.75200	Medium	1.60	Low	0.73	High	3.07	Medium	1.87	Medium	1.41	High	2.08	High	2.31	Medium	1.68	High	2.70
IYHPNINSNGSICLDILRSQWSPALTVSK	7	1	1	119389044	3226.66953	Medium	1.52	Medium	2.43	Medium	2.50			High	3.78							High	3.45
WTQKYAM	8	1	1	119389044	927.44316	Low	0.24	Low	0.31	Low	0.05			Low	0.17	Low	0.36	Low	0.32	Low	0.34	Low	0.48
IYHPNINSNGSICLD	18	1	1	119389044	1659.76755	Low	0.69	Low	0.60	Low	0.53	Low	0.63	Low	0.84	Low	0.99	Low	1.12	Low	0.81		
VLLSICSLLCDPNPD	2	1	1	119389044	1601.78484	Low	0.31			Low	0.16												

ILRSQWSPALTVSK	1	1	1	11938 9044	1585.9 0610	Low	0.4 8															
YPFKPPKIAFTTKIYHPNINSNGS ICLD	1	1	1	11938 9044	3178.6 0764	Low	0.0 9															
GSHMALKR	3	1	1	11938 9044	899.48 796			High	2.3 7			Medi um	1.8 4								Medi um	1.6 0
YNRHAR	9 2	1	1	11938 9044	816.42 223			Medi um	1.1 8	Medi um	1.1 7	Low	0.8 4	Medi um	1.3 6	Medi um	1.3 1	Medi um	1.3 0	Medi um	1.3 7	Medi um	1.1 7
GSHMALKRIQK	6	1	1	11938 9044	1268.7 2746			Low	0.7 8							High	2.9 8						
IAQIYKSD	1 7	1	1	11938 9044	937.49 828			Medi um	0.9 5	Medi um	1.0 0	Low	0.6 8	Low	0.4 6	Low	0.8 6	Low	0.6 7	Medi um	0.9 2	Low	0.5 7
LFHWQATIMGPPDSAYQGGVFF LTVHFPTDYPFKPPK	1	1	1	11938 9044	4237.1 0952			High	4.2 7														
SAYQGGVFFLTVHFPTD	1	1	1	11938 9044	1885.9 0190			Low	0.1 0														
DPLVPDIAQIYKSD	4	1	1	11938 9044	1573.7 9900					Low	0.3 0							Low	0.1 8			Low	0.4 8
LQRDPPAHCSAGPVGDD	2	1	1	11938 9044	1734.7 7959							Low	0.1 6									Low	0.3 2
IAFTTKIYHPNINSNGSICLDILR	2	1	1	11938 9044	2703.4 0223							Low	0.9 4										
LSDLQRDPPAHCSAGPVGD	1	1	1	11938 9044	1934.9 1318							Low	0.9 8										
GSSHHHHHHSSGLVPRGSHMA LK	3	1	1	11938 9044	2493.2 1638											Medi um	2.0 4						
VLLSICSLLCDPNPDDPLVPD	3	1	1	11938 9044	2238.1 0324											Medi um	2.0 5	Low	0.7 8	Low	0.1 3		
IAQIYKSDK	1	1	1	11938 9044	1065.5 8953											Low	0.0 7						
IQKELSD	1	1	1	11938 9044	832.44 078													Low	0.0 3				
ILRSQWSPALTVSKVLLSICSLLC DPNPD	1	1	1	11938 9044	3168.6 4809													Low	0.5 1				
DLFHWQATIMGPPD	1	1	1	11938 9044	1627.7 4260																	Low	0.2 3
KYNRHAR	1	1	1	11938 9044	944.51 354																	Medi um	1.1 7
GSSHHHHHHSSGLVPRGSHMA LKR	1	1	1	11938 9044	2649.3 2793																	Low	0.5 4

Sequence	# PSMs	# Proteins	# Protein Groups	Protein Group Accessions	MH+ [Da]	2b_NoPEP_15min	Xcorr 2b_NoPEP_15min	2b_NoPEP_30min	XCorr B7 2b_NoPEP_30min	2b_PEP_15min	Xcorr 2b_PEP_15min
VLLSICSLLCDPNPDDPLVPDIAQIYK	10	1	1	119389044	2954.50559	High	5.34			High	2.97
GSSHHHHHHSSGLVPR	183	1	1	119389044	1768.84966	High	4.90	High	5.02	High	4.87
SAYQGGVFFLTVHFPTDYPFKPPK	6	1	1	119389044	2743.39469	High	3.75	High	2.77	High	3.34
IYHPNINSNGSICLDILR	7	1	1	119389044	2042.04411	High	3.54	High	2.22	High	2.61
SQWSPALTVSK	144	1	1	119389044	1203.63738	High	3.32	High	3.45	High	3.42
HAREWTQK	16	1	1	119389044	1055.53850	High	2.51	High	2.52	High	2.47
DPLVPDIAQIYK	18	1	1	119389044	1371.75151	High	2.45	Medium	1.25	High	2.59
EWTQKYAM	4	1	1	119389044	1056.48235	High	2.23	High	2.34	High	2.53
GSHMALKR	2	1	1	119389044	899.48827	Medium	1.99			High	2.30
YNRHAR	34	1	1	119389044	816.42137	Medium	1.73	Medium	1.22	Medium	1.37
ELSDLQR	12	1	1	119389044	860.44725	Medium	1.61	Medium	1.98	Medium	1.95
YPFKPPK	4	1	1	119389044	876.49797	Medium	1.39	Medium	1.68	Medium	1.39
IAQIYKSD	7	1	1	119389044	937.49895	Low	0.75	Medium	1.13	Low	0.52
GSHMALKRIQK	4	1	1	119389044	1268.71379	Low	0.45	Low	0.52	Low	0.60
SAYQGGVFFLTVHFPTDYPFKPPKIAFTTK	1	1	1	119389044	3404.74663	Low	0.27				
IYHPNINSNGSICLD	3	1	1	119389044	1659.76773	Low	0.23	Low	0.91	Low	0.63
WTQKYAM	2	1	1	119389044	927.44341	Low	0.07			Low	0.39
DPLVPDIAQIYKSD	2	1	1	119389044	1573.80559			Low	0.39	Low	0.57
IAFTTKIYHPNINSNGSICLDILR	3	1	1	119389044	2703.40688			Low	0.03	Low	0.74
SAYQGGVFFLTVHFPTD	1	1	1	119389044	1885.92754					Low	0.55
IQKELSD	1	1	1	119389044	832.44103					Low	0.17
IAFTTKIYHPNINSNGSICLD	1	1	1	119389044	2321.15947					Low	0.12

Sequence	# PSMs	# Proteins	# Protein Groups	Protein Group Accessions	MH+ [Da]	2C_NoPEP_15	Xcorr 2C_NoPEP_15	2C_NoPEP_30	XCorr 2C_NoPEP_30	2C_PEP_15	XCorr 2C_PEP_15
VLLSICSLLCDPNPDDPLVPDIAQIYK	10	1	1	119389044	2954.52188	High	5.03	High	4.46	High	3.55
GSSHHHHHHSSGLVPR	116	1	1	119389044	1768.85076	High	4.70	High	4.97	High	4.59
SQWSPALTVSK	151	1	1	119389044	1203.63738	High	3.41	High	3.57	High	3.45
SAYQGGVFFLTVHFPTDYPFKPPK	7	1	1	119389044	2743.39634	High	3.30	High	3.09	High	3.07
EWTQKYAM	2	1	1	119389044	1056.48198	High	2.28			Medium	1.20
ELSDLQR	25	1	1	119389044	860.44725	High	2.27	Medium	1.88	High	2.23
IYHPNINSNGSICLDILR	4	1	1	119389044	2042.04819	High	2.19	High	3.51		
HAREWTQK	5	1	1	119389044	1055.53801	High	2.16	High	2.51		
VLLSICSLLCDPNPDDPLVPD	1	1	1	119389044	2238.09355	High	2.01				
GSHMALKR	5	1	1	119389044	899.48772	Medium	1.94	Medium	1.74		
DPLVPDIAQIYK	11	1	1	119389044	1371.75102	Medium	1.84	High	2.12	Low	0.56
YPFKPPK	4	1	1	119389044	876.49767	Medium	1.69	Medium	1.42	Medium	1.53
YNRHAR	9	1	1	119389044	816.42174	Medium	0.95	Low	0.49	Low	0.42
IAQIYKSD	5	1	1	119389044	937.50408	Low	0.49	Low	0.76		
GSHMALKRIQK	6	1	1	119389044	1268.71379	Low	0.39	Low	0.79	Low	0.57
DPLVPDIAQIYKSD	3	1	1	119389044	1573.82590	Low	0.27	Low	0.50		
SQWSPALTVSKVLLSICSLLCDPNPDDPLVPD	1	1	1	119389044	3422.74106	Low	0.21				
SQWSPALTVSKVLLSICSLLCDPNPD	1	1	1	119389044	2786.40508	Low	0.05				
IQKELSD	2	1	1	119389044	832.44121	Low	0.04	Low	0.20		
ILRSQWSPALTVSK	2	1	1	119389044	1585.90654					Medium	1.18
SAYQGGVFFLTVHFPTD	1	1	1	119389044	1885.90557					Low	0.76
VLLSICSLLCDPNPD	1	1	1	119389044	1601.79924					Low	0.64
YNRHARE	1	1	1	119389044	945.47148					Low	0.03

Sequence	# PSMs	# Proteins	# Protein Groups	Protein Group Accessions	MH+ [Da]	3_NoPEP_0min	Xcorr 3_NoPEP_0min	3_NoPEP_5min	XCorr 3_NoPEP_5min	3_NoPEP_10min	XCorr 3_NoPEP_10min	3_NoPEP_15min	XCorr 3_NoPEP_15min	3_NoPEP_30min	Xcorr 3_NoPEP_30min	3_PEP_0min	XCorr 3_PEP_0min	3_PEP_5min	XCorr 3_PEP_5min	3_PEP_10min	Xcorr 3_PEP_10min	3_PEP_15min	XCorr 3_PEP_15min
GSSHHHHHHSSGLVPR	446	1	1	119389044	1768.85076	High	3.93	High	5.03	High	4.98	High	4.76	High	4.38	High	5.10	High	5.15	High	4.93	High	4.26
SQWSPALTVSK	146	1	1	119389044	1203.63750	High	2.30	High	3.47	High	2.90	High	2.28	High	3.16	High	3.72	High	2.70	High	2.78	High	3.18
ELSDLQR	37	1	1	119389044	860.44707	Medium	1.68	Medium	1.80	Medium	1.94			Medium	1.84	Medium	1.72	High	2.02	Medium	1.43	Medium	1.48
GSHMALKR	54	1	1	119389044	899.48821	Medium	1.48	High	2.11	High	2.54	High	2.41	High	2.10	High	2.11	Medium	1.73	High	2.10	Medium	1.95
EWTQKYAM	8	1	1	119389044	1056.48174	Medium	1.38	Medium	1.70	Low	0.88			Medium	1.80			Medium	1.39			High	2.01
YPFKPPK	10	1	1	119389044	876.49791	Medium	1.22	Medium	1.31	Medium	1.85			Medium	1.59	Medium	1.92	Medium	1.55	Low	0.27	Medium	1.55
DPLVPDIAQIYK	8	1	1	119389044	1371.75212	Medium	1.13	High	2.50	High	2.55			High	3.22	High	2.00	High	2.55			High	2.39
YNRHARE	4	1	1	119389044	945.45714	Low	0.74					Low	0.45							Low	0.80		
IAQIYKSD	9	1	1	119389044	937.49870	Low	0.48	Low	0.31	Low	0.16					Medium	1.01	Low	0.26	Low	0.55	Low	0.33
DPLVPDIAQIYKSD	10	1	1	119389044	1573.82341	Low	0.32	Low	0.71	Low	0.33					Low	0.37	Low	0.33			Low	0.26
DLFHWQATIMGPPD	1	1	1	119389044	1627.74114	Low	0.32																
HAREWTQK	13	1	1	119389044	1055.53752	Low	0.28	Medium	1.27	Low	0.06	Low	0.04	Low	0.08	Low	0.13	Low	0.14	Low	0.09	Low	0.48
YNRHAR	19	1	1	119389044	816.42168	Low	0.28	Medium	1.39	Medium	1.69					Low	0.78	Low	0.49	Low	0.21	Low	0.31
IQKELSD	2	1	1	11938	832.44	Low	0.2					Lo	0.3										

				9044	725		5					w	1									
VLLSICSLLCDPNPDDPLVPDIAQIYK	5	1	1	11938 9044	2954.5 1419	Low	0.04			High	4.70							High	3.14	Low	0.27		
SAYQGGVFFLTVHFPTDYPFKPPK	12	1	1	11938 9044	2743.3 8883			High	2.57	High	2.61			High	2.66			High	3.30			High	2.97
GSHMALKRIQK	5	1	1	11938 9044	1268.7 2588			Medium	2.07	High	3.15					High	2.56						
IYHPNINSNGSICLDILR	12	1	1	11938 9044	2042.0 4607			Medium	1.80					High	3.44	Medium	1.17					Medium	1.00
IAFTTKIYHPNINSNGSICLDILR	2	1	1	11938 9044	2703.4 2569			Low	0.44							Low	0.03						
YPFKPPKIAFTTKIYHPNINSNGSICLD	1	1	1	11938 9044	3178.6 6257					Low	0.96												
KYNRHAR	1	1	1	11938 9044	944.52 648					Low	0.18												
YPFKPPKIAFTTK	3	1	1	11938 9044	1537.8 8541							Low	0.32							Low	0.24		
LSDLQRDPPAHCSAGPVGD	2	1	1	11938 9044	1934.8 8718							Low	0.12							Low	0.61		
IYHPNINSNGSICLDILRSQWSPALTVSK	2	1	1	11938 9044	3226.6 6953									High	2.96								
IAFTTKIYHPNINSNGSICLD	1	1	1	11938 9044	2321.1 4743											Low	1.15						
SAYQGGVFFLTVHFPTD	1	1	1	11938 9044	1885.9 3059													Low	0.06				
IAQIYKSDK	1	1	1	11938 9044	1065.6 0185															Low	0.34		
LQRDPPAHCSAGPVGDD	1	1	1	11938 9044	1734.7 7854																	Low	0.35

Sequence	# PSMs	# Proteins	# Protein Groups	Protein Group Accessions	MH+ [Da]	4_PEP_5min	XCorr 4_PEP_5min	4_PEP_10min	Xcorr 4_PEP_10min	4_PEP_15min	Xcorr 4_PEP_15min
VLLSICSLLCDPNPDDPLVPDIAQIYK	1	1	1	119389044	2954.51518	High	3.65				
IYHPNINSNGSICLDILR	4	1	1	119389044	2042.04892	High	3.52				
SAYQGGVFFLTVHFPTDYPFKPPK	3	1	1	119389044	2743.39139	High	3.37				
GSSHHHHHHSSGLVPR	97	1	1	119389044	1768.85002	High	3.21	High	4.32	High	4.58
SQWSPALTVSK	36	1	1	119389044	1203.63701	High	3.01	High	2.33	High	2.61
DPLVPDIAQIYK	2	1	1	119389044	1371.75188	High	2.09			High	2.53
EWTQKYAM	2	1	1	119389044	1056.48235	High	2.06			Medium	1.88
GSHMALKR	4	1	1	119389044	899.48796	Medium	1.92			Medium	1.63
ELSDLQR	4	1	1	119389044	860.44768	Medium	1.58	Medium	1.63	Medium	1.58
YPFKPPK	3	1	1	119389044	876.49736	Medium	1.52	Low	0.51	Medium	1.68
LSDLQRDPPAHCSAGPVGD	1	1	1	119389044	1934.91556	Medium	1.41				
DPLVPDIAQIYKSD	3	1	1	119389044	1573.82256	Low	0.49			Low	0.17
YNRHARE	1	1	1	119389044	945.46361	Low	0.29				
HAREWTQK	3	1	1	119389044	1055.54717	Low	0.15	Low	0.62		
IAQIYKSD	3	1	1	119389044	937.49944			Low	0.47	Low	0.31
YNRHAR	5	1	1	119389044	816.42107			Low	0.23	Low	0.73
LQRDPPAHCSAGPVGDD	1	1	1	119389044	1734.78728					Medium	1.13
DLFHWQATIMGPPD	1	1	1	119389044	1627.74175					Low	0.70
SAYQGGVFFLTVHFPTD	1	1	1	119389044	1885.92681					Low	0.23

9.2 Appendix II

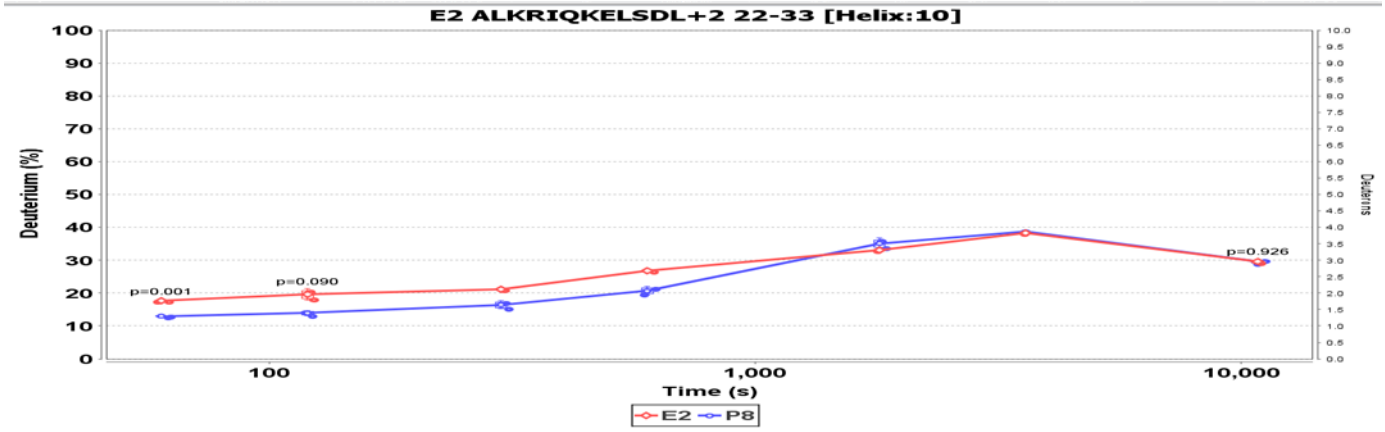
E2 ALKRIQKELSDL+2 22-33 [Helix:10]
Deuterium (%)
Deuterons
Time (s)
100
1,000
10,000
p=0.001
p=0.090
p=0.926
E2
P8

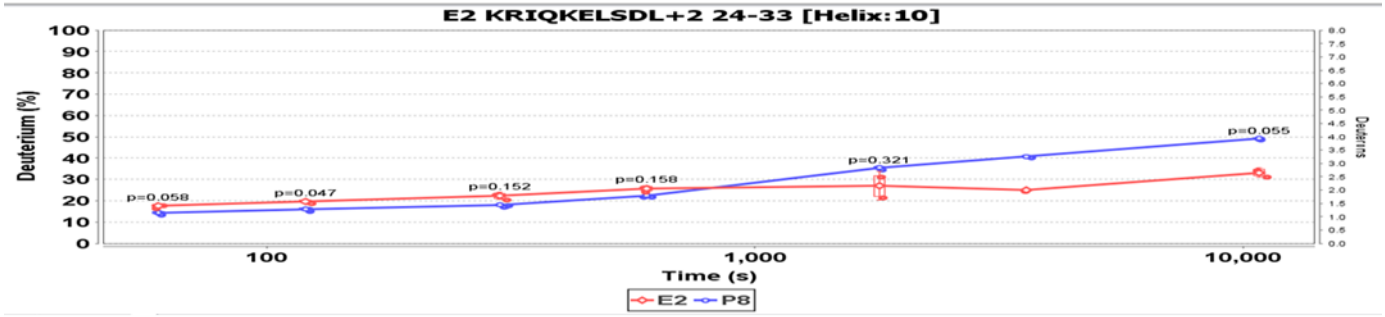
E2 KRIQKELSDL+2 24-33 [Helix:10]
Deuterium (%)
Deuterons
Time (s)
100
1,000
10,000
p=0.058
p=0.047
p=0.152
p=0.158
p=0.321
p=0.055
E2
P8

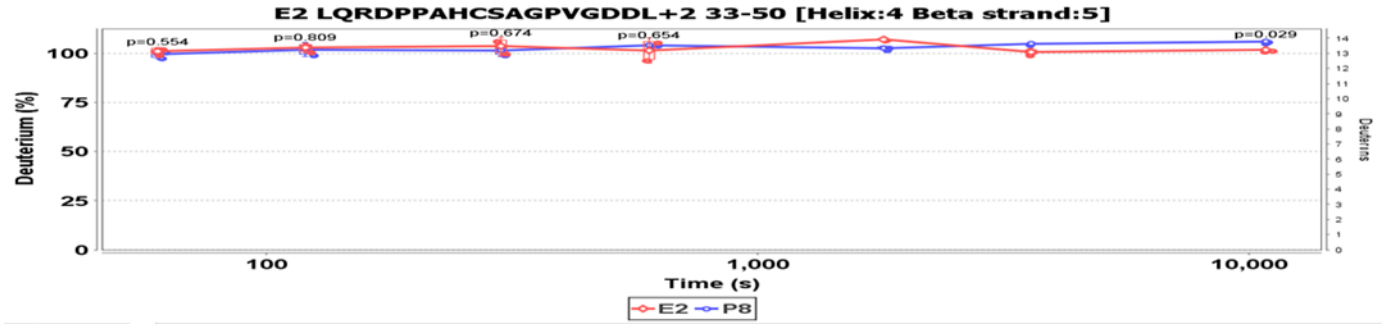
E2 LQRDPPAHCSAGPVGDDL+2 33-50 [Helix:4 Beta strand:5]
Deuterium (%)
Deuterons
Time (s)
100
1,000
10,000
p=0.554
p=0.809
p=0.674
p=0.654
p=0.029
E2
P8

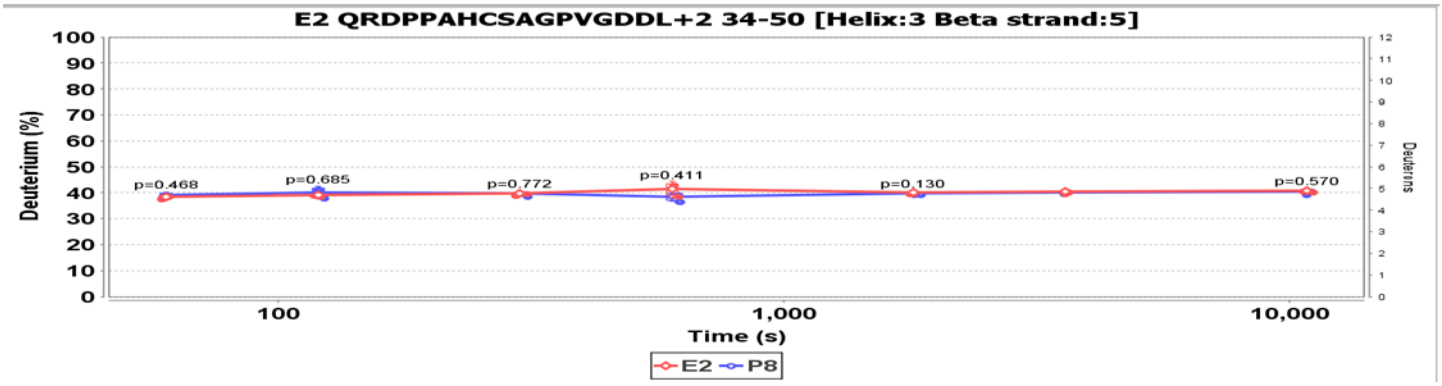
E2 QRDPPAHCSAGPVGDDL+2 34-50 [Helix:3 Beta strand:5]
Deuterium (%)
Deuterons
p=0.468
p=0.685
p=0.772
p=0.411
p=0.130
p=0.570
100
1,000
10,000
Time (s)
E2
P8

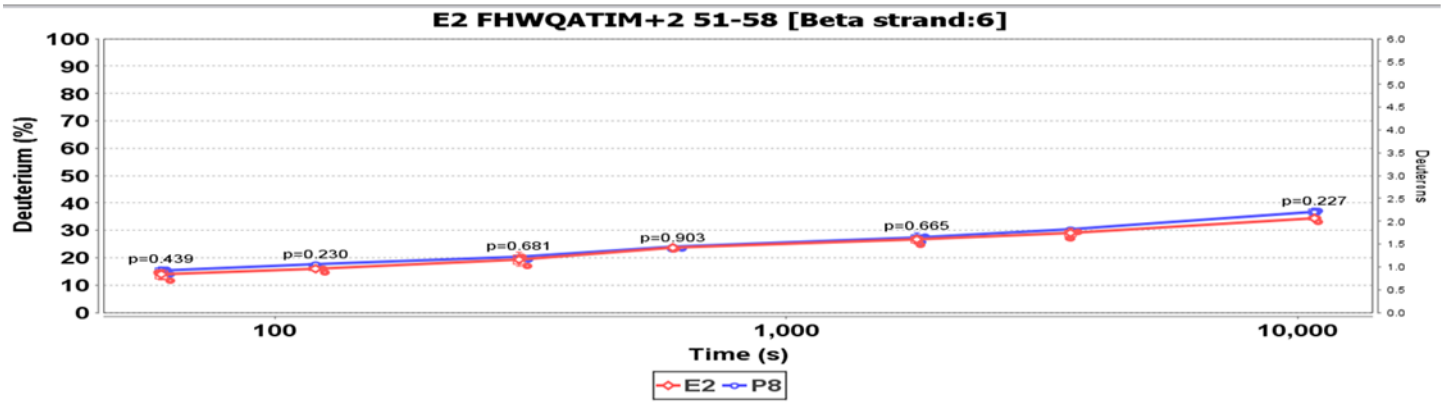
E2 FHWQATIM+2 51-58 [Beta strand:6]
Deuterium (%)
Deuterons
p=0.439
p=0.230
p=0.681
p=0.903
p=0.665
p=0.227
100
1,000
10,000
Time (s)
E2
P8

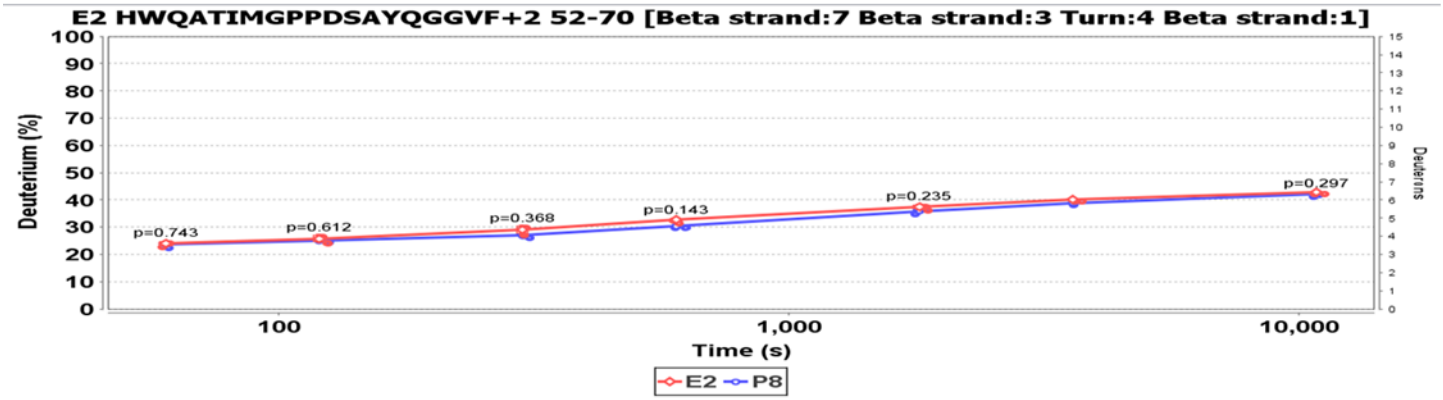
E2 HWQATIMGPPDSAYQGGVF+2 52-70 [Beta strand:7 Beta strand:3 Turn:4 Beta strand:1]
Deuterium (%)
Deuterons
p=0.743
p=0.612
p=0.368
p=0.143
p=0.235
p=0.297
100
1,000
10,000
Time (s)
E2
P8

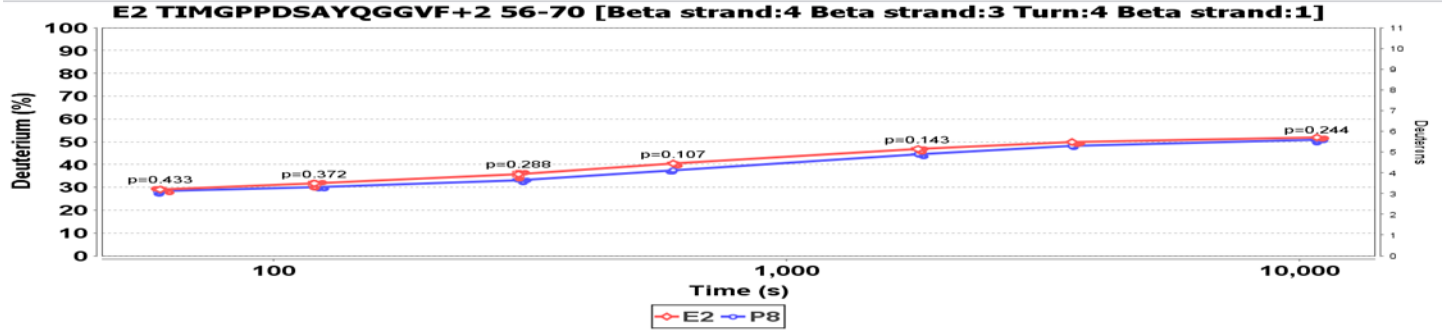
E2 TIMGPPDSAYQGGVF+2 56-70 [Beta strand:4 Beta strand:3 Turn:4 Beta strand:1]
Deuterium (%)
Deuterons
p=0.433
p=0.372
p=0.288
p=0.107
p=0.143
p=0.244
100
1,000
10,000
Time (s)
E2
P8

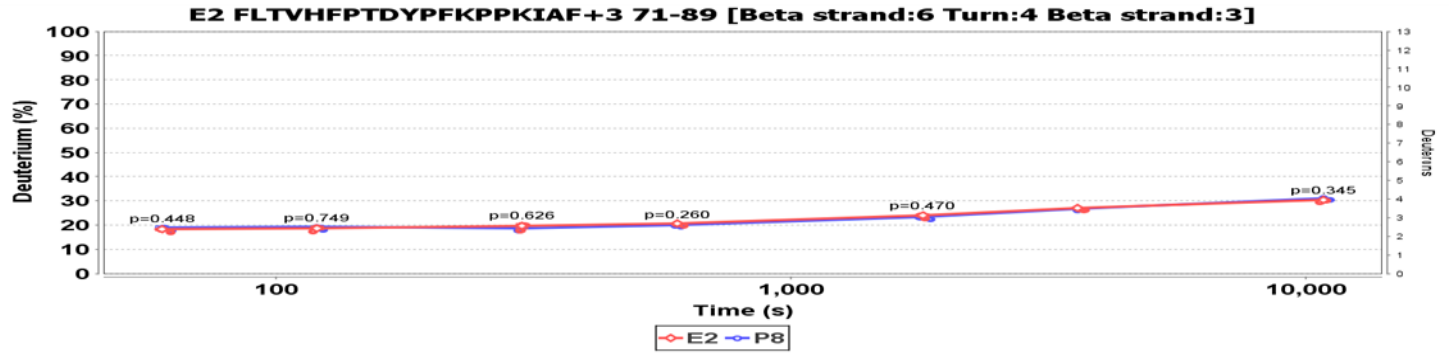
E2 FLTVHFPTDYPFKPPKIAF+3 71-89 [Beta strand:6 Turn:4 Beta strand:3]
Deuterium (%)
Deuterons
p=0.448
p=0.749
p=0.626
p=0.260
p=0.470
p=0.345
100
1,000
10,000
Time (s)
E2
P8

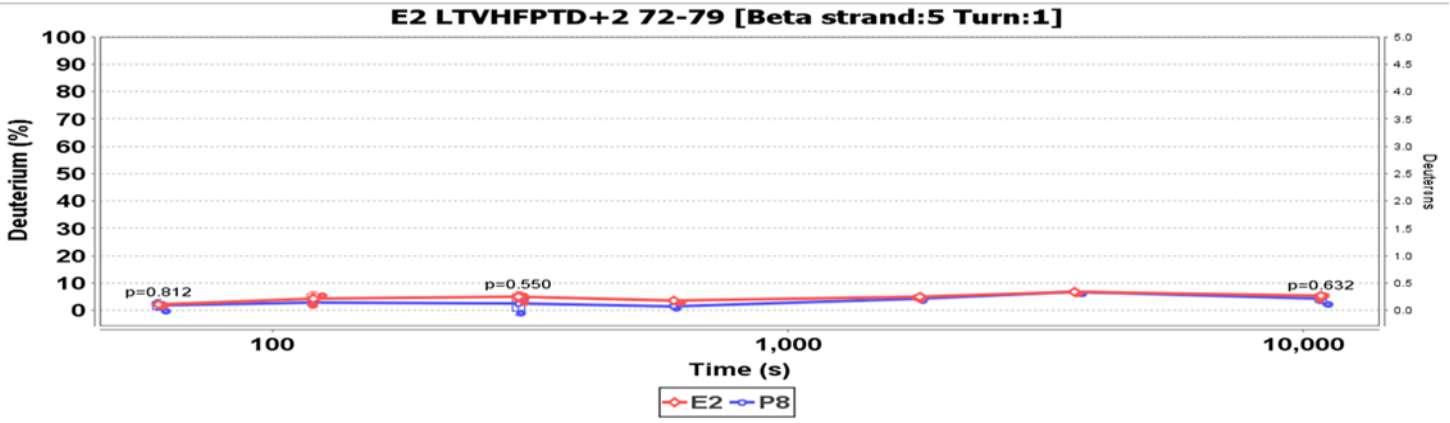
E2 LTVHFPTD+2 72-79 [Beta strand:5 Turn:1]
Deuterium (%)
Deuterons
p=0.812
p=0.550
p=0.632
100
1,000
10,000
Time (s)
E2
P8

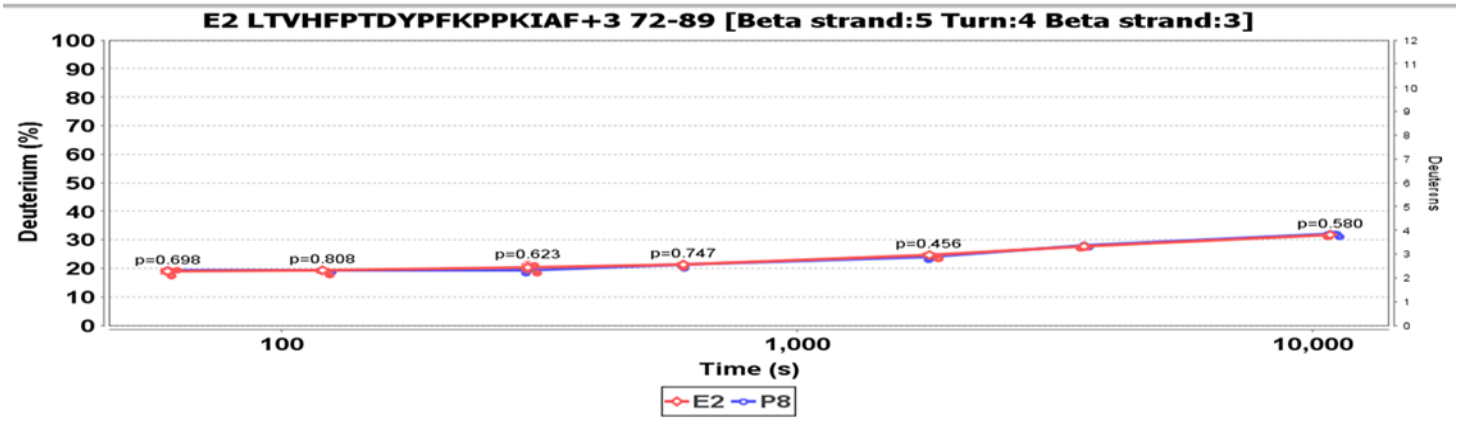
E2 LTVHFPTDYPFKPPKIAF+3 72-89 [Beta strand:5 Turn:4 Beta strand:3]
Deuterium (%)
Deuterons
p=0.698
p=0.808
p=0.623
p=0.747
p=0.456
p=0.580
100
1,000
10,000
Time (s)
E2
P8

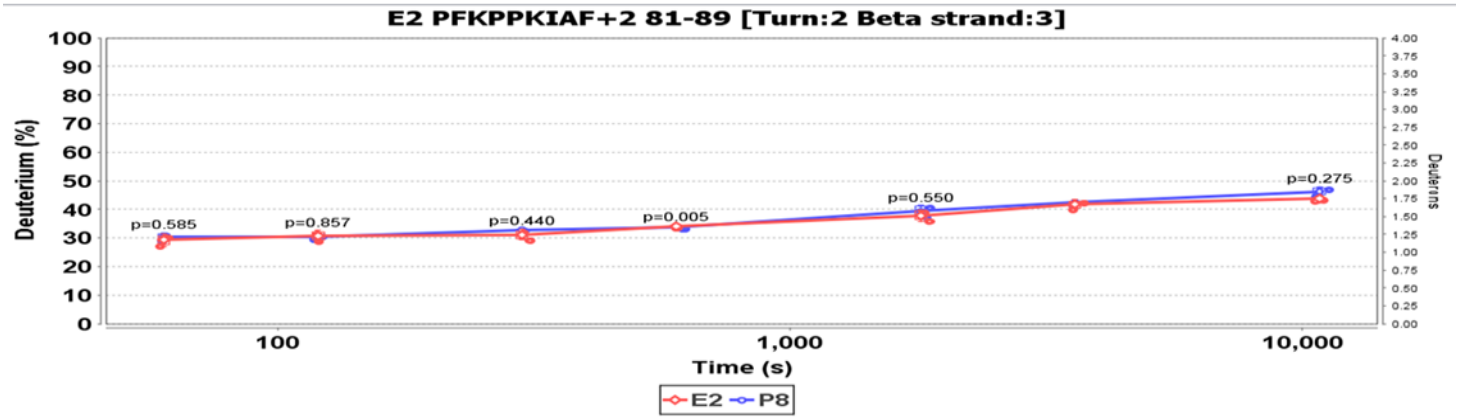
E2 PFKPPKIAF+2 81-89 [Turn:2 Beta strand:3]
Deuterium (%)
Deuterons
p=0.585
p=0.857
p=0.440
p=0.005
p=0.550
p=0.275
100
1,000
10,000
Time (s)
E2
P8

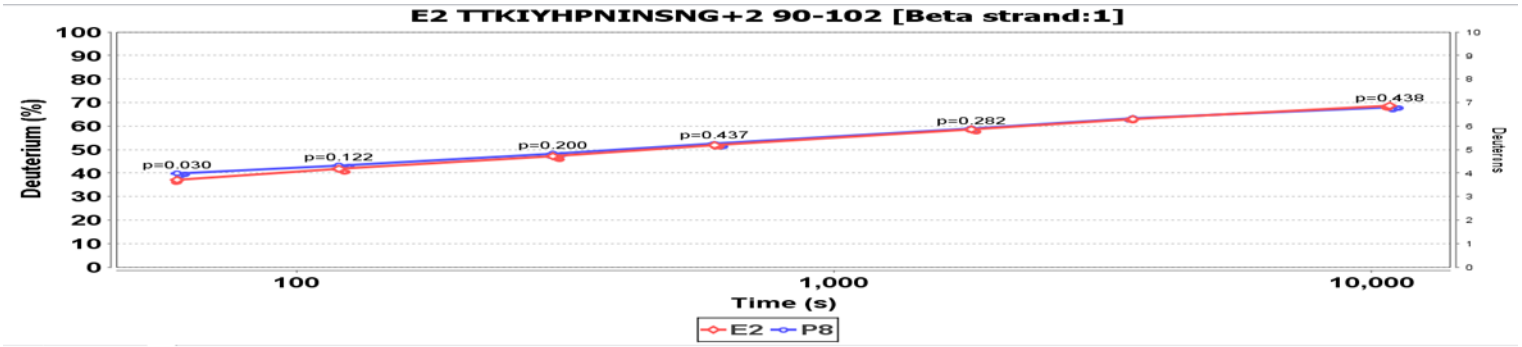
E2 TTKIYHPNINSNG+2 90-102 [Beta strand:1]
Deuterium (%)
Deuterons
Time (s)
100
1,000
10,000
p=0.030
p=0.122
p=0.200
p=0.437
p=0.282
p=0.438
E2
P8

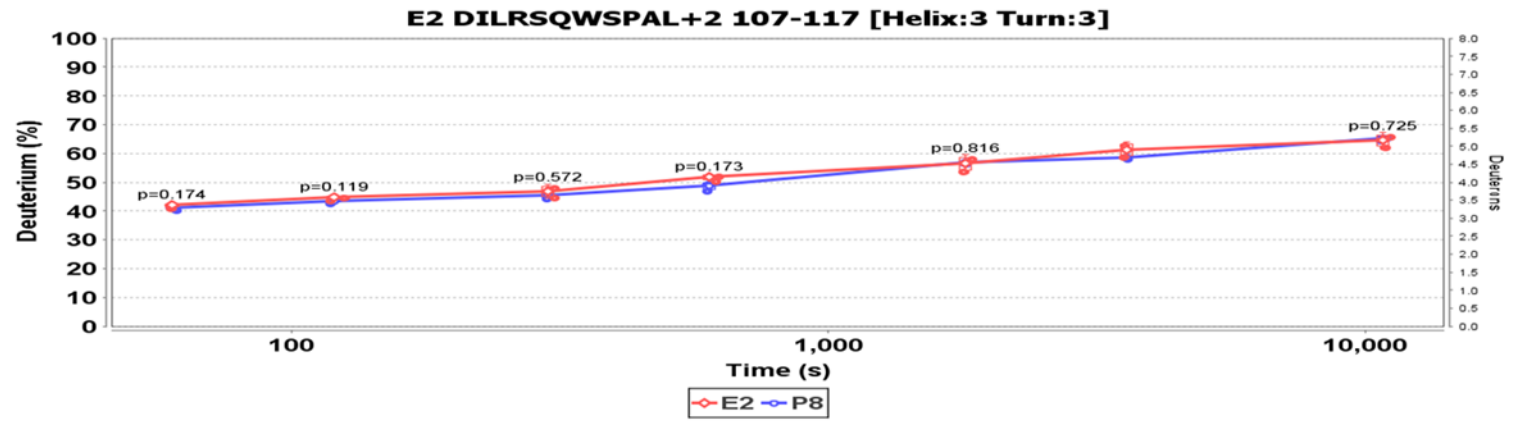
E2 DILRSQWSPAL+2 107-117 [Helix:3 Turn:3]
Deuterium (%)
Deuterons
Time (s)
100
1,000
10,000
p=0.174
p=0.119
p=0.572
p=0.173
p=0.816
p=0.725
E2
P8

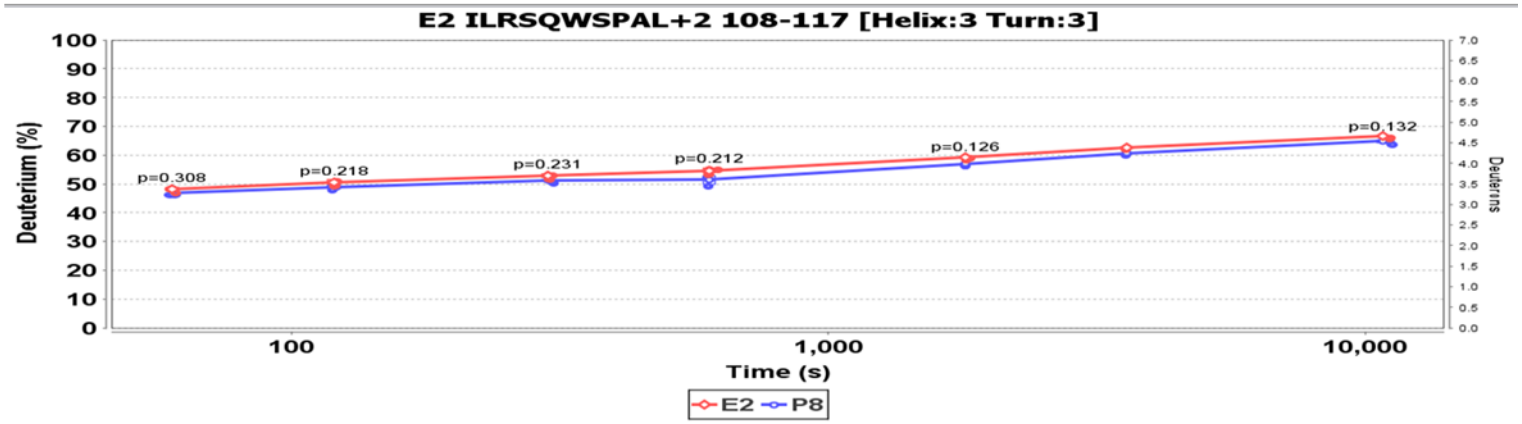
E2 ILRSQWSPAL+2 108-117 [Helix:3 Turn:3]
Deuterium (%)
Deuterons
Time (s)
100
1,000
10,000
p=0.308
p=0.218
p=0.231
p=0.212
p=0.126
p=0.132
E2
P8

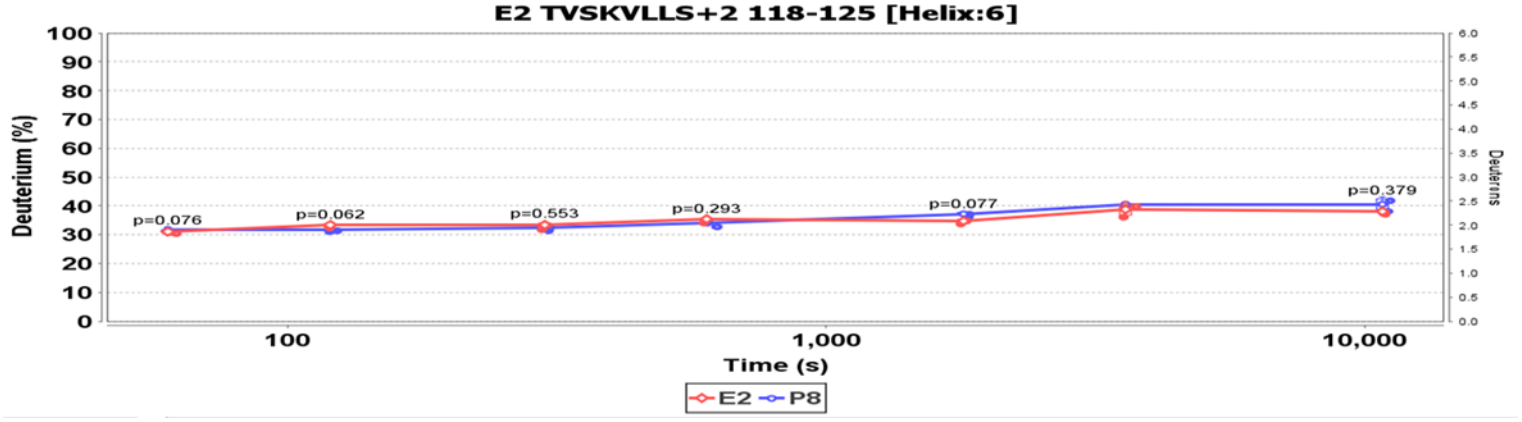
E2 TVSKVLLS+2 118-125 [Helix:6]
Deuterium (%)
Deuterons
Time (s)
100
1,000
10,000
p=0.076
p=0.062
p=0.553
p=0.293
p=0.077
p=0.379
E2
P8

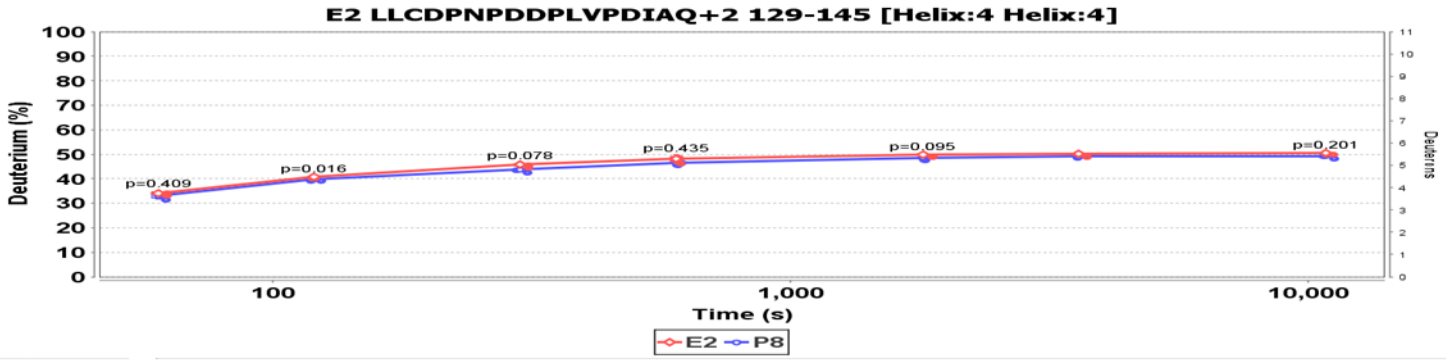
E2 LLCDPNPDDPLVPDIAQ+2 129-145 [Helix:4 Helix:4]
Deuterium (%)
Deuterons
Time (s)
100
1,000
10,000
p=0.409
p=0.016
p=0.078
p=0.435
p=0.095
p=0.201
E2
P8

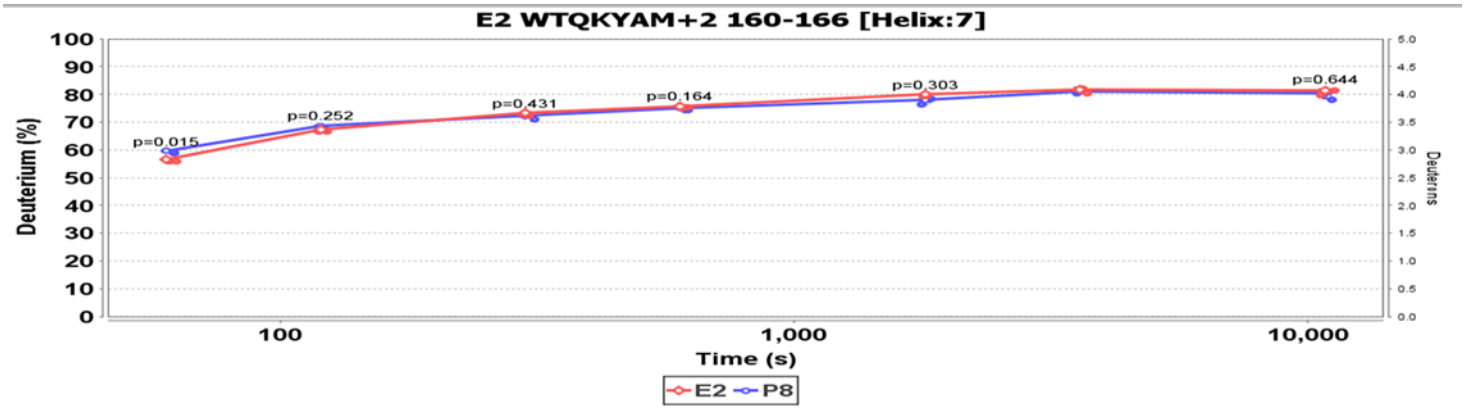
E2 WTQKYAM+2 160-166 [Helix:7]
Deuterium (%)
Deuterons
Time (s)
100
1,000
10,000
p=0.015
p=0.252
p=0.431
p=0.164
p=0.303
p=0.644
E2
P8

9.3 Appendix III

Nanosensing protein allostery using a bivalent mouse double minute two (MDM2) assay

Anna F. Robson[a], Ted R. Hupp[b,1], Fiona Lickiss[b], Kathryn L. Ball[b], Karen Faulds[a], and Duncan Graham[a,1]

[a]Centre for Molecular Nanometrology, WestCHEM, Department of Pure and Applied Chemistry, University of Strathclyde, Glasgow G1 1XL, United Kingdom; and [b]Edinburgh Cancer Research Centre, Cell Signaling Unit, Institute of Genetics and Molecular Medicine, University of Edinburgh, Edinburgh EH4 2XU, United Kingdom

Edited by Carol Prives, Columbia University, New York, NY, and approved March 28, 2012 (received for review October 14, 2011)

The tumor suppressor protein, p53, is either mutated or absent in >50% of cancers and is negatively regulated by the mouse double minute (MDM2) protein. Understanding and inhibition of the MDM2-p53 interaction are, therefore, critical for developing novel chemotherapeutics, which are currently limited because of a lack of appropriate study tools. We present a nanosensing approach to investigate full-length MDM2 interactions with p53, thus providing an allosteric assay for identifying binding ligands. Surface-enhanced Raman scattering (SERS)-active nanoparticles, functionalized with a p53 peptide mimic (peptide 12.1), display biologically specific aggregation following addition of MDM2. Nanoparticle assembly is competitively inhibited by the N-terminal MDM2-binding ligands peptide 12.1 and Nutlin-3. This study reports nanoparticle assembly through specific protein–peptide interactions that can be followed by SERS. We demonstrate solution-based MDM2 allosteric interaction studies that use the full-length protein.

assay system | biosensing | nano-assembly | protein interaction studies | Raman spectroscopy

The p53 tumor suppressor protein is often referred to as the "guardian of the genome" owing to its key role in cell-cycle regulation and its activity in a number of different cancer pathways (1–3). The antiproliferative action of p53 arises from the induction of cell-cycle arrest and apoptosis in cells subjected to DNA damage in response to stress. As such, p53 is central to protecting cells from uncontrolled growth and malignant transformation with inactivation or mutation of p53 found in over 50% of human cancers (1–3). Under nonstressed conditions, mouse double minute (MDM)2 negatively regulates p53, primarily through the ubiquitin degradation pathway but also via transrepression (4, 5). Studies have shown up-regulation of MDM2 in malignancies where p53 is fully functional, making the MDM2-p53 feedback loop of great interest in chemotherapeutic studies (6, 7).

MDM2 is a multidomain protein that exerts E3-ligase activity on a number of proteins, including p53 (5, 8, 9). The ubiquitination activity of MDM2 is a multisubunit process whereby the N-terminal hydrophobic pocket and central acidic domain of MDM2 are used in p53 binding, to the N-terminal and central domains of p53, respectively (10). The complexity of this multisubunit interaction makes it relatively difficult to investigate the allosteric nature of MDM2. This is made more difficult by the problems in acquiring a structure of full-length MDM2 because of intrinsically disordered regions on the protein that reduce likelihood of crystallization. Focus solely on the N-terminal domain of MDM2 has identified Nutlin-3-type molecules that activate p53 in cells; however, these also act as allosteric agonists that stimulate rather than inhibit p53 ubiquitination (10–15). The putative dimerization of MDM2 through the C-terminal really interesting new gene (RING) domain is reported to be critical for E3-ligase activity; however, molecular reasoning for this is not fully understood (8, 16–18). To date, studies on MDM2 structure have been conducted with purified domain constructs, which is not representative of full-length protein activity in nature.

Using full-length MDM2, which has the capacity to exhibit allosteric interactions (19, 20), would provide an assay for the screening of MDM2 ligands. Domain construct studies have investigated the multiple binding interactions of MDM2, but few, thus far, have used unlabeled full-length protein to simultaneously interrogate two binding events. The assay described in this report monitors both N-terminal and C-terminal activities of MDM2 simultaneously using full-length protein, which is critical to understanding the biological action of the native protein. The methodology provides a step forward in the capability for investigating such intricate interactions, and a unique insight is provided into the allosteric nature of native MDM2 that cannot be observed using other techniques.

Current methodologies used to probe interactions in biological systems commonly use readout tools such as fluorescence (21–23). This technique is subject to a high background from biological media and is limited by broad emission bands and the inability to probe interactions over distances of more than 10 nm. Surface-enhanced Raman scattering (SERS) is a vibrational spectroscopy that can provide similar sensitivity to fluorescence, but narrower spectral peaks allow for simultaneous detection of multiple species (24, 25). SERS interrogates an analyte, adsorbed onto a roughened metal surface, from which further Raman signal enhancement is achieved by coinciding the laser excitation wavelength with the analyte absorbance maxima (26, 27). SERS can also be enhanced or "turned on" by aggregation of nanoparticles (NPs) in solution because of "hot spots" of higher electromagnetic fields at NP junctions (26–28). Cotton et al. pioneered the use of NP and SERS for proteomic investigations and developed the first SERS-based enzyme immunoassay in 1989 (29). Subsequently, a number of SERS-based immunoassays have been documented (30–39). Assembly of functionalized NPs via protein–ligand interactions has been previously demonstrated using techniques such as extinction spectroscopy, transmission electron microscopy, and gel electrophoresis, all of which lack the sensitivity of SERS (40–44). Such interactions have been detected via SERS on metal surfaces, where binding events are compromised by protein orientation and conformation at the surface. Solution-based studies allow structural integrity of the full-length protein to be maintained, thus providing accurate information about complex interactions: however, such investigations have yet to be reported (36).

In this report, we outline a method for NP assembly through the interaction of full-length MDM2 with an N-terminal-domain peptide ligand. By exploiting the sensitivity and selectivity of SERS, we provide insight into the allosteric nature of MDM2 in

Author contributions: A.F.R., T.R.H., and D.G. designed research; A.F.R. and F.L. performed research; T.R.H., K.L.B., K.F., and D.G. contributed new reagents/analytic tools; A.F.R., T.R.H., and D.G. analyzed data; and A.F.R., T.R.H., and D.G. wrote the paper.

The authors declare no conflict of interest.

This article is a PNAS Direct Submission.

[1]To whom correspondence may be addressed. E-mail: ted.hupp@ed.ac.uk or duncan.graham@strath.ac.uk.

This article contains supporting information online at www.pnas.org/lookup/suppl/doi:10.1073/pnas.1116637109/-/DCSupplemental.

solution, which is not achievable by current methodologies, which only monitor one binding interaction, involve protein labeling, or require surface immobilization.

Results

Protein–Peptide Nanoparticle Assembly. We propose a solution-based approach to investigate the interaction of full-length MDM2 with a p53 peptide mimic exploiting the sensitivity and selectivity of SERS. p53 is known to bind the N-terminal hydrophobic pocket of MDM2 by forming an ampipathic helix containing the peptide motif, FxxxWxxL (45). Peptide 12.1 (MPR**F**MD**Y**W**E**G**L**N) originates from a library of p53 peptide mimics and demonstrates high-affinity binding to the MDM2 hydrophobic cleft (46). Tryptophan, a key residue involved in aromatic-aromatic interactions with MDM2 (47, 48), was replaced with alanine to create the mutant peptide $12.1_{W\Delta A}$, which provided a negative control to ensure biological specificity of the interaction. In theory, putative dimerization of full-length MDM2 (through its RING domain) would present two N-terminal hydrophobic pockets free (per dimer) to interact with ligands such as peptide 12.1. N-terminal interactions with peptide ligand, therefore, allow the MDM2 dimer to bring together two peptide 12.1 functionalized silver NP, peptide silver nanoparticle (PSN)-12.1, in solution (Fig. 1*A*, *i*). An alternative model for PSN-12.1 assembly, via a secondary peptide 12.1-binding site, is also illustrated (Fig. 1*A*, *ii*). The latter is unlikely because there is no evidence for two different peptide 12.1-binding sites on MDM2, and cell based studies suggest MDM2 is oligomeric in solution (16). MDM2-induced aggregation can be monitored over time by extinction spectroscopy and premodifying peptide 12.1 with a benzotriazole Raman tag, BT, enables the

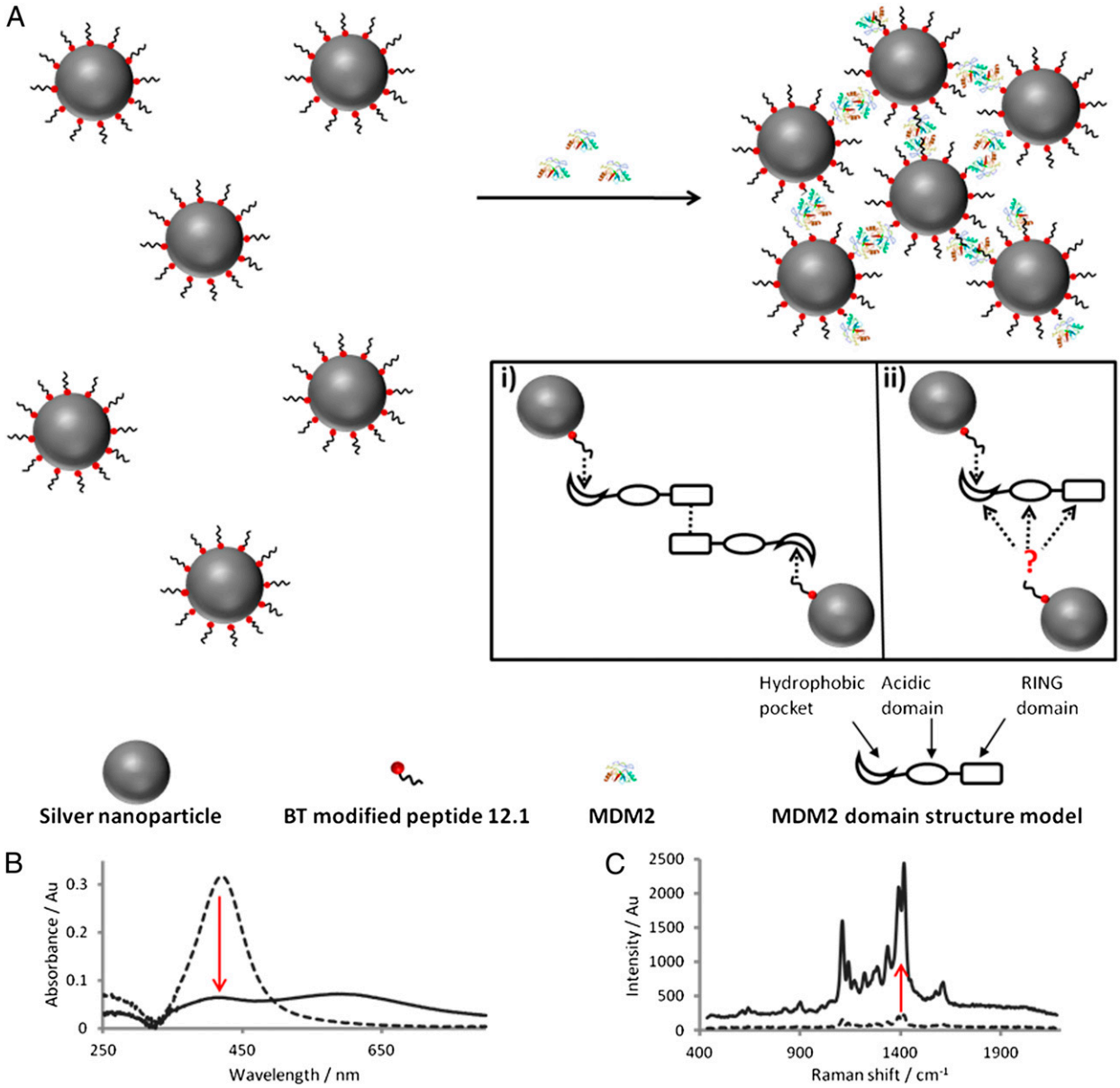

Fig. 1. (*A*) Schematic of the proposed assembly of PSN through specific interactions between MDM2 and peptide 12.1 (not to scale). *Inset* shows two proposed models for MDM2 bivalency resulting in PSN aggregation from a MDM2 dimerization (e.g., "oligomeric") conformation (*i*) and monomeric MDM2 (*ii*) have two distinct binding sites with the known and an alternative peptide 12.1 binding site (not to scale). (*B* and *C*) Extinction spectroscopy (*B*) and SERS analysis (*C*) before (dashed) and after (solid line) addition of MDM2 to PSN-12.1.

process to be explored using SERS. Both extinction and SERS intensity can be monitored over time to investigate the biological interactions driving this NP-assembly process.

Peptide Silver Nanoparticles. Reproducibility of spectra from Raman reporters used in SERS-based immunoassays is extremely important to obtain reliable results. Benzotriazole dyes adsorb onto silver nanoparticle surfaces in the same orientation irrespective of concentration, resulting in reproducible Raman spectral intensities (49). This is attributable to steric hindrance presented by covalent interactions between N_1 and N_3 lone electron pairs with the silver surface (50, 51). BT has an absorbance λ_{max} of 487 nm and, as such, is close in resonance when using an excitation wavelength of 514 nm. The most prominent peak in the BT Raman spectrum occurs at a shift of 1,416 cm^{-1} (Fig. 1*C*) and can be attributed to the azo stretch in the dye structure (Fig. S1).

Peptide 12.1 and mutant peptide $12.1_{W\Delta A}$ were modified with BT and directly conjugated to EDTA-reduced silver NP (AgEDTA) in a one-step reaction. BT consists of a triazole moiety with an affinity for silver surfaces, a Raman active chromophore, and a stabilizing polyethylene glycol spacer (Fig. S1). Circular dichroism (CD) analysis of peptide 12.1 and BT-modified peptide 12.1 showed the modification to have no inhibitory effect on the peptide adopting a helical conformation (Fig. S2). BT-modified peptide 12.1 and mutant peptide $12.1_{W\Delta A}$ displayed high- and low-level binding, respectively, to MDM2 in ELISA competition assays (Fig. S3). Successful PSN formation was shown by an increase in particle size through extinction spectroscopy, and matrix-associated laser desorption ionization–mass spectroscopy (MALDI-MS) analysis was used to identify BT-peptide molecules anchored on the nanoparticle surface (Figs. S4 and S5).

MDM2-Induced PSN Aggregation. Unlabeled full-length MDM2 was added to PSN solutions at various concentrations based on a molar excess of protein to PSN. This is in line with previously published data using streptavidin for controlled assembly of biotin-functionalized gold NP (40). Aggregation of 15 pM PSN-12.1 in solution was observed following the addition of MDM2 in a concentration-dependent manner, as shown by the plasmon band decrease monitored by extinction spectroscopy (Figs. 2 and 3). A dampening in the band at 419 nm and an increase at longer wavelengths are indicative of aggregate formation, verified by the change in NP size distribution shown by dynamic light scattering (Fig. 2*B*). Biological specificity of the MDM2–peptide 12.1 interaction was confirmed by using mutant PSN-$12.1_{W\Delta A}$ samples in which aggregation was observed to a much lesser extent at MDM2 concentrations up to a NP: protein ratio of 1:1,000 (15 pM PSN, 15 nM MDM2) (Figs. 2 and 4 and *SI Text*). This confirms the importance of specific amino acid residues in the binding event between MDM2 and NP-bound peptide. At protein concentrations higher than this, the extent of aggregation between PSN-12.1 and PSN-$12.1_{W\Delta A}$ solutions cannot be distinguished by extinction spectroscopy or dynamic light scattering (Figs. 2 and 3). At these concentrations, MDM2 is present in such excess that binding to the mutant peptide $12.1_{W\Delta A}$ is comparable to that of peptide 12.1, indicating a saturation point to the assay. Extinction spectroscopic measurements of samples taken 96 h after MDM2 addition show a much greater distinction in aggregation extent between PSN-12.1 and the mutant PSN-$12.1_{W\Delta A}$ up to the saturation concentration of 15 nM MDM2 (Fig. 2*A*); however, such a time duration for an immunoassay is impractical. The PSN assembly process can be monitored over time by measuring the extinction change at the λ-max, and aggregation was seen to plateau within the first 30 min (Fig. 3*A*). These data correlate with previous literature describing binding of p53 BOX-I to the MDM2 hydrophobic cleft to be a stable, high-affinity interaction. PSN-12.1 assembly can be interpreted through either of the models proposed in Fig. 1*A*; however, because there is no evidence to support the latter, the most likely explanation for the observed PSN aggregation is an active MDM2-dimer (or "oligomer").

MDM2-Induced Aggregation "Turns On" SERS. Initial SERS studies involved analysis of PSN samples after completion of aggregate assembly monitored by extinction spectroscopy. SERS enhancement was measured by comparing the standardized peak height at 1,416 cm^{-1} (Fig. 1*B*) for each sample in relation to unaggregated PSN solutions. Raman signal intensity increased in a positive correlation with MDM2 concentration up to a molar ratio of 1:1,000 PSN:MDM2 (15 pM PSN, 15 nM MDM2) (Fig. 4). This corresponds with previous extinction spectroscopy investigations indicating assay saturation at this concentration. When MDM2 was present at a larger molar excess than 1:1,000, a decrease in SERS intensity was observed (Fig. 4*A*). At these concentrations, protein can form almost monolayer coverage on the PSN surface, thus dampening Raman signals associated with BT but still allowing aggregation, as seen by extinction spectroscopy (Fig. 3*B*). Another possibility is that large aggregates

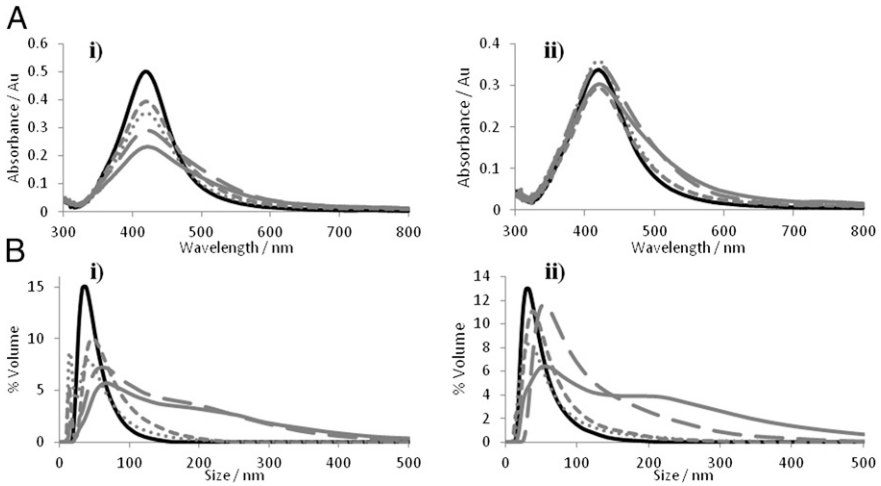

Fig. 2. Extinction spectroscopy and particle size analysis of PSN solutions before and after addition of MDM2. (*A* and *B*) Extinction profiles (*A*) and particle size distributions (*B*) of PSN-12.1 (*i*) and PSN-$12.1_{W\Delta A}$ (*ii*) samples without MDM2 (black) and 96 h after addition of 300 (dotted gray), 500 (short dashed gray), 1,000 (long dashed gray), and 2,000 (solid gray) MDM2 monomers per PSN.

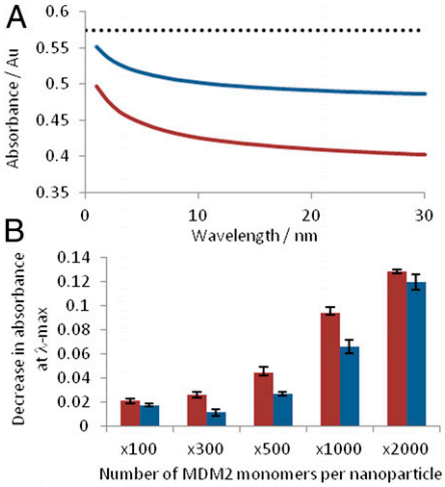

Fig. 3. Extinction spectroscopy analysis of PSN aggregation. (*A*) Extinction spectroscopy monitored for a 30-min duration following MDM2 addition to PSN-12.1 (red) and PSN-12.1$_{W\Delta A}$ (blue) at a PSN:MDM2 molar ratio of 1:1,000. Dotted line indicates the average plasmon band intensity before MDM2 addition. (*B*) Change in the plasmon band monitored from the 1–30 min after MDM2 addition. Error bars illustrate the SD.

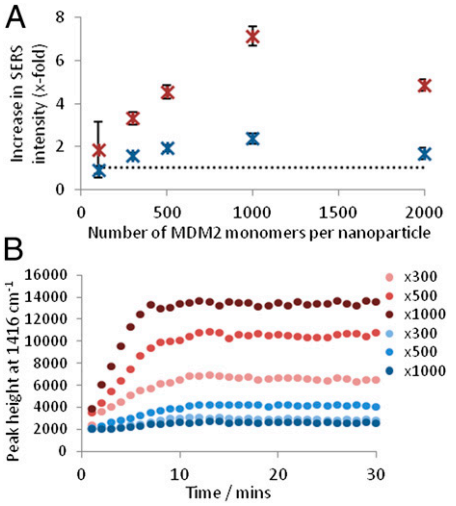

Fig. 4. SERS analysis of PSN aggregation. (*A*) Calculated x-fold increase in SERS intensity following MDM2 addition to PSN-12.1 (red) and PSN-12.1$_{W\Delta A}$ (blue). (*B*) Peak height at 1416 cm^{-1} monitored every 60 seconds for 30 min following addition of varying amounts of MDM2 to PSN-12.1 (red) and PSN-12.1$_{W\Delta A}$ (blue). X-value represents the excess of MDM2 monomers per PSN. Dotted line indicates PSN samples when MDM2 is absent. Error bars illustrate the SD.

form that fall out of solution; however, this explanation is contradicted by the partial aggregation observed in scanning electron microscopy (SEM) (Fig. S6). At a molar ratio of 1:1,000 PSN:MDM2 (15 pM PSN, 15 nM MDM2), an eightfold increase in peak height was observed compared with samples where protein was absent. No such signal enhancement was apparent for PSN-12.1$_{W\Delta A}$ samples or when MDM2 was replaced with a control protein, BSA (Fig. 4*A* and Fig. S7). This demonstrated the high biological specificity of the interaction, further validated by additional MDM2 binding studies (Fig. S8). SERS analysis of MDM2-induced PSN aggregation enables protein detection at a molar excess of 100 MDM2 per PSN (15 pM PSN, 1.5 nM MDM2), demonstrating a lower limit of detection than was achievable using extinction spectroscopy (Figs. 3*B* and 4*A*). Comparable results for PSN-12.1 and PSN-12.1$_{W\Delta A}$ samples were also more distinguishable when applying SERS rather than extinction spectroscopy (Figs. 3 and 4). These data indicate that SERS presents a more sensitive analysis technique than extinction spectroscopy for NP assembly controlled by biological interactions.

Temporal SERS Analysis of Aggregation. Our findings show that the assembly of PSN-12.1 with MDM2 is a time- and concentration-dependent process (Fig. 3). To this end, SERS analysis was investigated to monitor the PSN assembly process over time. To minimize SERS signal variations, PSN preparation and final solution concentrations were optimized. Focus of the laser through the bulk of the solution and continuous sample rotation ensured consistent sampling of the components throughout the duration of the experiment.

The rate at which SERS intensity reached saturation was seen to increase with MDM2 concentration, and it can be interpreted from the data that the formation of PSN assemblies approaches completion within 11, 9, and 7 min for PSN:MDM2 ratios of 1:300, 1:500, and 1:1,000, respectively (15 pM PSN, 4.5–15 nM MDM2) (Fig. 4*B*). This is quicker than observed in extinction spectroscopy (Fig. 3*A*), demonstrating the higher sensitivity of SERS as an analytical tool for monitoring NP aggregation. These data demonstrate that SERS can be used as a viable tool for monitoring time-dependent NP assembly, although it must be realized that it does not represent the system found in nature owing to PSN solution kinetics.

Inhibition of the MDM2-PSN Interaction. To test the potential for development of the assay for investigating MDM2 interactions with small molecules, we exposed MDM2 to N-terminal-binding ligands to competitively inhibit the aforementioned PSN-12.1 assembly. MDM2 is likely to exhibit a higher binding affinity to free peptide 12.1 (inhibitor 12.1) than to NP-bound peptide 12.1, because of the solution kinetics. Nutlin-3 is a potent and well studied small molecule inhibitor of the MDM2-p53 interaction (15). For all inhibition experiments, a molar ratio of 1:1,000 PSN:MDM2 (15 pM PSN, 15 nM MDM2) was used owing to the large extent of the aggregation observed (Figs. 2–4). MDM2 was preincubated with a 100-fold molar excess of inhibitor (0.96 mM MDM2, 96 mM inhibitor) before mixing with PSN-12.1 solutions (6.25 mL added to 400 mL of 15 pM PSN), and temporal analysis was carried out using extinction spectroscopy. A lesser decrease in the plasmon band was observed for PSN-12.1 solutions treated with MDM2 preincubated with either inhibitor 12.1 or Nutlin-3 than was evident following the addition of native MDM2 (Fig. 5). A much greater enhancement in Raman signal was also observed in the presence of native MDM2 compared with MDM2 preincubated with inhibitor (Fig. 5*B*). Inhibitor 12.1 and Nutlin-3 were able to bind the MDM2 hydrophobic cleft, thus blocking the binding site for peptide 12.1 molecules on PSN-12.1 and disallowing MDM2-mediated PSN assembly. Signal changes in SERS and extinction spectroscopy associated with PSN aggregation were, therefore, not observed to the same extent (Fig. 5*B*). It was subsequently observed that lowering the excess of inhibitor resulted in a decrease in inhibition efficiency by extinction spectroscopy and SERS (Fig. 5*C*). Varying the molar excess of inhibitor 12.1 prebound to MDM2 in this way demonstrates PSN-assembly inhibition in a dose-dependent manner. The extinction spectroscopy and SERS data, together, demonstrate a competitive inhibition of MDM2–peptide 12.1-driven NP assembly by inhibitor 12.1 and Nutlin-3. A 1.4× increase in SERS response was detected at the highest concentration of inhibitor 12.1, suggesting that some PSN assembly occurred (Fig. 5*C*). Depletion in extinction plasmon band for the same sample in extinction spectroscopy is negligible (Fig. 5*C*), thus identifying SERS as the superior technique to investigate inhibitor potency. SERS analysis also provides a positive response for NP assembly that is

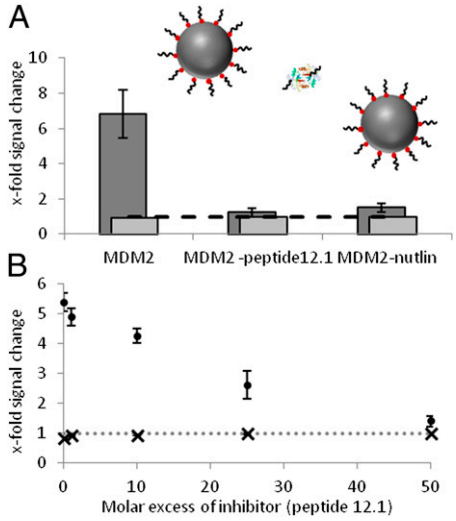

Fig. 5. Competitive inhibition of MDM2-induced PSN aggregation. Schematic illustrates proposed MDM2-induced PSN aggregation inhibition with inhibitor peptide 12.1 and Nutlin-3. (*A* and *B*) X-fold decrease in the plasmon band monitored by extinction spectroscopy [light gray (*A*) and X (*B*)] and x-fold SERS intensity change following 30 min incubation of MDM2 with varying concentrations of inhibitor molecule [dark gray (*A*) and circle (*B*)].

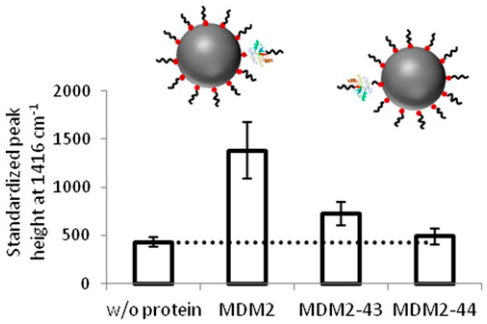

Fig. 6. Competitive inhibition of MDM2-induced PSN aggregation. Schematic illustrates proposed MDM2-induced PSN assembly inhibition with dimerization-motif self-peptides 43 and 44. Data show SERS peak height measurements, at 1,416 cm^{-1}, recorded for PSN-12.1 samples after completion of temporal analysis. Dotted line indicates PSN samples when MDM2 is absent. Error bars illustrate the SD.

advantageous over extinction spectroscopy where a decrease in signal is monitored.

Disruption of the Dimerization Interface. To further test the assay capabilities for investigating MDM2 and verify the requirement for MDM2 oligomerization in PSN assembly, MDM2 was premixed with self-peptides from one linear motif that stabilizes the MDM2/MDMX heterodimer at the N-terminal junction of the C-terminal RING domain (amino acids 430-LPLNAI-435) (8) at a molar ratio of 1:100 MDM2:peptide (0.96 mM MDM2, 96 mM peptide). SERS analysis of PSN solutions (15 pM) was carried out following the addition of MDM2 preincubated with peptides 43 (DKEESVESSLPLNAI) and 44 (PLNAIEPCVICQGRP) (6.25 mL added to 400 mL), which represent overlapping sequences from the dimerization interface (Fig. S9). Preincubation of MDM2 with peptides 43 and 44 resulted in a decrease in PSN-12.1 assembly, as monitored using SERS (Fig. 6). Despite both dimerization-motif peptides demonstrating an inhibitory effect on PSN-12.1 assembly, a 1.69-fold increase in SERS was observed in the presence of peptide 43 compared with a 1.14-fold increase with peptide 44. The difference in PSN-12.1 assembly inhibition potency of these two ligands indicates a positional effect of peptide-ligand binding to the MDM2 dimerization interface in preventing dimerization. As a control, the binding of peptides 43 and 44 to MDM2 using ELISA demonstrated no affect on N-terminal-binding activity (Fig. S9*B*). These data highlight the difference between a standard ligand-binding assay that does not distinguish between the oligomeric or monomeric nature of the target protein (Fig. S9) and a SERS-based ligand-binding assay that requires target protein "oligomerization" (Fig. 6; PSN assembly model illustrated in Fig. 1*A*, *i* and *ii*).

Discussion

A number of SERS-based immunoassays have been developed for the detection of biological interactions; however, few NP–protein aggregation studies have been published. This report presents the use of protein–peptide interactions as a controlled NP-assembly template capable of "turning on" SERS. Furthermore, the protein interactions investigated are of particular biological interest owing to the critical role of MDM2 in cancer progression. PSN assembly and associated SERS enhancement were successfully inhibited by preincubating MDM2 with small-molecule-binding ligands.

We have demonstrated that full-length MDM2 is able to successfully aggregate PSN-12.1, suggesting that the MDM2 protein is in dimeric (oligomeric) state in solution, while maintaining biological activity of the hydrophobic pocket. These studies present an innovative method for interrogating the allosteric interactions of full-length unlabeled MDM2 using biologically driven NP assembly. We also demonstrate a proof-of-concept with which to use SERS-based ligand-binding assays to investigate other allosteric proteins that undergo complex conformational interactions.

Methods

Peptide–BT Conjugation. Peptides 12.1 (SGSG-MPRFMDYWEGLN-resin) and 12.1$_{W\Delta A}$ (SGSG-MPRFMDYAEGLN-resin) were obtained bound to Wang resin via the C terminus (Almac Sciences), with the N terminus deprotected. Modification with BT was carried out via amide coupling in the solid phase and cleaved from the resin using 95% TFA (*SI Methods*).

Nanoparticle Bioconjugation. AgEDTA nanoparticles were synthesized with a 40-nm diameter using the method described by Heard et al. in 1983 (52). Nanoparticles were centrifuged at 1,900 × *g* for 20 min and resuspended in buffer [25 mM Hepes and 20 mM KCl (pH 7.5)] before addition of BT or peptide–BT at a final concentration of 10^{-6} M. After shaking for a minimum of 1 h, the conjugation solutions were centrifuged at 5,000 rpm for 20 min and resuspended in buffer (×3) to remove any excess analytes. Complete BT–peptide conjugates were characterized using extinction spectroscopy, dynamic light scattering, and MALDI-MS.

Dynamic Light Scattering. One-milliliter samples were analyzed via dynamic light scattering using a Malvern high-performance particle sizer (HPPS) using standard disposable cuvettes.

Extinction Spectroscopy. Absorbance readings were taken from 250–650 nm using a Cary Eclipse extinction spectrometer. All spectra were baseline corrected using 25 mM Hepes buffer (pH 7.5), 20 mM KCl, as a blank. NP concentrations were calculated using the extinction coefficient for 40-nm silver nanoparticles at λ-max ($\varepsilon = 2.87 \times 10^{10}$). Peptide–BT concentrations were calculated using the extinction coefficient for BT at 487 nm ($\varepsilon = 12017$).

MALDI-MS. Peptide samples were analyzed using a 1:1 ratio of sample to matrix, α-cyano-4-hydroxycinnamic acid (α-cyano). Ionization was conducted in the positive reflectron mode. A linear three-point calibration was achieved using a preprepared peptide mixture: 379.1 *m/z* (α-cyano matrix), 757.4 *m/z* (Bradykinin fragment), and 1,046.5 *m/z* (angiotensin II). To analyze nanoparticle-bound peptide samples, conjugates were removed from the nanoparticles and desalted. Nanoparticle samples were treated with DTT (10 mM) for a minimum of 30 min to displace BT from the metal surface. Following centrifugation at 5,000 rpm for 20 min, 150 μL of supernatant was desalted using PepClean C-18 spin columns (Thermo Scientific) MALDI-MS carried out on the recovered sample.

Protein Preparation. MDM2 was purified as indicated in *SI Methods*. Purified full-length MDM2 was stored at −20 °C in storage buffer [25 mM Hepes (pH 7.5), 10% (vol/vol) glycerol, 1 mM benzamidine, 5 mM DTT, 290 mM KCl], and buffer exchange into assay buffer [25 mM Hepes (pH 7.5), 20 mM KCl] was performed using a concentrator with a 10-kDa molecular mass cutoff filter (Millipore). BSA was obtained from Sigma and dissolved in assay buffer. MDM2 and BSA stocks were prepared at a concentration of $\sim 8 \times 10^{-7}$ M in assay buffer for use in NP aggregation assays. MDM2 protein was validated in the dual-site-binding assay that measures the ability of Nutlin to stimulate the interaction of MDM2 with the Rb1 peptide (10). Rb1 peptide binds to the acidic domain of MDM2 and mimics the interaction of MDM2 with the p53 central DNA-binding domain (10).

SERS Analysis. SERS spectra were collected using a Renishaw inVia microscope system. Excitation at 514.5 nm was achieved via an Ar^+ laser attenuated using neutral density filters. Spectra were obtained using 180° backscattering with the grating centered at 1400 cm^{-1} using a 20× long-working distance objective. Static scans with a 2-s collection time were obtained for analysis of postassay samples in disposable cuvettes. Temporal SERS analysis of samples was conducted using an NMR tube spinner microscope attachment. A 1-s scan duration was used, and one spectrum was acquired every 60-s for 30 min.

ACKNOWLEDGMENTS. We thank Vivien Landre and Jude Nicholson for insights into the MDM2 RING domain structure, dynamics, and function. This work was supported by a Biotechnology and Biological Sciences Research Council doctoral studentship (to A.F.R.), a Cancer Research UK doctoral studentship (to F.L.), and a Royal Society Wolfson Research Merit Award (to D.G.).

1. Carson DA, Lois A (1995) Cancer progression and p53. *Lancet* 346:1009–1011.
2. Lane DP (1992) Cancer. p53, guardian of the genome. *Nature* 358:15–16.
3. Vousden KH, Lu X (2002) Live or let die: The cell's response to p53. *Nat Rev Cancer* 2: 594–604.
4. Arva NC, et al. (2005) A chromatin-associated and transcriptionally inactive p53-Mdm2 complex occurs in mdm2 SNP309 homozygous cells. *J Biol Chem* 280: 26776–26787.
5. Fang SY, Jensen JP, Ludwig RL, Vousden KH, Weissman AM (2000) Mdm2 is a RING finger-dependent ubiquitin protein ligase for itself and p53. *J Biol Chem* 275: 8945–8951.
6. Momand J, Zambetti GP, Olson DC, George D, Levine AJ (1992) The mdm-2 oncogene product forms a complex with the p53 protein and inhibits p53-mediated transactivation. *Cell* 69:1237–1245.
7. Oliner JD, Kinzler KW, Meltzer PS, George DL, Vogelstein B (1992) Amplification of a gene encoding a p53-associated protein in human sarcomas. *Nature* 358:80–83.
8. Linke K, et al. (2008) Structure of the MDM2/MDMX RING domain heterodimer reveals dimerization is required for their ubiquitylation in trans. *Cell Death Differ* 15: 841–848.
9. Pettersson S, Kelleher M, Pion E, Wallace M, Ball KL (2009) Role of Mdm2 acid domain interactions in recognition and ubiquitination of the transcription factor IRF-2. *Biochem J* 418:575–585.
10. Wallace M, Worrall E, Pettersson S, Hupp TR, Ball KL (2006) Dual-site regulation of MDM2 E3-ubiquitin ligase activity. *Mol Cell* 23:251–263.
11. Dastidar SG, Lane DP, Verma CS (2008) Multiple peptide conformations give rise to similar binding affinities: Molecular simulations of p53-MDM2. *J Am Chem Soc* 130: 13514–13515.
12. Ding K, et al. (2005) Structure-based design of potent non-peptide MDM2 inhibitors. *J Am Chem Soc* 127:10130–10131.
13. Ding K, et al. (2006) Structure-based design of spiro-oxindoles as potent, specific small-molecule inhibitors of the MDM2-p53 interaction. *J Med Chem* 49:3432–3435.
14. García-Echeverría C, Chène P, Blommers MJJ, Furet P (2000) Discovery of potent antagonists of the interaction between human double minute 2 and tumor suppressor p53. *J Med Chem* 43:3205–3208.
15. Vassilev LT, et al. (2004) In vivo activation of the p53 pathway by small-molecule antagonists of MDM2. *Science* 303:844–848.
16. Poyurovsky MV, et al. (2007) The Mdm2 RING domain C-terminus is required for supramolecular assembly and ubiquitin ligase activity. *EMBO J* 26:90–101.
17. Uldrijan S, Pannekoek WJ, Vousden KH (2007) An essential function of the extreme C-terminus of MDM2 can be provided by MDMX. *EMBO J* 26:102–112.
18. Kostic M, Matt T, Martinez-Yamout MA, Dyson HJ, Wright PE (2006) Solution structure of the Hdm2 C2H2C4 RING, a domain critical for ubiquitination of p53. *J Mol Biol* 363:433–450.
19. Worrall EG, Worrall L, Blackburn E, Walkinshaw M, Hupp TR (2010) The effects of phosphomimetic lid mutation on the thermostability of the N-terminal domain of MDM2. *J Mol Biol* 398:414–428.
20. Wawrzynow B, et al. (2009) A function for the RING finger domain in the allosteric control of MDM2 conformation and activity. *J Biol Chem* 284:11517–11530.
21. Huang SX, Chen Y (2008) Ultrasensitive fluorescence detection of single protein molecules manipulated electrically on Au nanowire. *Nano Lett* 8:2829–2833.
22. Tang L, Dong C, Ren J (2010) Highly sensitive homogenous immunoassay of cancer biomarker using silver nanoparticles enhanced fluorescence correlation spectroscopy. *Talanta* 81:1560–1567.
23. Xia ZY, Rao JH (2009) Biosensing and imaging based on bioluminescence resonance energy transfer. *Curr Opin Biotechnol* 20:37–44.
24. Faulds K, Jarvis R, Smith WE, Graham D, Goodacre R (2008) Multiplexed detection of six labelled oligonucleotides using surface enhanced resonance Raman scattering (SERRS). *Analyst (Lond)* 133:1505–1512.
25. Sabatté G, et al. (2008) Comparison of surface-enhanced resonance Raman scattering and fluorescence for detection of a labeled antibody. *Anal Chem* 80:2351–2356.
26. Graham D, Faulds K, Smith WE (2006) Biosensing using silver nanoparticles and surface enhanced resonance Raman scattering. *Chem Commun (Camb)* 42:4363–4371.
27. Cunningham D, et al. (2006) Practical control of SERRS enhancement. *Faraday Discuss* 132:135–145, discussion 147–158.
28. Faulds K, Littleford RE, Graham D, Dent G, Smith WE (2004) Comparison of surface-enhanced resonance Raman scattering from unaggregated and aggregated nanoparticles. *Anal Chem* 76:592–598.
29. Rohr TE, Cotton T, Fan N, Tarcha PJ (1989) Immunoassay employing surface-enhanced Raman spectroscopy. *Anal Biochem* 182:388–398.
30. Campbell FM, et al. (2008) SERRS immunoassay for quantitative human CRP analysis. *Analyst (Lond)* 133:1355–1357.
31. Dou X, Takama T, Yamaguchi Y, Yamamoto H, Ozaki Y (1997) Enzyme immunoassay utilizing surface-enhanced Raman scattering of the enzyme reaction product. *Anal Chem* 69:1492–1495.
32. Douglas P, Stokes RJ, Graham D, Smith WE (2008) Immunoassay for P38 MAPK using surface enhanced resonance Raman spectroscopy (SERRS). *Analyst (Lond)* 133: 791–796.
33. Driskell JD, et al. (2005) Low-level detection of viral pathogens by a surface-enhanced Raman scattering based immunoassay. *Anal Chem* 77:6147–6154.
34. Grubisha DS, Lipert RJ, Park HY, Driskell J, Porter MD (2003) Femtomolar detection of prostate-specific antigen: An immunoassay based on surface-enhanced Raman scattering and immunogold labels. *Anal Chem* 75:5936–5943.
35. Han XX, et al. (2008) Fluorescein isothiocyanate linked immunoabsorbent assay based on surface-enhanced resonance Raman scattering. *Anal Chem* 80:3020–3024.
36. Han XX, et al. (2008) Simplified protocol for detection of protein-ligand interactions via surface-enhanced resonance Raman scattering and surface-enhanced fluorescence. *Anal Chem* 80:6567–6572.
37. Narayanan R, Lipert RJ, Porter MD (2008) Cetyltrimethylammonium bromide-modified spherical and cube-like gold nanoparticles as extrinsic Raman labels in surface-enhanced Raman spectroscopy based heterogeneous immunoassays. *Anal Chem* 80: 2265–2271.
38. Ni J, Lipert RJ, Dawson GB, Porter MD (1999) Immunoassay readout method using extrinsic Raman labels adsorbed on immunogold colloids. *Anal Chem* 71:4903–4908.
39. Wang G, Park H-Y, Lipert RJ, Porter MD (2009) Mixed monolayers on gold nanoparticle labels for multiplexed surface-enhanced Raman scattering based immunoassays. *Anal Chem* 81:9643–9650.
40. Aslan K, Luhrs CC, Perez-Luna VH (2004) Controlled and reversible aggregation of biotinylated gold nanoparticles with streptavidin. *J Phys Chem B* 108:15631–15639.
41. Andresen H, Gupta S, Stevens MM (2011) Kinetic investigation of bioresponsive nanoparticle assembly as a function of ligand design. *Nanoscale* 3:383–386.
42. Du BA, Li ZP, Cheng YQ (2008) Homogeneous immunoassay based on aggregation of antibody-functionalized gold nanoparticles coupled with light scattering detection. *Talanta* 75:959–964.
43. Gupta S, Andresen H, Stevens MM (2011) Single-step kinase inhibitor screening using a peptide-modified gold nanoparticle platform. *Chem Commun (Camb)* 47: 2249–2251.
44. Onoda A, Ueya Y, Sakamoto T, Uematsu T, Hayashi T (2010) Supramolecular hemoprotein-gold nanoparticle conjugates. *Chem Commun (Camb)* 46:9107–9109.
45. Kussie PH, et al. (1996) Structure of the MDM2 oncoprotein bound to the p53 tumor suppressor transactivation domain. *Science* 274:948–953.
46. Böttger V, et al. (1996) Identification of novel mdm2 binding peptides by phage display. *Oncogene* 13:2141–2147.
47. Li C, et al. (2010) Systematic mutational analysis of peptide inhibition of the p53-MDM2/MDMX interactions. *J Mol Biol* 398:200–213.
48. Liu M, et al. (2010) A left-handed solution to peptide inhibition of the p53-MDM2 interaction. *Angew Chem Int Ed Engl* 49:3649–3652.
49. Graham D, et al. (1998) Synthesis of novel monoazo benzotriazole dyes specifically for surface enhanced resonance Raman scattering. *Chem Commun* 11:1187–1188.
50. Naumov S, Kapoor S, Thomas S, Venkateswaran S, Mukherjee T (2004) SERS of benzotriazole on Ag colloid: Surface structure characterization using the DFT approach. *Theochem. J Mol Struct* 685:127–131.
51. Pergolese B, Muniz-Miranda M, Bigotto A (2004) Study of the adsorption of 1,2,3-triazole on silver and gold colloidal nanoparticles by means of surface enhanced Raman scattering. *J Phys Chem B* 108:5698–5702.
52. Heard SM, Grieser F, Barraclough CG, Sanders JV (1983) The characterization of Ag Sols by electron-microscopy, optical-absorption, and electrophoresis. *J Colloid Interface Sci* 93:545–555.